NASA CR
151541

INVESTIGATION OF THREADED FASTENER STRUCTURAL INTEGRITY

(NASA-CR-151541) INVESTIGATION OF THREADED FASTENER STRUCTURAL INTEGRITY Final Report (Southwest Research Inst.) 206 p HC A10/MF A01 CSCL 13E
N78-10473
Unclas
G3/37 52079

FINAL REPORT
Contract No. NAS9-15140
DRL T1190, CLIN 3
DRD MA129TA
SwRI Project No. 15-4665

October 1977

SOUTHWEST RESEARCH INSTITUTE
SAN ANTONIO CORPUS CHRISTI HOUSTON

SOUTHWEST RESEARCH INSTITUTE
Post Office Drawer 28510, 6220 Culebra Road
San Antonio, Texas 78284

INVESTIGATION OF THREADED FASTENER STRUCTURAL INTEGRITY

FINAL REPORT
Contract No. NAS9-15140
DRL T1190, CLIN 3
DRD MA129TA
SwRI Project No. 15-4665

October 1977

Approved:

R K Swanson

R. K. Swanson, Project Manager

John R. Barton

John R. Barton, Vice President
Instrumentation Research Division

ABSTRACT

A review of the fastener literature and industry standards indicates that a high majority of bolted joints are assembled by reference to installation torque only, resulting in preload variation of at least 30%. Direct tension control, which offers great improvement in preload accuracy, generally requires the use of special fasteners or hardware, adding cost and weight.

The NDE literature discloses three general nondestructive approaches to shank tension determination: (1) measurement of shank elongation (strain); (b) measurement of compressive stresses in the head; and (c) measurement of the acoustic response of the fastener with load. Specific methods based on these three approaches were experimentally evaluated.

A magnetic approach, restricted to ferromagnetic steel fasteners, and an ultrasonic birefringence technique, useful on all fastener materials, were both found capable of determining shank tension by measurements made on the fastener head. However, two fundamental problems were found to exist: (a) allowed dimensional variations in standard fasteners can produce indicated stress variations as high as 20%, and (b) residual stresses in the head produce significant data scatter in the measured results. Of the two methods, the birefringence technique is considered the more promising.

Preload can be determined by measuring fastener elongation as it is tightened. Two acceptable elongation techniques were demonstrated. One of these was a commercially available pulse-echo system, and the other an experimental ultrasonic resonance approach. Accurate shank load can be determined with either of these methods, provided calibration information is available.

Two acoustic impact methods were evaluated without promising results. While it was consistently possible to determine whether bolts were "tight" or "loose", differences between various conditions of shank tension were undetectable.

Recommendations include serious effort to implement tension control by ultrasonic elongation measurements, and further attention to the development of the shear-wave birefringence technique as a means of post-installation inspection. To minimize error due to dimensional tolerances, a special "NDE Grade" bolt classification is also recommended.

TABLE OF CONTENTS

Page

LIST OF ILLUSTRATIONS vii

LIST OF TABLES xi

I. INTRODUCTION 1

II. FASTENER INTEGRITY CRITERIA 2

- Brief Historical Review of Bolt Torquing 2
- Efforts to Improve Preload Repeatability 3
- Effect of the Reduction in Preload Scatter 6
- Review of NASA MSFC Threaded Fastener Failures 8

III. REVIEW OF TORQUE-TENSION STANDARDS 12

- Description of Some Torque Recommendations 12
- Summary of Torque-Tension Standards 21

IV. REVIEW OF JOINT TENSIONING TECHNIQUES 22

- General Considerations in Joint Tensioning 22
- Strain-Gage Bolts 22
- Preload Indicating Washers 23
- Visual Indicators 24
- Direct Tensioning 25
- Torque-Tension Systems 25
- Torque Versus Angle 26
- Torque Versus Time 28
- Ultrasonic Length Measurement 30
- An Idea that Failed 30
- Summary of Tensioning Systems 30

V. POTENTIAL NEW APPROACHES TO TENSION CONTROL 37

- Parameters of Interest 37
- Evaluation Procedure 38
- X-Ray Diffraction 40
- Nuclear Magnetic Resonance 40
- Exo-Electron Emission 41
- Magnetic and Electromagnetic Methods 42
  - Magnetic Permeability 42
  - Low-Frequency Magneto-elastic Effects 43
  - Eddy Current 43
  - Barkhausen Noise Analysis 43
  - Electromagnetic Generation of Ultrasound 44

PRECEDING PAGE BLANK NOT FILMED

TABLE OF CONTENTS (Contd.)

Page

Ultrasonic Methods 44
- Ultrasonic Pulse-Echo Extensometer 45
- Reflection Oscillator Ultrasonic Spectrometer (ROUS) 45
- Acoustic Impact Technique (AIT) 45

Shear Wave Birefringence 46
Conclusions 46

VI. APPLICATION OF STRESS DETERMINATION METHODS 47

Finite Element Analysis 47
MS21250 Bolt 55
Conclusions 65

VII. EXPERIMENTAL EVALUATION OF SELECTED NDE METHODS 68

Magnetic Methods 68
Review of Magnetism and Magnetic Effects 69
Specimen Selection for Magnetics Experiments 71
Design of Magnetics Experiments 73
Magnetic Parameter Experimental Results 78
Barkhausen Effect Experiments 79
Results of Barkhausen Experiments 84
Hex-head Bolts 84
Inner Probe Only 84
Two-Probe Ratio Measurement 95
Multiple Regressions Analysis 106
Residual Stress Considerations - Data Analysis 108
Residual Stress Experiments on Hex-Head Bolts 110
Experiments with MS21250 Aircraft Bolts 120
Residual Stress Considerations in MS21250 Bolts 123
Residual Stress Experiments with MS21250 Bolts 128
Acoustic and Ultrasonic Methods 128
Application of Acoustic Energy to Stress Measurement 132
Longitudinal Wave Techniques 133
Shear Wave Techniques 134
Mechanical Impact Techniques 135
Acoustics Experiments 136
The ROUS System 137
Evaluation of ROUS Data 145
Douglas-Erdman Extensometer 146

TABLE OF CONTENTS (Contd.)

Page

Operation of the Extensometer 147
Extensometer Experiments 147
Post-Installation Load Determination 148
Results of Extensometer Evaluation 159
Shear-Wave Birefringence Experiments 159
Results of Birefringence Experiments 160
Conclusions from Birefringence Experiments 171
Mechanical Impact Techniques 171
Preliminary Ball-Drop Impact Experiment 175
Transverse Impact 178
Instrumented Hammer Impact 178
Instrumented Hammer Impace with Modified Fixture 182
Conclusions from Acoustic Impact Experiments 190

VIII. CONCLUSIONS AND RECOMMENDATIONS 191

Conclusions 191
Recommendations 193

REFERENCES 194

LIST OF ILLUSTRATIONS

Figure Page

1. The Effect of Preload Scatter Reduction on Joint Efficiency 7
2. Torque vs. Fastner Rotation Curve 27
3. Typical Response of "Timed Torque" System in which Increasing Force Pulses are Applied until Torque no longer Increases as at "D". 29
4. Comparison of Preload by Three Tightening Systems 32
5. Miscellaneous Commercially Available Washer-Type Pre-Load Indicators 34
6. Specification of AN8 Series Bolts used in Finite Element Analysis 49
7. Finite-Element Model of Symmetrical Bolt showing Elements used in Analysis. 50
8. Surface Stress across Top of Bolt Head 51
9. Surface Stress down Side of Bolt Head 52
10. Surface Stress across Top of Bolt Head 53
11. Surface Stress down Side of Bolt Head 54
12. Surface Stress across Top of Bolt Head 56
13. Surface Stress down Side of Bolt Head 57
14. Finite-Element Model used in "Case II" Dimensional Analysis 58
15. Surface Stress across Top of Bolt Head 59
16. Surface Stress down Side of Bolt Head 60
17. Specification for MS21250 Aircraft Bolt 61
18. Finite-Element Model used for Analysis of MS21250 Aircraft Bolt 62
19. MS21250 Bolt - Surface Stress across Bottom of Hole in Head 63
20. MS21250 Bolt - Surface Stress along I. D. of Bolt Head 64
21. MS21250 Bolt - Surface Stress across Top Edge of Bolt Head 66
22. MS21250 Bolt - Surface Stress on Outside Flange 67
23. Typical Hysteresis Loop for Iron 70
24. Specifications for one Bolt Type used in the Magnetics Experiments 72
25. Laboratory Set-Up for Barkhausen Noise Investigation of Stress in Bolts. 74
26. Closeup View of Skidmore-Wilhelm Loader and Magnetic Circuit 75
27. Schematic of Barkhausen Bolt Inspection System 76
28. Concentric Probe Configuration 77
29. Magnetic Circuit Arrangement for Measurement of Fringing Flux as an Indication of "B" 80

LIST OF ILLUSTRATIONS (Contd.)

Figure		Page
30.	Magnetic Hysteresis Loop Measurements vs. Magnetic Current at 0 and Full Load	81
31.	Schematic Diagram of Essential Components of Stress Measuring Instrument based upon the Stress Dependence of the Barkhausen Effect	83
32.	Barkhausen Signature, 3/8" Bolt, Measured at Center of Head vs. Shank Load	85
33.	Barkhausen Signature, 3/8" Bolt, Measured at Outer Periphery on Top of Bolt Head	86
34.	Ratio of Outer to Inner Barkhausen Measurement, 3/8" Bolt	87
35.	3/8" Grade 5 Bolts #30-#39, Inner Probe Measurements	88
36.	1/2" Grade 8 Bolts	89
37.	1" Grade 8 Bolts	91
38.	MS90727 Bolt #2, Inner Probe Reading	92
39.	1/2" Grade 8 Bolts	93
40.	1/2" Grade 8 Bolts, MS90727	94
41.	3/8" Grade 5 Bolts, #30-#39, Outer Probe Measurements	97
42.	1/2" Grade 8 Bolts #2-0 through #2-24, Outer Probe	98
43.	1" Grade 8 Bolts #1-0 through #1-24, Outer Probe	99
44.	1/2" Grade 8 Bolts #1 & #4-#12, First Loading	100
45.	1/2" Grade 8 Bolts #1 and #4-#12, Second loading	101
46.	MS90726 Grade 5 Bolts 3/8", Barkhausen Ratio vs. Shank Load	102
47.	Barkhausen Ratio vs. Load 1/2" Bolts	103
48.	Barkhausen Ratio vs. Load 1" Bolts	104
49.	1/2" Grade 8 Bolts #1 and #4-#12, First Loading	105
50.	1/2" Grade 8 Bolts #1 and #4-#12, Second Loading	107
51.	Typical Barkhausen Responses	108
52a.	3/8" Bolts-Uncorrected Barkhausen Data	111
52b.	3/8" Bolts - Corrected for Residual Stress	111
53a.	1/2" Bolts - Uncorrected Barkhausen Data	112
53b.	1/2" Bolts - Corrected for Residual Stress	112
54a.	1" Bolts - Uncorrected Barkhausen Data	113
54b.	1" Bolts - Corrected for Residual Stress	113
55a.	1/2" MS90727 Bolts, First Run Inner Probe, Uncorrected	114
55b.	1/2" MS90727 Bolts, Corrected for Residual Stress	114
56a.	1/2" MS90727 Bolts, Second Run, Uncorrected	115
56b.	1/2" MS90727 Bolts, Corrected for Residual Stress	115
57a.	1/2" MS90727 Bolts, First Run, Outer Probe, Uncorrected	116
57b.	1/2" MS90727 Bolts, Corrected for Residual Stress	116
58a.	1/2" MS90727 Bolts, Second Run, Outer Probe	117
58b.	1/2" MS90727 Bolts, Corrected for Residual Stress	117

LIST OF ILLUSTRATIONS (Contd.)

Figure		Page
59.	MS90727 Bolts Before and After Heat Treatment	118
60.	MS90727 Bolts before and after 1100F Heat Treatment	119
61.	Loading Fixture as Modified for Barkhausen Experiments with MS21250 12-point Aircraft Bolts	121
62.	MS21250 Bolts 1/2" Measurements on Head	122
63.	MS21250 Bolt #1 Barkhausen Signal vs Load at 4 Orientations, Probe at Center	124
64.	MS21250 Bolt #1, Barkhausen Signal vs Load at 4 Orientations, Probe on Inside Wall	125
65.	MS21250 Bolts, Uncorrected Data	126
66.	MS21250 Bolts, Corrected for Residual Stress	127
67.	MS21250-05 before and after Heat Treatment at 800 and 1100F	129
68.	MS21250-06 before and after Heat Treatment at 800 and 1100F	130
69.	Plot of Atomic Position in an Ultrasonic Wave	131
70.	Block Diagram of ROUS System for Measuring Shift in Resonant Frequency of Bolt vs Load	138
71.	Frequency Shift Data for the Steel Bolts with Least Squares fit to Data Plotted	140
72.	Frequency Shift Data for the Aluminum Bolts with Least Squares fit to Data Plotted	141
73.	Frequency Shift Data for the Titanium Bolts with Least Squares fit to Data Plotted	142
74.	Frequency Shift Data for the "As Received" Aluminum Bolt with Least Squares fit to Data Plotted	143
75.	Frequency Shift Data for the "As Received" Titanium Bolt at Two Resonant Frequencies with Least Squares Fit to Data	144
76.	Elongation Measured by Douglas-Erdman Instrument on Grade 8 Steel Bolts with Prepared Ends	152
77.	Elongation Measured by Douglas-Erdman Instrument on Untouched Grade 8 Steel Bolts	153
78.	Variation with Cycling of the Elongation Measurements on Grade 8 Steel Bolt with Ground Ends	154
79.	Variation with Cycling of the Elongation Measurements on Grade 8 Bolt with Unprepared Ends	155
80.	Elongation of Aluminum Bolt Measured by the Douglas-Erdman Instrument	156
81.	Variation in Elongation Measurements with Changes in Calibration Setting for Aluminum Bolt	157
82.	Elongation Measurements on a Titanium Bolt using the Doublas-Erdman Instrument	158

LIST OF ILLUSTRATIONS (Contd.)

Figure		Page
83.	Echo Patterns for Various Orientations of Propagation of 5 MHz Ultrasonic Wave through 5/8" Grade 8 Steel Bolt Head	161
84.	Experimental Arrangement for Measurement of Ultrasonic Birefringence Effect on Hex-Head Bolt during Loading	162
85.	Fit to Data on 5/8" Steel Bolts (Grade 8) with Standard Deviation Boundaries Plotted	165
86.	Plot of Birefringence for the Three Orientations of Propagation through the Bolt Head for Bolt #6	167
87.	Birefringence in an 1/2" Aluminum Bolt	169
88.	Birefringence in a 1/2" Titanium Bolt	170
89.	Shear Wave Birefringence on Four 3/4" Steel Bolts	173
90.	Instrumentation for Ball-Drop Experiment	176
91.	Accelerometer Time Responses and System Frequency Responses obtained from Ball-Drop Tests	177
92.	Frequency Measurement Apparatus Employing an Instrumented Hammer	179
93.	Fast Fourier Transform Analyzer, Graphic Terminal and Hardcopy Unit	180
94.	Frequency Spectrum of Mechanical Impulse	181
95.	Frequency Response with Bolt Snug	183
96.	Frequency Response with Bolt Loaded to 31% Proof Load	183
97.	Frequency Response with Bolt Loaded to 63% of Proof Load	184
98.	Frequency Response with Bolt Loaded to 94% of Proof Load	184
99.	Modified Hammer-Impact Apparatus	185
100.	Frequency Response of Modified Fixture with Bolt Snug and Impact on Bolt Head	186
101.	Frequency Response of Modified Fixture with Bolt Loaded to 34% of Proof Load and Impact on Bolt Head	186
102.	Frequency Response of Modified Fixture with Bolt Loaded to 63% of Proof Load and Impact on Bolt Head	187
103.	Frequency Response of Modified Fixture with Bolt Loaded to 89% of Proof Load and Impact on Bolt Head	187
104.	Frequency Response of Modified Fixture with Bolt Snug and Impact on Top Plate	188
105.	Frequency Response of Modified Fixture with Bolt Loaded to 34% of Proof Load and Impact on Top Plate	188
106.	Frequency Response of Modified Fixture with Bolt Loaded to 63% of Proof Load and Impact on Top Plate	189
107.	Frequency Response of Modified Fixture with Bolt Loaded to 89% of Proof Load and Impact on Top Plate	189

LIST OF TABLES

Table		Page
I	Typical Minimum Bolt Tension Values Achieved by Two Methods of Tightening	5
II	Review of NASA Threaded Fastener Failures by Category	9
III	Some Representative Recommended Torques for 1/2-20UNF Steel Bolts	13
IV	Steel Bolt Mechanical Properties	15
V	Normalized Torques and Preloads for 1/2-20UNF Steel Bolts	17
VI	Preloading Devices and Systems	35
VII	Post Tension Devices and Systems	36
VIII	Stress Measurement Methods of Potential Interest to Threaded Fastener Integrity	39
IX	Dimensional Values used for Stress Analysis of AN8 Bolt	48
X	Descriptive Data on Bolts	137
XI	Summary of Absolute Measured Resonant Frequency	139
XII	Calculated and Theoretical Values of K	145
XIII	Nine 1/2" Grade 8 Steel Bolts, One Loading Cycle	149
XIV	1/2" Steel Bolt with Ground Ends, Five Loading Cycles	149
XV	1/2" Steel Bolt (#10), as received, Five Loading Cycles	150
XVI	Two Grade 8 Steel Bolts at Full Load	150
XVII	Effect of Temperature on Grade 8 Steel Bolt #9, zero to proof load	151
XVIII	Effect of Error in Calibration Setting on Aluminum Bolt	151
XIX	Titanium Bolt	151
XX	Shear Wave Birefringence of 5/8" Grade 8 Steel Bolts	163
XXI	Variation of Shear Wave Birefringence with Orientation of Bolt Head	166
XXII	Shear Wave Birefringence Data for a 1/2" Alum. Bolt	168
XXIII	Shear Wave Birefringence Data for a 1/2" Titanium Bolt	168
XXIV	Shear Wave Birefringence Data on Four 3/4" Bolts	172
XXV	Shear Wave Birefringence Data for Selected Orientations	174

I. INTRODUCTION

Threaded fasteners form a large and varied category of structural components. Properly designed joints using accurately installed threaded fasteners serve an essential and inexpensive function. Such joints, however, are subject to failure when improperly constructed, and as a consequence, their correct use has received a great deal of attention throughout the period since the industrial revolution. The use of threaded fasteners has extended into the space age, where their reliability often becomes a critical matter. Not only can failure of critical fasteners in aircraft or spacecraft jeapordize the mission, but excessive safety factors designed into such bolted joints may dictate a severe weight penalty due to overdesign. If adequate means were available for accurately determining the integrity of the joint after assembly, considerable weight savings could accrue through the use of fewer and smaller fasteners, more critically stressed.

A principal purpose of the research reported in this document has been the assessment of technical nondestructive evaluation (NDE) approaches to the determination of fastener integrity. Existing instruments and methods have been examined, and industry procedures now being followed have been evaluated. An attempt has been made to quantitatively define the goals of instruments which might be applied to fastener integrity determination.

A corollary to the proper installation of fasteners at assembly is the extension of inspection methods to include post-installation applications. There are no commercial methods available which currently serve this function, other than the use of special fastener hardware. Such special hardware inevitably carries a weight and cost penalty.

In performing this research, the NDE literature has been carefully surveyed and all methods potentially applicable to the measurement of preload isolated and assessed. The parameter of interest is fastener shank stress, and by implication strain. Thus the search centered on those methods capable of determining stress or strain.

In the determination of fastener integrity criteria, manufacturers' data and the open literature were carefully searched for pertinent information.

II. FASTENER INTEGRITY CRITERIA

Brief Historical Review of Bolt Torquing

The principal use of threaded fasteners is to draw layers of material together into structural joints. There is no record of the invention of the first threaded fastener, although the concept of the screw thread was known by Archimedes (d. 212 B.C.) who used it in a water lift device. There is little doubt that the inventor of the first nut to complement a screw had no idea of the revolution he began. Today, literally billions of threaded fasteners are used throughout industry, in a wide variety of sizes and shapes. It has been said that one automobile manufacturer a few years ago used 11,500 different fasteners in his product.

A considerable body of research(1) has been devoted to the elements of a satisfactory bolted joint; that is, a joint that will reliably carry its intended load. It is well understood by designers that in a tension-type joint, the initial load (called preload) put into the bolt at the time of installation, must be greater than any subsequent load on the bolt. A basic problem has always been the accurate determination of the desired preload at the time of assembly. Insufficient preload results in a poor joint, and too much preload may cause the bolt to fail.

The earliest attempt to accurately control the preload was by relating it to the torque applied to tighten the nut. This method, in one form or another, is still by far the most widely used. More will be said of this in a later section. Because approximately 90 percent of the applied torque is needed to overcome thread and bearing surface friction, and since friction is a variable quantity, it is difficult to obtain uniform and accurately known preloads by measuring the applied torque only. To add to this difficulty are problems caused by cross-threads, misaligned holes and the like, which give a false indication of preload because of the abnormally high torque level experienced.

Depending on the thread lubricant used, the hardness of the bearing washer, and the smoothness of torque wrench operation, tension variations of ±30%(2) are not uncommon with torque measurement systems and they may be much greater. Some recent(3), very carefully controlled laboratory-type tests have reported variations of ±5% in tension but it is doubtful such could be approached in field applications. Tension variability or scatter can never be completely eliminated, and it would appear that ±10% is, at least for now, a reasonable limit for production methods using torque measurement. As will be described later, there are special bolts which can be tightened to within ±2% or so of the desired value, but the bolts are expensive and the process is not adapted to most production methods.

All of the factors affecting the bolt tightening process contribute to the preload variability. Some of these are material strength, bolt diameter, hole fit, thread and bearing friction, speed of tightening, fastening device indication tolerance, etc. The goal in accurate preload determination is the reduction or the elimination of the effect of these factors on the tightening process.

Efforts to Improve Preload Repeatability

The first effort to improve the repeatability of fastener preload was through the use of calibrated manual torque wrenches. These used gauges, snap-springs and other limiting devices to control applied torque. The improvement in preload accuracy was limited due to the great variability of thread friction in the fastener itself. In spite of this, continued effort has been devoted to better torque-only methods, particularly for use in high speed production work.

The impact wrench, with a preset torque cut-off point, was one of the early attempts to integrate torque control into production-type tools. It is also notably unreliable, producing torque scatter to ±25%. (This is torque scatter; tension variability could be twice this amount.) Very often, torque verification by random sampling with a manual torque wrench is used on the production line, but this introduces additional problems. The break-away torque needed to restart the nut is almost always greater than the dynamic torque last applied to the nut, because static friction is usually higher than dynamic friction. Since neither friction coefficient is deterministic, the break-away torque is only loosely related to the actual tightening torque.

Stall-type torque drives, if well maintained, represent an improvement, potentially achieving torque repeatability of ±10%. Again, however, there is no way to monitor the actual torque applied.

Stall-type drives have been instrumented to monitor the actual torque and to display its value. This improves the "confidence" in the system, but does not reduce the torque variability, nor does it improve the torque-tension relationship. Using the uninstrumented stall-type drive as a base of 100, the instrumented drive increases the cost of a bolted joint to 140 to 275, depending on whether partial or 100% monitoring is employed.

The next step involves the use of feedback. The torque signal in a monitor-type stall system is fed back electronically, directly controlling the drive motor when the torque reaches the desired value. Very low inertia air motors and extremely fast acting air valves had to be developed for this type of system, but ±5% torque variability (not tension variability) has reportedly been achieved. The relative cost per installed fastener is about 325(4).

A different approach to the problem was proposed by the American Association of Railroads (1). They conducted experiments which showed that a good degree of reliability in tensioning could be achieved by turning the nut one revolution past the hand-snugged position. Such a procedure was adopted in 1955. By turning the nut one revolution, the stretch of the bolt was controlled and hence the preload.

Unfortunately, hand snugging to achieve a uniform initial change was not reliable due to dirt, thread imperfections, mis-alignment, etc. The self-locking features on aerospace fasteners has prevented uniform snugging and has practically precluded the use of the turn-of-the-nut method in the aerospace industry. In an attempt to avoid inherent problems in the method, Bethlehem Steel Corporation defined snugging as that achieved by a preset impact wrench, with the final tightening achieved by turning the nut 1/2 to 3/4 turn, depending upon bolt length.

In applications where the threads are clean, parts properly aligned and flat, and threaded holes sufficiently deep, the turn-of-the-nut method has proven better than the torque-only methods for achieving a uniform tension. Automated systems combining the use of torque to provide the initial clamp, and nut turn to obtain the final preload, are in popular use. Their relative per joint cost is about 475(4).

In recent years very sophisticated systems have been devised that sense the point when the bolt begins to yield as the nut tightens and then shuts off. These systems achieve good uniformity of tension, on the order of ±3 standard deviation spread which represents a ±10% variation in the tension. Not only is the tension more uniform with these systems, but the bolt is loaded to its ultimate capacity. This often allows for fewer or smaller fasteners to do the job.

A graphic example of the size and weight reduction possible through accurate tensioning is shown in Table 1, based on data from the manufacturer of one of these sophisticated tension-controlled systems. The circled numbers show how tension control can increase the nominal preload and at the same time reduce the size of the bolt required. The numbers in the squares illustrate a double effect of employing tension control and upgrading the bolt quality. The total weight saving in each of the three examples is about 32%.

Two types of tension control systems are available and these are described in more detail in a later section. Relative cost for these systems is about 500(4).

TABLE I

Typical Minimum Bolt Tension Values Achieved by Two Methods of Tightening

Bolt Size, In.		1/4	5/16	3/8	7/16	1/2	9/16	5/8	3/4	7/8	1
Nominal Weight, Ten 3-in. Bolts, lb.		0.524	0.824	1.19	1.70	2.36	2.99	3.88	5.95	8.67	11.9
Bolt Quality	**Method of Tightening**	Shank Tension, lbs. x 100 (min)									
SAE Grade 5 Steel	Calibrated Torque Wrench	16	26	38	52	65	89	110	163	225	296
	Tension Control	26	43	63	87	121	148	183	272	375	494
SAE Grade 8 Steel	Calibrated Torque Wrench	22	37	54	74	93	127	157	233	322	423
	Tension Control	37	61	90	124	170	211	262	401	536	705

Effect of the Reduction in Preload Scatter

The preceding discussions have emphasized the efforts made over many years to reduce the scatter in the preload value due to the tightening process. By reducing the variability caused by torquing, fastener breakage can be reduced, underfastening can be better avoided, fastener size and thus weight can be reduced, or the number of fasteners can be reduced.

The effect of preload scatter reduction on the tightening process may be realized through reference to Figure 1. The solid line represents the tension-strain curve for a given bolt size. The dashed line represents a similar curve for a smaller bolt of the same material. Load A represents the design load or the minimum desired preload. Load B is the maximum load on the bolt brought about by the ±30% scatter in the tightening process. At point B the bolt has yielded by an amount represented by the slope of the curve at B.

If the tightening process reduces the scatter to ±10%, the maximum bolt load is at C, not yet into the yield condition, and the joint is not very efficient.

On the other hand, if at the same time that the tightening process holds the tension scatter to ±10% the bolt size is reduced, as represented by the dashed line, the load at C now brings the material into the yield regime. If the slope at load C for the smaller bolt is the same as at load B for the larger, both bolts are tightened to the same relative degree but the excess load capacity of the larger bolt is no longer needed because the scatter in the tensioning method is reduced.

In spite of the improvement in preload control achieved over the years, none of the systems give actual preload and, more important to reuseable aerospace systems, none give a post application preload indication. The ability to determine post application preload is important from at least two standpoints. First, it should reveal loosening of the bolt as may result from structural overload, and second, the normal loss of preload with time should become apparent. Neither of these may be perceptible to ordinary examination. Studies have shown that a threaded fastener loses an average of 5% of its tension immediately upon completion of the fastening process, probably due to elastic recovery. The recent tension control systems described above make some attempt to overcome this initial relaxation in their multiple spindle designs by supplying to the fasteners after final torquing a simultaneous last "jolt" of torque. Long term creep in the fastener and joint may also cause relaxation, particularly in the high strength fasteners which are tightened to near their ultimate strength. At present, the only approach to post-application inspection is by laboriously re-torquing each fastener, or by using special fastener hardware.

4521

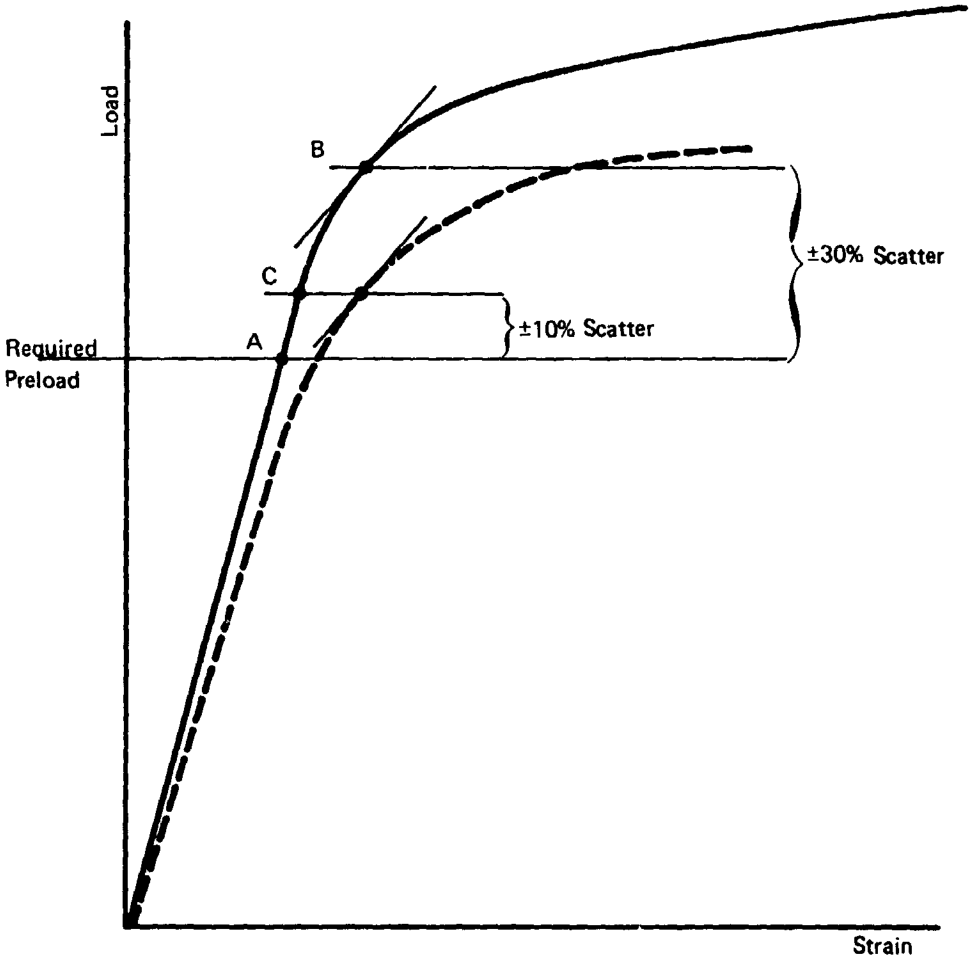

Fig. 1. The Effect of Preload Scatter Reduction on Joint Efficiency

In order to determine the actual preload, a number of devices and systems have been placed on the market. In a few cases these devices allow for the determination of post application preload, or at least indicate the loss of the initial preload. These devices are for the most part expensive, restrictive in application, or add undesirable weight to the joint. They are described in a later section

Review of NASA MSFC Threaded Fastener Failures

The NASA Skylab program experienced a number of problems during the mission phases concerning loss of integrity of bolted joints. Components became misaligned, parts failed, and electric and hydraulic circuits failed.

In order to obtain some grasp of the magnitude and nature of the problem, a review was made of NASA failure analysis reports at the Manned Space Flight Center in Houston. The failures reported were those arising out of component and system checkout, qualification, receiving, and assembly of NASA built parts. Assembly problems are generally caught on the floor where QA/QC inspectors monitor all fastening operations for compliance with appropriate specifications. For the most part, fastener problems in contractor furnished assemblies are the contractor's responsibility and only confront NASA during interfacing.

Unfortunately, the name "failure report" was found to be largely a misnomer. The reports in this file consist only of unacceptable joints or fasteners discovered during an inspection step. Actual service failures are not documented, and consequently if they exist (as they almost certainly do), their causes remain unknown.

Microfilm copies of these failure (or inspection) analysis reports were examined. File access was made through the use of various key words such as: fastener, bolt, bolt assembly, screw, nuts, nut plates, nut subassembly, studs, torque and torquer. Only those reports were considered that related to some physically identifiable failure of the fastener. For example, a fastener dropped into another assembly causing some secondary failure was not considered. Corrosion during storage was also not considered, nor was accidental contamination of dry film lubricant.

From the rather voluminous file, eighty reports were considered valid fastener failures, and these have been categorized in the breakdown shown in Table II Some examples of the failures found in each category are described in the following paragraphs:

TABLE II

Review of NASA Threaded Fastener Failures by Category

Inadequate Design	Improper Assembly	Poor Manufacture or Faulty Part	Damaged in Handling	Excess or Insufficient Torque
19	23	8	19	11

Breakdown of Failures due to Improper Torque

Torque wrench calibration error	3
Faulty bolt led to overtorque	2
Improper use of torque wrench	3
Loose (unknown cause)	3
	11

A. Due to Inadequate Design

1. The set screw for a switch knob was sheared off. Tests showed that this could occur during rapid switching. Design was changed to a "D" shaft to reduce shear load on set screw. Detected during qualification testing of assembly.

2. Two mounting bolts froze in bushings during installation. Bushing designed clearance was inadequate. Undersized bolts were used. Occurred during acceptance test of system.

3. Interference of sharp-edged part with tie-down bolts in some installations caused metal gouging, requiring bolt replacement. Parts modification was required for correction. Observed during acceptance inspection.

4. Titanium bolts broke during proof pressure test. Load too high for titanium. Replaced by corrosion resistant steel bolts. Occurred during design verification test.

B. Due to Improper Assembly

1. Hold-down bolt was cross-threaded during installation. The threads stripped but mating part was undamaged. Bolt replaced. Occurred during functional tests of the system.

2. Screw broke off in a bellows mounting ring. Lubricant was supposed to be used but was not. Subsequent installations specified the use of dry film lubricated screws to eliminate requirement for applying lubricant. Occurred during qualification test.

3. Mounting screws were developing burred heads. The screws were intended for one time use but were actually being reused several times. Discovered during vehicle ground checkout at Cape Kennedy.

4. It was impossible to get to a bolt to tighten it. It was determined that during prior assembly phases the interfering part had slipped into the improper position. The immediate problem was corrected by filing the offending part away. Occurred during assembly.

C. Due to Poor Manufacture or Faulty Part

1. Small mounting screw for electronic assembly was sheared in the as-received condition. Poor surface quality of the screw led to excessive friction-induced torques and subsequent breakage during assembly, testing, and disassembly at the contractor facility. An alternate screw manufacturer whose product had a better finish was used for subsequent units. Discovered during visual inspection.

2. A pre-launch check of a strain-gaged load indicating tie-down bolt was negative. The bolt proved defective and was replaced. Occurred during functional test at Cape Kennedy.

D. Damaged in Handling or by Corrosion in Storage

1. Stud threads in an electronic assembly were damaged either in manufacturing or handling. Noted during visual inspection.

2. Wires leading from strain gaged bolt were damaged when bolt was dropped on them. Occurred during system assembly at Cape Kennedy.

3. Foreign material, probably epoxy, fell into nut insert during assembly. This caused interference and the bolt sheared. Occurred during qualification testing.

4. Electronic readout torque wrench did not indicate in both tightening and loosening modes. Leads had been damaged by use of wrong solder during repair.

E. Due to Excess or Insufficient Torque

1. Mounting bolt broke during system installation. Analysis revealed over-torquing. May have been due to nonobservance of procedure.

2. Threads on a bolt were stripped during installation. Torque wrench was found to be out of calibration, indicating 140 in. /lb. when actually releasing at 163 to 174 in. /lb.

3. Strain gaged bolt broke during torquing. Strain indicating equipment was faulty such that actual bolt load was 47, 000 lb. instead of the required 40, 000 lb.

4. Retainer nut was found to be loose after a proof pressure test failure. Nut had not been torqued originally. Procedure was revised to include specific check of torques. Error was discovered during acceptance test.

III. REVIEW OF TORQUE-TENSION STANDARDS

There are numerous sources in the literature giving the torque required to tighten a bolted connection. Unfortunately, much of the data contained in these sources are incomplete. The criteria used to relate the torque and the preload are not stated. Often the preload to be achieved by the applied torque is missing. The grade or quality of the bolt material is not specified. Added to these problems are those relating to the effect of friction, hole size, and washer or surface material hardness on the torque/tension relationship and it becomes quickly evident that choosing a reliable source for torque values required to achieve a given joint clamping force is not a clear-cut response.

Description of Some Torque Recommendations

Table III lists a number of representative sources for torque for 1/2-20 UNF bolts. The list is not inclusive and is biased toward aerospace and aircraft applications. The recommended torques are initially arranged, to the extent possible, into "lubricated" and "unlubricated" categories. Within each of the categories the data are arranged by SAE bolt grade, or minimum ultimate tensile strength if no SAE grade is defined for that material strength.

Table IV gives the mechanical properties of steel bolts of the various grades considered in Table III, to the extent that the material is specified in the referenced document.

A comparison between recommended torques for similar grade bolts and comparable lubrication conditions in Table III is of interest. For comparable bolt grades in source Items 3 and 5 (minimum ultimate tensile stress 125,000 psi) the recommended torque values do not differ a great deal, approximately ±2% above the average. The recommended torque values for unlubricated Grade 8 bolts, as shown in source Items 5 and 7, are also nearly the same, but the torque recommendation in Item 6 for the same bolt is much higher. Considering the average torque from these three references, the recommended torque varies ±21%. Further, comparing bolts of steel having minimum ultimate tensile stress of 180,000 psi in Items 2 and 5, the recommended torque values are almost the same*, but similar bolts in Item 8 call for torque values almost 50% higher.

Part of the explanation for the difference in recommended torque for bolts of the same grade under similar conditions, lies in the criteria chosen for defining the fastener preload. The basis for fastener preload is given under the category "CONDITIONS" in Table III. It is evident that where such data are available, no unanimity exists regarding these criteria. Some criteria

---

*This is not too surprising since both of these references are NASA publications.

TABLE III

SOME REPRESENTATIVE RECOMMENDED TORQUES FOR 1/2-20UNF STEEL BOLTS

Item	Reference	Torque in.-lb.	Preload lb.	Strength	Conditions
1	Tech. Manual; Aircraft, Missle, and Related Aerospace Equip. Repair. Structural Hardware (USAF T.O. 1-1A-8), (Navy NAVWEPS 01-1A-8), 1 Jan. 1959.	550/750		Use when Maint. Tech. Manual of specific vehicle does not list torques.	Free spinning self-locking plain nut.
		1100 max.		90,000 psi in bolt (probably SAE Grade 8)	Oil free cadmium plated threads.
2	NASA Prime Contractor Material Processing specification "Installation of Threaded and Collared Fasteners" MA 0101-301	290/410		Min. UTS 40,000 psi	Bolt hole clearance such that bolt may be installed by finger push.
		585/840		Min. UTS 140,000 psi	
		1200/1320		UTS 180,000 to 240,000 psi	Bolt hold clearance such that bolt may be installed by finger push.
3	Tech. Manual; Std. Maint. Procedures (Navair 02-1-517), (USAF T.O. 2-1-111), (Army DMWR 55-2800-206), 15 Oct. 1975 P&WA Aircraft Engines	750 max. 550, 675 min*		Min. UTS 125,000 psi	Oil lubricated.
		515 max. 390, 460 min*		Min. UTS 125,000 psi	Antiseize coated.
4	Tech. Manual; Overhaul Turboprop Engine, AF Model T56-A-15 (T.O. 2J-T56-43) 1 April 1968	564/648		Engine grade fasteners.	Dry. Apply torque to head or nut.
5	NASA Std. Torque Limits for Threaded Fasteners, MSFC-STD-486, Amend. 1, 14 July 1970	420		SAE Grade 2**, Min. UTS 74,000 psi	Cadmium plated. unlubricated; torque to produce 65% of tensile yield by Johnson's 2/3 method.
		610		SAE Grade 5, Min. UTS 120,000 psi	
		690		Min. UTS 125,000 psi	
		905		SAE Grade 8, Min. UTS 150,000 psi	For UNC and UNF threads
		950		Min. UTS 160,000 psi	For UNC and UNF threads
		1260		Min. UTS 180,000 psi	For UNC and UNF threads
		315		SAE Grade 2	Cadmium plated or unplated, lubricated; torque to produce 65% of tensile yield by Johnson's 2/3 method.
		540		SAE Grade 5	
		576		Min. UTS 125,000 psi	
		790		SAE Grade 8	For UNC and UNF threads
		830		Min. UTS 160,000 psi	For UNC and UNF threads
		940		Min. UTS 180,000 psi	For UNC and UNF threads

---

* Use lower value where alignment of cotter pin locking holes reqd. Otherwise use higher value.

** SAE J429h, Mechanical and Material Requirements for Externally Threaded Fasteners, September 1974.

ORIGINAL PAGE IS
OF POOR QUALITY

TABLE III (con't.)

Item		Torque in.-lb.	Preload lb.	Strength	Conditions
6	*Machine Design*, Reference Issue, Vol. 41, 11 Sept. 1969, p. 20. (No source given for data; some obvious errors corrected.)	660	6,600	SAE Grade 2	Unlubricated. Torque to produce 75% of proof load. Friction factor = 0.20.
		1020	10,200	SAE Grade 5	
		1260	12,600	SAE Grade 7	
		1440	14,400	SAE Grade 8	
		495	6,600	SAE Grade 2	Lubricated. Torque to produce 75% of proof load. Friction factor = 0.15.
		764	10,200	SAE Grade 5	
		944	12,600	SAE Grade 7	
		1080	14,400	SAE Grade 8	
7	Thor Power Tool Co., Fastener Tension & Torque Manual	505	5,800	SAE Grade 2	Unlubricated; torque to produce 75% of proof load. Coef. friction = 0.135
		781	8,960	SAE Grade 5	
		1100	112,700	SAE Grade 8	
		404	5,800	SAE Grade 2	Lubricated; torque to produce 75% of proof load. Coef. friction = 0.108
		625	8,960	SAE Grade 5	
		882	12,700	SAE Grade 8	
8	Almay Research & Testing Corp. "Development of Technology for Installation of Mechanical Fasteners," NAS 8-20779, N71-26568, 1971.	2040 Nut	23,000	MS 21250 (Min. UTS 180,000 psi)	Cadmium plated, unlubricated; torque to produce 90% of tensile yield by Johnson's 2/3 method
		2400 Head	23,000		
		1920 Nut	23,000	MS 21250	Cadmium plated, dry film lubricated; torque to produce 90% of tensile yield by Johnson's 2/3 method.
		2280 Head	23,000		
		1400 Nut 1500 Head	16,000	NAS 1108 (Min. Ult. Tens. 160,000 psi)	Cadmium plated, dry film lubricated; torque to produce 90% of tensile yield by Johnson's 2/3 method.

TABLE IV
STEEL BOLT MECHANICAL PROPERTIES

Designation	100% Proof Load Stress, psi	Min. Yield Stress, psi	Min. Ult. Tens. Stress, psi	65% of Tensile Yield
SAE Grade 2	55,000	57,000*	74,000	37,050*
SAE Grade 5	85,000	92,000*	120,000	59,800*
SAE Grade 7	105,000	115,000	133,000	74,750*
125,000 psi Min. UTS	---	---	125,000	---
SAE Grade 8	120,000	130,000*	150,000	84,500*
160,000 psi Min. UTS		142,000**	160,000	92,300**
180,000 psi Min. UTS		150,000**	180,000	97,500**

* Determined from 0.2% offset method

** Determined from Johnson's 2/3 method

are based on a percentage of proof load and others are based on various percentages of the yield stress as determined by different methods. The proof load is defined by the SAE as "...a specified load which the product must withstand without permanent set." Practically, the proof load is computed as a fraction of the yield stress.

In order to compare the torque/tension results on a more uniform basis, all of the torque values for Items 6 through 8 in Table III have been recalculated to the extent possible on the basis of 65% of yield stress, the criterion applied in Item 5. These are shown in Table V. Even so, Table V still reveals considerable variation in torque for bolts of comparable strength.

The torque data in Item 5 of Table V are the same as those in Item 5 of Table III since the recalculated results will be compared to these data. The basis for determining the torque in Item 5 is not given, other than to note that the torque is that necessary to produce a preload stress equal to 65% of the yield stress as found by the Johnson 2/3 method.

It is proper to note at this point that of the eight references cited in Table III, only Items 6, 7 and 8 give the preload as well as the torque. Yet it is the preload that is important in joint integrity; the torque is merely a means to estimate the preload, and it may be a poor one indeed.

The preload as well as the torque to produce the preload is given in Item 6. The preload was determined in that reference from the following equation:

$$P = \sigma \times A_r \times p \qquad (1)$$

where
P = preload, lb.
σ = allowable tensile stress level, psi
A_r = thread stress area*, in.^{2}
p = percentage fraction stress

For example, referring back to Table III, the preload for a Grade 5 bolt was computed from

$$P = 85,000 \times 0.1599 \times 0.75$$
$$= 10,200 \text{ lb.}$$

Here, the 85,000 psi is the 100% proof load stress(8) from Table IV and 0.1599 in.^{2} is the stress area for a 1/2-20 UNF thread. The preload is to be 75% of the maximum proof load, hence the 0.75 in Equation (1).

---

* Stress area is based on a diameter which is the mean of the pitch and minor diameters.

TABLE V

NORMALIZED TORQUES AND PRELOADS FOR 1/2-20UNF STEEL BOLTS

Item from Table I	Reference	Torque in.-lb.	Preload lb.	Strength	Basis for Preload
5	NASA Std. Torque Limits for Threaded Fasteners, MSFC-STD-486, Amend. 1, 14 July 1970	420		SAE Grade 2	Cadmium plated, unlubricated; torque to produce 65% of tensile yield by Johnson's 2/3 method.
		610		SAE Grade 5	
		690		Min. UTS 125,000	
		905		SAE Grade 8	
		950		Min. UTS 160,000	
		1260		Min. UTS 180,000	
		315		SAE Grade 2	Plated or unplated, lubricated; torque to produce 65% of tensile yield by Johnson's 2/3 method
		540		SAE Grade 5	
		576		Min. UTS 125,000	
		790		SAE Grade 8	
		830		Min. UTS 160,000	
		940		Min. UTS 180,000	
6	Machine Design, Reference Issue, Vol. 41, 11 Sept. 1969	592	5920	SAE Grade 2	Unlubricated; torque to produce 65% of min. tensile yield by 0.2% offset method. Friction factor = 0.20.
		957	9560	SAE Grade 5	
		1200	12000	SAE Grade 7	
		1350	13500	SAE Grade 8	
		444	5920	SAE Grade 2	Lubricated; torque to produce 65% of min. tensile yield by 0.2% offset method. Friction factor = 0.15.
		718	9560	SAE Grade 5	
		900	12000	SAE Grade 7	
		1010	13500	SAE Grade 8	
7	Thor Power Tool Co., Fastener Tension and Torque Manual	454	5210	SAE Grade 2	Unlubricated; torque to produce 65% of min. tensile yield by 0.2% offset method. Coef. fric.= 0.135
		733	8400	SAE Grade 5	
		1035	11900	SAE Grade 8	
		363	5210	SAE Grade 2	Lubricated; torque to produce 65% of min. tensile yield by 0.2% offset method. Coef. fric.= 0.108
		586	8400	SAE Grade 5	
		828	11900	SAE Grade 8	

ORIGINAL PAGE IS
OF POOR QUALITY

TABLE V (con't.)

Item from Table I	Reference	Torque in.-lb.	Preload lb.	Strength	Basis for Preload
8	Almay Research & Testing Corp., "Development of Technology for Installation of Mechanical Fasteners," NAS 8-20779, N71-26568, 1971	1380 Nut 1630 Head	15,600 15,600	MS21250 (Min. UTS 180,000 psi)	Cadmium plated, unlubricated; torque to produce 65% of tensile yield by Johnson's 2/3 method.
		1300 Nut 1550 Head	15,600 15,600		Cadmium plated, dry film lubricated; torque to produce 65% of tensile yield by Johnson's 2/3 method.
		1010 Nut 1080 Head	11,500 11,500	NAS 1108 (Min. UTS 160,000 psi)	Cadmium plated, dry film lubricated; torque to produce 65% of tensile yield by Johnson's 2/3 method.

In Table V the 85,000 psi proof load stress has been replaced by the minimum yield stress of 92,000 psi(8) and the 0.75 has been replaced by 0.65 for a 65% fraction stress level. The yield stress of 92,000 psi is determined at 0.2% offset since the yield according to the Johnson's 2/3 rule was not known.

The torque to produce this preload in Item 6 was determined, in that reference, from the following equation:

$$T = KDP \tag{2}$$

where
T = torque, in.-lb.
K = torque-friction coefficient; 0.20 for dry, 0.15 for lubed threads
D = nominal bolt diameter, in.
P = preload, lb.

This is an empirical equation where the coefficient K relates the torque and the preload. The revised torque values in Item 6 are about 50% higher than those for equivalent bolt grades in Item 5, in spite of their both using preloads computed on a similar basis.

The preloads are given in Item 7 but they are less than those specified in Item 6. The preloads in Item 7 are determined such that the maximum stress due to the combination of tension and shear (from the torquing action) is 65% of the minimum tensile yield stress. It will be remembered that the preload in Item 6 was obtained from a consideration of the direct tensile loading only, ignoring the effect of the simultaneous shear.

The relationship between torque and preload in Item 7 is a theoretical one taking into account thread friction, the thread angle and lead angle, and the tension in the bolt. The computed values are less than those cited in Item 6. Interestingly enough, the recommended torque values from Item 7 are very nearly the same as those in Item 5 for which no preload values were given and for which no method for determination of the torque was cited.

Because of the choice of materials and bolt grades, it is only possible to compare directly Item 8 with Item 5, at 160,000 psi and 180,000 psi ultimate tensile strength. The recommended torque values in Item 8 are higher than those in Item 5. Further, values are different when torque is applied to the head as compared to the nut of the fastener. This is a unique differentiation in torque tables, although Item 4 states that the listed torque values are applicable for either nut or bolt head tightening. Presumably, in the absence of specific admonition, this is true of the other torque standards described.

The torque and preload values in Item 8 were experimentally determined. The preload in Table I is defined by use of the following equation:

$$P = \frac{BYS}{BTS} \times MTL \times 0.9 \qquad (3)$$

where

P = preload, lb.

BYS/BTS = ratio of test yield stress to test ultimate tensile stress

MTL = minimum recommended bolt load, lb.

$= \sigma_{ult} \times A$

σ_{ult} = minimum ultimate tensile strength, psi

A = area

Because Item 8 is devoted exclusively to military and aerospace standard fasteners covered by MIL-STDs, the MTL are maximum loads called for in the standards.

If the relationship for MTL is substituted into Equation (3), and if the experimental ultimate tensile stress is equal to the minimum ultimate tensile strength, the result is

$$P = BYS \times A \times 0.9 \qquad (4)$$

which is similar to Equation (1).

The values of the preload for Item 8 in Table V were obtained from Equation (3) by using 0.65 as the percentage fraction stress instead of 0.9, and, in the case of the 180,000 psi material, correcting the value of MTL to reflect a load based on the stress area A_r instead of the basic pitch diameter as is done in the procurement military standard.* No basis for the determination of the minimum recommended bolt load for the 160,000 psi material was given in the procurement standard** so that in this case the only correction to be applied to the preload values of Table III to obtain those in Table V is that of using 0.65 instead of 0.9.

---

*Bolt, Tensile, Steel, 180KSI Ftu, 450°F, External Wrenching, Flanged Head, MIL-B-8831A, 28 January 1972.

**Bolt, Shear-Hexagon Head Modified, Short Thread, NAS 1103-1120, 31 January 1975

The torque values corresponding to the preload values were found experimentally by measuring the torque needed to achieve the desired preload as calculated by Equation (3). Representative torque-tension curves are practically linear in the areas of interest(3) so that the torque values given in Table V for Item 8 represent a reduction from those values in Table III proportional to the reduction in preloads.

In spite of all of the corrections applied to Item 8, the recommended torque values are still higher than those of Item 5. The difference probably lies in the elusive friction between threads and between the turning element (nut or head) and the contact surface, usually a washer. Item 6 points out in several instances the variable effect of friction and attempts to be specific regarding the thread conditions (plating type, lubricant type, etc.) and the turning element contact surface (washer hardness, etc.) when recommending the torque required to achieve a given preload.

Summary of Torque-Tension Standards

A considerable degree of variation exists in tables of recommended torque for similar grades of steel bolts. Part of the variation is due to differences in the preload criteria, and part is due to differences in the assumed friction between threads and bearing surfaces. Other factors may be the degree of care exercised in the collection and interpretation of experimental data, and the application or lack of application of a statistical approach to the data.

There are large variations in the pertinent material properties of fasteners, including yield stress. While the torque values recommended by almost any of the cited references are so conservative that they will always provide a secure joint without overtorquing, the data presented in Table III and as revised in Table V suggest strongly that for critical joints an experimental program using samples of the intended fasteners should be performed prior to making specific torque recommendations.

Since torque measurement is relatively easy and affords an inexpensive method for achieving useful bolt preloads, it is not likely to be eliminated in industry or military applications in the foreseeable future. Of considerable value, therefore, would be torque data statistically related to mean and standard deviation of preloads. This would enable a designer to evaluate the potential integrity of his joint design over the long term, in an accepted statistical manner. Reliability calculations could then be performed, and predictions made based on these calculations.

IV. REVIEW OF JOINT TENSIONING TECHNIQUES

General Considerations in Joint Tensioning

The previous chapter described the variation in recommended torques for bolts of similar grades of material necessary to achieve a certain preload. Because of material variability itself, even the application of a given torque to several bolts within an installation will result in a considerable spread in the preload. Because of these variations in preload for a given torque, the torque levels are designed to give an average preload of only a fraction of that which could be safely achieved.

The recommended torque must be such that the probable maximum preload will not exceed the bolt yield; yet the minimum expected preload is too low for an efficient joint. It has been shown experimentally(6) that even with a torque wrench exhibiting torque reading scatter of only ±10%, the corresponding scatter in tension for a series of tests on a group of steel bolts ranged from about 3,400 lb. to 5,400 lb. at an average of 4,400 lb., or 73% of yield stress. Using one of the forms of tension control described later in this section, it was possible to reduce the three standard-deviation scatter from 5,000 to 5,600 lb. at an average of about 5,300 lb. or 87% of yield. The implication is clear. If the tension scatter can be reduced, it is possible, on the average, to achieve preloads which utilize a greater percentage of the capacity of the bolt without occasionally exceeding the capacity. In Table III in the previous section, the recommended torques were those required to give a preload of about 65% of the yield stress (the exception was Item 8 which represents careful laboratory work and may not be representative of industrial capabilities). Using various types of load control, preload values as high as 80% of yield are recommended by various manufacturers.

In recognition of the problem of tension scatter using a torque-only method, and appreciating that torque is only a means to obtaining the preload, considerable effort has been devoted to means other than through torque measurement to determine preload. Some of these commercially available methods, not necessarily in any significant order, are discussed on the following pages. The listing is only representative, and not all-inclusive. The devices are listed in Table VI (see Page 34).

Strain-Gage Bolts

Bolts containing foil-type strain gages cemented to the walls of a centrally drilled hole in the bolt shank offer a direct means for determining the preload at the time of initial application as well as later. The drilled hole is confined to the unthreaded shank area of the bolt and is sized such that the remaining solid area is not less than the thread root area.

The strain gages may be obtained in three configurations. A quarter-bridge consists of two gages wired in series, located 180° apart on the hole circumference. There are three external leads, including a separate ground lead. The arrangement compensates for bending and torque, but it does require an external bridge completion circuit.

The double quarter-bridge also uses two gages located 180° apart, but they are not wired together and have four external leads. The signal from this arrangement may be twice that of the quarter bridge. Again, an external bridge completion circuit is needed. Finally, a full bridge circuit is available using four gages and having four external leads.

Connections to the bolt may be made through a separable connector, soldered wire connector, or a factory installed permanently affixed connector.

Strain gage bolts are available in size #10 up to 1-1/2 inches, in SAE Grade 8 material having a minimum ultimate tensile strength of 150,000 psi. Other materials and sizes are available on a custom installation basis. The bolts may be gaged for use at temperatures to 150F or to 300F.

The recommended preload for these bolts is based on 70% of the yield stress which for a 1/2-20 UNF SAE Grade 8 bolt is 13,200 lb. Claimed accuracy is within 1% of the desired load. Each bolt comes with its own calibration certification.

Basic price for a 1/2-20 UNF Grade 8 bolt with a quarter bridge, solder type connector, rated 150F operation, is $72. The same bolt with a full bridge, for 300F operation, with a separable connector is $177.

Preload Indicating Washers

A relatively simple device for indicating the attainment of a given preload consists of two concentric rings or cylinders of slightly different heights sandwiched between two face washers. This assembly may be placed under the bolt head or under the nut. As load is applied, the taller of the two concentric rings is loaded by the face washers into the plastic regime, to a point such that the outer, shorter, concentric ring just makes contact with the face washers and cannot be turned by hand. At this condition the calibrated preload has been achieved. Care must be taken to avoid overtightening. Normally, the washers are sized to give a preload equal to 80% of yield strength although other preloads may be designated. Preload accuracy is claimed to be ±10% of designed value. If the preload subsequently releases, the inner ring, because it was stressed plastically, will not return to its former size. Then the outer ring once more becomes loose and indicates loss of preload.

The load indicating washers have three main drawbacks: they cannot be reused; they must be used for the specific preload for which they have been designed, and they add length and weight to the bolted assembly.

Preload indicating washers come in standard sizes from #10 to 1-1/2 inch, calibrated to produce a preload of 80% of tensile yield. Standard material is alloy steel for the concentric rings and carbon steel for the face washers. Other materials may be used if desirable.

Prices vary according to size and quantity. For example, washers for 1/2 inch bolts in the 160,000 or 180,000 psi ultimate tensile strength category are priced at $182/hundred in lots of 100 and $110/hundred in lots of 1,000.

Visual Indicators

A unique preload indicating system consists of a colored insert placed in a cavity in the head and a portion of the shank of a bolt. The insert contains a proprietary material, probably from the family of liquid crystals, which changes color when strain is applied to the bolt. When the color changes to match that of a ring surrounding the insert, the bolt tension is at the designed value. Studies have shown that over a wide spectrum of observers of various ages, background, education, etc., the ability to properly color match is excellent. Actual figures are not available however.

These load indicating bolts have two drawbacks. They must be used for the specific preload for which they were designed, and the physical size of the insert reduces the strength of the bolt below the value normal for the size and grade. This latter problem is compensated by using the next higher grade bolt for the application. For example, if a Grade 5 bolt is called for, a Grade 7 bolt, derated by the installation of the visual indicator, might provide the equivalent strength of the Grade 5 bolt.

The system is adaptable to any bolt material. Applications for steel bolts are normally limited to Grades 5 and 8 or better. Operating temperatures can range from -20 to +225°F. Bolts incorporating the visual system are not available from stock since each application is unique. Each bolt is checked prior to shipment at the designed load for color matching using photocells.

The costs for this system vary with the application but normally add about $1 to the cost of the bolt for Grades 5 and 8 steel bolts.

Direct Tensioning

The ultimate reason for torquing a nut on a bolt or stud is to apply preload to the bolt. A very direct method has been developed whereby a specially designed device applies tension to the threaded end of a bolt or to a stud to achieve a desired stretch and preload. The nut is then snugged, the tensioning device removed, and the joint is preloaded.

The tension is applied hydraulically through a cylinder and piston arrangement screwed to the threads extending beyond the nut. The system is obviously not applicable to tightening through the bolt head. Once the tension is applied, a handwheel turns the nut socket until the nut is firmly seated, without hard torquing. Once this has been achieved, the hydraulic pressure is released, the unit is removed, and the bolt is preloaded. Compensation for some small amount of tension relaxation after removal of the tensioner must be made.

This system is custom designed and built, no "standard" or off-the-shelf units are available. Units have been designed to handle stud diameters from 5/16 inch to over 12 inches, with loadings from 100 lb. to over 7 million lbs. For best results on multi-bolt connections, such as large pipe and pressure vessel flanges, 3 or 4 units are used simultaneously.

Some representative costs for simple, straight forward applications, are from $1,500 to $1,600 each in sets of 4 units in the 1/2-inch bolt size. Single units are priced in this size from about $2,200 each. Larger sizes and complex installations are higher priced. The hydraulic loading system is extra.

Torque-Tension Systems

Several systems have been developed in the past few years that are capable of torquing a fastener to the yield range, and at assembly line speeds. It has been recognized for a long time that the most efficient use of a bolt is achieved when the preload stress is just into the yield range. Under these conditions the bolt has slightly stretched and is providing the greatest safe clamping force.

The problem, of course, is to turn the nut and stretch the bolt into that yield range without either fracturing the bolt, in the case of high strength materials which exhibit poorly defined yield points, or exceeding the yield range into plastic deformation. It was pointed out in an earlier section that relating torque to preload is not a highly accurate method of measuring stress, and one is as likely to stretch the bolt too much as to achieve insufficient preload for the same torque reading.

Through the use of sophisticated electronic systems it has become possible to rapidly sense changes in torque during the tightening operation such that the wrench can be stopped close to the threshold of yield. In general, two different systems are used and these are described in the following sections.

Torque Versus Angle

There are two principal manufacturers of this type of system in this country and the following is a composite description of the operation.

This method in effect notes the change in torque for equal increments of nut rotation, and when the torque differential decreases a predetermined amount for a given increment of nut movement, the system stops. The drive mechanism is air operated and electronically controlled.

Figure 2 plots nut torque vs. rotation angle. The system runs down the nut to the snug condition at A before being activated. This action clamps the parts. From this point on, the slope of the torque curve increases until point B is reached, after which the torque slope decreases as the bolt is stressed into the elastic range. The change in slope is compared to the maximum slope achieved at B and the system cuts off at a predetermined value of slope change. Upper and lower limits to both torque and angle may be set into the system so as to provide an acceptance "window". Light signals may be utilized in production line applications to signal joints that are out of specifications.

The preload level obtained under various joint conditions is approximately equal to the bolt proof load or about 70 to 80% of the actual ultimate tensile strength. A ±3 standard deviation scatter of the preload falls within ±10% of the mean for a sample of high grade bolts, with lower grades showing more scatter.

This system is available in single and multiple spindle units. The capacity of fixed single spindles is about 400-500 ft-lb and with torque multipliers, the torque capacity may be extended beyond this. Hand-held portable angle-drive units have been used to 300 ft-lb, but unless special safety precautions are taken, the maximum capacity is about 85 ft-lb. One manufacturer does not produce a hand-held portable drive because he feels adequate control over the tightening cannot be achieved with such units.

Depending on the manufacturer, various degrees of flexibility are available in the capacity of the fixtured multiple spindle units. One manufacturer claims his system will tighten several sizes of fasteners, or various grades of fasteners simultaneously, each spindle being controlled separately yet linked together such that the final tightening is achieved by all bolts at the same time. He claims his system will sense any abnormal condition and

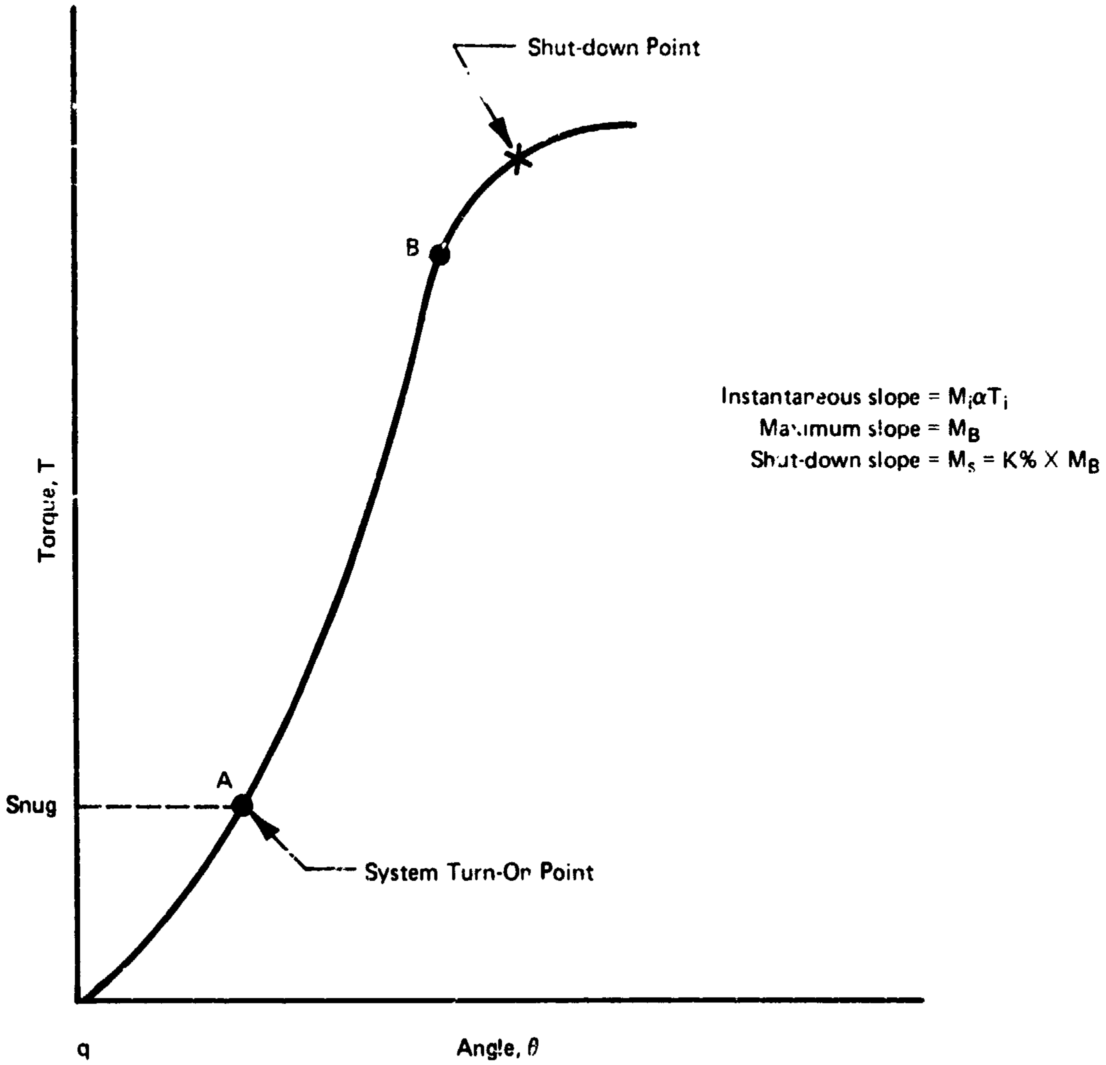

Fig. 2. Torque vs. Fastener Rotation Curve

4522

will refuse to act on that fastener, thus avoiding bolt breakage. Approximate cost for this complete system ranges from $12,000 to $14,000/spindle. The system may be purchased, leased or lease-purchased.

A second manufacturer sells the units only and the complete cost is approximately $5,000/spindle.

Torque Versus Time

This system, once the nut has been snugged, applies timed pulses of ever-increasing torque to the nut until the torque increase drops off a predetermined amount, at which time the system shuts off. The system is air driven and electronically controlled.

Figure 3 illustrates typical system behavior. The nut is rapidly run down to point A at which point the system moves into the pulse mode. Timed torque pulses are applied to the nut setter and the resulting torque is measured by the built-in transducer. Each torque pulse is greater than the one preceding it, as for example at B_1 and B_2. As the pulse occurs, the peak signal is examined to determine whether the torque is increasing, within the specified time interval, at or above the desired rate, such as C. If the applied torque does not increase at the desired minimum rate during the timed pulse cycle, such as at D, the system shuts off, as at E. In Figure 3, the upper horizontal line represents a maximum torque at which the system will stop if yield has not already occurred.

Actual tests on a sample of bolts (1/2-20 UNF) of 180,000 psi minimum ultimate tensile strength using this system resulted in a ±3 standard deviation scatter or ±11% of the mean. The manufacturer claims that this figure can be bettered.

This system is available in single and multiple spindle units. The multiple units, designed for a single size and grade of bolt, operate with selective restraining action in such a manner that all bolts are brought to the tight condition simultaneously.

Spindle capacity is nominally 550 ft.-lb. in both the multiple spindles and the hand-held portable angle-drive unit. The hand-held spindles require special safety precautions at the higher torques.

Costs are dependent upon size and spindle arrangement. Costs for single spindle hand-held units range from $3,800 to $5,000. Multiple spindle units range from $4,500 to $7,000 per spindle, complete.

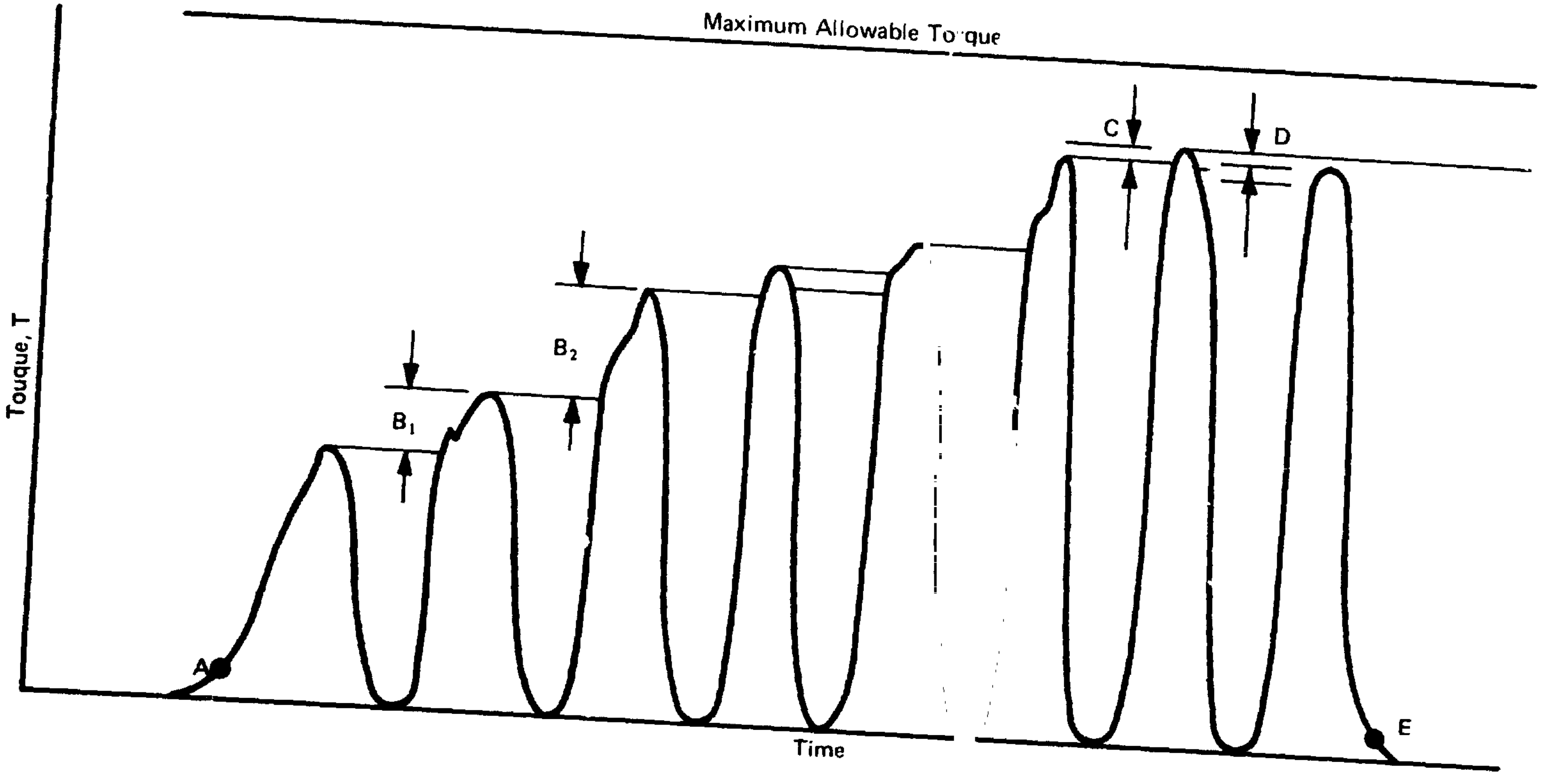

FIGURE 3. TYPICAL RESPONSE OF "TIMED TORQUE" SYSTEM IN WHICH INCREASING FORCE PULSES ARE APPLIED UNTIL TORQUE NO LONGER INCREASES AS AT "D".

Ultrasonic Length Measurement

Bolt elongation in the elastic range may be directly related to the bolt load. A commercial system has been developed and is available which measures the round-trip time of an ultrasonic pulse through the bolt length and determines the change in length as the bolt is torqued, to an accuracy of ±0.0001 inch, the limit of resolution of the readout equipment.

The ultrasound is generated by a piezoelectric transducer, operating at a nominal frequency of 5 MHz, coupled to the bolt head by a magnetic holding device. A thin film of oil is used as a couplant.

From limited data it appears that at strains of 0.0030 in./in. the accuracy of strain (elongation) measurement is within 3%. At smaller values of strain the accuracy is less, but for high strength aerospace quality steel fasteners, strains much less than 0.0030 in./in. are not of great interest. No data are available which correlate actual preload (stress) to the measured strain.

This system is described in greater detail in a following section of this report, devoted to the evaluation of NDE approaches to determination of fastener integrity.

The cost of the instrument is in the range of $7,500.

An Idea that Failed

Often the simplest, most direct means to a goal is the best. Unfortunately, this is not a universal truth. A case in point, typical of dozens of patented tension control devices, involves a preload-indicating bolt containing an unstressed rod passing through a central hole in the bolt and fixed at one end by an interference fit. The other end of the rod protruded past the bolt head surface by a few thousands of an inch. When the bolt was tightened it stretched, but the unstressed rod did not. When the rod and bolt head surface were flush, the designed preload had been achieved. Subsequent tension relaxation was evident by the protrusion of the rod tip above the head.

High costs associated with production, quality control and limited market led to this type of fastener being discontinued by two manufacturers.

Summary of Tensioning Systems

The salient features of the previously described bolt tensioning systems are summarized in Tables VI and VII. Table VI covers those systems that are capable of applying a given tension initially, and Table VII covers those capable of indicating post-application tension as well as applying the initial tension. Within each table the systems are separated into those that require special bolts and those that are largely applicable to any bolt.

Each system, noted in the first four items in Table VI, while achieving basically the same thing, i.e., tension control instead of torque control, possess different advantages and disadvantages as well as cost. Item 1 can be used with the very largest pressure vessel fasteners, while Items 2 through 4 are applicable to production lines processing thousands of smaller bolts per hour.

For purposes of comparison, Items 5 and 6 have been included to describe briefly the predecessors to the torque tension systems. The torque-turn system may be considered one degree less sophisticated than the torque-tension systems, and the torque only with feedback is one degree less sophisticated than the torque-turn system.

The torque-turn system runs the nut down quickly to a snug condition at a specified threshold torque. Then, utilizing a slow speed motor, the nut is turned a predetermined number of degrees to achieve the final tightness. Unfortunately, poorly machined or ill-fitting parts can cause the system to achieve threshold torque prior to achieving a snug joint, after which the turn of the nut does not result in a properly tightened joint. For well machined surfaces and properly threaded fasteners, the torque-turn system can approach the results of the torque-tension system.

The torque system with feedback represents one degree less sophistication than the torque-turn system. It still uses torque as the basis for achieving tension, but, by the use of feedback to a very fast acting air shut-off valve, exercises better control over the motor that applies the torque. Tension is still subject to a ±20% variation.

Figure 4, abstracted from Reference 7, provides an excellent example of the differences in tightening provided by the torque-only, torque-turn, and torque-tension systems. Because the torque-only method has such a wide scatter in tension, the maximum allowable tension is derated to prevent over-tightening. The torque-tension system, with its more precise control of the tightening parameters, brings the tension to the initial yield point. The torque-turn method requires the turn of the nut to be great enough to compensate for variations in the bolt strength and joint compression stiffness. This in turn may lead to large bolt deformations, well into the yield region.

The systems summarized in Table VII are specialized and represent various degrees of complexity in use. The strain gaged bolts offer the most flexibility of use inasmuch as the actual tension attained is measured. On the other hand, this flexibility is costly not only for the fastener, but also for the electronic measuring equipment needed. Post-tension determination is absolute, but does require the use of complex electronic equipment. The bolts are reusable to the extent that reuse may be practiced with highly stressed bolts(1, 3).

4524

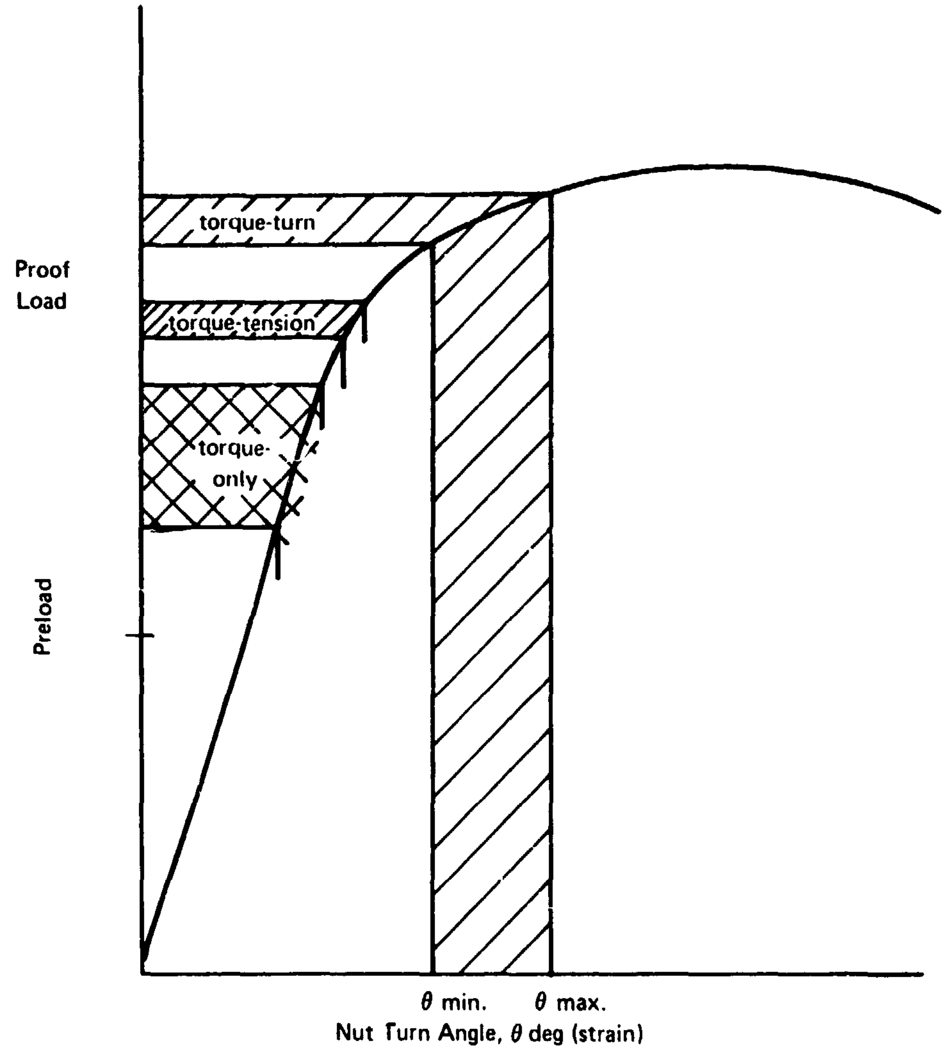
torque-turn
Proof Load
torque-tension
torque-only
Preload
θ min.
θ max.
Nut Turn Angle, θ deg (strain)

Fig. 4. Comparison of Preload by Three Tightening Systems

The load indicating washers are much cheaper than the strain gaged bolts, but they are only useful at their designed load, can give a relative measure only of post-tension, are not reusable, and add weight to the installation. A variety of types are available, several of which are shown in Figure 5.

Even less expensive than the washers are the visual indicator bolts but these again are useful only at their design load. Also, the initial cost is somewhat deceptive since a better grade of bolt is needed to make up for the derating effect of the indicator. Post tension is only relative. The current saying "what you see is what you get" appears to apply to a choice of these post-tension systems.

The ultrasonic system is too new to accurately compare with these other systems from a cost standpoint. The system is applicable to standard bolts but appears complex in use. It further requires the generation and retention of paper work to allow for post-tension comparisons, if indeed it is applicable to this inspection application at all.

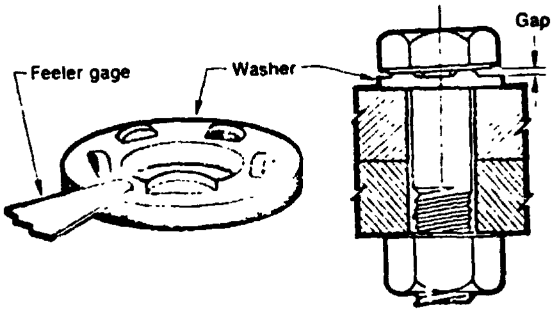
Gap
Feeler gage
Washer

a. Depressed Dimple (left)

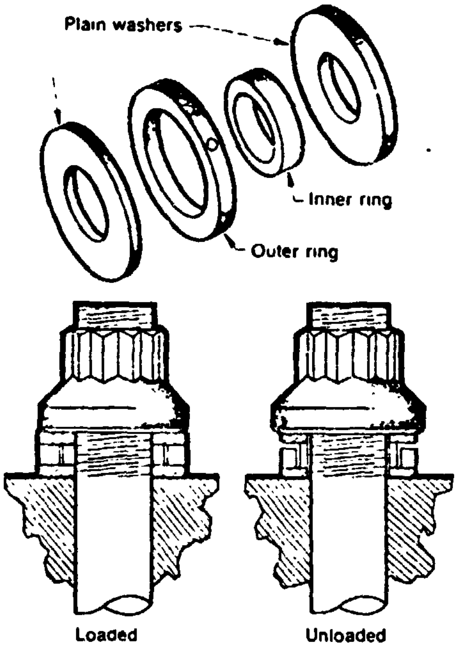
Plain washers
Inner ring
Outer ring
Loaded
Unloaded

4525

b. Dual Washer (right)

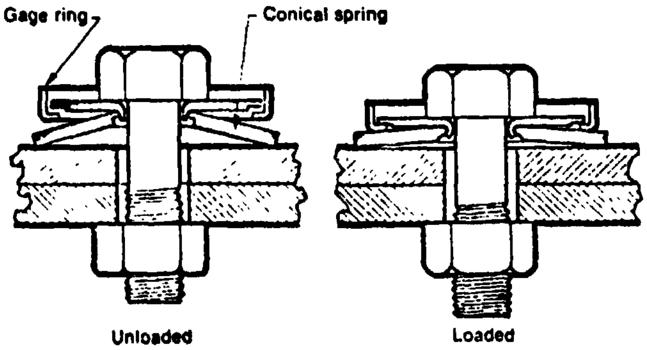
Gage ring
Conical spring
Unloaded
Loaded

c. Spinning Ring (left)

FIGURE 5. MISCELLANEOUS COMMERCIALLY AVAILABLE WASHER-TYPE PRE-LOAD INDICATORS (Machine Design V49, No. 20, Sept. 8, 1977)

TABLE VI. PRELOADING DEVICES AND SYSTEMS

Item	Type	Sizes	Material	Features	Cost	Mfg. Code	Claimed Tension Accuracy	Capacity
1	Tensioner	5/16 to 12 in. bolts and studs; other sizes can be accommodated.	Can be designed to handle bolts of any material.	No std. units; not applicable to mass production-line use. Only applicable to studs or nut end of bolt.	1/2 in. bolt size about $2200. ea.; $1500 in groups of 4, exclusive of hydraulic system. System cost would be amortized over no. of bolts tensioned.	D	±2% of desired tension	Usually designed for 65% yield.
2	Torque-tension; torque vs. angle of twist	Up to 6000 in. -lb. of torque in 2-speed spindles; higher capacity in single speed spindles. About 7/8 in. bolt.	Any material for which stress and strain relationship is known.	Portable single spindle angle units and multiple spindle units. Multiple units can simultaneously handle different sizes and materials; production line capability; spindles selectively shut-off for damaged fastener. Electronic read-out, signals, etc.	$12,000 - $14,000 per spindle; lease, purchase lease-purchase. Does not include air system.	E	±10% of desired tension	70 to 80% of ultimate strength
3	Torque-tension; torque vs. angle of twist	Up to 6000 in. -lb. of torque in 2-speed multiple spindles; about 7/8 in. bolt.	Any material for which stress/strain relationship is known.	No hand-held portable units; most applications multiple spindle; production line capability.	$5000/spindle; purchase only; cost does not include air system.	F	±10% of desired tension	70 to 80% of ultimate strength
4	Torque-tension; torque vs. time	Up to 6600 in. -lb. of torque;about 7/8 in. bolt.	Any material for which stress/strain relationship is known.	Hand-held single-spindle portable units & multiple spindle units; multiple units average out torques during tightening operation; production line capability.	$3800 - $7000/spindle; cost does not include air system.	G	±11% of desired tension	70 to 80% of ultimate strength
5	Torque-turn; with monitoring.	60 to 7200 in. -lb. capacity.	Any fastener application; most effective w/matls. having long flat yield region.	Mostly multiple spindle; production line capacity; largely ignores effect of friction in fastener; can achieve higher preloads with safety than Item 6.	$4600/spindle in multiple spindle systems; does not include air system	E F G		
6	Torque; feedback control with monitoring.	60 to 7200 in. -lb. capacity.	Any fastener application.	Mostly multiple spindle; production line capacity; fast response driven shut-off valves. Based on torque as measure of tension.	$4200/spindle in multiples of 5-6 spindles; does not include air system	E F G	±5% of set torque	Usually 75% of proof load

ORIGINAL PAGE IS
OF POOR QUALITY

TABLE VII. POST TENSION DEVICES AND SYSTEMS

Item	Type	Sizes	Material	Features	Cost	Mfg. Code	Claimed Tension Accuracy	Capacity
1	Strain Gaged Bolts	#10 to 1-1/2 in. std.	SAE Grade 8 std.	Available for service to 300°F. Various connectors & bridge styles. Must keep records of readings to determine post tension. Reusable.	From $72 to $177. for 1/2-20 UNF depending on temperature capability, connector type and bridge style.	A	±1% of indicated load	70% of yield
2	Load indicating washers (various types which deform & indicate proper preload by position)	#10 to 1-1/2 in. std.	Steel, standard. Other as desired.	Caution to prevent overstressing. Relative indication of post tension; not reusable: may be used with any type bolt.	From $1.82 to $1.10 for 1/2 in. depending on quantity	B	±10% of design value	80% of yield
3	Visual indicators	Minimum size unknown	Bolt of any material may be used.	Temp. range -20 to +225°F. Unuseable at other than design load. Bolt strength derated; each application uses next higher grade bolt. No stock sizes or materials. Reusable.	Adds about $1 to cost of Grades 5 & 8 steel bolts	C	Unknown	75% of yield
4	Ultrasonic length measure device	Probably any size	Steel only; applicability to other materials unknown	Very new; limited use to date. Requires records to determine post-tension.	Unknown. System cost would be amortized over no. of bolts checked.	H	±3% probably	Any desired; based on elongation

Legend for Manufacturer's Code:

A - Strainsert
Union Hill Industrial Park
West Conshohocken, Pennsylvania 19428

B - PLI Washers
Standard Pressed Steel
Aerospace Products Division
Jenkintown, Pennsylvania 19046

C - Tell-Torq
Modulus Corporation
1000 Modulus Road
Mount Pleasant, Pennsylvania 15666

D - Biach Steel Tensioners
Torque and Tension Equipment, Inc.
1624 Dell Avenue
Campbell, California 95008

E - Joint Control System
SPS Special Products
A Division of Standard Pressed Steel Co.
135 Commerce Drive
Ft. Washington, Pennsylvania 190[illegible]

F - Ingersol-Rand Company
Automatic Production Systems
23400 Halstead Road
Farmington Hills, Michigan 48024

G - Par II and Comp-Par
Thor Power Tool Company
Stewart Warren Companies
175 North State Street
Aurora, Illinois 60507

H - Douglas-Erdman Ultrasonic Preloader
Torque and Tension Equipment, Inc.
1624 Dell Avenue
Campbell, California 95008

ORIGINAL PAGE IS
OF POOR QUALITY

V. POTENTIAL NEW APPROACHES TO TENSION CONTROL

It can be seen from the preceding chapters that the determination of fastener integrity is limited in several regards. First, the present standard for preload indication is installation torque, and torque is less than ideal as an accurate measurement parameter. Second, the recommended torque values specified by various standards are generally so conservative, because of the variability of torque measurement, as to impose a weight penalty on most designs; and third, direct methods of tension control, such as special bolts, washers, etc., are expensive and add weight, complexity and cost. These limitations are not based on any uncertainty in the theory, since it is well known that for a given material, correct fastener preload is both critical and sufficient to the success of a properly designed joint. Consequently, lack of a convenient means of direct measurement of preload is responsible for many of the limitations on fastener applications.

Even more serious, perhaps, is the lack of methods which can inspect the condition of a fastener at a later time. Such highly desirable, routine examination is an excellent candidate for nondestructive evaluation (NDE). The inspection of a structure for improperly tensioned bolts may be equally critical to its operation as the discovery of fatigue cracks or other flaws. Since NDE implies the determination of the condition of a component before failure, the evaluation of a fastened joint should be amenable to NDE methods.

During the accomplishment of this program, an extensive review of the NDE literature, including the patent literature, was performed in a search for methods showing promise for the determination of fastener integrity.

Parameters of Interest

In order to apply NDE methods to fasteners, inspection parameters must be defined and characterized. A number of factors may affect the performance of a finished bolted joint, but the basic parameter is the clamping force. It has been shown in the previous chapters that clamping force during the life of the joint is directly related to the initial preload. This preload is defined as the tensile stress in the shank of the fastener at the time of installation. Assuming a fastener of known material properties, proper tensile stress in the shank is sufficient to insure its integrity, regardless of the torque applied to produce the stress. Thus the two most significant factors are (1) the fastener material and (2) the shank stress. High-quality threaded fasteners are generally well controlled, and their properties held within close tolerances. If the proper bolt is selected, then the significant NDE parameter is the tensile stress in the shank, and those methods capable of determining stress become the techniques of importance.

An extensive literature is devoted to the nondestructive measurement of stress. Vary(9) in a compendium of current NDE methods, lists a total of seventy basic NDE techniques, of which 26 are related to the measurement of stress. Many of these are not suitable for the application to fasteners, but of this list, 14 were selected as worthy of further investigation.

Evaluation Procedure

An extensive literature search was performed through the Nondestructive Testing Information Analysis Center (NTIAC) operated by Southwest Research Institute for the Department of Defense. Titles of direct relevance to fastener inspection, fastener preload and clamping force, as well as those related to stress measurement in general, were reviewed. The principal data files utilized in the search included the National Technical Information Service File (NTIS), Physics Abstracts, Engineering Index, the NTIAC file, and the U. S. Patent file. More than 2500 abstracts were reviewed.

The 26 stress measurement methods listed by Vary form the principal basis for the techniques considered. Each of the 26 methods was evaluated in a preliminary way by members of the project team, on the basis of several factors of primary importance. First, the methods were categorized according to their sensitivity to (1) surface stress, and (2) subsurface stress. Second, literature reference to the use of a method with fasteners automatically qualified the method for further consideration. Finally, adaptability of the method to a manufacturing environment was evaluated. Evaluation factors included complexity, safety and state of development. The results of this preliminary assessment are summarized in Table VIII in which a total of 14 techniques of the original 26 survive.

Two of these, the ultrasonic pulse-echo technique and the ultrasonic resonance technique, are now in a relatively advanced stage of development. Both measure fastener elongation, and thus their practical application to post-tensioning inspection is questionable, although as preload indicators, they perform well. Two other techniques, the acoustic impedance technique and the Barkhausen noise analysis method, have been reported in the literature in connection with fastener inspection. Neither, however, are fully developed methods. All four of these techniques are included in the list of potential methods.

After the selection of the 14 candidate techniques, a thorough theoretical and engineering investigation of their application to fasteners was conducted. Brief summaries of the results of this evaluation are given in the following paragraphs. Those techniques showing the highest potential then became the basis for the experimental evaluation program discussed in following chapters of this report.

TABLE VIII

Stress Measurement Methods of Potential Interest to Threaded Fastener Integrity

Characteristic	NUCLEAR AND X-RAY METHODS			ELECTROMAGNETIC METHODS							ULTRASONIC METHODS			
	X-Ray Diffraction	Nuclear Magnet Resonance	Exo-Electron Emission	Magnetic Permeability	AC Magnetoelastic Effects(RAMMP, etc.)	Eddy Current	Magnetoabsorption	Barkhausen Noise Analysis	Electromagnetic Generation of Ultrasound	Electric Current (Resistivity)	Pulse Echo	Shear Wave Birefringence	Continuous-Wave Resonance (ROUS)	Acoustic Impact
	1	2	3	4	5	6	7	8	9	10	11	12	13	14
A. Sensitivity														
1. Sensitivity to Surface Stresses	Excel	Excel	Fair	Good	Good	Good	Excel	Excel	Good	Fair	None	None	Good	None
2. Sensitivity to Subsurface Stresses	None	None	None	None	Poor	Poor	Poor	Poor	Poor	Fair	Good	Good	Good	Fair
3. Adequacy of Stress Range	Good	Excel	?	Fair	Fair	Fair	Fair	Fair	Good	Fair	Good	Good	Good	?
B. Literature Ref. to Fasteners	No	No	No	No	No	No	No	Yes	No	No	Yes	No	Yes	Yes
C. Adaptability to Field Use														
Safety of Operation	Good	Excel	Good	Good	Excel	Excel	Excel	Excel	Good	Good	Excel	Excel	Excel	Good
2. Complexity of Instrument	High	High	High	Mod.	High	Low	Mod.	Low	High	Mod.	Mod.	Mod.	Mod.	Mod.
3. Difficulty of Data Interpretation	Mod.	High	High	High	High	Mod.	Mod.	Mod.	Mod.	Mod.	Mod.	High	Mod.	High
D. Potential for Development for Fasteners	Poor	Fair	Poor	Fair	Poor	Fair	Fair	Fair	Fair	Fair	Avail	Mod.	Good	Fair

Possible Ratings: Excel., Good, Fair, Poor, None
High, Moderate, Low, None

X-Ray Diffraction

Presently X-ray diffraction is the most widely accepted method for nondestructively measuring surface stress. The method is applicable to crystalline materials having randomly oriented small grains, and is based on the fact that the wavelengths of X-rays are the same general order of magnitude as the atomic spacings in metallic crystals. The short wavelength of X-rays makes it possible for the rays to penetrate the crystalline lattice to some extent and be reflected back from the atomic planes which they have penetrated. The reflected beams from successive parallel planes of atoms are reinfoced in one direction establishing a diffraction pattern defined by Bragg's law. Stresses distort the lattice and shift the diffraction peak (Bragg angle). Quantitative stress determinations are derived by measuring this shift in the diffraction peak.

Two general techniques are used in the recording of diffraction patterns: (a) photographic film and (b) X-ray diffractometers. Unfortunately, diffractometers are usually massive, slow, and require considerable power. These are conditions which are generally incompatible with tasks requiring great portability. X-ray diffraction probably has little applicability to fastener inspection, but it is included as a reference standard against which other techniques may be compared.

Nuclear Magnetic Resonance

The nuclear magnetic resonance absorption is obtained when a specimen is exposed simultaneously to a polarizing magnetic field, and either a radiofrequency field or an acoustic stress/strain wave. The resonance absorption is obtained over a narrow band of frequencies centered about a frequency which is a constant, different for each nuclear species, times the intensity of the steady magnetic field. For example, at a magnetic field of 1000 Gauss, the resonant absorption frequency for aluminum is 1.1 MHz.

The radiofrequency field is used if only surface measurements are desired since the conductivity effects limit penetration to 10^{-3} millimeters at the frequencies employed. For bulk stress measurements, acoustic excitation is used.

The frequency of the absorption and/or the width of the absorption band are modified by the surface and internal fields in the metals. In ferromagnetic metals, there is an internal magnetic field which may be much, much higher than the 1000 Gauss mentioned above. Measurements indicate that internal field values in iron are as high as 70,000 Gauss which gives a resonance frequency for the nucleus of iron of 9.67 MHz. Residual or applied stress in the sample changes this internal magnetic field and the frequency of the NMR absorption of the iron nuclei. Therefore, a plot of resonance frequency as a function of stress can be obtained for iron with either electromagnetic fields for surface measurements or acoustic waves for subsurface penetration.

In nonmagnetic materials such as aluminum, the internal electric fields cause changes in the magnetic resonance absorption frequencies and the width of the absorption band. These internal fields will also be changed by residual or applied stress so that the NMR responses can be used to determine stress. Here again, electromagnetic waves are useful for surface measurements while acoustic waves give deeper penetration.

For many cases, the steady magnetic field and the radiofrequency field are supplied around or encircling the sample. Recent developments permit nuclear magnetic resonance absorption to be obtained by nonencircling techniques, which now make it possible to obtain NMR absorption, using either electromagnetic or acoustic excitation, from only one side of the specimen. This appears to make the technique applicable to fasteners. Complexity and cost of this system are likely to be a problem, but it must definitely be considered a potential approach.

Exo-Electron Emission

It is well-known that electrons are emitted from surface atoms under certain conditions that provide sufficient energy. Such conditions can be correlated closely with surface changes produced by wear, cracks and material fatigue in general. No mention has been found in the literature of the application of this technique to fasteners, but it is conceivable that such a process might be applied. Conceptually, such a method would involve the following steps:

1. A device would be sealed over a fastener so that the fastener head or an area of material around the fastener could be isolated in vacuum.

2. Torquing force would be applied to the fastener with the vacuum chamber in place.

3. The surface of the fastener head or of the joint material would be scanned with a beam of radiation, e.g. ultraviolet light, which would stimulate emission of electrons from the stressed surface.

4. The emitted electrons would presumably be emitted in a pattern representative of the stress gradient across the head, or of the clamping force on the joint, and these electrons would be counted.

There is nothing to indicate that such a method would be affected by phenomena within the shank, but would be dependent upon the clamping force, or surface stress on the fastener head. The effect is time-dependent, decaying with time following the application of stress. Thus the method is probably not applicable to any function other than monitoring the torquing operation itself. In view of the difficulties involved in applying any method in the field requiring a high-vacuum, the potential of this method to routine determination of torquing force must be rated low.

Magnetic and Electromagnetic Methods

The electromagnetic approaches to stress measurement are based upon the stress-dependence of electrical conductivity and magnetic properties of materials. All these methods share common difficulties, chief of which is that these properties tend to vary markedly with composition, metallurgical constitution, heat treatment, and magnetic history as well as with stress. Furthermore, the sensitivities to stress in ferromagnetic materials are nonlinear, decreasing as the stress level increases, at moderate stress levels. However, attempts are being made to minimize these difficulties through the use of multiparameter measurements followed by multiple regression analysis. Some investigation of magnetic methods for application to stress measurement in steel fasteners are reported and the results tend to indicate that these may be the most promising of all the methods for inspecting installed fasteners without re-torquing them.

1. Magnetic Permeability

It is sometimes possible to relate the state of stress within a ferromagnetic specimen to the material permeability (B/H) at a preselected, constant value of H. The procedure for doing this is to introduce the specimen into a known external magnetic field and then measure the flux density, B, of the specimen. The specimen is usually made a part of a magnetic circuit, and changes in the flux density made with a Hall effect device. This technique could be applied to an exposed fastener head.

While changes in permeability may be well enough related to compressive stress in the head to assist in torquing the fastener, they are unlikely to independently provide a method of inspection of installed bolts; the technique warrants further study.

2. Low Frequency Magneto-elastic Effects

These encompass a number of magnetic-hysteresis methods including all that relate a measureable parameter of the hysteresis loop of a ferromagnetic specimen to its state of stress. The magnetic parameters which may be measured and used in nondestructive evaluation include: (1) coercive force, (2) maximum flux density, (3) maximum permeability, (4) retentivity, (5) hysteresis power loss, and (6) magnetoabsorption.

Recently an extension of these methods has been reported by Battelle-Columbus. The technique has the acronym RAMMP (Real-Time Analysis of Magnetic Material Properties). Basically it measures a series of magnetic material properties as the specimen is cycled through increasing magnetic hysteresis loops until saturation is reached. A unique (and sophisticated) data analysis scheme called Multivariant Analysis is used which is a numerical/statistical technique based on a modified regression analysis. This determines the optimum combination of the magnetic measurements for isolating the stress parameter in a composite predictive equation. Results appear promising, but the method is complex and expensive to employ in a portable instrument. At this time it is not likely to have application to the fastener problem. Simplification may be feasible.

3. Eddy Current

Eddy currents have been used for a number of purposes including the measurement of stress. Internal stresses resulting from uneven plastic working of ferromagnetic materials are relatively easily detected with eddy current measuring instruments when using low field strength (below one-half of the coercive force). The sensitivity is rather high; the ratio of magnetization of a stress-free sample to that of one with internal stresses can be as high as 5:1. The effect is even more pronounced in magnetostrictive materials and increases with increasing values of magnetostriction. Even though eddy currents can identify stress zones through harmonic analysis, Barkhausen and magnetoabsorption methods are more fully developed and easier to interpret. A number of factors other than stress influence the eddy current characteristics, as they do in all electromagnetic stress effects. The simplicity of application to fasteners, however, may recommend its further assessment. It appears applicable to post-installation inspection of fasteners, but its application for this purpose is not reported in the literature.

4. Barkhausen Noise Analysis

If the bulk magnetization of a ferromagnetic specimen is reversed, abrupt, localized, and irreversible changes, called "Barkhausen jumps", occur which correspond to the movement of magnetic domain walls within the material. These jumps may be detected by an appropriately positioned inductive search coil connected to suitable amplifiers and signal processing devices. Certain features of the resultant signal may be correlated with the state of mechanical stress within the material. Using this approach, instrumentation has been reported for residual stress measurement. The Barkhausen-effect approach has a number of operationally advantageous features: (1) the instrumentation is comparatively simple and portable; (2) the probes require limited access space; (3) operator training is minimal; (4) the approach lends itself to semiautomation; and (5) permanent records could be made available in real time. The method is sensitive only to surface stress. Investigation of Barkhausen noise analysis applied to fasteners has been reported in the literature.

5. Electromagnetic Generation of Ultrasound

It is known that magnetostriction is a useful parameter to monitor in a nondestructive test for the stress or strain of a material. It has been established at Rockwell International Science Center that the efficiency of an electromagnetic transducer, in ferromagnetic materials, is determined by the magnetostrictive properties of the material. Hence, a measurement of this efficiency, i.e., of the amplitude of the ultrasonic wave generated, can be used to determine stress. As in other magnetic methods, one has to determine the effects of cold work, texture, and other material changes. However, the parameter may possibly be used to separate effects produced by these variables from those produced by stress.

Ultrasonic Methods

The use of various acoustic and ultrasonic techniques represents one of the few classes of approach to direct measurement of internal fastener stress caused by tensioning. Ultrasonic phenomena identified in the literature as applicable to stress measurement include (1) shear-wave birefringence, (2) surface-wave dispersion, (3) surface-wave velocity, (4) longitudinal-wave velocity, (5) attenuation with magnetization, and (6) continuous-wave resonance. In addition, a related method known as the acoustic impedance, or acoustic impact technique (AIT) offers some potential.

These methods are based on changes in the lattice structure of crystalline materials due to strain. Thus elongation, acoustic velocity, impedance, ultrasonic resonance or some other property of the material affecting acoustic wave motion is measured as stress is applied. Difficulties are encountered in application of these methods, of course.

First, the effect of stress on ultrasonic velocity, impedance, attenuation, etc., is very small, and can be masked easily by other effects, specifically by material properties such as grain orientation and size. Interpretation of data derived from practical specimens presents serious difficulty due to both physical and material tolerances. Launching an ultrasonic wave of proper characteristics into a complex item such as a fastener, requires mechanical transducer coupling, the parameters of which are critical. Since all the acoustic properties of a material are primarily affected by strain, variations in temperature must be accurately accounted for. Some special preparation of the fastener (grinding ends parallel, providing special surfaces, etc.) may be required.

1. Ultrasonic Pulse-Echo Extensometer

One commercial instrument is available, and considerable work has been reported, on the pulse-echo extensometer. In operation, an ultrasonic transducer is attached to the top of the bolt head, and a short pulse of acoustic energy coupled through the length of the bolt. At the opposite end, the energy is reflected back to the transducer, which then functions as a receiver. The transit time is measured by the relative time of arrival of the received energy. As the bolt is stressed, the transit time changes slightly, due to elongation of the bolt.

This method requires exact knowledge of the stress-strain relationship of specific bolts, as well as extremely accurate instrumentation. Bolt ends may require some preparation.

2. Reflection Oscillator Ultrasonic Spectrometer (ROUS)

NASA Langley Research Center has developed a system called the Reflection Oscillator Ultrasonic Spectrometer (ROUS) which simultaneously makes use of several ultrasonic parameters that reflect stress. The system consists of a closed-loop feedback oscillator, and utilizes CW rather than a pulse-echo mode. When applied to a fastener, stress affects several parameters of the fastener, including its resonant frequency. These frequency changes are monitored by the closed-loop oscillator, which reportedly permits changes in frequency of 1 part in 10^7 to be detected. The system is in a rather high state of development, but is not available commercially.

3. Acoustic Impact Technique (AIT)

Extensive Air Force sponsored research has been reported in which an impact technique for determination of joint integrity has been investigated. Most of this work has been directed to inspection of the material being clamped, where cracks originating at the hole impair the joint. Some reference has been made to fastener integrity also.

In the technique, a controlled acoustic impact is coupled into the fastener head. The resulting acoustic impulse, measured by transducers on the fastener or on the joint surface, is analyzed, and the response is reportedly indicative of the joint integrity.

Shear-Wave Birefringence

Ultrasonic shear waves, in which the particle motion is perpendicular to the wave direction, may be propagated in a material. If the grain structure is anisotropic, the velocity of propagation of a wave polarized in a direction parallel to the direction of propagation will be different from that of a wave polarized perpendicular to the direction of propagation. Anisotropy is the result, among other things, of applied stress. If stress is the only cause of the anisotropy, the preferred direction of propagation is perpendicular to the direction of the stress. This difference in velocity in the two polarization directions, known as birefringence, can then be used to determine the preferred direction, and hence the anisotropy. The method has been investigated as a stress-measurement technique.

In evaluating the approach applied to fasteners, it appears that the method might be useful in determining the average bulk stress in the head of a bolt. Shear-wave velocities through the width of the head could be determined and preload inferred from stresses in the head. This is in contrast to the magnetic methods which are only capable of measuring surface stresses.

Conclusions

A total of fourteen NDE methods with potential application to fastener integrity were located in an extensive review of the literature and subsequent analysis of specific techniques. The most promising of these 14 methods consist of two ultrasonic systems which measure fastener elongation (strain), an ultrasonic bi-refringence method for measuring bulk stress, and several magnetic approaches to the direct measurement of surface stress on the fastener head. Nuclear magnetic resonance absorption shows promise, but its complexity and cost are matters of concern.

VI. APPLICATION OF STRESS DETERMINATION METHODS

The stress of principal interest in evaluating fastener integrity is the tensile stress along the axis in the shank. Since the shank is generally inaccessible in practical joints, useful methods must be capable of being applied to the head or, occasionally, to the threaded end of the fastener, and measurements made in the axial direction. Unfortunately, as can be seen from Table VIII, most of the candidate techniques are only sensitive to surface stress, and application directly to the shank is not possible. The shear-wave birefringence technique, while sensitive to subsurface stress, must be oriented in a direction perpendicular to the stress, which again makes its application directly to the shank impractical.

Stress can be indirectly measured by measuring the resulting strain. Loading a bolt causes it to stretch in the axial direction, the amount of stretch or elongation directly proportional to the applied stress. A sufficiently accurate elongation measurement can be related to preload if the material properties are accurately known. In particular, methods including the ultrasonic pulse-echo technique, or the ROUS ultrasonic spectrometer system, by measuring elongation during installation, are potentially capable of determining the preload.

Application of other methods is necessarily confined to measurements of stresses on the head (or occasionally the nut). When a bolt is stressed in tension, the head, in general, responds by going into compression, as the forces tend to pull the head through the joint. Thus, intuitively at least, it appears that shank stress may be measured indirectly by determining the compressive stresses in the head.

Finite Element Analysis

To investigate the feasibility of determining preload by stress measurements made on the head of a fastener, a finite-element stress analysis technique, based on computer modeling of the stresses throughout the entire bolt, was employed. This technique allows calculation of surface stresses on the bolt head at desired shank loads. Such surface stresses would be applicable, for example, to the use of magnetic stress measurement techniques, such as magneto-absorption, eddy currents, or Barkhausen noise analysis.

The finite element analysis was first applied to a typical hexagon head aircraft-quality bolt. Of particular interest was the surface stress distribution (especially radial stress) on the bolt head and the effect of dimensional changes as allowed by manufacturing tolerances on the magnitude of the surface stresses. The hex-head bolt selected for analysis was a 1/2-inch bolt described by specification AN8. Figure 6 is a copy of the specification. Dimensions as allowed by tolerances in the specification were selected in two combinations to have maximum effect on the surface stress on top of the head. Dimensions are shown as Case I and Case II in Table IX . The lettered dimensions in the table are referenced to the bolt drawing in Figure 6.

TABLE IX

DIMENSIONAL VALUES USED FOR STRESS ANALYSIS
OF AN8 BOLT

	Case I	Case II
Shank Diameter (A)	0.499 inch	0.499 inch
Head Width (B)	0.752	0.740
Head Height (D)	0.265	0.297
Washer Face Diameter (H)	0.752	0.710
Fillet Radius (R)	0.010	0.010
Inside Diameter of Washer	0.520	0.520
Outside Diameter of Washer	0.875	0.875
Washer Thickness	0.032	0.032

The first computer model developed for this bolt and an associated washer is shown in Figure 7. Since the bolt is symmetrical, only half of it was necessary for the model. Note that the head shape represented by the model is round as opposed to the true hexagonal shape of the bolt head. Dimensions used in this model are shown in Case I in Table IX; however, no fillet radius at the shank-head junction was utilized in this initial model. Calculations were performed for a bolt load of 12,800 pounds which corresponds to 90% of the yield strength for an AN8 steel bolt at the effective shank diameter at the threads. Figure 8 is a plot of the calculated surface stresses (both radial and hoop) on top of the bolt head from the center to the outer edge. The stress analysis technique does not calculate surface stress at the absolute center point of the bolt head so this point is omitted on the plot. The radial surface stress is 39,000 psi compression near the center which is 60% of the magnitude of the 65,000 psi tensile stress in the shank. The radial stress then tapers off to a zero value near the edge and into a slight tensile stress at the edge. Figure 9 is a plot of the axial and hoop surface stresses on the side flat of the bolt head plotted from top to bottom.

To make the bolt model more precise, a fillet radius at the shank-head junction was added. Figures 10 and 11 are plots of the calculated surface stresses on the top and sides of the bolt head with the fillet radius included. Note that the radial surface stress on top of the head near the center has increased to 43,500 psi compression from the previous value of 39,000 psi. This tends to indicate that the dimensions of the fillet radius could influence the surface stress values. The fillet radius is included in all additional studies.

ORIGINAL PAGE IS
OF POOR QUALITY

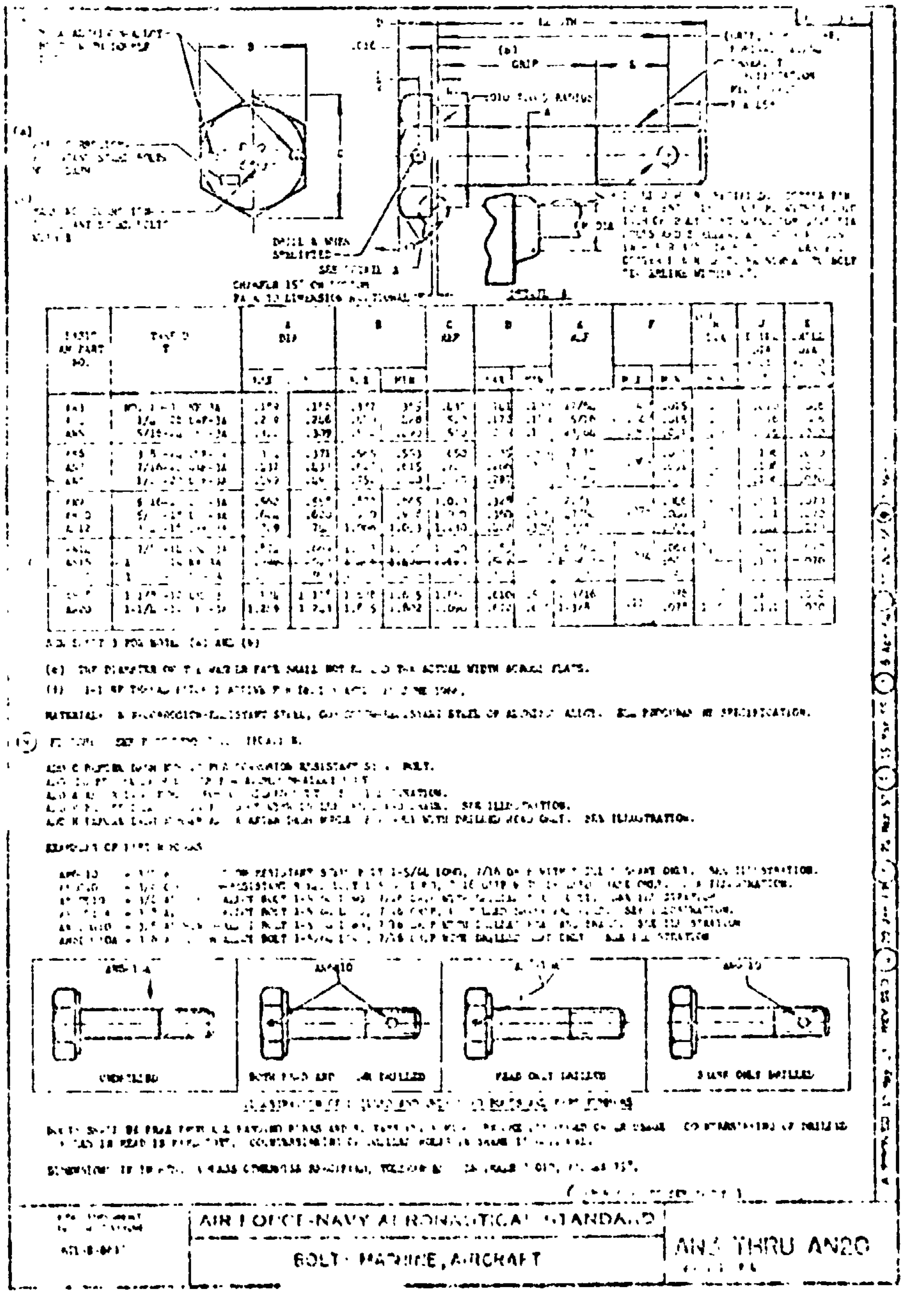
AIR FORCE-NAVY AERONAUTICAL STANDARD

BOLT - MACHINE, AIRCRAFT

AN3 THRU AN20

GRIP
DETAIL A
UNDRILLED
HEAD ONLY DRILLED
SHANK ONLY DRILLED

FIGURE 6. SPECIFICATION OF AN8 SERIES BOLTS USED IN FINITE ELEMENT ANALYSIS.

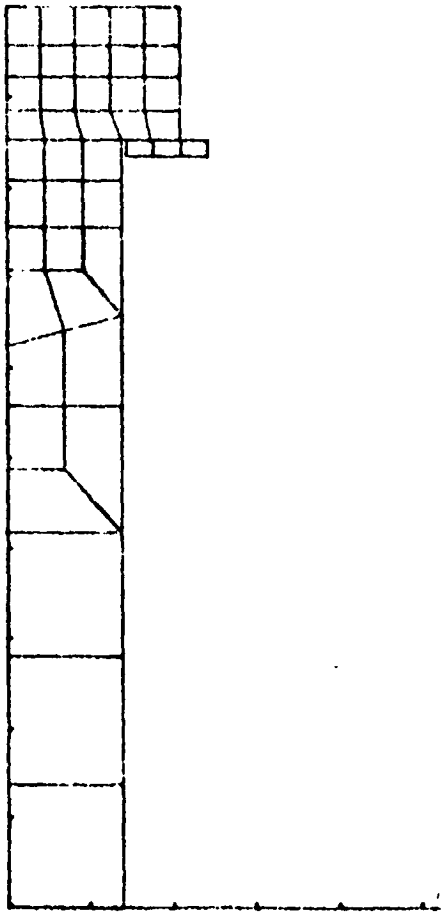

4526

FIGURE 7. FINITE-ELEMENT MODEL OF SYMMETRICAL BOLT SHOWING ELEMENTS USED IN ANALYSIS

FIGURE 8.
SURFACE STRESS ACROSS TOP OF BOLT HEAD--.5IN. SHANK, 12,800LB. LOAD

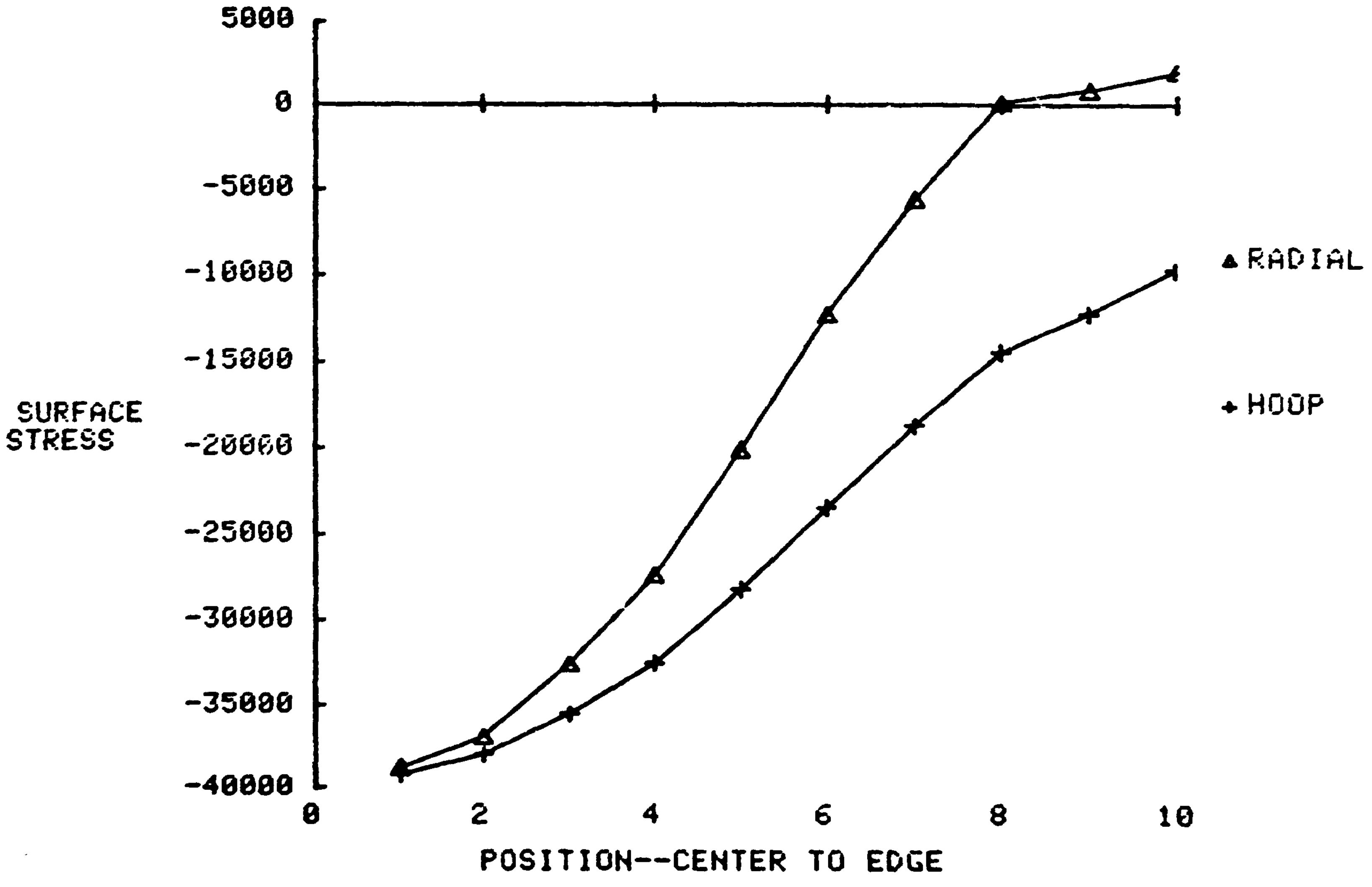

FIGURE 9.
SURFACE STRESS DOWN SIDE OF BOLT HEAD--.5IN. SHANK, 12,800LB. LOAD

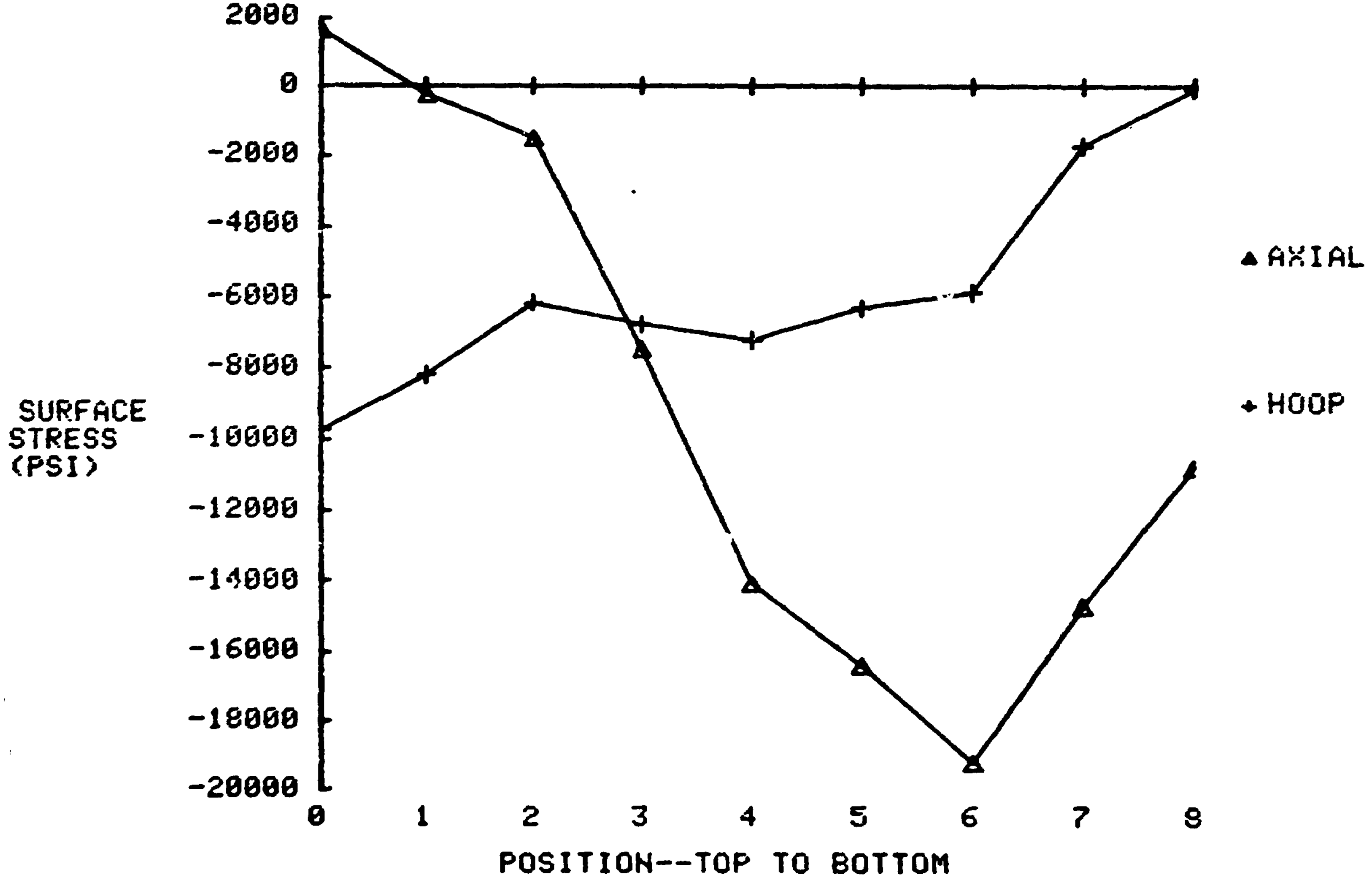

FIGURE 10.
SURFACE STRESS ACROSS TOP OF BOLT HEAD--.5IN. SHANK, 12800LB. LOAD
FILLET RADIUS IN MODEL

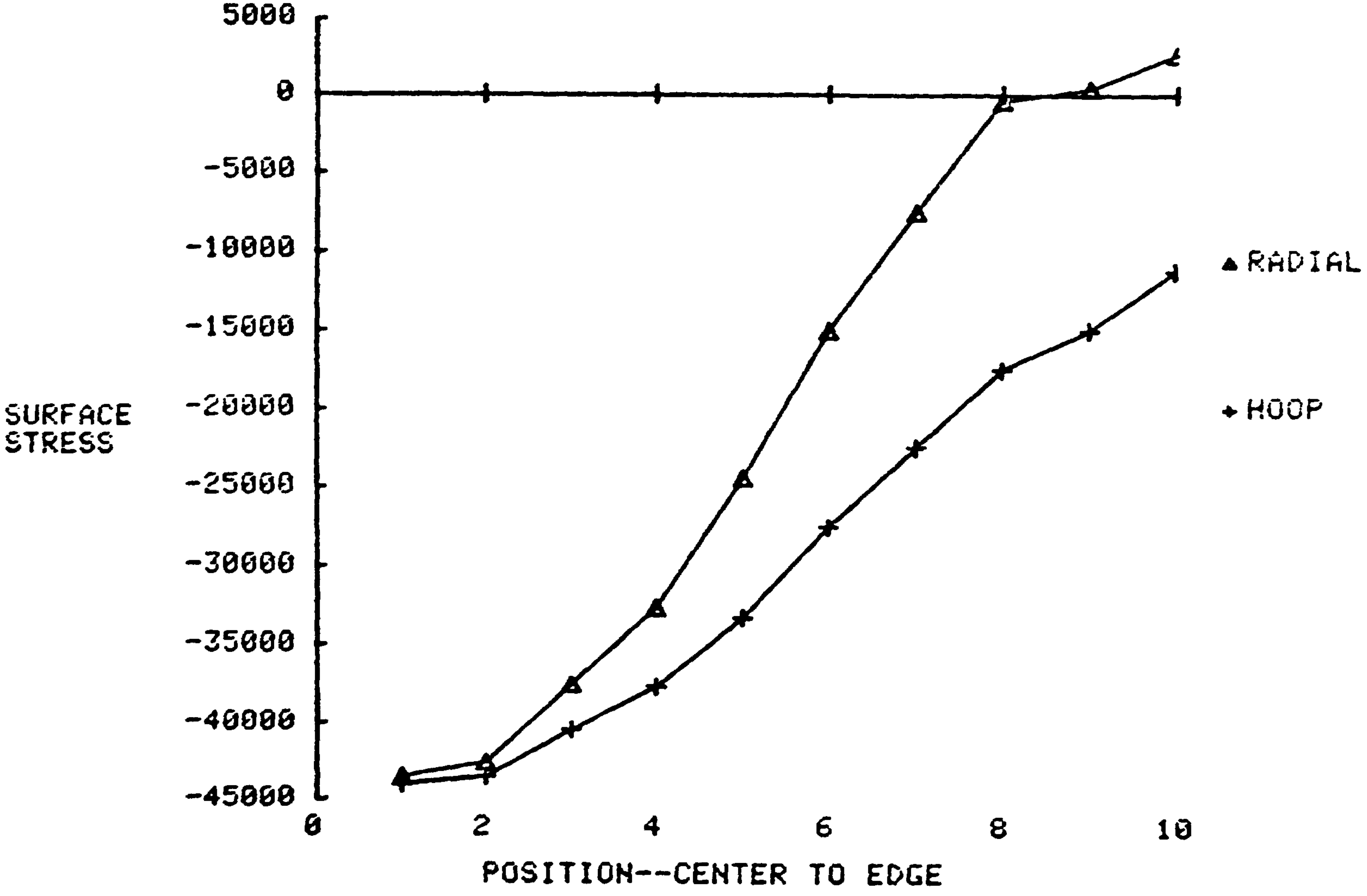

FIGURE 11.

SURFACE STRESS DOWN SIDE OF BOLT HEAD--.5IN. SHANK, 12,800LB. LOAD

FILLET RADIUS IN MODEL

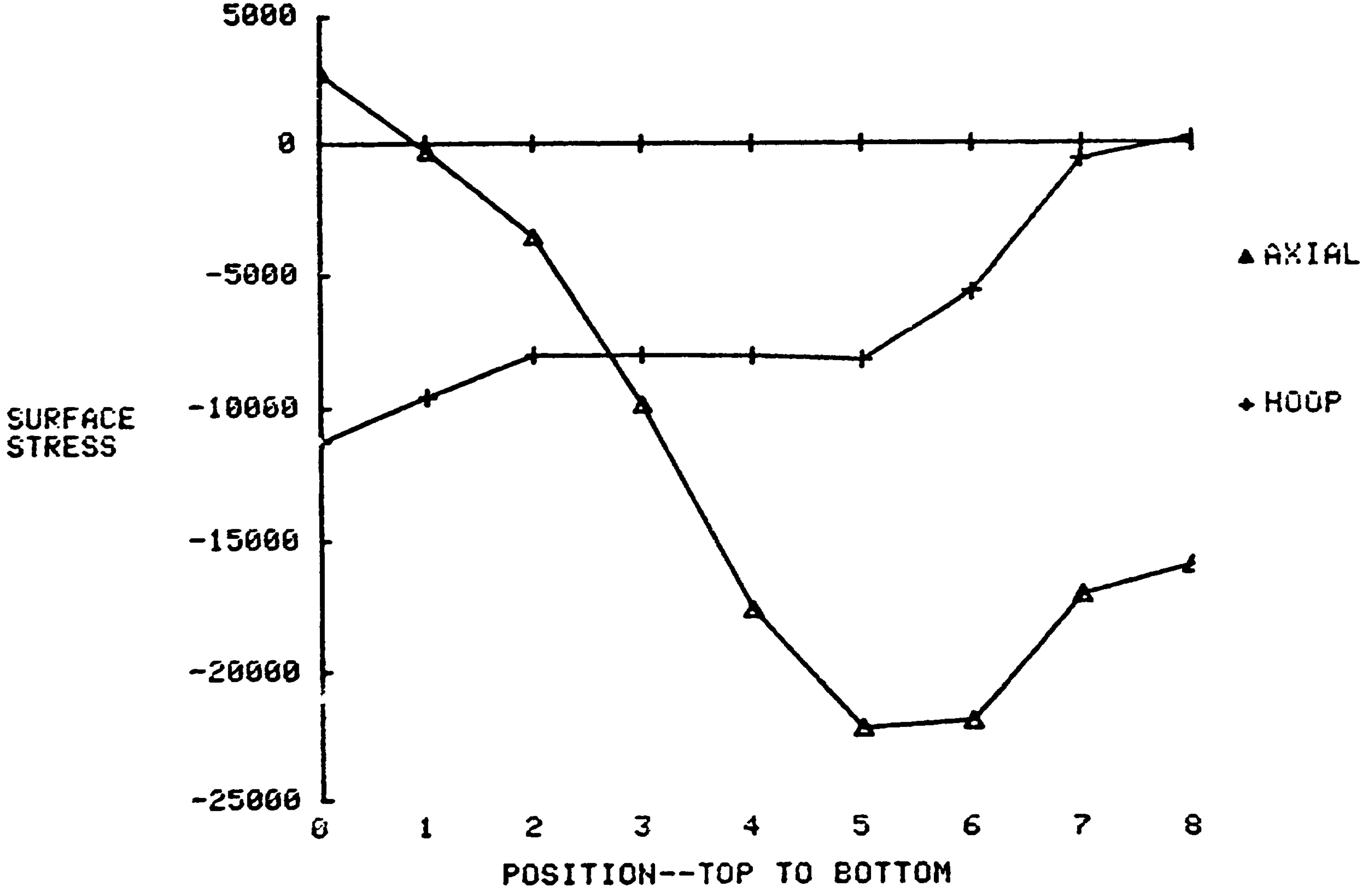

To determine the effects of washer inside diameter on the surface stress, computations were made with washer diameters of 0.520 and 0.620 inch. The 0.520 inch diameter is the smallest washer size which could be utilized without physical interference with the fillet radius. The 0.620 diameter is the maximum inside diameter of washer MS20002 which is specifically designed for use under bolt heads. The results are plotted in Figures 12 and 13. Surprisingly, the larger washer diameter only increased the radial surface stress near the center from 43,500 to 44,000 psi, a 1% change.

As a final part of the study, surface stress calculations were made to determine the maximum influence of dimensional changes in the bolt head. The computer model was modified slightly to obtain surface stress calculations at more closely spaced intervals. For the Case II dimensions, the washer face diameter of the bolt (dimension H in Figure 6) was no longer the same as the head width, so the model was also modified to include this change. Figure 14 is the model utilized for Case II dimensions. Figures 15 and 16 are composite plots comparing the results of both Case I and Case II dimensions. Again, bolt load is 12,800 pounds. As can be seen in the plots, the dimensional changes are quite significant. The radial surface stress near the center is 44,500 psi compression for the Case I dimensions and 36,300 psi for the Case II dimension. This represents a change of 20%. It is thus apparent that dimensional changes in bolts allowed by manufacturing tolerances play a significant role in the shank-bolt head stress relationship and can limit the accuracy of shank stress determination techniques based solely on surface stress measurements on the bolt head.

MS21250 Bolt

A bolt selected specifically for the experimental program was also studied using the finite element analysis. Since this bolt has such a complex head geometry, it was necessary to calculate the stress patterns to determine optimum stress measurement positions. The bolt is described in MIL STD MS2 1250 and is a 12-point external wrenching bolt (see Figure 17). The washer is MS20002. Figure 18 is a cross-sectional drawing of the bolt and an associated washer as used for the finite element stress analysis. Dimensions used are the nominal dimensions given in the bolt specifications. Dimensional changes were not investigated. Calculations were made at a bolt load of 23,000 poinds which corresponds to 90% of the yield stress at the effective stress area at the threads.

Figure 19 is a plot of surface stresses along the bottom of the hole inside the head. The pattern here is similar to that on top of the hex head bolts. The radial surface stress near the center is 81,000 psi compression. This is 69% of the magnitude of the surface stress in the shank. Figure 20 is a plot of the axial and hoop surface stresses from bottom to top along the

FIGURE 12.
SURFACE STRESS ACROSS TOP OF BOLT HEAD--.5IN. SHANK, 12800LB. LOAD
WASHER ID .520-.620
CASE 1 DIMENSIONS

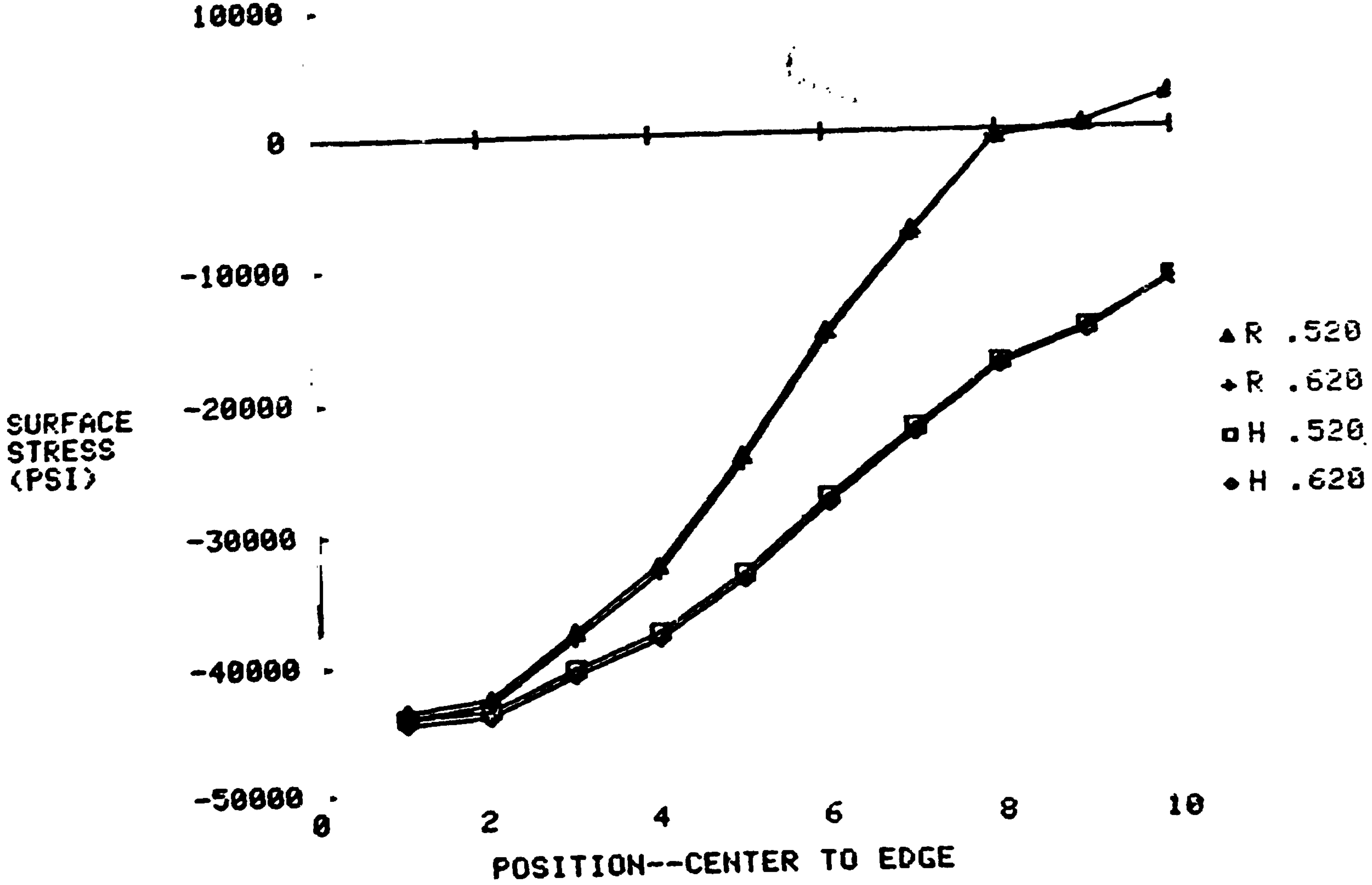

FIGURE 13.
SURFACE STRESS DOWN SIDE OF BOLT HEAD--.5IN. SHANK, 12800LB. LOAD
WASHER ID .520-.620
CASE 1 DIMENSIONS

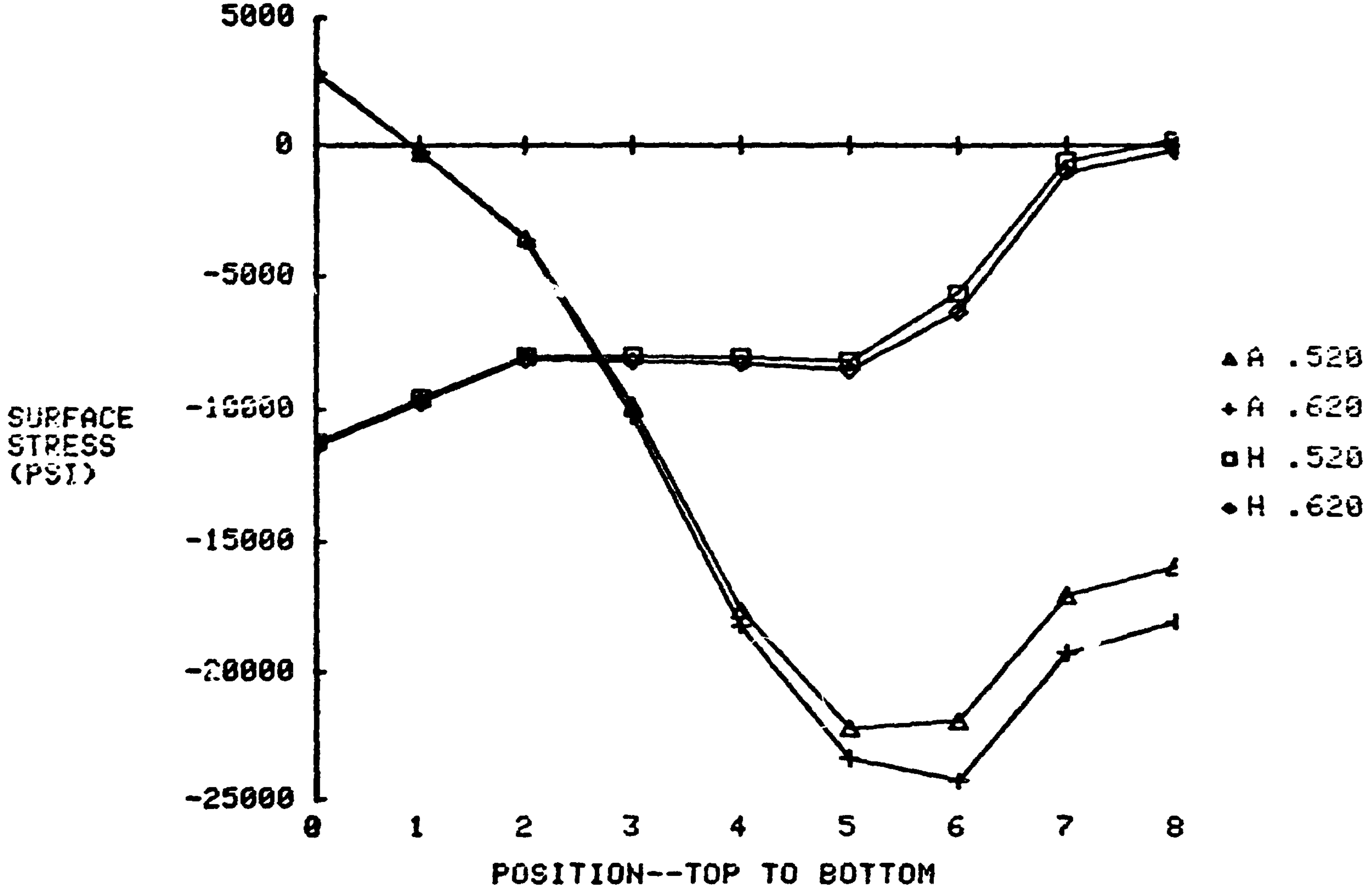

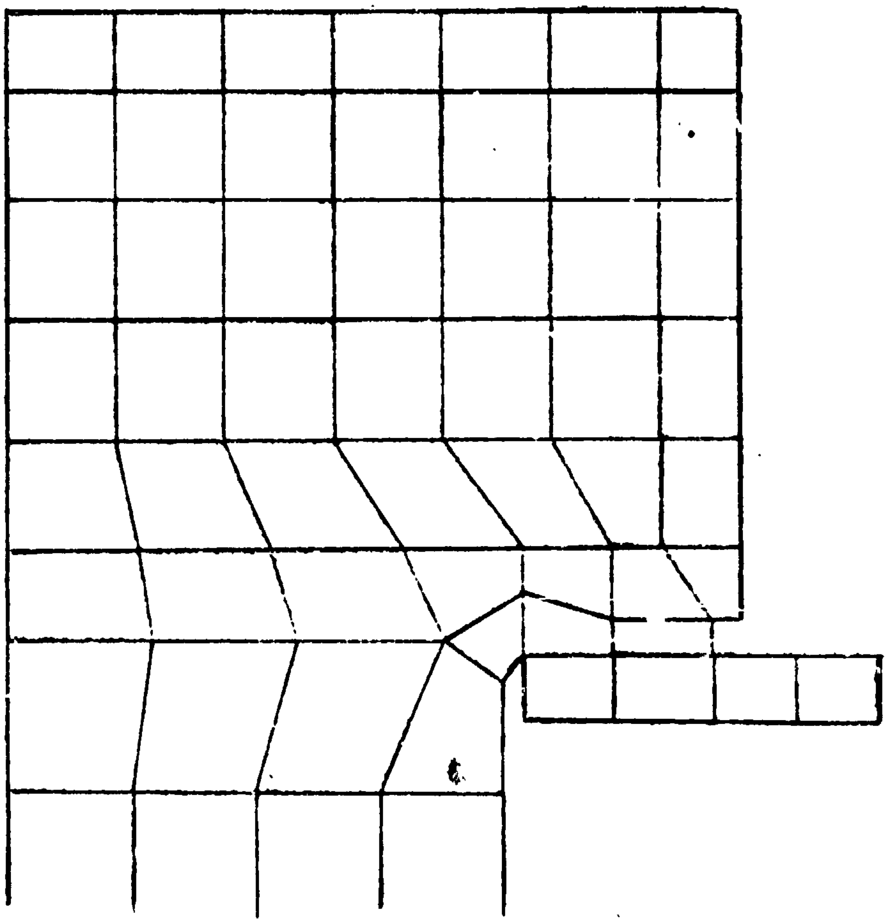

FIGURE 14. FINITE-ELEMENT MODEL USED IN "CASE II" DIMENSIONAL ANALYSIS (from Table IX)

4527

FIGURE 15:
SURFACE STRESS ACROSS TOP OF BOLT HEAD-- 0.5IN. SHANK, 12800 LB. LOAD
CASE I AND CASE II DIMENSIONS

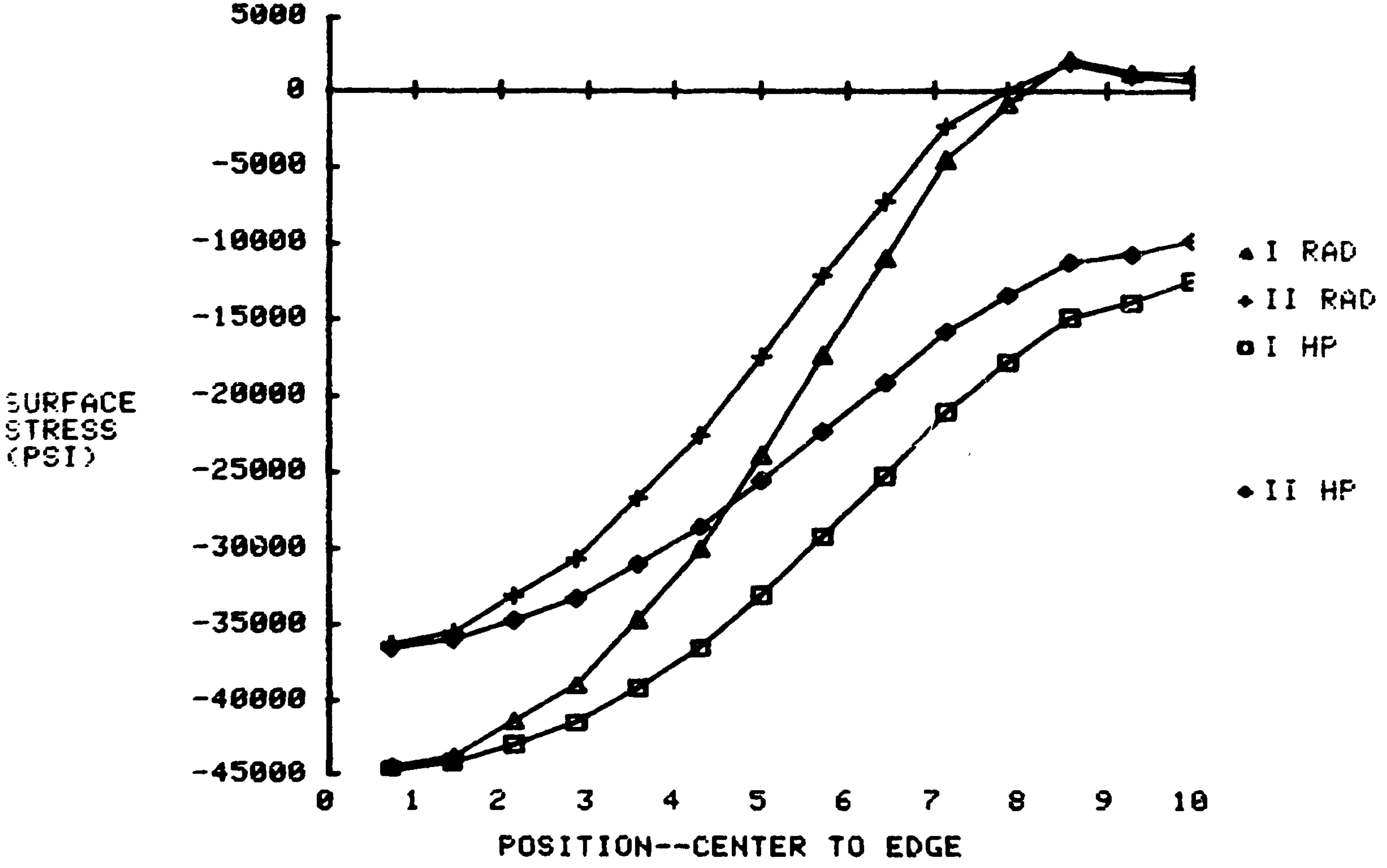

ORIGINAL PAGE IS
OF POOR QUALITY

GURE 16.
RFACE STRESS DOWN SIDE OF BOLT HEAD--0.5IN. SHANK, 12800 LB. LOAD
SE I AND CASE II DIMENSIONS

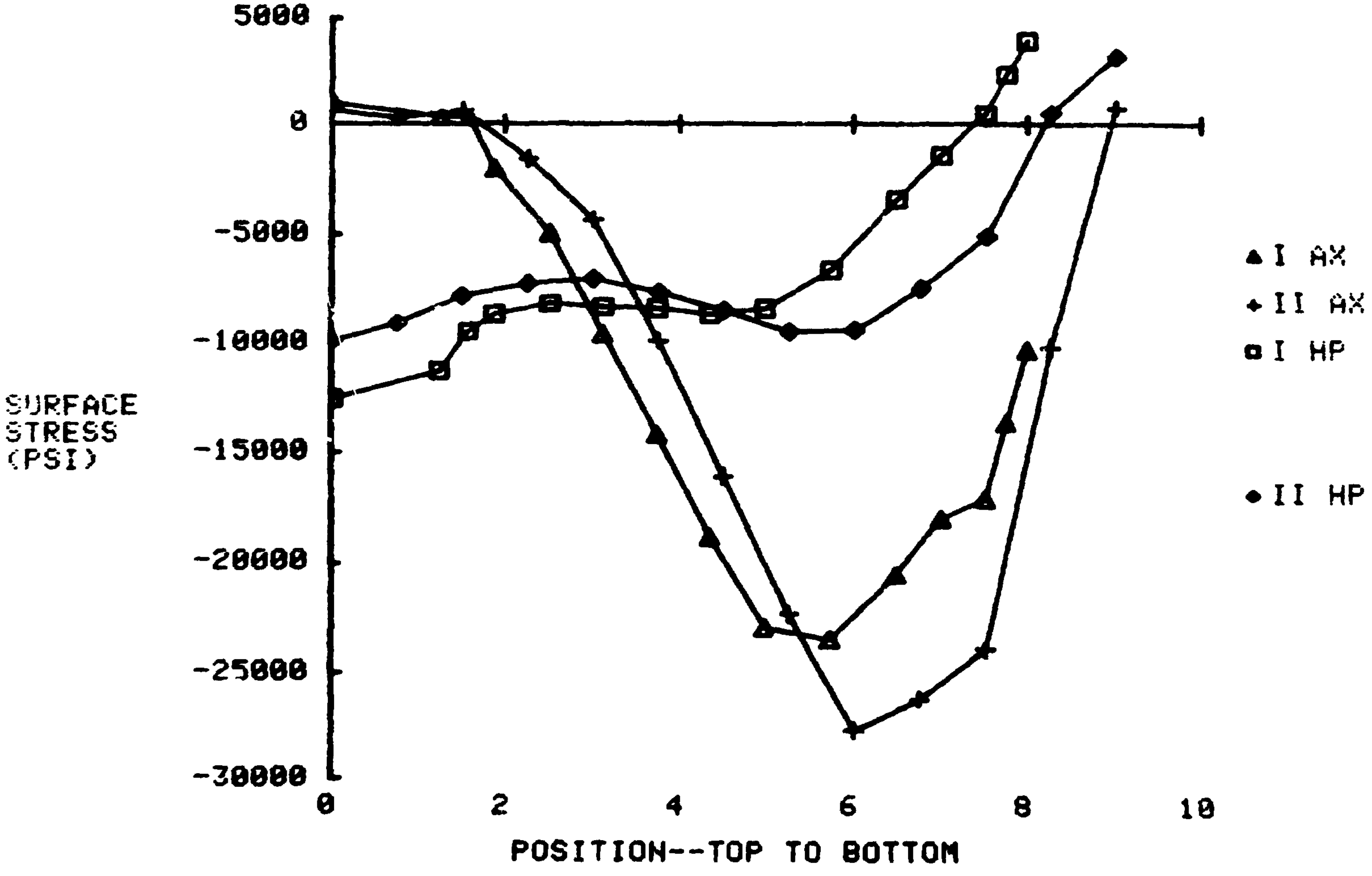

ORIGINAL PAGE IS
OF POOR QUALITY

FED SUP CLASS
5306

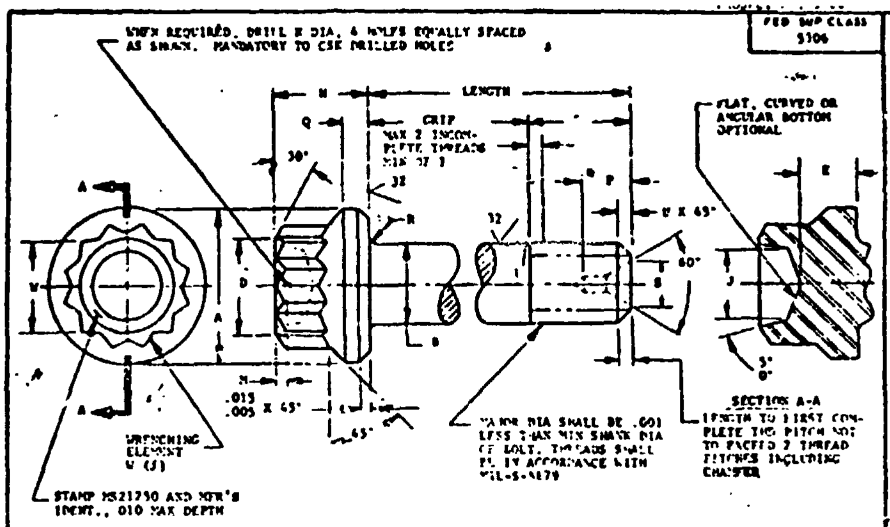
WHEN REQUIRED, DRILL E DIA, 6 HOLES EQUALLY SPACED AS SHOWN. MANDATORY TO CSK DRILLED HOLES
H
LENGTH
Q
GRIP
MAX 2 INCOMPLETE THREADS MIN OF 1
30°
32
R
A
A
V
D
A
B
32
I
P
U X 45°
60°
S
FLAT, CURVED OR ANGULAR BOTTOM OPTIONAL
K
J
5°
0°
SECTION A-A
.015
.005 X 45°
45°
WRENCHING ELEMENT
W (J)
MAJOR DIA SHALL BE .001 LESS THAN MIN SHANK DIA OF BOLT. THREADS SHALL BE IN ACCORDANCE WITH MIL-S-8879
LENGTH TO FIRST COMPLETE THD PITCH NOT TO EXCEED 2 THREAD PITCHES INCLUDING CHAMFER
STAMP MS21250 AND MFR'S IDENT., .010 MAX DEPTH

NOTES:

1. MATERIAL: STEEL ALLOY, MIL-S-5626 (AISI 4140) MIL-S-5000 (AISI 4340) MIL-S-6049 (AISI 8740) MIL-S-8503 (AISI 6150)
2. PLATING: CADMIUM PLATE IN ACCORDANCE WITH QQ-P-416, TYPE II CLASS 2. (CLASS 3 MAY BE USED UNTIL 1 JAN 1976)
3. SURFACE TEXTURE IN ACCORDANCE WITH ANSI (ASA) B46.1-1962. UNLESS OTHERWISE SPECIFIED, THE SURFACE TEXTURE SHALL NOT EXCEED 125 MICROINCHES.
4. DIMENSIONS IN INCHES, UNLESS OTHERWISE SPECIFIED, TOLERANCES: DECIMALS ±.010, ANGLES ±2°.
5. DIMENSIONS TO BE MET AFTER PLATING.
6. TENSILE STRENGTH TO BE 180,000 TO 200,000 PSI.
7. DIAMETER DASH NO. AT TOP OF TABLE, SHEET 3, PLUS GRIP DASH NO. FIRST COLUMN ON LEFT OF TABLE CONSTITUTE A COMPLETE DASH NO. IDENTIFYING SPECIFIED LENGTHS OF A GIVEN SIZE OF BOLT.
8. ADD LETTER H BEFORE DASH NO. TO DESIGNATE DRILLED HEAD. FIRST TWO DASH NUMBERS DESIGNATE DIAMETER IN SIXTEENTHS, LAST THREE DASH NUMBERS DESIGNATE GRIP LENGTH IN SIXTEENTHS. UNASSIGNED DASH NUMBERS SHALL NOT BE USED.

   EXAMPLES OF PART NUMBERS: MS21250-04008 = .2500-28 BOLT, 1.012 LONG .500 GRIP, UNDRILLED HEAD
   MS21250H04008 = .2500-28 BOLT, 1.012 LONG .500 GRIP, DRILLED HEAD
   MS21250-05012 = .3125-24 BOLT, 1.349 LONG .750 GRIP, UNDRILLED HEAD
   MS21250H05012 = .3125-24 BOLT, 1.349 LONG .750 GRIP, DRILLED HEAD

   SEE TABLE ON SHEET 3 FOR GRIP DASH NUMBERS.
   GRIP LENGTH OF BOLT SHALL BE MEASURED FROM UNDERSIDE OF HEAD TO THE END OF FULL CYLINDRICAL PORTION OF THE SHANK.
9. HARDNESS: RC39-43

FOR DESIGN FEATURE PURPOSES, THIS STANDARD TAKES PRECEDENCE OVER PROCUREMENT DOCUMENTS REFERENCED HEREIN. REFERENCED DOCUMENTS SHALL BE OF THE ISSUE IN EFFECT ON DATE OF [illegible] FOR BID.

(G) REVISED

APPROVED 13 NOV 60 REVISED (D) 11 AUG 71 (E) 21 JUN 74 (F 23 MAY 75 (G) 12 DEC 75

P A NAVY - AS Other Cust USAF-11 ARMY-AV	TITLE BOLT, TENSION, STEEL, 180 KSI FTU, 450 F, 12 POINT, EXTERNAL WRENCHING, FLANGED	MILITARY STANDARD MS21250
PROCUREMENT SPECIFICATION MIL-B-8831	SUPERSEDES MS21250(ASG)	SHEET 1 OF 3

FIGURE 17. SPECIFICATION FOR MS21250 AIRCRAFT BOLT

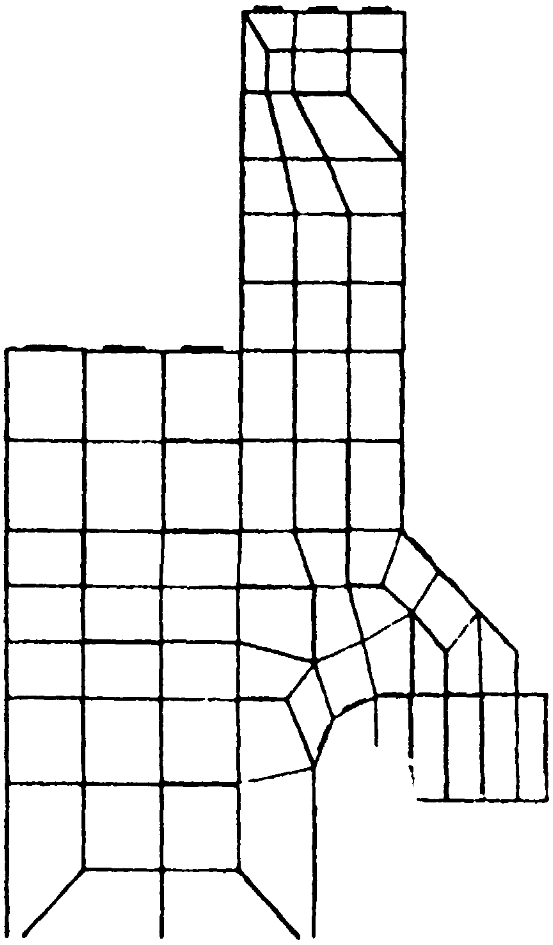

FIGURE 18. FINITE-ELEMENT MODEL USED FOR ANALYSIS OF MS21250 AIRCRAFT BOLT

FIGURE 19.
MS21250 BOLT---SURFACE STRESS ACROSS BOTTOM OF HOLE IN HEAD
23000 LB. LOAD

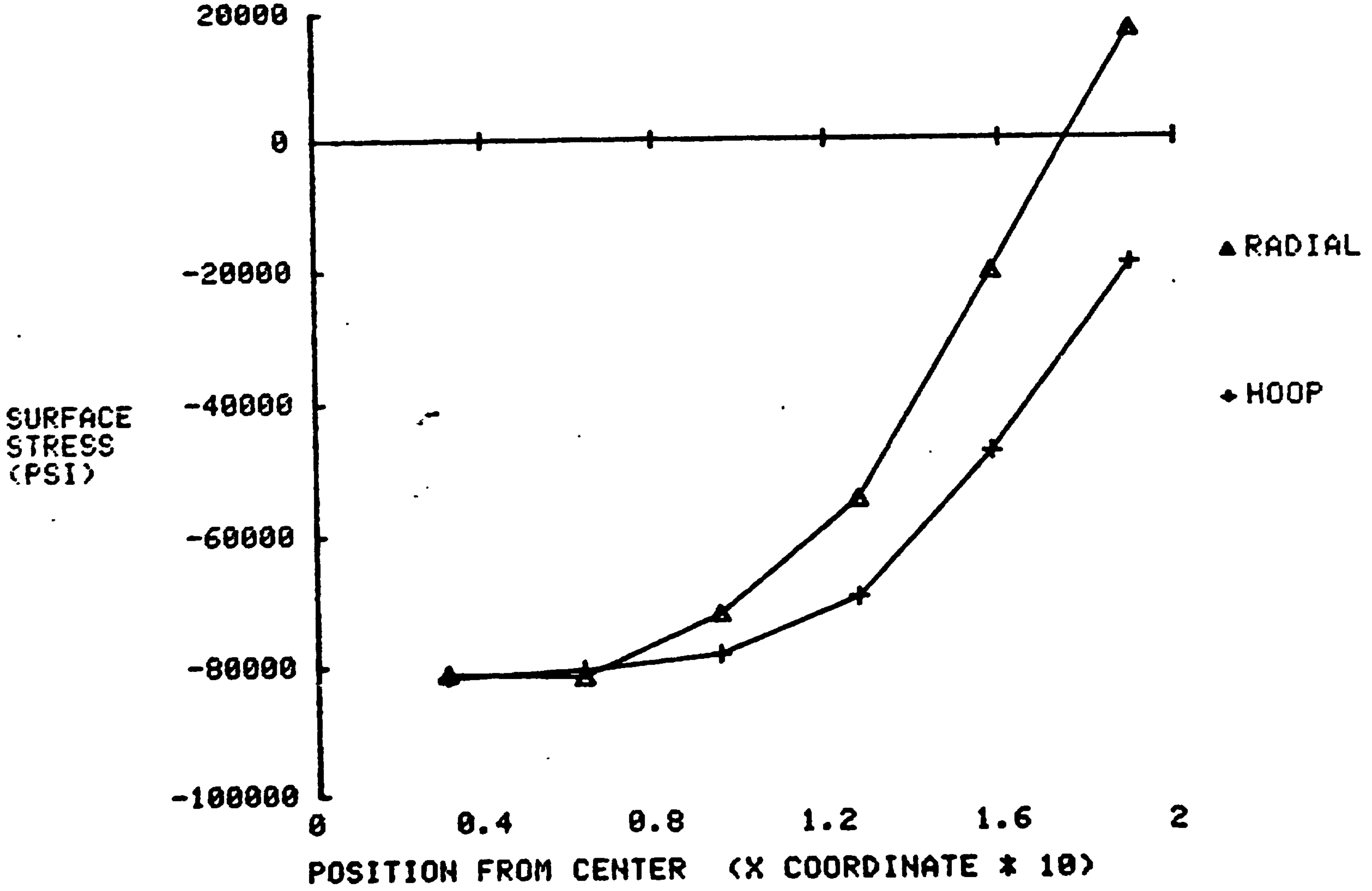

FIGURE 20.
MS21250 BOLT---SURFACE STRESS ALONG I.D. OF BOLT HEAD
23000 LB. LOAD

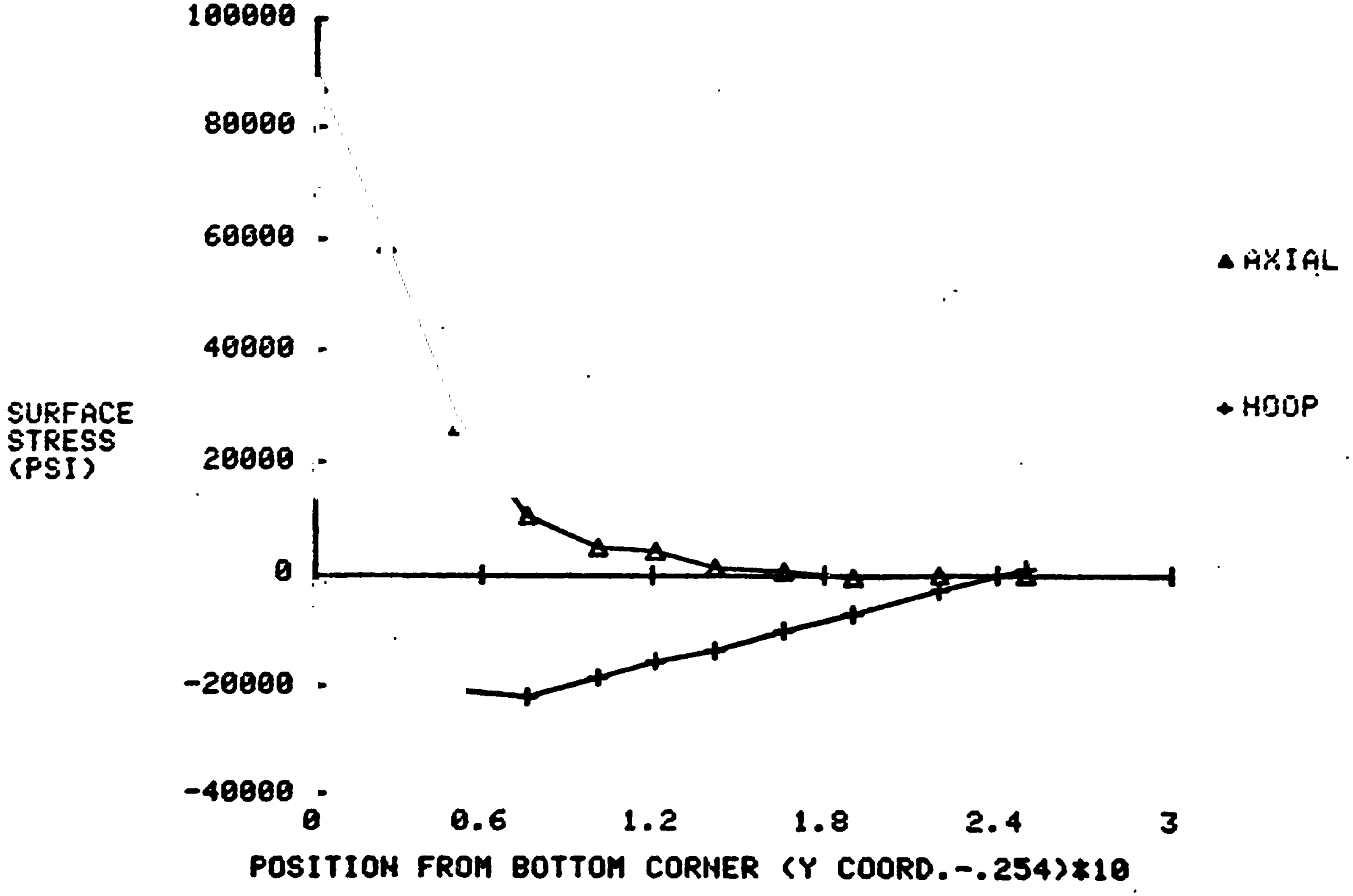

inside wall. Here a large tensile axial surface stress of 88,000 psi exists near the bottom corner. Figure 21 is a plot of the radial and hoop stresses on the top edge of the bolt head. Very small stresses are present here. Stresses were not computed for the outer vertical wall since this area is a wrenching element. Stresses along the flanged area are plotted in Figure 22.

Conclusions

The finite-element computer model analysis of fastener stress has shown that variations in the head dimensions as allowed by specified dimensional tolerances can significantly affect the relationship between shank load and the resultant surface stress values on the fastener head. A maximum variation of 20% (±10% about the average) in the radial surface stress at the top center of an AN8 hex-head bolt at full shank load resulted when two combinations of maximum and minimum bolt head dimensions (head height, head width, and washer face diameter of the bolt head) were used in the computations. Although the effect of each dimensional change was not investigated individually, it appears that variations in head height have the greatest influence, since head dimensions have the greatest permissible tolerances.

A separate part of the study showed that the fillet radius at the bolt shank-head junction affects the surface stress, although effects of dimensional changes in the fillet radius were not investigated.

An evaluation of variations in inside diameter of the washer, however, showed minimal effect (1%) on the surface stress.

It is apparent from these analyses that the accuracy of preload measurement techniques which rely on fastener head surface-stress measurement is inherently limited by the degree of control of the dimensional tolerances.

FIGURE 21.
MS21250 BOLT---SURFACE STRESS ACROSS TOP EDGE OF BOLT HEAD
23000 LB. LOAD

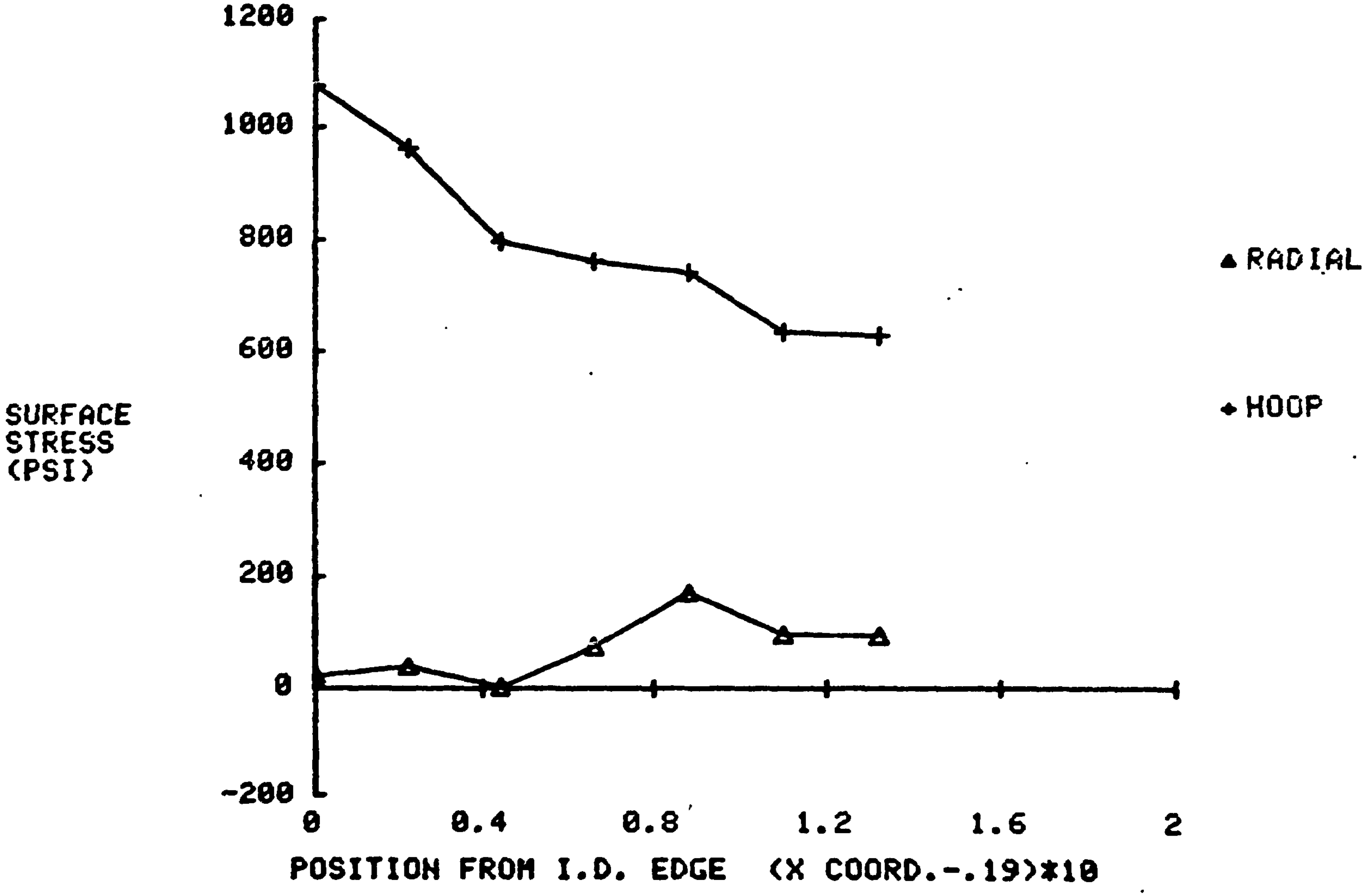

FIGURE 22.
MS21250 BOLT---SURFACE STRESS ON OUTSIDE FLANGE
23000 LB. LOAD

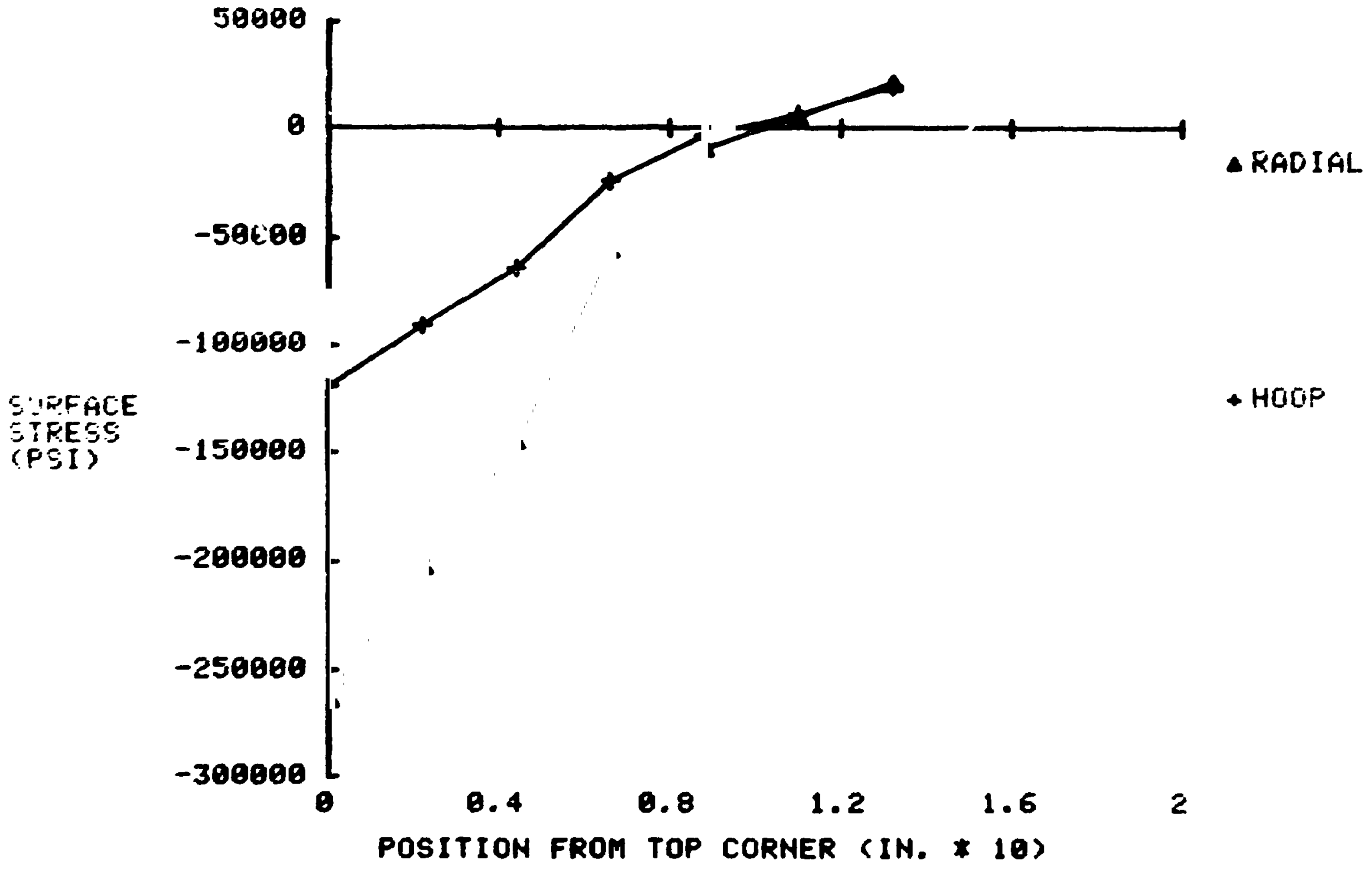

VII. EXPERIMENTAL EVALUATION OF SELECTED NDE METHODS

In Chapter V the selection of NDE methods appropriate for consideration to fastener integrity determination was summarized. A total of 26 methods generally related to the measurement of stress was refined to a list of 14 techniques showing specific promise to fastener application. On the basis of more detailed theoretical and engineering evaluation of the 14 techniques including their stage of development, three general approaches were determined to be most applicable to the problem; these included - several magnetic techniques applicable to ferromagnetic fasteners only, two ultrasonic methods of fastener elongation measurement, and two ultrasonic or acoustic approaches to bulk stress determination. Some experimental evaluation of each of these methods was undertaken although, because of the limited scope of the project, equal weight could not be given to each.

Magnetic Methods

Several magnetic approaches were found to offer potential as surface-stress measurement techniques on ferromagnetic steel fasteners. At least one of these, the Barkhausen noise analysis method has been mentioned in the literature in connection with fastener integrity determination(10).

The general shape of the magnetic hysteresis curve of ferromagnetic material is known to be altered by the application of stress. This fact results in a number of measurement possibilities, all related to the hysteresis effect, including measurement of the hysteresis loop itself, measurement of magnetic permeability, remnant field, coercive force, etc.

The eddy current technique, an accepted NDE method for flaw determination, is also known to be sensitive to stress. Eddy current testing involves the effects of inducing electric currents, called eddy currents, into a specimen. Characteristics of these eddy currents and their resulting secondary magnetic field are dependent upon magnetic and electrical properties of the material which are affected by stress.

Electromagnetic generation of ultrasound, based on an effect known as magnetostriction, results from dimensional changes in a specimen upon application of a magnetic field. Magnetostriction is known to be affected by stress.

Magnetoabsorption is a measure of the change in the radio frequency energy absorbed by a specimen as a low frequency magnetic bias field is applied. Magnetoabsorption has been shown to be stress sensitive(11).

Other methods involving combinations of magnetic parameters are also possible. Recognizing that all these magnetic effects are closely related to basic magnetic properties of a ferromagnetic material, all are likely to share common difficulties, chief among which is that the stress effects tend to vary markedly with the material composition, heat treatment and magnetic history. The two most well-developed of the magnetic techniques appear to be the Barkhausen noise approach and the eddy current technique. of the two, the Barkhausen method was selected for evaluation experiments because of its relatively high sensitivity to surface stress. Also, previously reported investigation applied to fasteners gave a good point of departure for more comprehensive work.

Measurement of other magnetic parameters simultaneously with the Barkhausen effect, although complicated by bolt geometry, was thought promising as a possible means of separating some of the effects of material properties. These relatively independent measurements might be combined into a simplified multiple regression analysis to improve the accuracy of stress measurement.

Review of Magnetism and Magnetic Effects

The strength of a magnetic field, the "magnetic intensity", is denoted by H and is measured in Oersteds. The magnetic flux per unit area is the "magnetic induction", B, and is measured in Gauss. The "magnetization", M, is defined from B and H by the relation

$$M = \frac{B}{\mu_o} - H \quad (5)$$

where

μ_o = the permeability of free space.

In a ferromagnetic material such as steel, B (magnetic induction in the material) is related to the applied magnetic field strength H by the equation $B = \mu H$ where μ is the magnetic permeability of the material. The permeability of a ferromagnetic material is not constant so that B is not a linear function of H. In addition, the relationship between B and H as determined by the permeability depends upon the magnetic history of the material. A typical relationship between B and H in iron is found by an experimentally measured plot of B as a function of H, more commonly known as a hysteresis loop as shown in Figure 23.

The hysteresis loop begins with an unmagnetized specimen and as H is increased from zero, B increases rapidly, then less rapidly, and finally begins to saturate (B_s). As H is then decreased, B also decreases in a generally reversed fashion, but at H = 0, B still retains a significant value known as the remnant field (B_r). At this point the material has the properties

4529

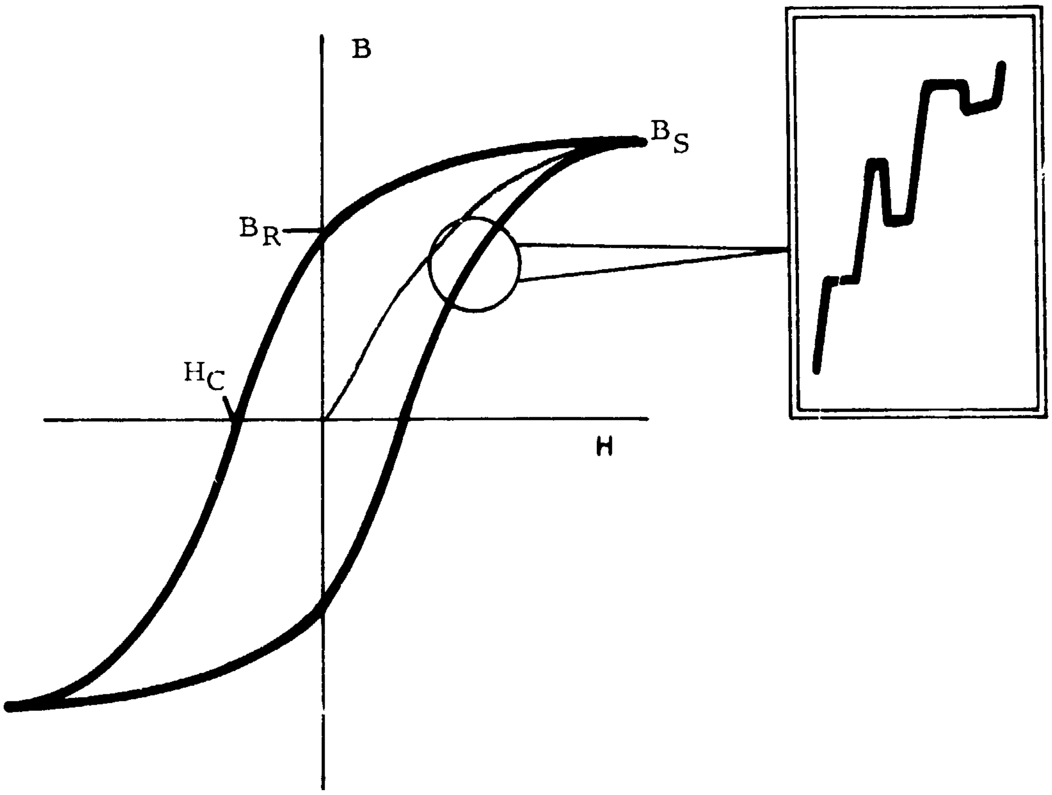

FIGURE 23. TYPICAL HYSTERESIS LOOP FOR IRON. Inset shows a magnified portion of the curve as consisting of discrete "jumps".

a permanent magnet. If the polarity of H is reversed and increased in the negative direction, B continues to decrease to zero. The value of H at this point is the coercive force (H_c). As the magnetization cycle is continued, the hysteresis curve follows the same pattern into the negative region. Repetition of the application of H causes the complete BH curve to be retraced.

An examination of the BH relationship on a microscopic scale suggests that an unmagnetized ferromagnetic material consists of small regions called magnetic domains, each of which is always magnetized to saturation. The random orientation of these domains or microscopic permanent magnets results in an average net bulk magnetization of zero. As an external magnetic field (H) is applied, the domains tend to become reoriented in a direction such that each domain is aligned with the applied field. The domain wall boundaries shift, as domains favorably oriented with respect to the applied field grow at the expense of unfavorably oriented domains. These actions account for changes in B in the specimen. If the magnetic hysteresis loop is examined on a sufficiently small scale, it is seen to be composed of small abrupt shifts rather than continuous, smooth changes. These shifts, illustrated in Figure 23, are introduced by domain behavior.

The effect of tensile stress on magnetic parameters of iron is examined by Bozorth(12), who shows that the value of B at saturation as well as the remnant field, decreases with applied tensile stress. A slight decrease in the coercive force is also observed. The saturation induction (BH at saturation) should be unaffected by stress within the elastic limit.

The behavior of magnetic domains with stress is of course related to changes in the magnetic parameters of a material. Bozorth shows that application of stress tends to cause a realignment of the magnetic domains according to the direction and magnitude of the applied stress. Magnetic domain behavior with stress is reflected in measurements involving the Barkhausen effect, in which an applied cyclic magnetic field induces abrupt domain growth and reorientation which can be sensed as voltage pulses in an inductive pickup coil. The Barkhausen effect has been shown to be stress sensitive; tensile stress causes an increase in the sensed domain activity while a compressive stress results in a decrease in activity.

Specimen Selection for Magnetics Experiments

Specimen selection for the magnetics tests is obviously limited to bolts of ferromagnetic steels. Previous experiments utilizing the Barkhausen technique on bolts as reported by Reimherr and Barton(10) employed 3/8-inch grade 5 hex-head bolts nominally 3 inches long as specified by MIL STD MS90726. Since some experimental Barkhausen data were already available for these bolts, they were included as specimens for this experimental program. Figure 24 is the specification for these bolts.

ORIGINAL PAGE IS
OF POOR QUALITY

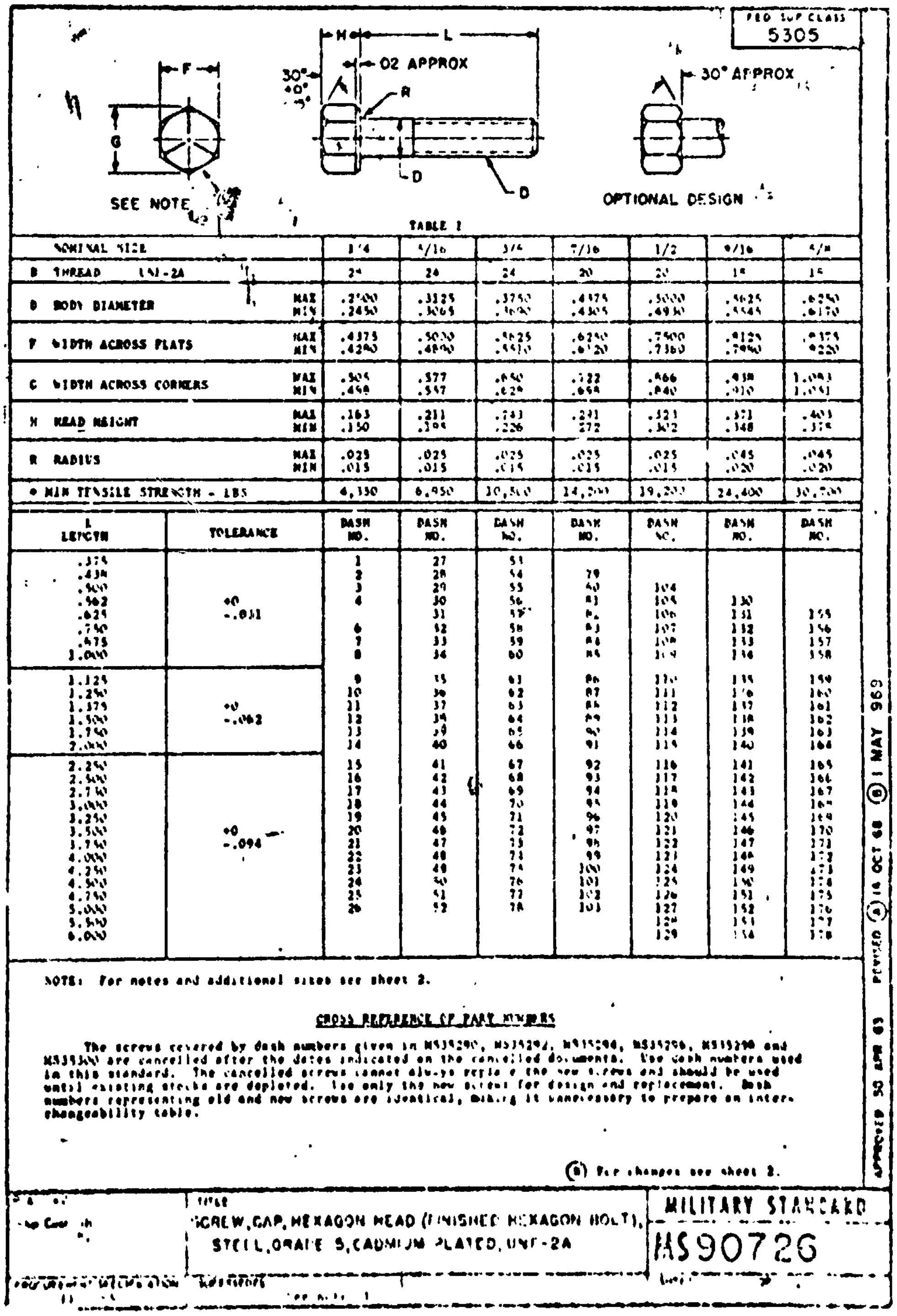
FED SUP CLASS
5305
H
L
.02 APPROX
30°
+0°
-5°
R
F
G
D
D
SEE NOTE
30° APPROX
OPTIONAL DESIGN
APPROVED 30 APR 63 REVISED (A) 16 OCT 68 (B) 1 MAY 969

TABLE I

NOMINAL SIZE		1/4	5/16	3/8	7/16	1/2	9/16	5/8
B THREAD UNF-2A		28	24	24	20	20	18	18
D BODY DIAMETER	MAX MIN	.2500 .2450	.3125 .3065	.3750 .3690	.4375 .4305	.5000 .4930	.5625 .5545	.6250 .6170
F WIDTH ACROSS FLATS	MAX MIN	.4375 .4280	.5000 .4890	.5625 .5510	.6250 .6120	.7500 .7360	.8125 .7950	.9375 .9220
G WIDTH ACROSS CORNERS	MAX MIN	.505 .488	.577 .557	.650 .628	.722 .698	.866 .840	.938 .910	1.083 1.051
H HEAD HEIGHT	MAX MIN	.163 .150	.211 .195	.243 .226	.291 .272	.323 .302	.371 .348	.403 .378
R RADIUS	MAX MIN	.025 .015	.025 .015	.025 .015	.025 .015	.025 .015	.045 .020	.045 .020
• MIN TENSILE STRENGTH - LBS		4,350	6,950	10,500	14,200	19,200	24,400	30,700

L LENGTH	TOLERANCE	DASH NO.	DASH NO.	DASH NO.	DASH NO.	DASH NO.	DASH NO.	DASH NO.
.375	+0 -.031	1	27	53				
.438		2	28	54	79			
.500		3	29	55	80	104		
.562		4	30	56	81	105	130	
.625			31	57	82	106	131	155
.750		6	32	58	83	107	132	156
.875		7	33	59	84	108	133	157
1.000		8	34	60	85	109	134	158
1.125	+0 -.062	9	35	61	86	110	135	159
1.250		10	36	62	87	111	136	160
1.375		11	37	63	88	112	137	161
1.500		12	38	64	89	113	138	162
1.750		13	39	65	90	114	139	163
2.000		14	40	66	91	115	140	164
2.250	+0 -.094	15	41	67	92	116	141	165
2.500		16	42	68	93	117	142	166
2.750		17	43	69	94	118	143	167
3.000		18	44	70	95	119	144	168
3.250		19	45	71	96	120	145	169
3.500		20	46	72	97	121	146	170
3.750		21	47	73	98	122	147	171
4.000		22	48	74	99	123	148	172
4.250		23	49	75	100	124	149	173
4.500		24	50	76	101	125	150	174
4.750		25	51	77	102	126	151	175
5.000		26	52	78	103	127	152	176
5.500						128	153	177
6.000						129	154	178

NOTE: For notes and additional sizes see sheet 2.

CROSS REFERENCE OF PART NUMBERS

The screws covered by dash numbers given in MS35290, MS35292, MS35294, MS35296, MS35298 and MS35300 are cancelled after the dates indicated on the cancelled documents. Use dash numbers used in this standard. The cancelled screws cannot always replace the new screws and should be used until existing stocks are depleted. Use only the new screws for design and replacement. Dash numbers representing old and new screws are identical, making it unnecessary to prepare an interchangeability table.

(B) For changes see sheet 2.

TITLE
SCREW, CAP, HEXAGON HEAD (FINISHED HEXAGON BOLT),
STEEL, GRADE 5, CADMIUM PLATED, UNF-2A

MILITARY STANDARD
MS90726

FIGURE 24. SPECIFICATIONS FOR ONE BOLT TYPE USED IN THE MAGNETICS EXPERIMENTS

In order to extend the measurements to a similar, but higher strength bolt, and to demonstrate measurements on a different bolt size, 1/2"-20 grade 8 bolts (3 inches long) as specified by MIL STD MS90727 were also selected. In addition to these specimens, it was considered desirable to obtain measurements from a good cross section of bolts as produced by different manufacturing techniques and materials. Consequently, two groups of commercial type bolts (non-MIL STD) were also selected. The bolt types were 1/2"-13 and 1"-8 grade 8 bolts (5 inches in length). The 1/2-inch bolts permitted a comparison with the MS90727 1/2-inch military bolts while the 1-inch bolts were selected to assess possible problems of magnetizing such large specimens.

In addition to hex-head bolts, the applicability of magnetic techniques to a type of fastener more frequently used in aircraft applications was investigated. Brenner(3) reports torque-tension measurements on a 1/2-inch, 12-point external wrenching 180 ksi FTU steel aircraft bolt as specified by MIL STD MS21250. The radically different head design of these bolts provided an opportunity to investigate the extension of magnetic techniques to much more complex bolt head geometry as compared to the hex-head bolts. Figure 17 is the MS21250 specification (page 60).

Design of Magnetics Experiments

The experimental arrangement for the magnetics experiments with bolts is illustrated in Figures 25 and 26. A Skidmore Wilhelm hydraulic bolt loading device with a hand operated pump was utilized for applying shank load to the bolts. Although load readout can be accomplished by a built-in hydraulic pressure gage, a Houston Scientific force-washer placed under the bolt head and a BLH digital strain indicator were employed for more precise load measurements.

The magnetic circuit consisted of an electromagnet with adjustable spacing of the magnet pole pieces and interchangeable pole tips to conform to each different bolt type. All bolts selected could be accommodated with this arrangement which is shown in Figure 27.

Barkhausen measurements were made with small inductive wire-coil probes. For hex-head bolts, the probe consisted of a concentric dual-coil arrangement. An inner (load sensitive) probe coil for all bolt sizes was 4.75mm diameter, while outer (reference) coils were specially constructed for each bolt size to fit the periphery of the bolt head. This probe configuration is shown in Figure 28.

4530

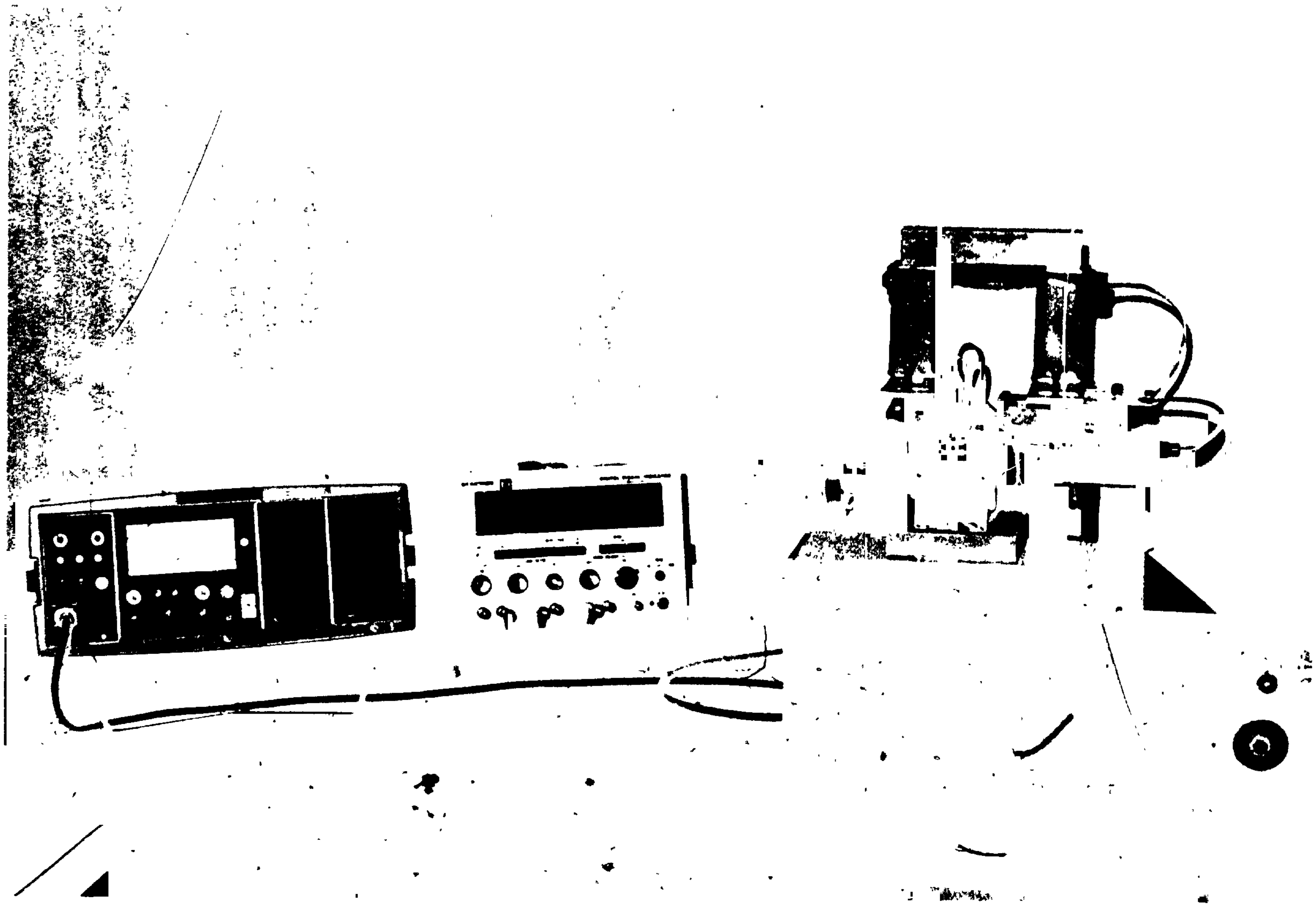

FIGURE 25. LABORATORY SET-UP FOR BARKHAUSEN NOISE INVESTIGATION OF STRESS IN BOLTS. From left a) Barkhausen instrument, b) Load indicator, c) Hydraulic bolt loader, d) Magnetization source

ORIGINAL PAGE IS
OF POOR QUALITY

4531

FIGURE 26. CLOSEUP VIEW OF SKIDMORE-WILHELM LOADER AND MAGNETIC CIRCUIT. Barkhausen probe is located over bolt head in center.

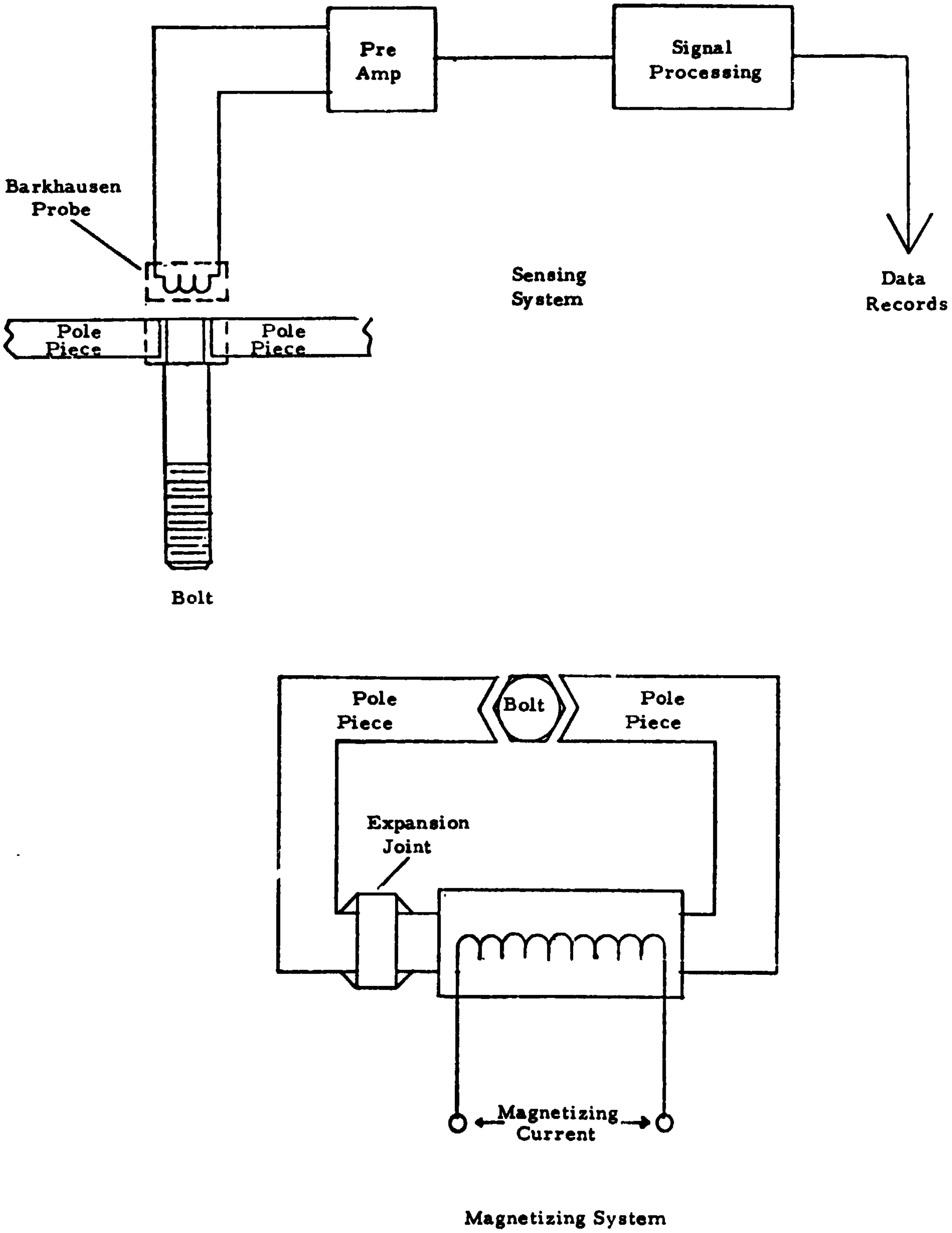
Pre Amp
Signal Processing
Barkhausen Probe
Sensing System
Data Records
Pole Piece
Pole Piece
Bolt
Pole Piece
Bolt
Pole Piece
Expansion Joint
Magnetizing Current
Magnetizing System

3842

FIGURE 27. SCHEMATIC OF BARKHAUSEN BOLT INSPECTION SYSTEM

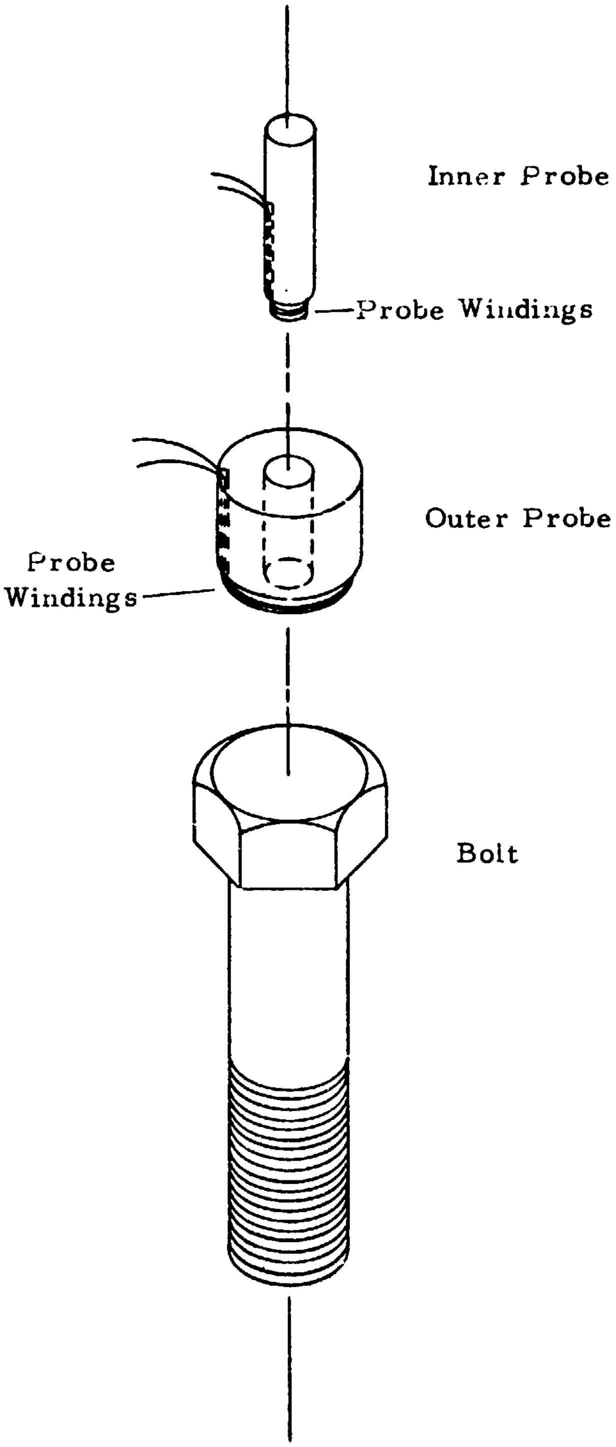
Inner Probe
Probe Windings
Outer Probe
Probe Windings
Bolt

3847

FIGURE 28. CONCENTRIC PROBE CONFIGURATION

The magnetic induction B and, consequently, the magnetization M within a ferromagnetic specimen are both functions of the applied magnetic field H and tend to be influenced by stress conditions within the material. In addition, the saturation induction (BH at saturation) should be independent of stress within the plastic limit. For these reasons it was envisioned that the measurement of these magnetic parameters could serve as a bolt load measurement system, but would most likely be useful as a complement to a Barkhausen noise analysis approach. The magnetic parameter measurements were planned to be taken simultaneously with Barkhausen measurements using the same magnetizing circuit arrangement.

The measurement of B, H and M was intended to be accomplished by generating a magnetic hysteresis loop for each bolt. The hysteresis loop, essentially a measurement of B as a function of H, normally is measured on special ring-shaped or long-rod specimens. Primary windings wrapped directly on the toroid or rod provide the applied magnetic field (H) when energized with an electric current, the magnitude of which is proportional to H. Secondary windings sense the magnetic induction (B) as an induced voltage when the applied magnetic field is rapidly changed. In either case, precise measurement of magnetic parameters can be accomplished only through the use of special specimen shapes. The relatively complicated bolt head geometry does not readily lend itself to measuring a hysteresis loop. For practical applications, the magnetic field must be applied to the bolt head through the pole pieces of an electromagnet.

A reasonably good approximation can be achieved by measuring the air gap flux near the bolt head surface. Due to the constraints of this arrangement, one can no longer measure B alone as a function of H, but can measure a quantity related to the specimen magnetization M. It is thus not possible to obtain an exact hysteresis loop for the specimen with well defined magnetic parameters. Changes in the magnetic parameters with stress should still, however, be reflected in the measured leakage flux.

In each series of magnetics experiments performed, a selected bolt specimen was loaded to various values of shank tension, from zero to proof load, in the tensioning equipment. At each load value, the appropriate magnetic parameters were recorded. Specific instrumentation is described in connection with specific experiments.

Magnetic Parameter Experimental Results

A 3/8-inch grade 5 bolt (MS90726) was selected for an experiment to determine the feasibility of the BH measurement approach. The bolt was loaded with the hydraulic loading fixture, equipped with an accurate load readout from a mechanical load cell and specimen magnetization was oriented across the hexagonal bolt head as shown in Figure 27. The electromagnet and pole pieces were constructed to conform to the bolt head.

A flat Hall-effect probe with an active area of 2mm x 4.75mm was used in conjunction with an RFL digital gauss meter for measuring the relative leakage flux vs. load cell readings. The Hall probe was oriented in a variable airgap in one side of the pole piece, as well as at various locations on and above the polepiece-bolthead junction. Optimum response was obtained with the probe located as shown in Figure 29, above a 1.6mm gap between the magnet pole piece and the bolt head. No other positions yielded a significant change in magnetic flux with mechanical load.

The magnetic leakage flux was measured at zero load and at bolt proof load (7,400 lbs.) as a function of magnetizing current, where the magnetizing current is directly proportional to the applied magnetic field intensity H. Figure 30 is a plot of the results. The maximum sensitivity to load occurred at 1.5 amps where a flux change of 15 Gauss was obtained over the entire load range of the bolt. This represents only a 3% signal change. No parameter could be isolated which was not stress sensitive at magnetic saturation and therefore might be related to material properties as discussed earlier. However, this was probably due to an inability to actually saturate the bolt head itself. The circuit could be driven to saturation, but because of the geometry, leakage flux was probably too great to saturate the bolt.

The measurement of B, H or M as a stress indicator or as an indicator of magnetic material properties in bolts is seen to be hampered by the complex geometry of the bolt head, the materials in the joint and other considerations. A precise determination of the exact magnetic parameters of interest, isolated from other parameters, is very difficult. Due to these complicating factors and the small stress effect over the entire load range, this offers little help in combination with a Barkhausen approach. For these reasons, tests involving hysteresis loop measurements were not pursued further.

Barkhausen Effect Experiments

In 1917, Barkhausen(13) discovered that voltages induced in a coil encircling a ferromagnetic specimen undergoing magnetization produced a noise when suitably amplified and applied to a speaker, even though the magnetization applied to the specimen was changed smoothly. From such experiments he inferred that the magnetization in the specimen does not increase in a strictly continuous way, but rather by small, abrupt discontinuous increments, now called "Barkhausen jumps". Such jumps are caused, principally, by the discontinuous movements of mobile magnetic boundaries (Bloch walls) between adjacent magnetic domains and occasionally by the initiation of new magnetic domain walls. Furthermore, the direction and magnitude of the mechanical stress existing in a macroscopic ferromagnetic specimen strongly influences the detailed dynamics of the domain wall motion and correspondingly influences the Barkhausen noise.

4532

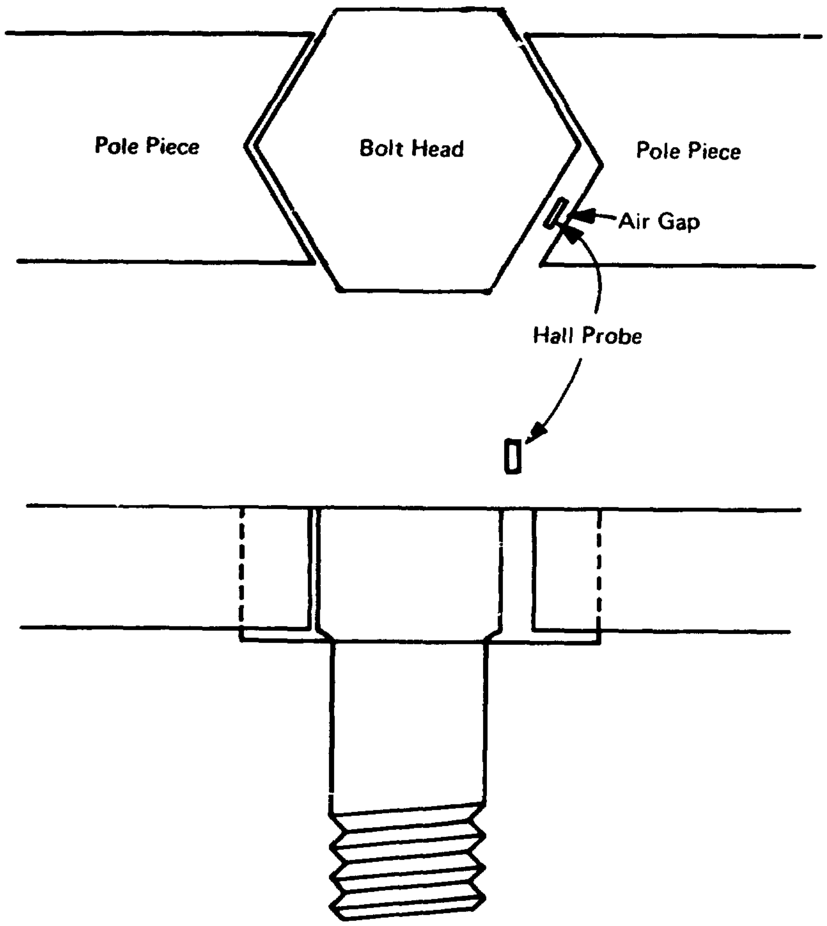
Pole Piece
Bolt Head
Pole Piece
Air Gap
Hall Probe

Fig. 29. Magnetic Circuit Arrangement for Measurement of Fringing Flux as an Indication of "B"

FIGURE 30. 3/8-in. Bolt
MAGNETIC HYSTERESIS LOOP MEASUREMENTS VS. MAG. CURRENT AT 0 AND FULL LOAD. BOLT NO. 32
PROBE LOCATED ABOVE .063IN. AIR GAP.

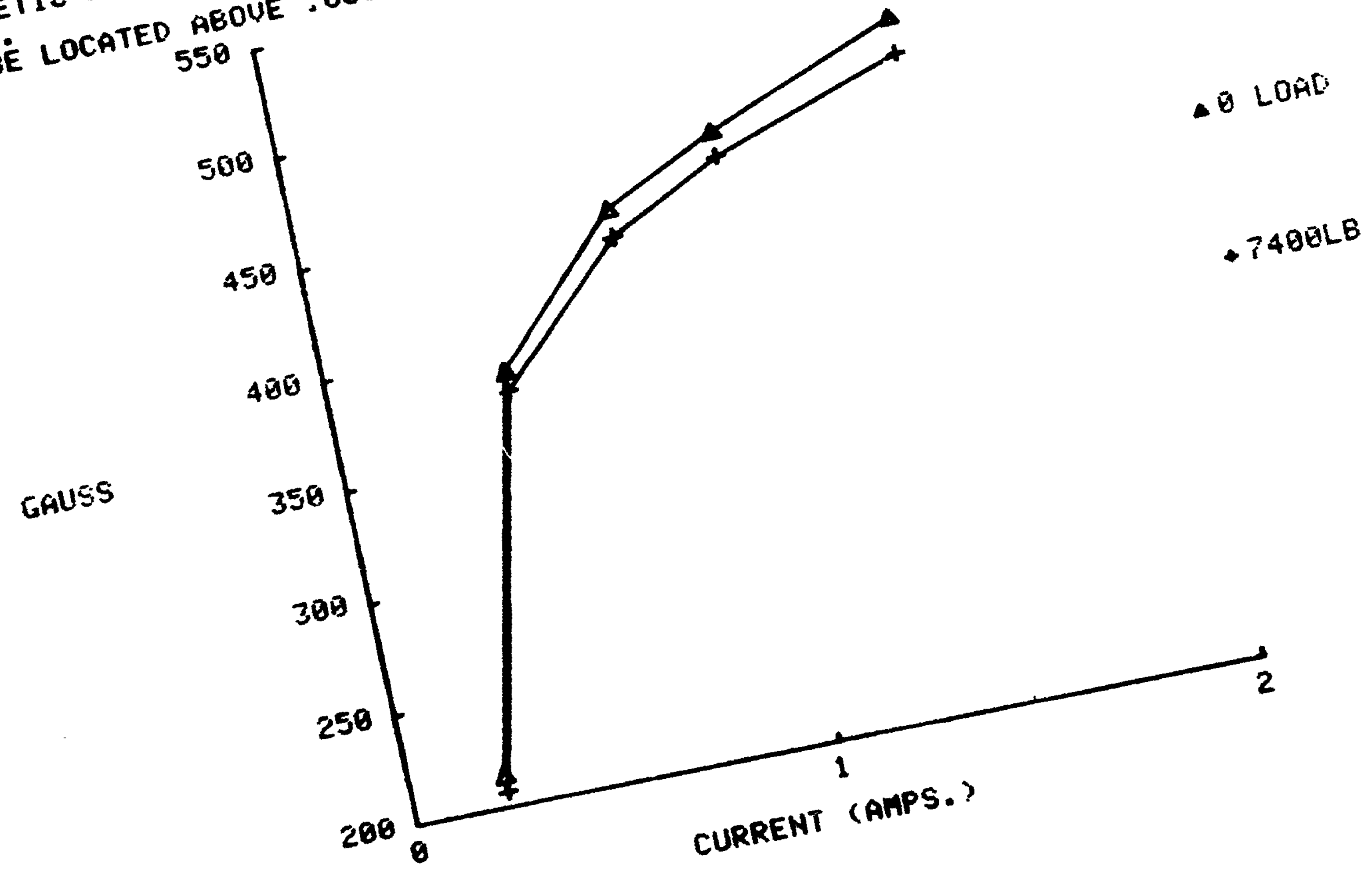

The Barkhausen technique as applied to shank tension measurement in bolts must rely on measurement of the resultant surface stress introduced in the bolt head by shank loading. For a typical hex-head bolt, the surface stress on top of the bolt head near the center experiences compression as the shank is loaded in tension. Investigation of this surface stress, reflecting the tensile stress in the shank in a loaded bolt, was reported in Chapter of this report. Compressive stress results in a decrease in Barkhausen noise activity as shank load is increased. This concept forms the basis for the Barkhausen tests performed in this program.

The Barkhausen noise response is produced by applying a cyclic (typically 1 Hz) magnetic field to the bolt head and sensing the Barkhausen signal bursts with an inductive pickup coil located at a region exhibiting good surface stress response to shank load. A schematic of a typical setup was shown in Figure 27, page 75. The Barkhausen response is primarily sensitive to stresses which lie in the direction of applied magnetization. Thus, with the arrangement shown in Figure 27, response to radial surface stress is obtained on top of the bolt head and response to hoop surface stress is obtained on the flat at the side of the head.

Since the resultant surface stress is not constant across the head, it is possible to utilize a dual measurement procedure in which Barkhausen noise is sensed at two locations on the head: one maximum and a reference probe located where stress response remains essentially zero. If the relatively constant signal from the reference probe is divided by the decreasing signal from the load sensing probe, a response results that increases with increasing tensile shank load. This ratio technique was reported by Reimherr and Barton to partially compensate for variations in Barkhausen response from bolt to bolt and to reduce probe lift-off effects which would result from raised markings existing on the bolt head. A diagram of a typical dual probe arrangement as utilized for ratio measurements was illustrated in Figure 28, page 76.

Instrumentation for supplying the magnetizing current and for processing the Barkhausen noise signatures was provided by a system shown schematically in Figure 31, developed by SwRI. A magnetizing current with adjustable frequency, slope and amplitude is supplied to the magnetic circuit. The Barkhausen noise pulses sensed by the pickup coil are amplified and then processed to obtain envelope detection of the Barkhausen noise burst. Amplifier gain is 66 dB from 1 kHz to 100 kHz. The peak amplitude of the detected signal is measured and read out by a digital voltmeter.

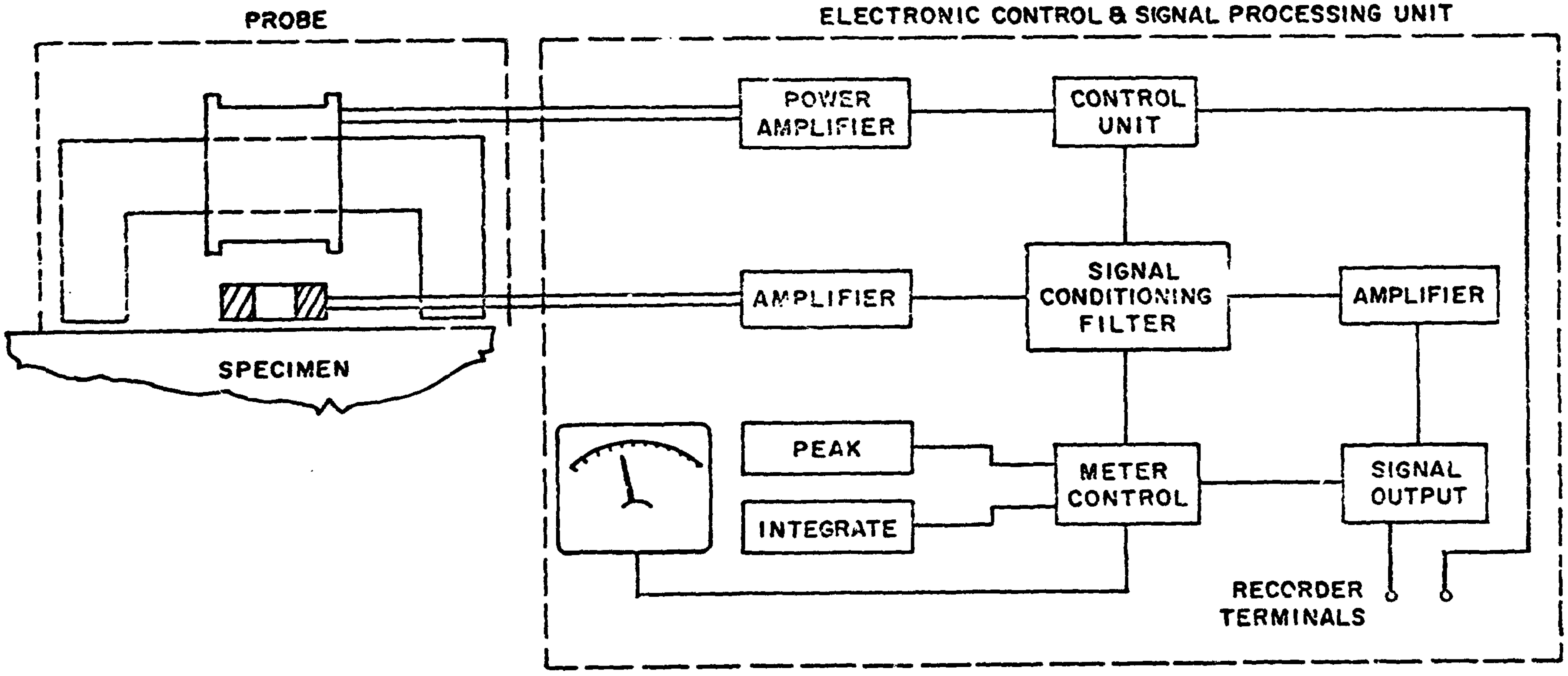
PROBE
SPECIMEN
ELECTRONIC CONTROL & SIGNAL PROCESSING UNIT
POWER AMPLIFIER
CONTROL UNIT
AMPLIFIER
SIGNAL CONDITIONING FILTER
AMPLIFIER
PEAK
INTEGRATE
METER CONTROL
SIGNAL OUTPUT
RECORDER TERMINALS

FIGURE 31. SCHEMATIC DIAGRAM OF ESSENTIAL COMPONENTS OF STRESS MEASURING INSTRUMENT BASED UPON THE STRESS DEPENDENCE OF THE BARKHAUSEN EFFECT

Results of Barkhausen Experiments

In these experiments Barkhausen noise response measurements were made on each of 76 bolts of five types, at five shank load values ranging from zero to proof load. Proof load values were obtained from the applicable SAE specification or MIL STD for each bolt.

Hex-head Bolts

As mentioned previously, dual concentric coil probes were utilized for measurements on hex-head bolts. The inner probe, nominally on the center of the head, is in the region over which the finite-element stress analysis shows maximum radial surface stress sensitivity to shank load. In addition, this region exhibits a low stress gradient, relatively insensitive to small changes in probe position. Figure 32 shows typical response to load from the inner probe only, obtained on a 3/8-inch grade 5 bolt. Outer (reference) probe measurements were also made near the periphery of the bolt head, in a region where stress sensitivity is much lower. Figure 33 is a plot of the response of the outer probe obtained from the same 3/8-inch grade 5 bolt. A combination of these two measurements into a ratio (outer/inner), results in the plot in Figure 34 in which response increases with increasing shank load. In the following data analysis, both inner probe measurements and ratio measurements are examined to determine optimum measurement techniques and associated problems.

Inner Probe Only

Inner and outer probe data were obtained from ten 3/8"-24 grade 5 bolts (MS90726) at shank loads of 0, 1850, 3700, 5550, and 7400 pounds, where 7400 pounds is the proof load value. Considering first the inner probe only, the mean of the measurements from this central head area for all ten bolts is plotted along with one standard deviation in Figure 35. Statistically, 68% of all the data should fall within this range of one standard deviation. The Barkhausen signal is shown to respond well to shank load; however, data scatter from bolt to bolt limits accuracy as predicted by the finite element analysis. From the plot it can be seen that measurement uncertainty at proof load is high. For example, consider a Barkhausen signal (on the arbitrary scale in the figure) of 2.2 volts. The plot indicates that this reading could indicate shank loads from 3500 to 7400 pounds, a total of 53% variation.

Data from twenty-five 1/2"-13 grade 8 commercial bolts (non MIL STD) were obtained in the same way, at shank loads of 0, 4250, 8500, 12,750, and 17,000 pounds, the latter representing proof load. The inner probe Barkhausen measurements are plotted in Figure 36. Here, the response to stress is also good; however, data scatter is seen to be high. A Barkhausen reading of 1.6 volts could represent shank loads ranging from 2,000 to 17,000 pounds, an 88% variation in load.

FIGURE 32 BARKHAUSEN SIGNATURE, 3/8" BOLT, MEAS. AT CENTER OF HEAD VS. SHANK LOAD

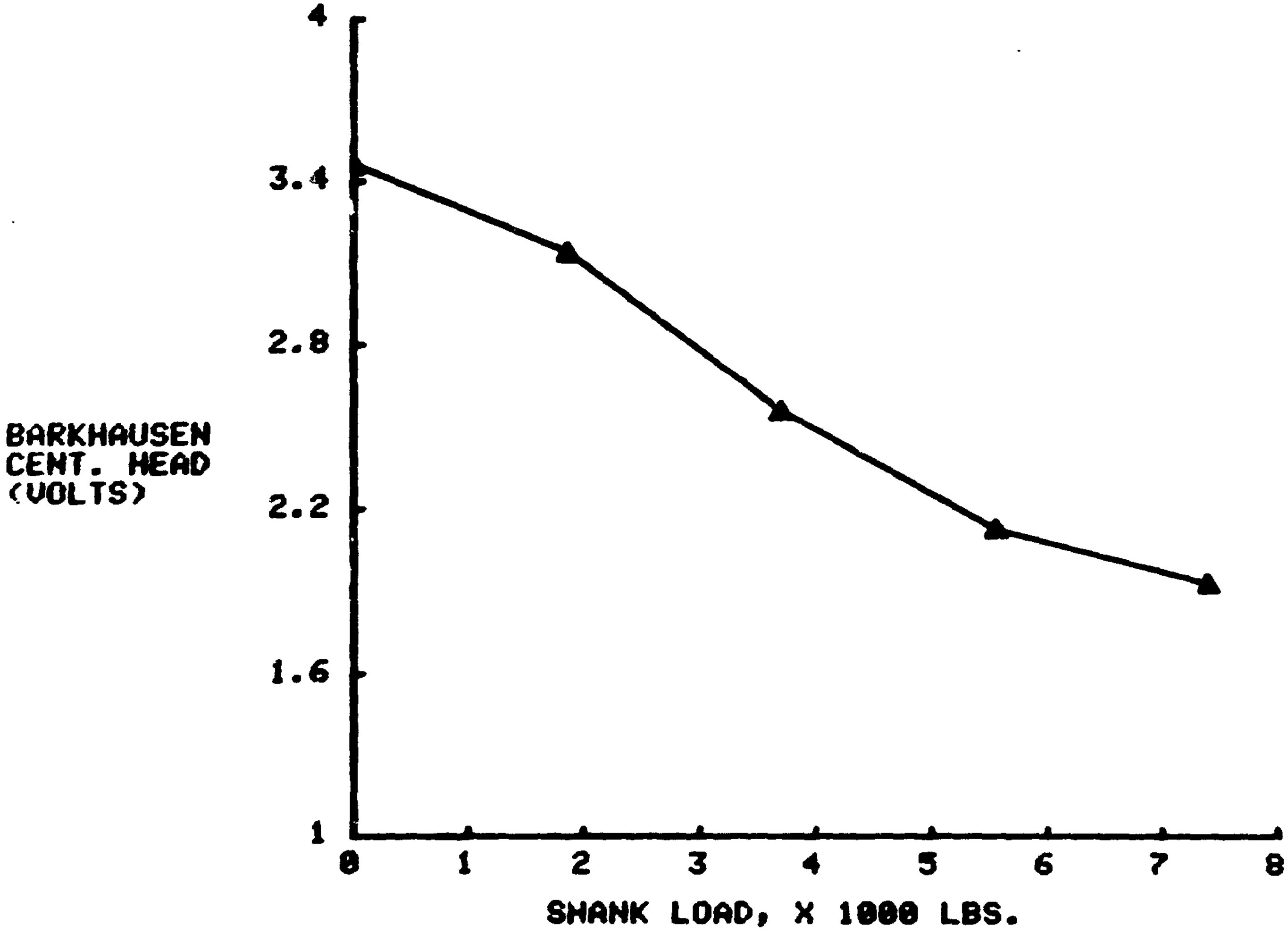

FIGURE 33 BARKHAUSEN SIGNATURE, 3/8" BOLT, MEAS. AT OUTER PERIPHERY ON TOP OF BOLT HEAD

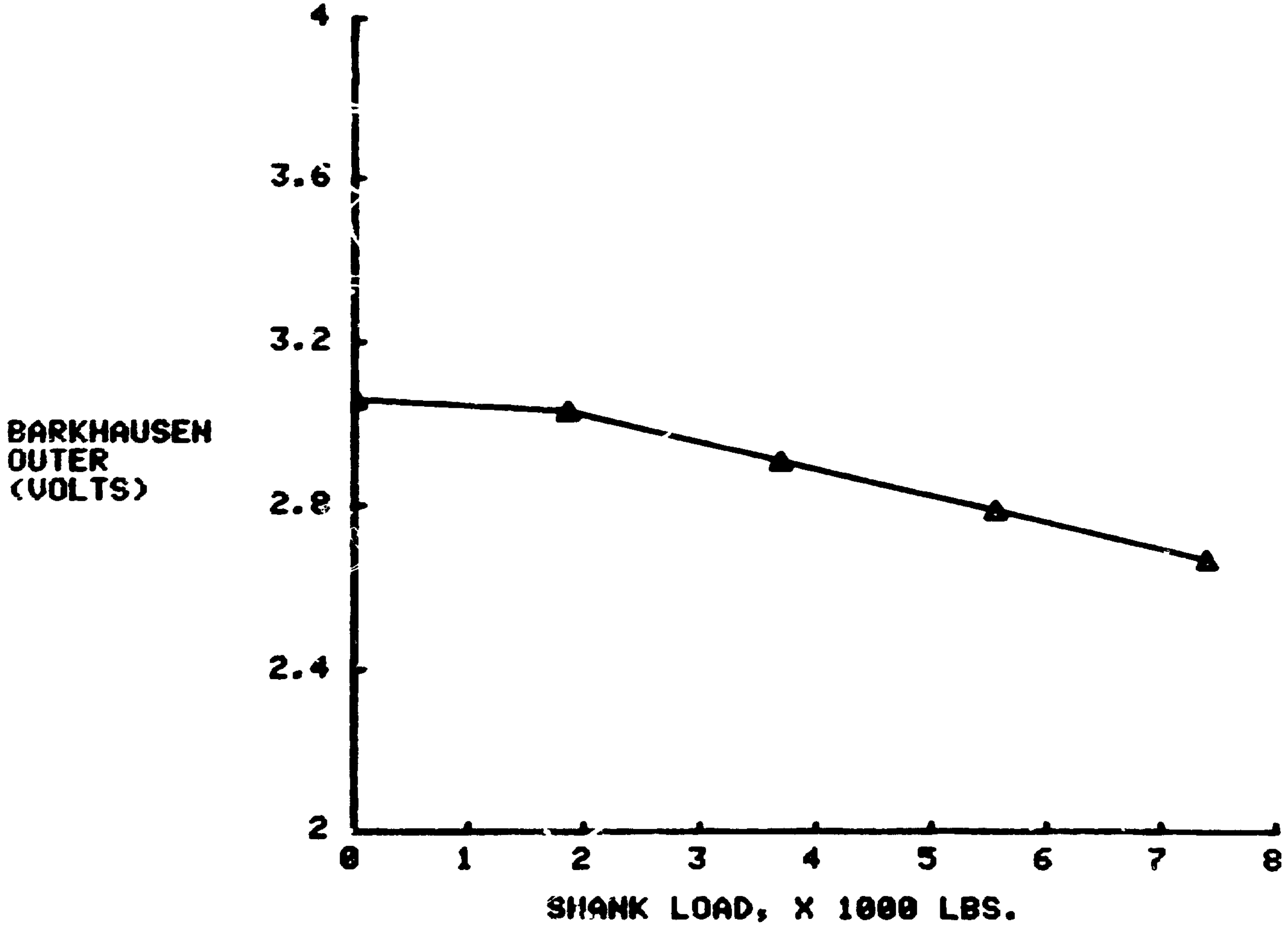

C-2

FIGURE 34 RATIO OF OUTER TO INNER BARKHAUSEN MEASUREMENT, 3/8" BOLT

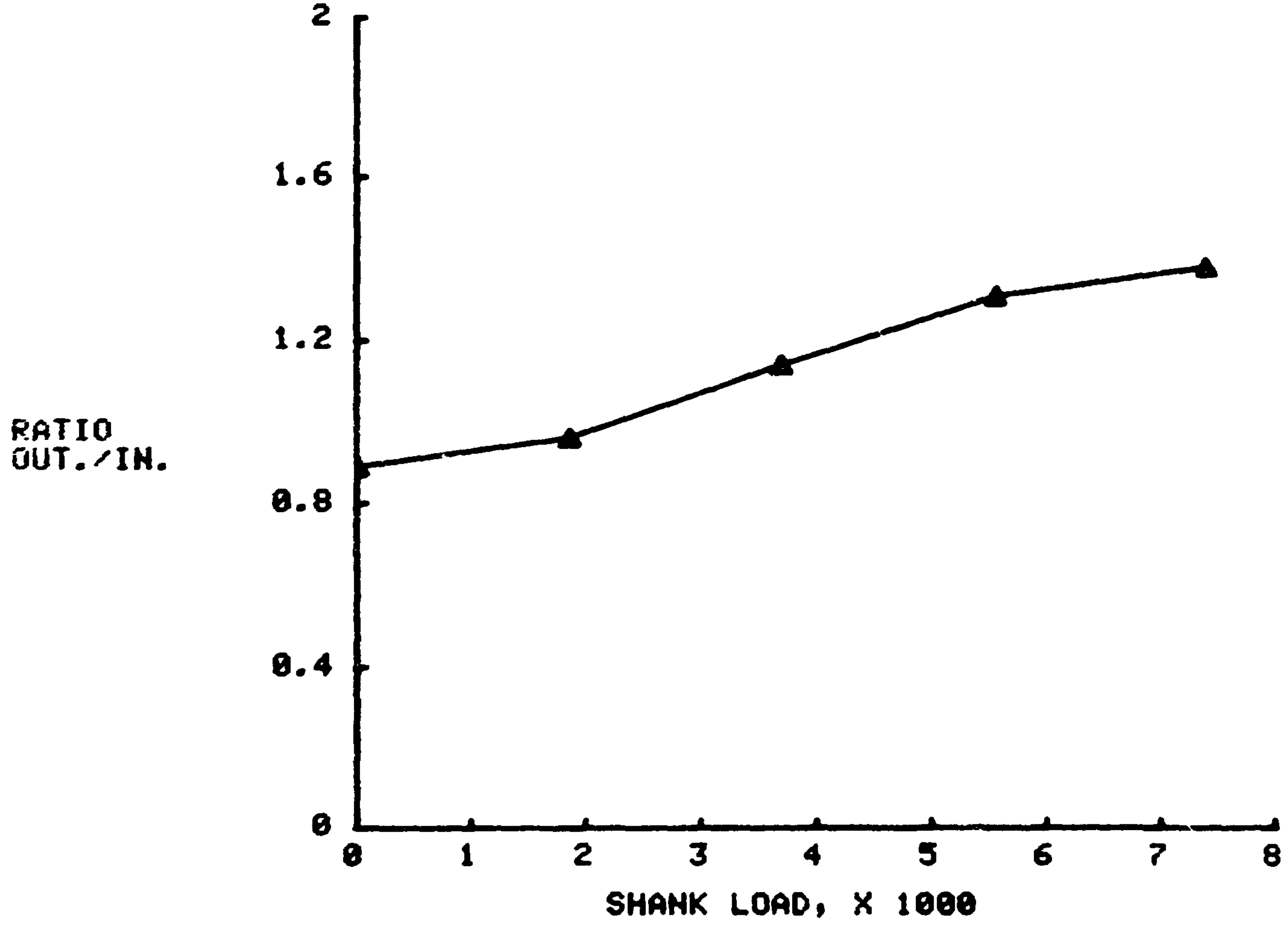

FIGURE 35.
3/8IN. GRADE 5 BOLTS #30-#39
INNER PROBE MEASUREMENTS

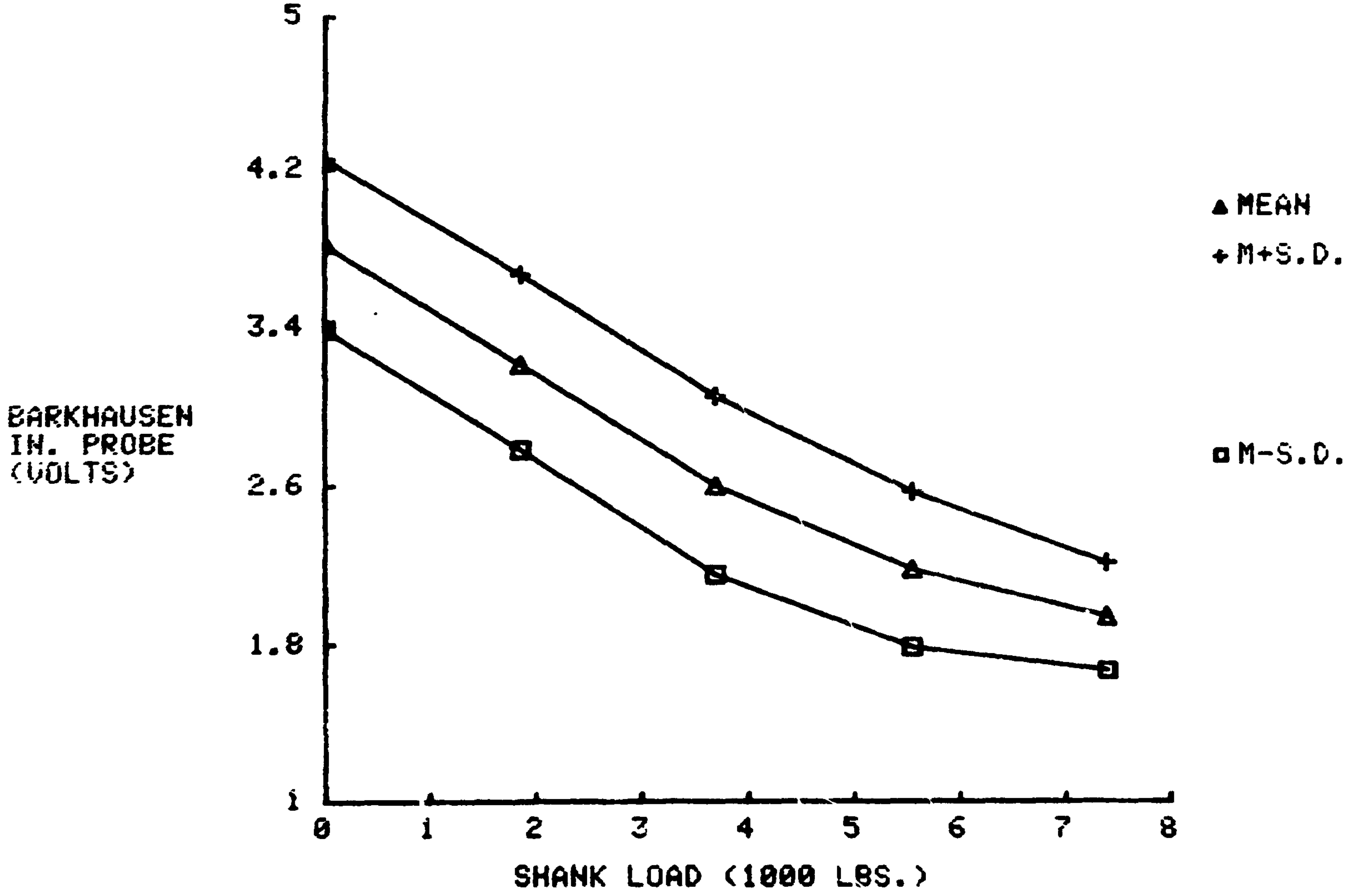

FIGURE 36.
1.2IN. GRADE 8 BOLTS (CAT.)
#2-0 THRU #2-24
INNER PROBE

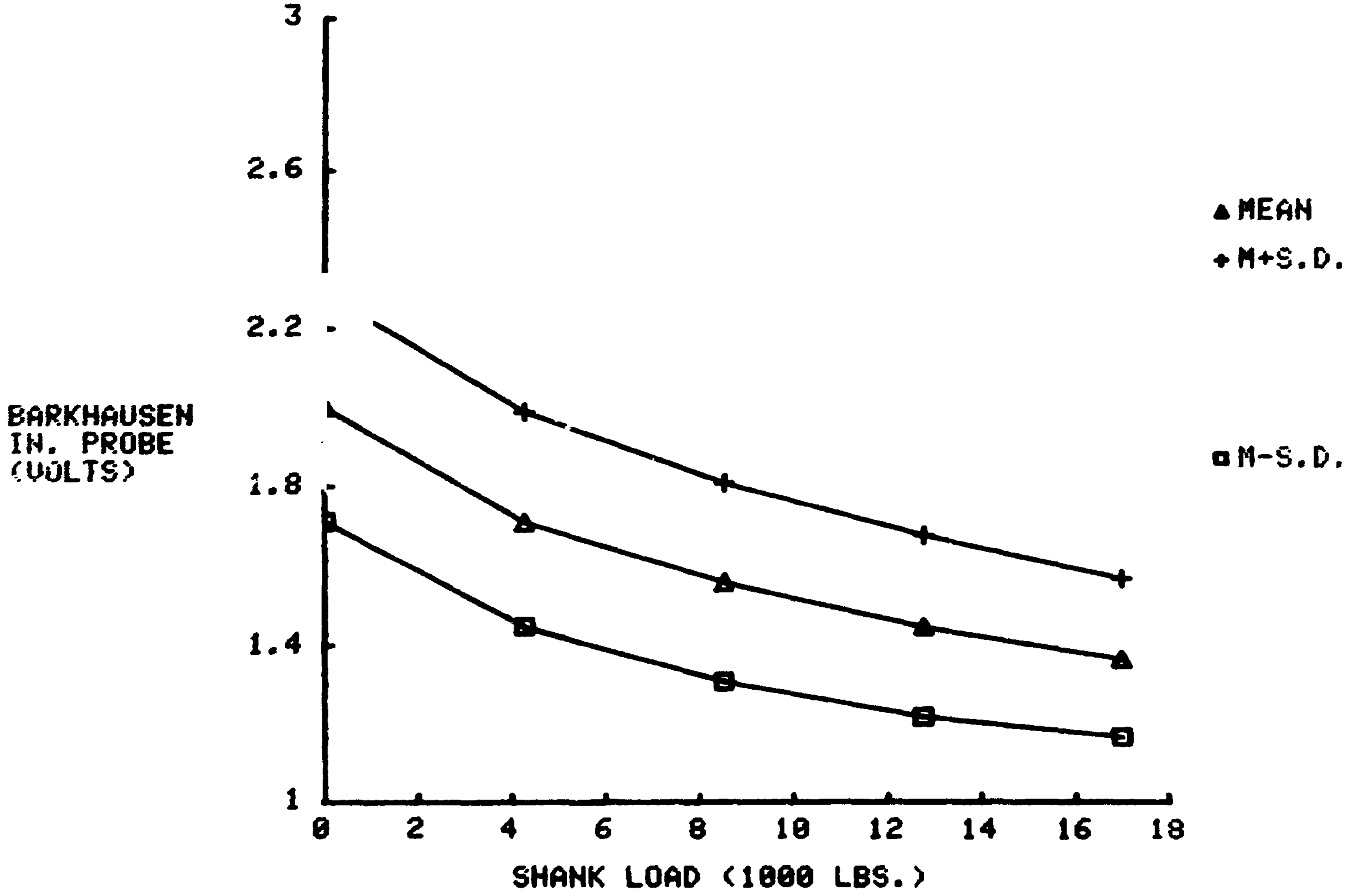

Twenty-five 1"-8 grade 8 commercial bolts similar to the 1/2"-13 bolts were also examined. Shank loads were 0, 18,175, 36,350, 54,525 and 72,700 lbs. Figure 37 is a plot of the inner probe data. Somewhat less scatter is observed in these data compared to the 1/2" bolts, but even so, a Barkhausen reading of 0.8 volts could represent a bolt load between 43,000 and 72,700 lbs. which represents a 41% variation in load.

A group of ten 1/2"-20 grade 8 (MS90727) bolts were also tested at shank loads of 0, 4800, 9600, 14,400, and 19,200 pounds. Measurements on these bolts produced surprising results, in that repeated loading of each bolt resulted in continually decreasing Barkhausen signatures at low shank loads, particularly at no load. This effect was not observed in the previous bolts, and may reflect magnetic material properties of a slightly unusual nature. One bolt was carried through eleven load cycles before the no-load signal amplitude stabilized. Figure 38 is a plot of the Barkhausen readings at no-load and proof load versus the number of load cycles. This plot shows that the largest change occurred between the first and second loading. Because of these results, measurements were made on all ten bolts in this group over two load cycles. Figure 39 is a plot of the mean and standard deviation for the first load cycle of all ten bolts as a function of shank load. Figure 40 is a similar plot taken during the second load cycle. A comparison of Figures 39 and 40 shows that Barkhausen measurements at low shank load have decreased significantly from the first to the second loading, while the readings at full load have remained approximately the same. The reason for this decrease is not entirely clear. The bolt material is apparently either experiencing a degree of plastic deformation with loading, or is particularly sensitive to magnetic history with stress. Whatever the cause, this represents a significant complication in the use of the magnetic measurements.

To be certain the bolts had been properly heat treated, hardness tests were performed on two sample bolts. Hardness values specified by MIL SPEC FF-S-85C allow a hardness range of Rockwell C-32 to C-38. Measured hardness values on these two bolts were C-32.5 and C-32.6. Although these values are on the low end of the allowable range, they are still within tolerance and far higher than would suggest any abnormal yield behavior.

An analysis of data scatter for the first loading of all ten bolts (Figure 39) shows that, as a worst case, a Barkhausen reading of 340 mv could indicate a bolt load between 7800 and 19,200 pounds, or a variation of 59%. Data scatter for the second loading (Figure 40) is even greater. Here, a Barkhausen reading of 340 mv could represent a shank load between 4400 and 19,200 pounds - a variation of 77%.

FIGURE 37.
1IN. GRADE 8 BOLTS
#1-0 THRU #1-24
INNER PROBE

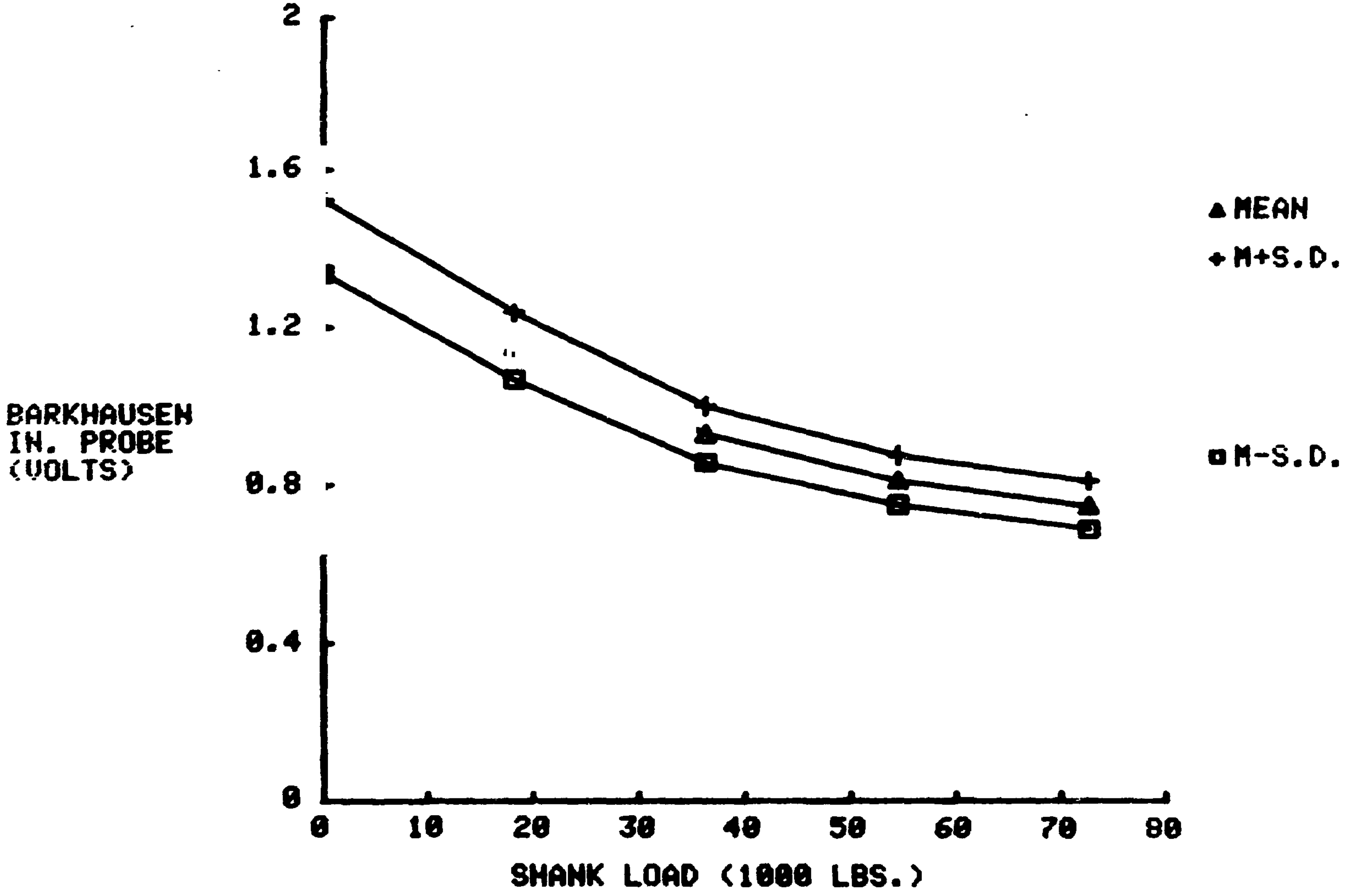

FIGURE 38.
[illegible]0727 BOLT #2
[illegible]ER PROBE READING AT 0 AND 19200 LB. LOAD VS. NUMBER OF LOADING CYCLES

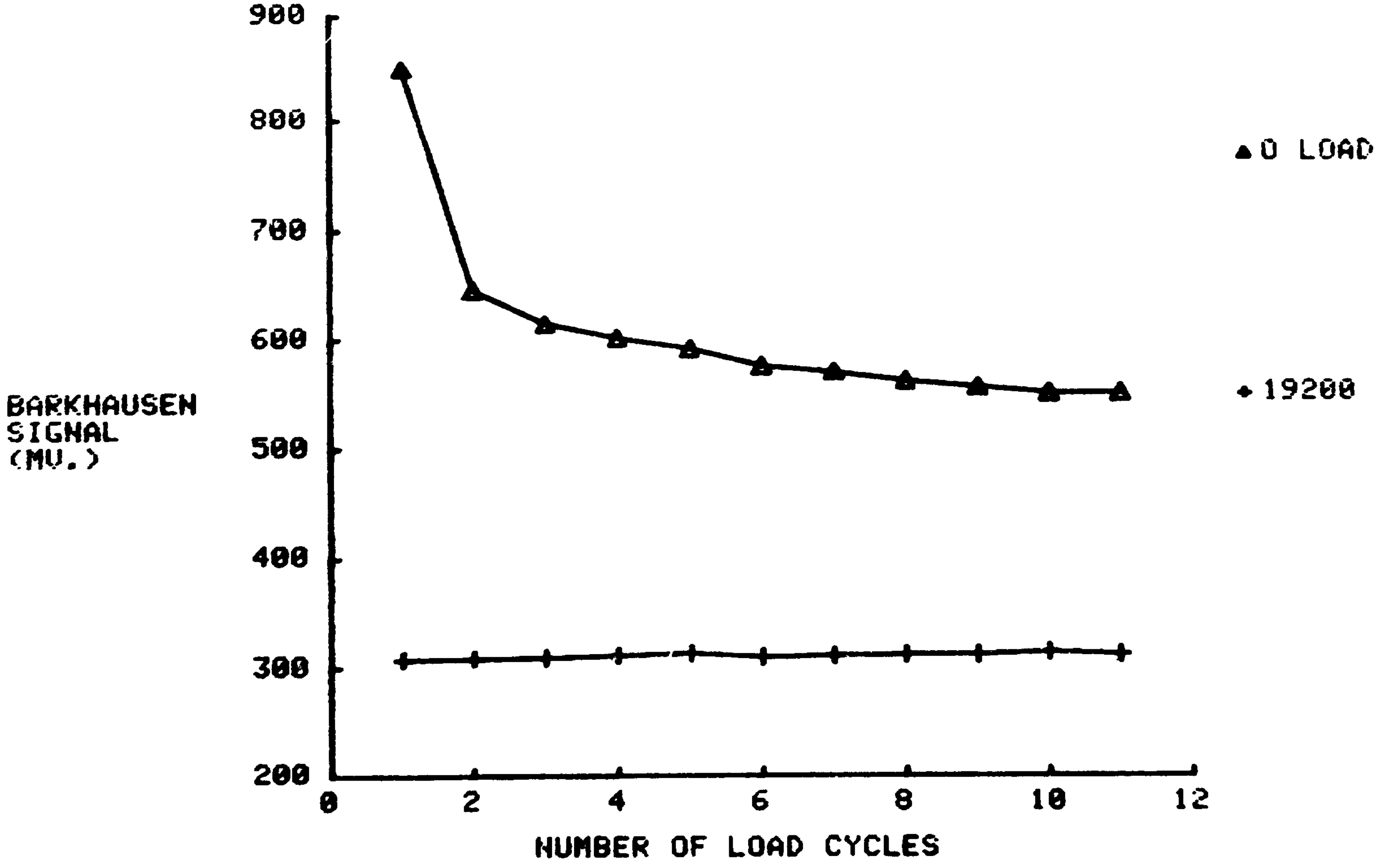

FIGURE 39.
1/2IN. GRADE 8 BOLTS (10)
FIRST LOADING
INNER PROBE

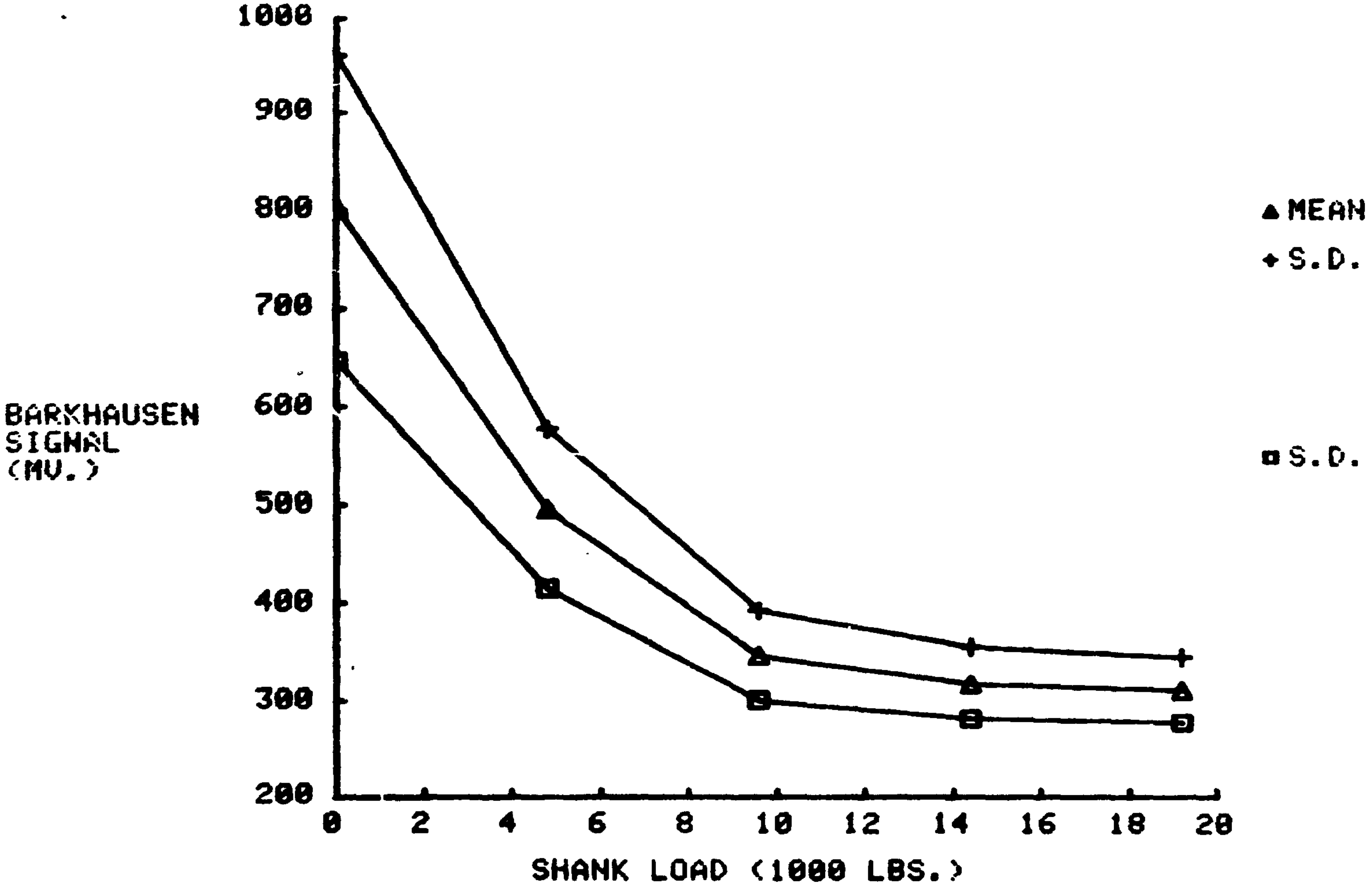

FIGURE 40.
[illegible] IN. GRADE 8 BOLTS MS90727 (10)
SECOND LOADING
INNER PROBE

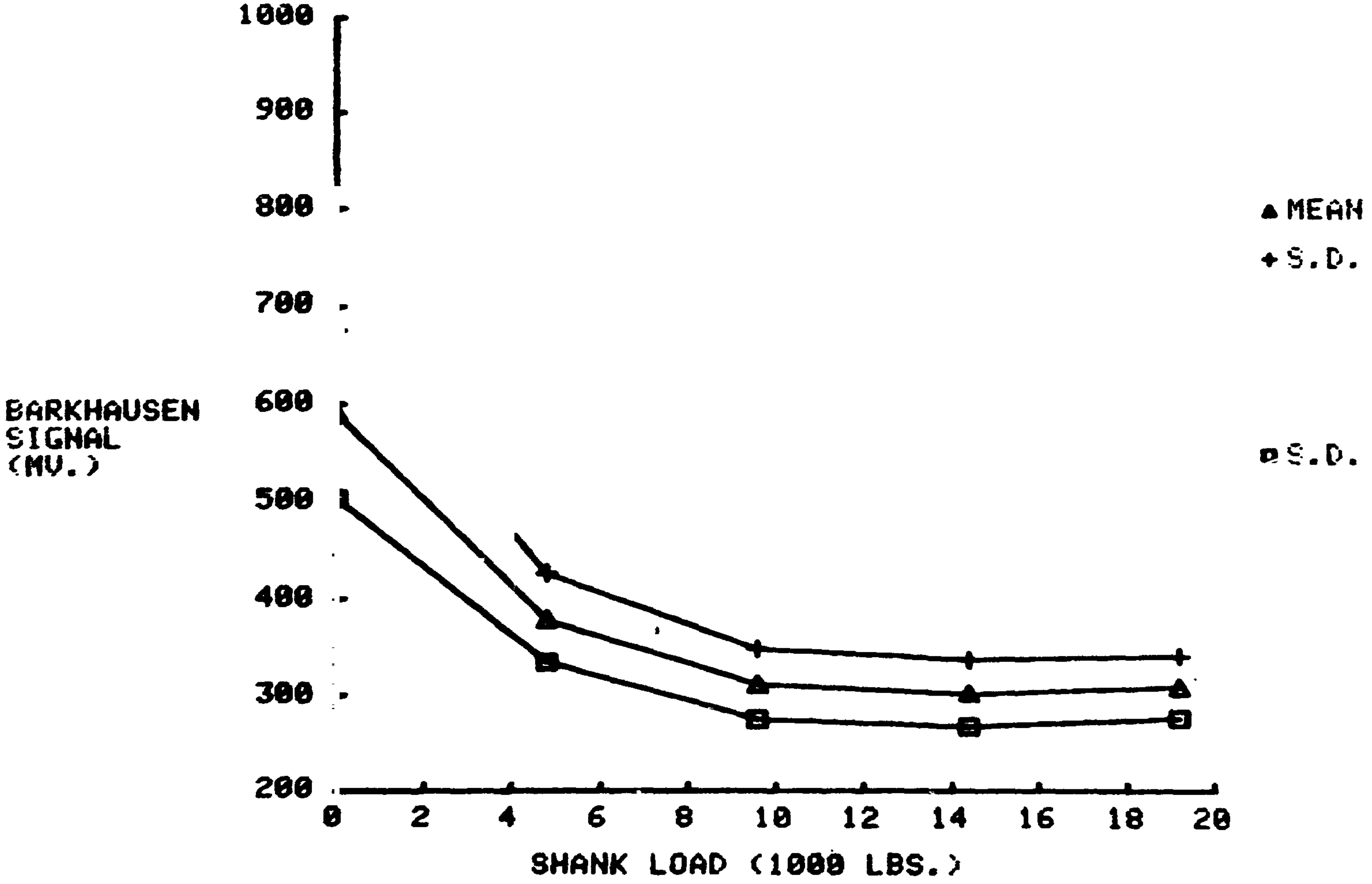

Data from all four bolt types examined shows that response to shank load can be obtained by Barkhausen measurements made on top of the bolt head. A considerable degree of data scatter exists, however, from bolt to bolt. Several factors can contribute to this situation.

First, the dimensional variations allowed by normal manufacturing tolerances were shown by the finite-element model to reflect stress variations in the head as great as 20%. This can only be accommodated by tighter dimensioning of the bolts, particularly of the head thickness.

Second, since the Barkhausen method is a magnetic technique, it is influenced by magnetic properties of the material. Changes in magnetic properties from bolt to bolt, particularly from different manufacturers and different lots, can influence the Barkhausen response to stress.

A third major influencing factor, and perhaps the most significant of all, is the effect of residual stresses present in the fastener head due to manufacture, particularly heat treatment. The Barkhausen method measures total surface stress, and distinction between residual and applied stress at a point is nondeterministic.

Another serious problem in the single-probe Barkhausen approach is the stress-saturation effect. It can be seen in the preceding plots of Barkhausen measurements that the slope of the Barkhausen response versus load is nonlinear, and tends to saturate at high shank loads. For the 1/2"-20 bolts (MS90727), this effect occurred at approximately one-half proof load on the second loading cycle. This saturation effect is typical of magnetic stress response.

Two-Probe Ratio Measurement

Barkhausen response measured by an outer probe located near the periphery of the bolt head was also recorded on the hex-head bolts. This outer probe was on an area relatively insensitive to shank loading. A ratio between the inner and outer probe measurements was then established. The ratio measurement tends to compensate probe placement errors including lift-off, and more important, should help compensate for residual stresses and material magnetic effects. A residual stress, measured by both probes, would tend to be cancelled by dividing one measurement by the other. Total residual stress compensation depends, however, on a constant residual stress level across the entire bolt head, and experiment has shown that this is not the usual case.

Outer probe measurements for the four groups of bolts examined are presented in Figures 41 through 45. The outer probe measurements are relatively insensitive to shank load, because the compressive stress reflected in the head is concentrated near the center. The response from the 3/8-inch bolts shows a 12% change from zero to full load, while the 1/2- and 1-inch grade 8 commercial bolts have an essentially flat response. The response from the 1/2-inch MS90727 grade 8 bolts is plotted for both the first and second loadings. Here, the average change over the full load range is 35% for the first loading and 20% for the second. The outer probe responses to load are in all cases much lower than the corresponding inner probe response.

The outer probe measurement for each bolt is divided by the inner probe measurement to produce a ratio measurement that increases with increased shank load. The ratio plot for the 3/8-inch grade 5 bolts is shown in Figure 46. Here, a worst case variation of data scatter at high load is represented by a ratio value of 1.4. This value could represent a bolt tightness range from 3900 to 7400 pounds or a 47% variation in load. This shows a slight but relatively insignificant improvement over the 53% load variation from the inner probe measurement only shown previously in Figure 32.

Ratio measurements for the 1/2-inch grade 8 commercial bolts are presented in Figure 47 . In this case, data scatter improvement using the ratio technique was slightly more pronounced. A worst case ratio reading of 1.75 represents a load range from 8600 to 17,000 pounds or a 79% variation in load, where the inner-probe-only data in Figure 36 showed an 88% variation in load.

The ratio data from the 1-inch grade 8 commercial bolts is shown in Figure 48. The degree of data scatter is represented by a ratio value of 1.7 which denotes a load range from 28,000 to 72,700 pounds or a 61% variation in load. Here, the ratio method actually made the data scatter worse, the inner-probe-only measurement yielding a 41% variation in load. The failure of the ratio method to improve the data from these bolts is likely related to the large head size of these bolts (1-1/2" across flats). Any residual stress gradients are likely to be greater from the center to the periphery than with smaller size bolts, introducing error into the reference probe correction. However, this remains only a supposition.

Ratio data were computed for both first and second loadings of the 1/2-inch grade 8 MS90727 bolts. Figure 49 is a plot of the first loading. Here, the ratio plot actually reverses at approximately 50% of full load. An examination of the inner and outer probe response (Figures 39 and 44), shows this effect

FIGURE 41.
3/8IN. GRADE 5 BOLTS #30-#39
OUTER PROBE MEASUREMENTS

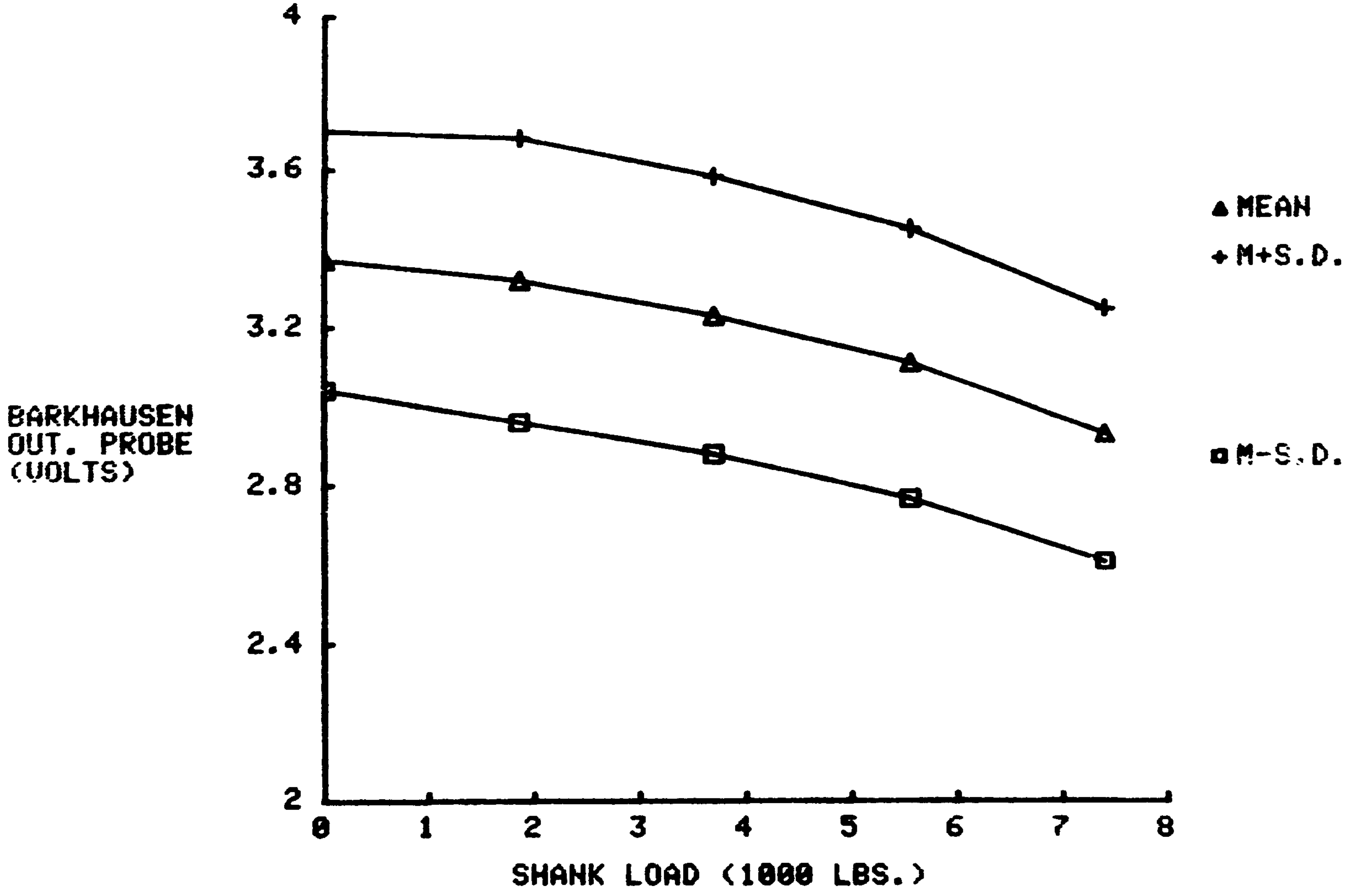

FIGURE 42.
1/2IN. GRADE 8 BOLTS (CAT.
#2-0 THRU #2-24
OUTER PROBE

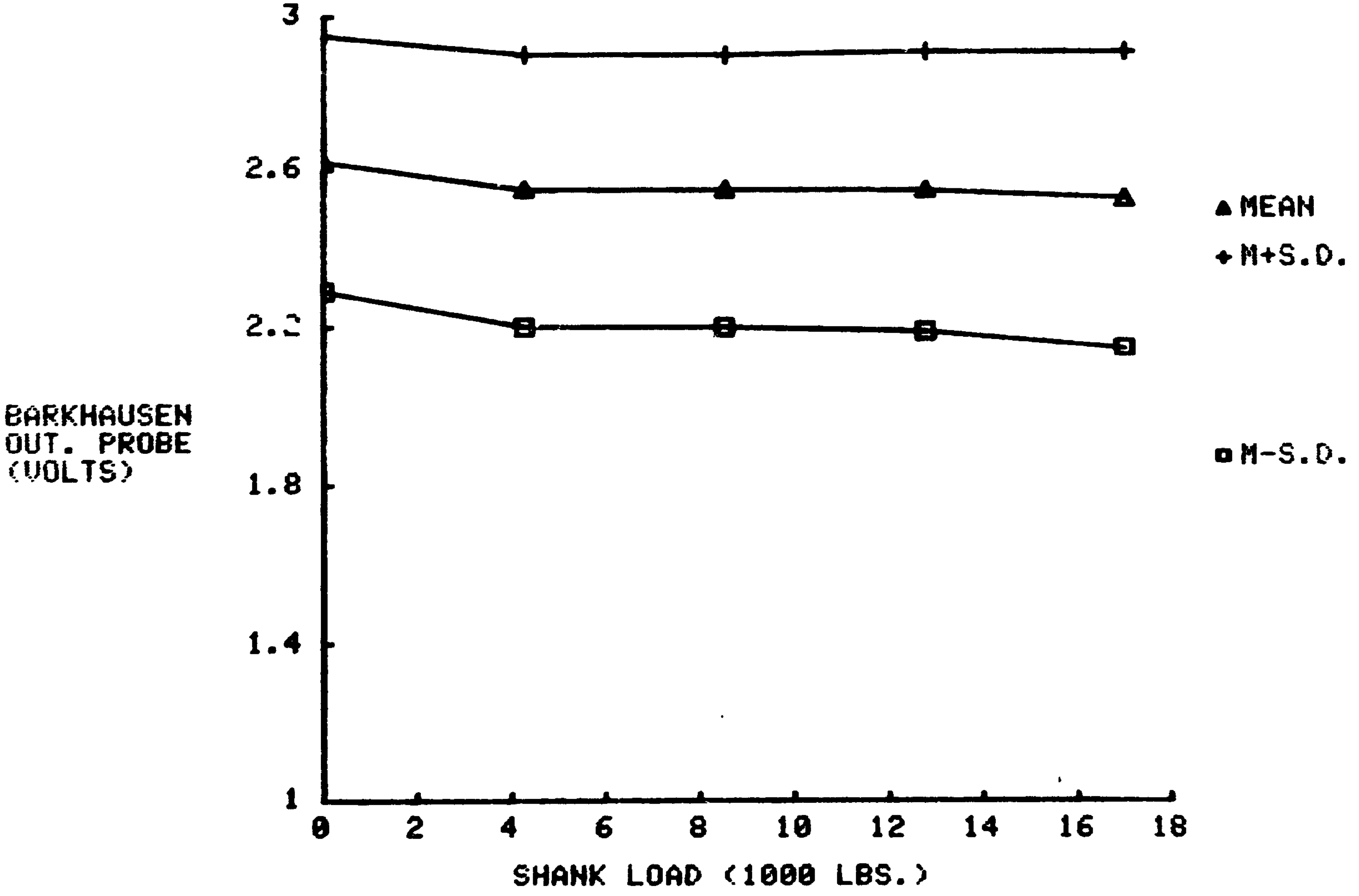

FIGURE 43.

1IN. GRADE 8 BOLTS (CAT.)
#1-0 THRU #1-24
OUTER PROBE

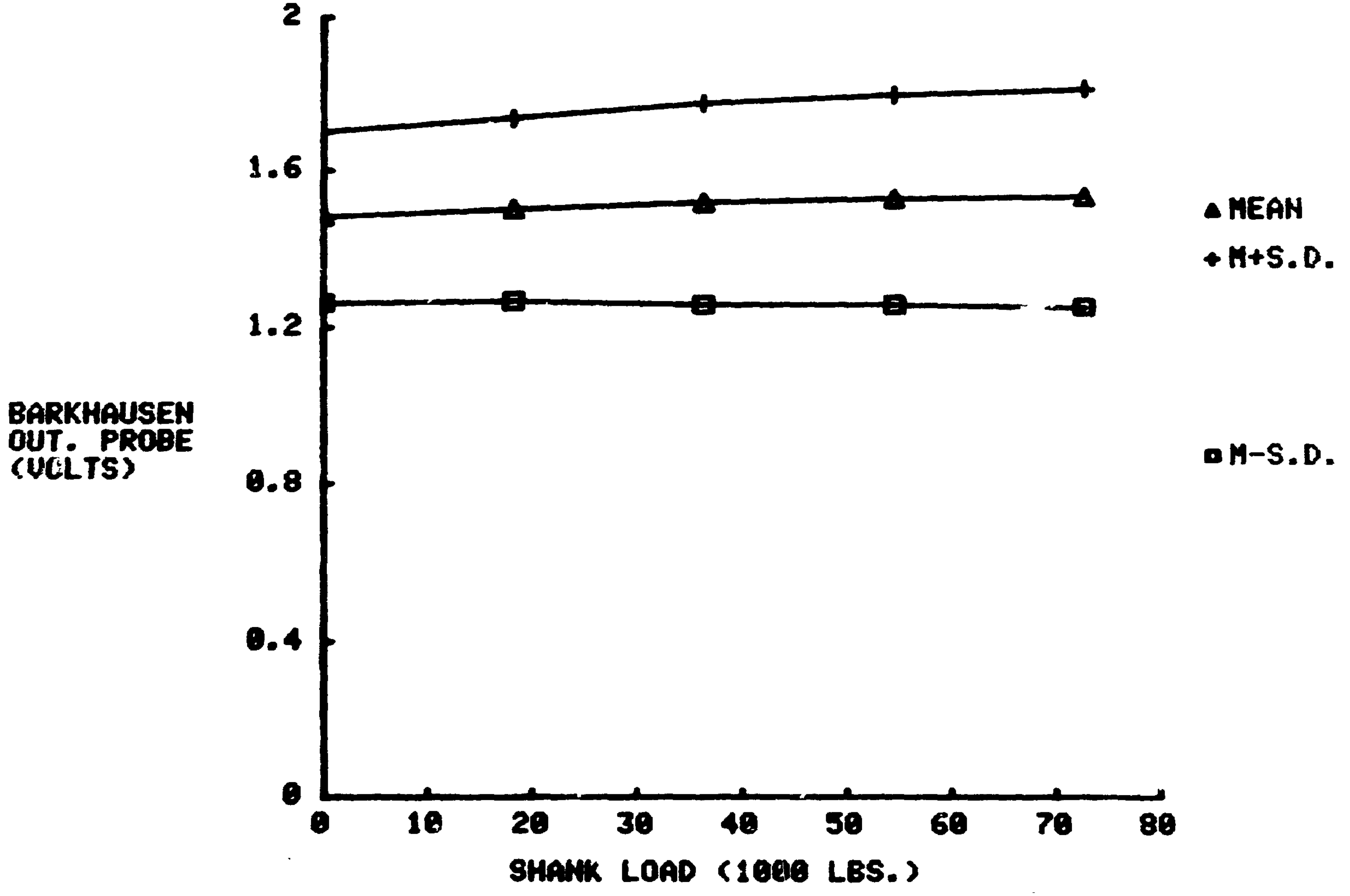

FIGURE 44.
1/2IN. GRADE 8 BOLTS #1 AND #4-#12
FIRST LOADING
MESUREMENTS FROM OUTER PROBE ONLY

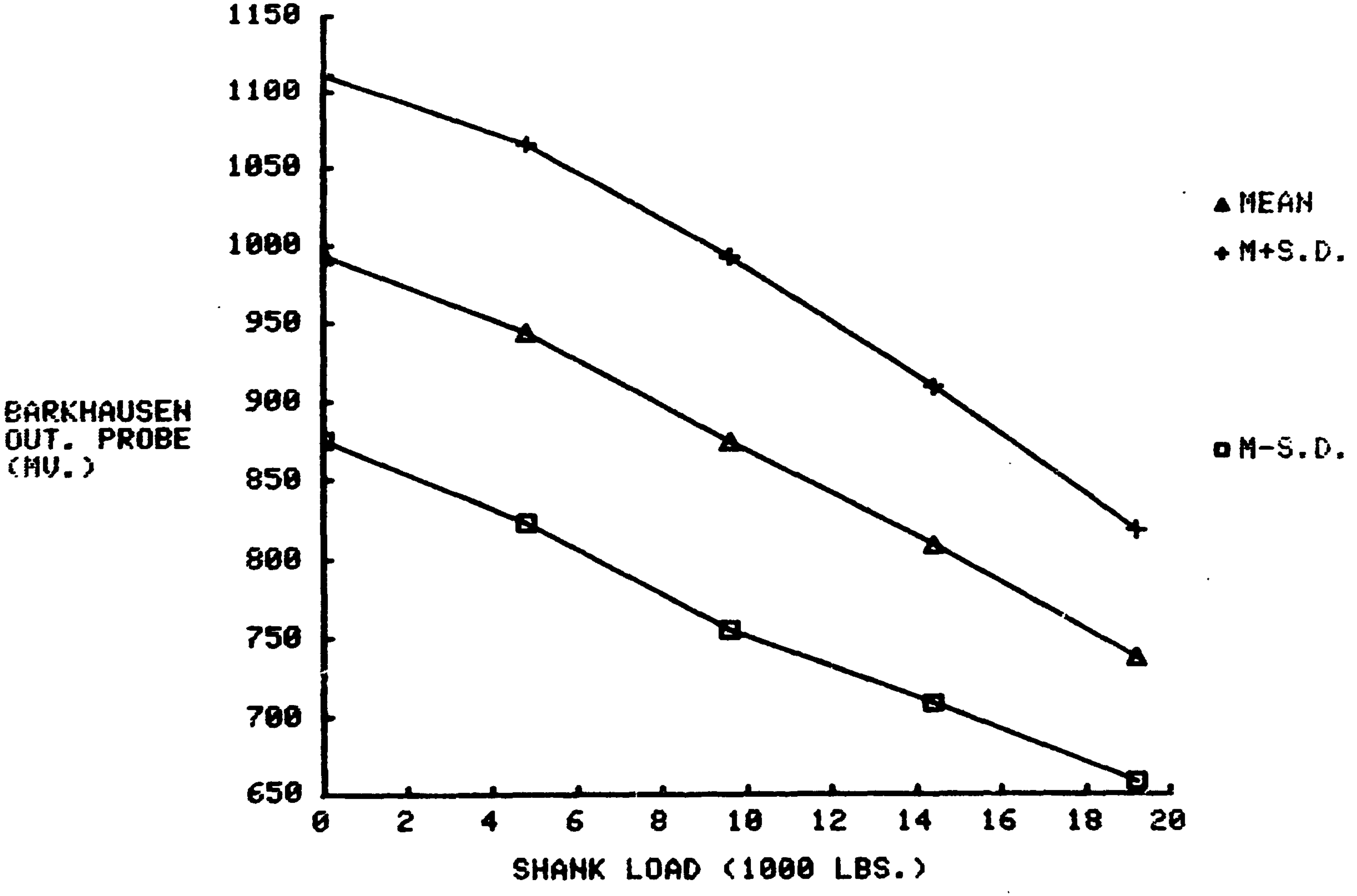

FIGURE 45.
1/2IN. GRADE 8 BOLTS #1 AND #4-#12
SECOND LOADING
MEASUREMENTS FROM OUTER PROBE ONLY

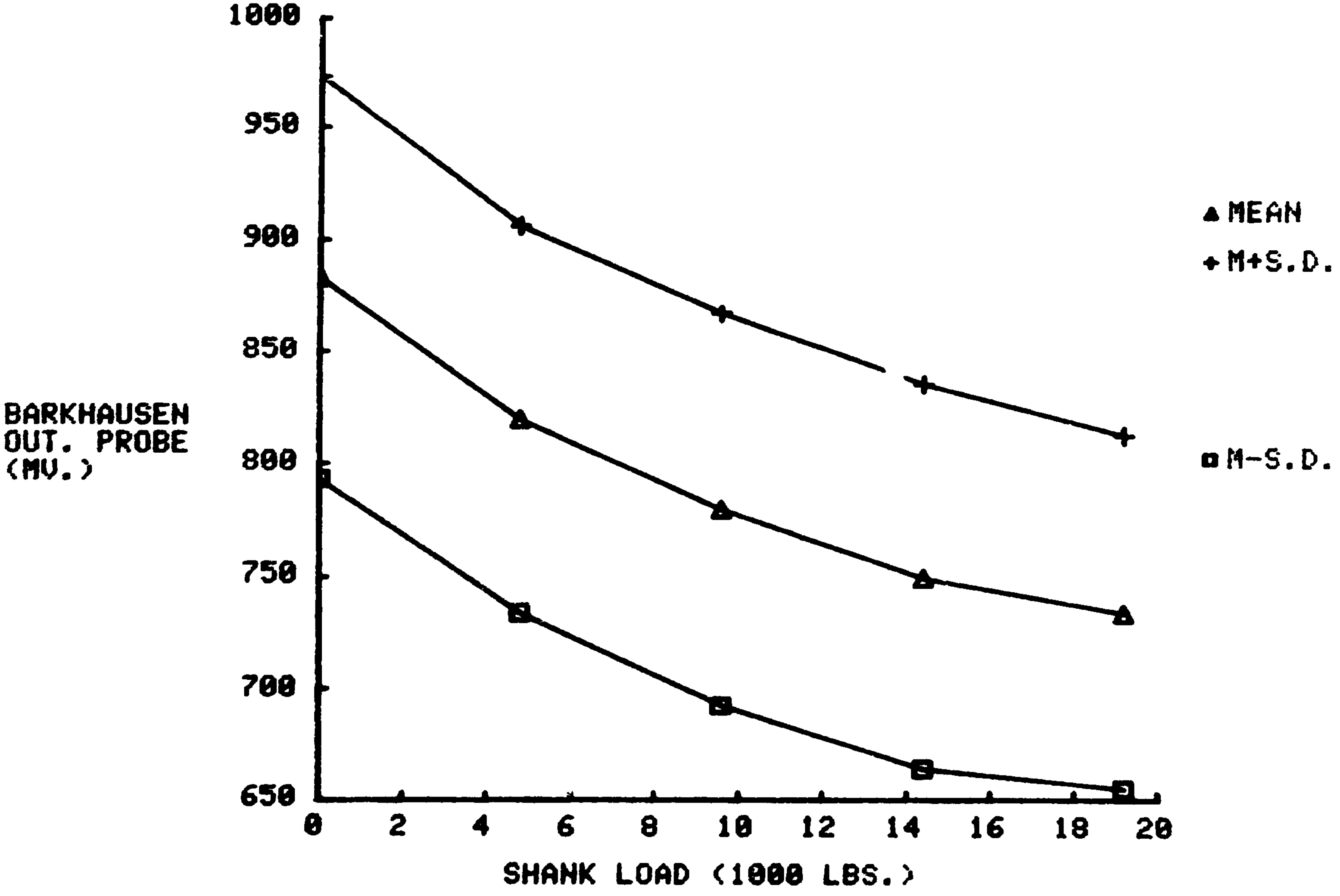

FIGURE 46.
MS90726 GRADE 5 BOLTS 3\8IN.
BARKHAUSEN RATIO VS. SHANK LOAD

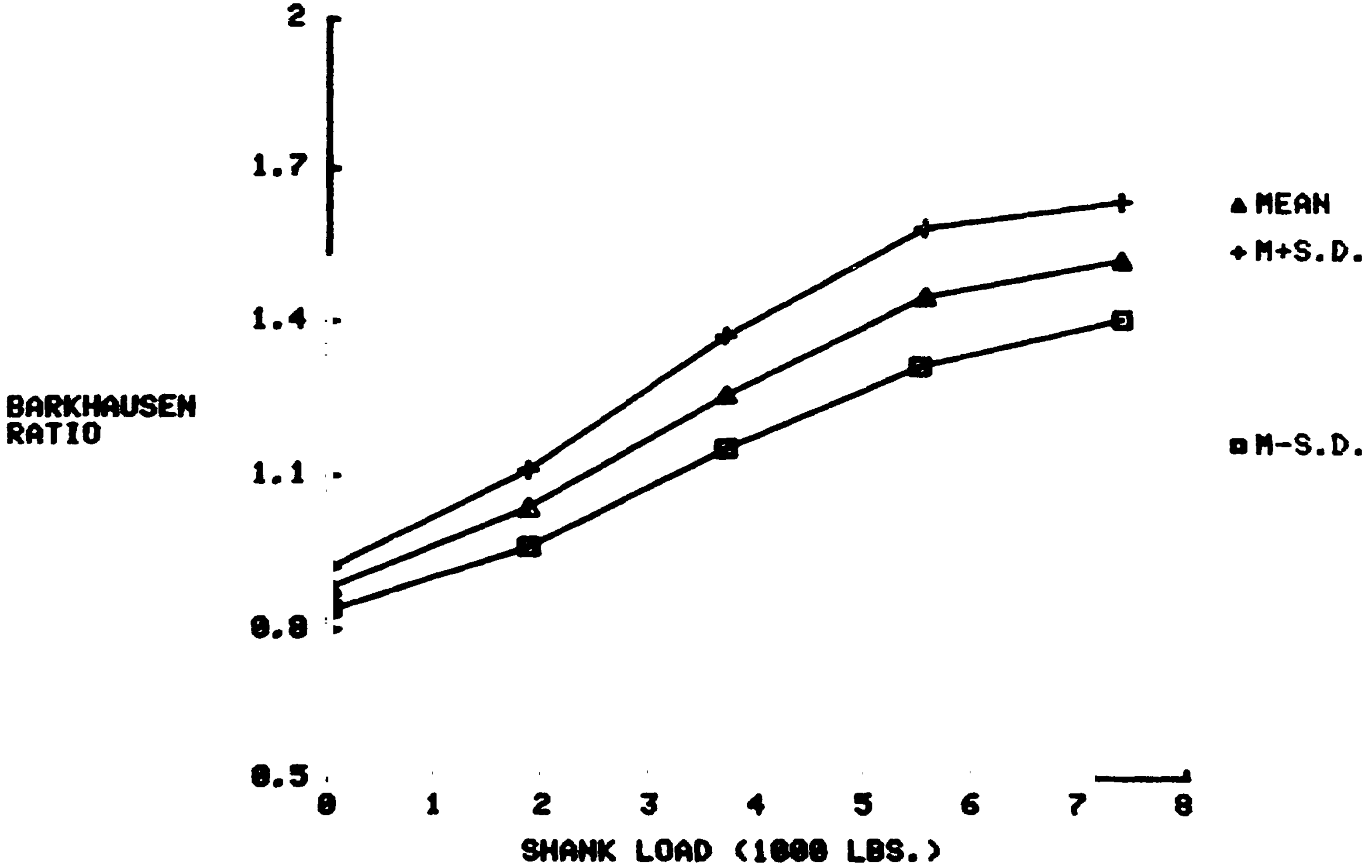

FIGURE 47.
BARKHAUSEN RATIO VS. LOAD
1/2IN. BOLTS #2-0 THRU 2-24

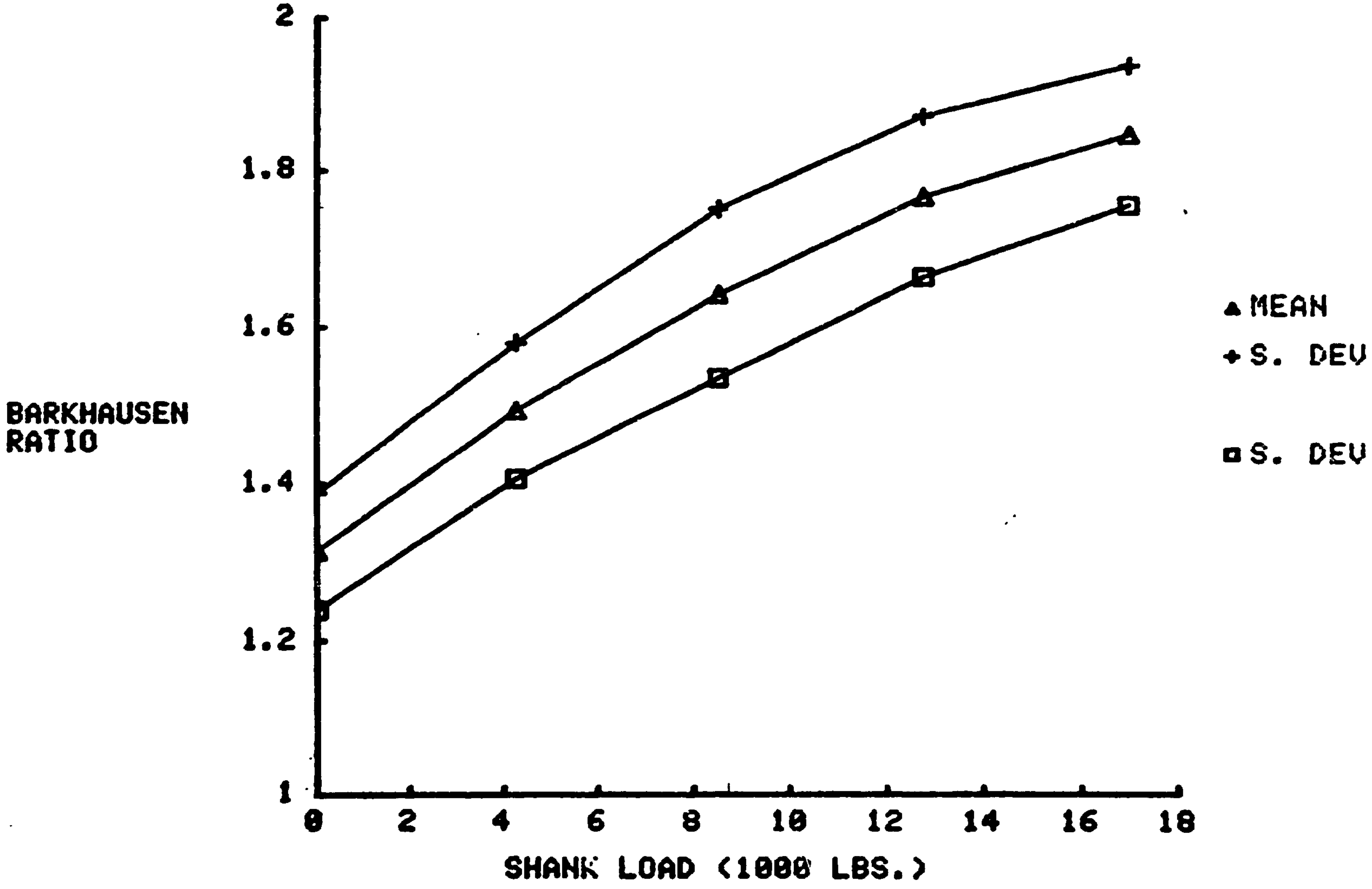

FIGURE 48.
BARKHAUSEN RATIO VS. LOAD
1IN. BOLTS #1-0 THRU 1-24

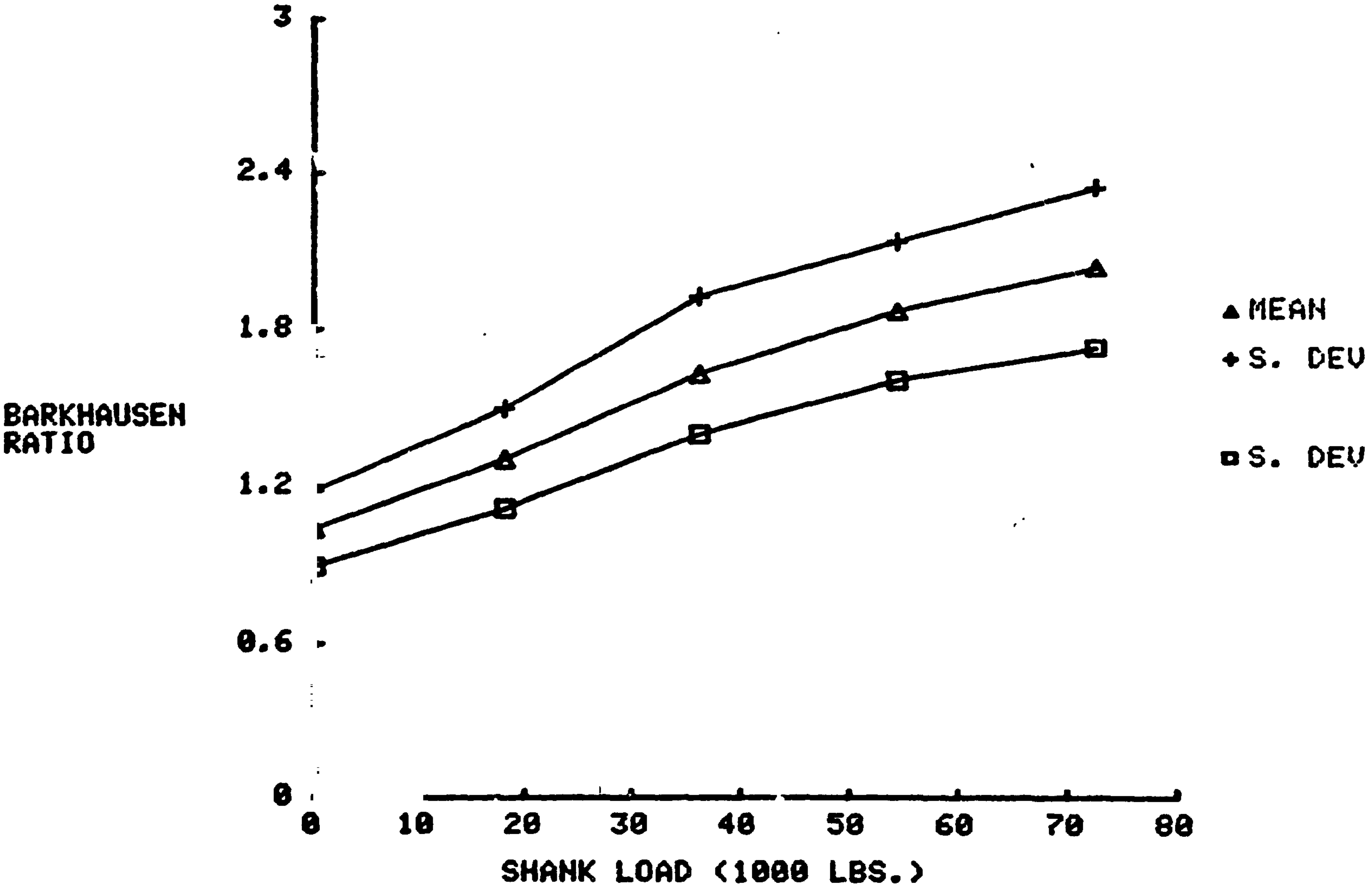

FIGURE 49.
1/2IN. GRADE 8 BOLTS #1 AND #4-#12
FIRST LOADING

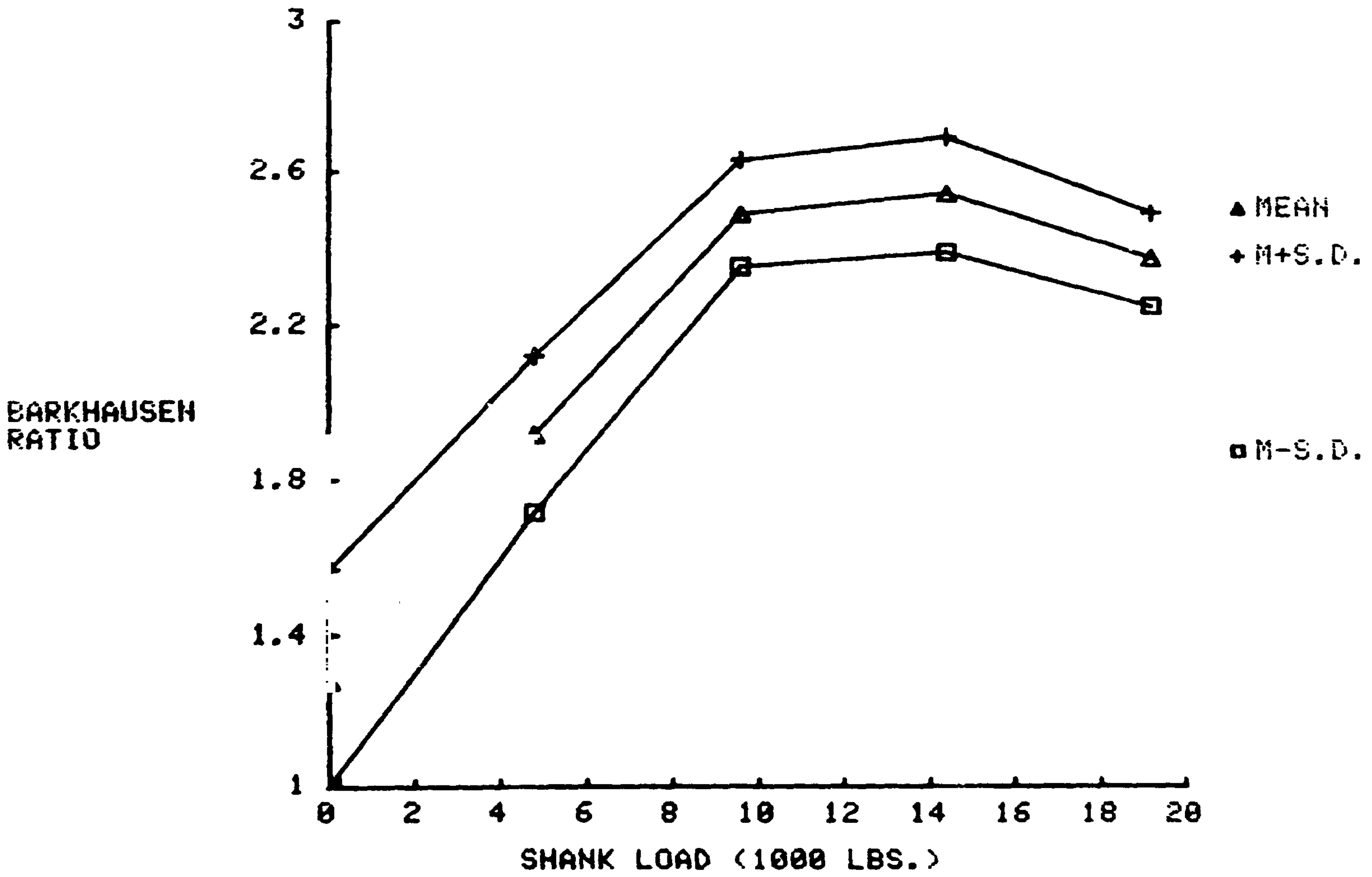

is due to early saturation of the inner probe signals with applied stress. Since the outer probe signal continues to react to increasing load, the ratio decreases. The worst case measurement error for the first loading case is represented by Barkhausen ratio of 2.25, which denotes a load range from 6,000 to 19,200 pounds, or a variation of 69%. This compares to the 59% variation in the inner-probe-only measurement value.

The second loading ratio data are presented in Figure 50. This plot is similar in shape to that of the first loading and a similar analysis can be applied. The increase in low load values results from the decrease in inner probe values from the first loading. Data scatter is greater than the first loading which results in an uncertainty of from 4,000 to 19,200 lbs. (79%) as compared to the inner probe measurement variation of 77%.

Multiple Regression Analysis

Measurements discussed so far have dealt entirely with the peak amplitude of the envelope-detected Barkhausen signal. In addition to these data, the relative timing of the occurance of the peak with respect to the magnetization cycle was measured for the 3/8-inch grade 5 and the 1/2-inch and 1-inch grade 8 commercial bolts. A shift in the timing of the response was observed as bolt load was increased. Limited evidence suggested that this shift might be a magnetization effect and thus related to bulk stress, and as a consequence might reflect a relatively independent measurement parameter.

A multiple linear regression computer program was employed to analyze these and other Barkhausen data and to determine which combination of measurements gave best correlation with load. The multiple regression analysis consists of obtaining a relationship between a dependent variable and "n" independent variables. The relationship is of the form

$$Y = a_o + a_1 x_1 + a_2 x_2 + \ldots + a_n x_n \qquad (6)$$

where Y = shank load, while
x = measured Barkhausen amplitude and time parameters.

The determination of "best fit" is made by examining the residuals, which are the difference between Y estimated from the equation and the actual Y. The program provides a term called R-square which is a function of these residuals. For a perfect fit, R-square is equal to one. As the fit becomes less satisfactory, the R-square value decreases.

The Barkhausen parameters for the 1/2-inch commercial bolts were evaluated individually as functions of load. Measurements utilized included peak amplitudes for both inner and outer probes, peak amplitude ratio (outer/inner),

FIGURE 50.
1/2IN. GRADE 8 BOLTS #1 AND #4-#12
SECOND LOADING

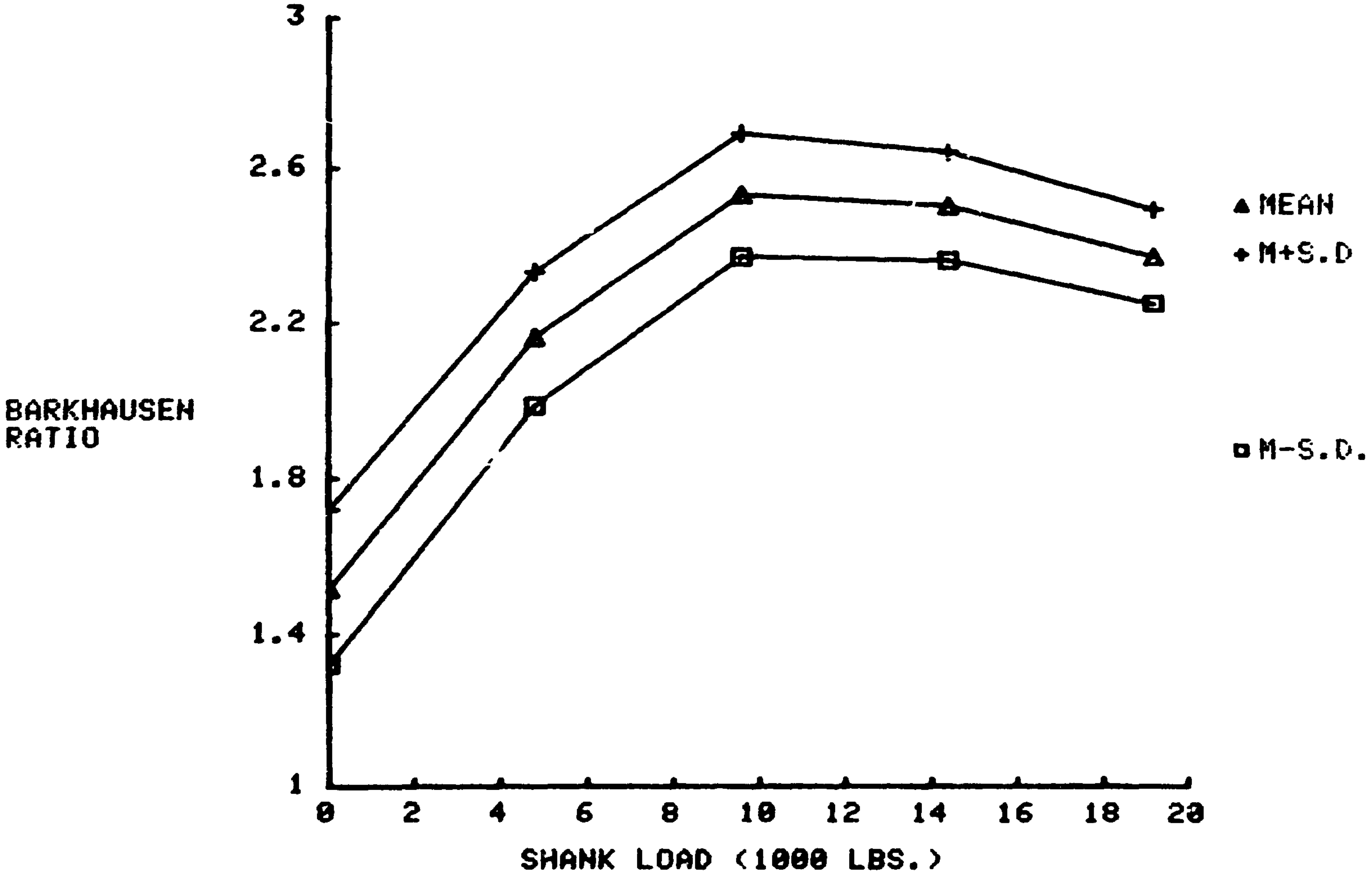

peak time shift for both inner and outer probes, and time shift ratio (outer/inner). The best individual fit was found to occur with the amplitude ratio (as in Figure 47), which produced an R-square value of 0.793. Several combinations of the parameters were applied, and the highest R-square value of 0.800 resulted when all the parameters were included. However, this represented only a 0.09% improvement over the amplitude ratio only, and was judged to be insignificant. The results indicate no significant improvement in data scatter by using parameters other than the peak amplitude ratio.

Residual Stress Considerations - Data Analysis

Residual stress was discussed earlier as a possible source of data scatter in the experimental results. Since occurrence of a residual stress appears very likely due to the head forming and heat treatment processes involved in bolt manufacture, additional study was directed toward examination of residual stress effects.

A typical Barkhausen response to compressive stress is illustrated in Figure 51 (a). The curve consists of a relatively linear region and a nonlinear saturation region. The effects of residual and applied stress on the Barkhausen response are considered to be additive so that the Barkhausen effect responds to a combination of both stresses. The appearance of the inner probe measurement curves for the four hex-head bolt types examined, tends to indicate operation over the part of the curve marked. The presence of residual stress (S_1) in the head would apparently bias the Barkhausen response upward or downward along the curve, and cause the dynamic Barkhausen response to occur over the corresponding, new region of the curve. A slightly lower residual compressive stress level (S_2) would bias the operating regime to a corresponding, lower range. The measured response to applied shank load for two bolts with these residual stress levels would then appear as the two curves in Figure 51 (b). Residual stress differences between bolts could result in apparently different response for each bolt, especially at low applied loads.

A data analysis procedure was established to determine if such an effect could be observed in the experimental data. For this analysis, the bolt from each group with the highest no-load Barkhausen response was selected. This bolt was assumed to have the lowest residual stress level, and is typified by curve "E" in Figure 51 (b). Other bolts in this group were all assumed to have higher residual stress levels of varying amounts, one of which might be represented by curve "F". The no-load point for curve "F" would then be shifted to the right by an amount "G" to intersect curve "E". This shift establishes the apparent difference in residual stress for these two bolts. All other load measurement points for the curve "F" are also shifted along the load axis by this same amount. When the shift is accomplished for all load points, then curves E and F should form a single composite curve representing the "true" Barkhausen response curve.

4533

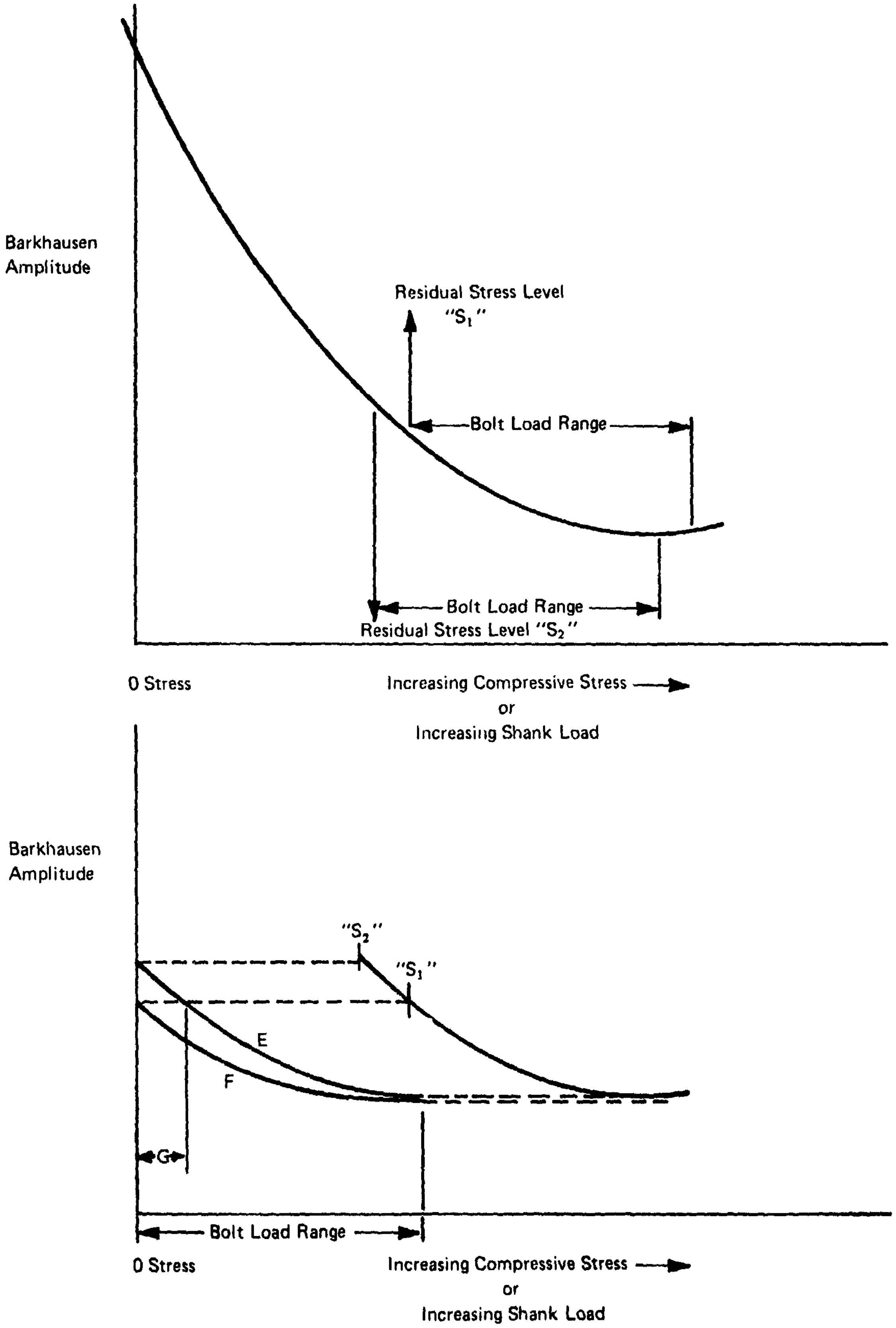

FIGURE 51 (a) TYPICAL BARKHAUSEN RESPONSE WITH COMPRESSIVE STRESS AT TWO LEVELS OF RESIDUAL STRFSS S_1 & S_2. (b) RESPONSE OF TWO BOLTS WITH SAME TWO RESIDUAL STRESS LEVELS S_1 & S_2 (curves E and F).

This "residual stress shift correction" technique was applied to the experimental data for all four groups of hex-head bolts examined. These data are summarized in Figures 52 through 58, each of which consists of two parts: (a) the original data from the Barkhausen response vs. stress measurement, and (b) the data re-plotted with a set of stress-axis corrections to compensate for residual stress. The solid curves are simply computer-generated functional fits to the data, and play no role in the data analysis.

As can be seen, the effect of this stress-axis correction is quite dramatic, and the data scatter has been markedly reduced. The good correlation of the experimental data with expected residual stress behavior presents strong evidence that much of the original data scatter observed was due to variations in residual stress levels from bolt to bolt. Most of the remainder is likely to reflect the dimensional variations.

Residual Stress Experiments on Hex-Head Bolts

In order to reinforce the idea that residual stresses are present and responsible for uncertainty in bolt head stress measurements, an additional experiment was designed in which several bolts were stress relieved by heat treatment. Four bolts were selected from the group of 1/2-inch MS90727 bolts. Two bolts were heat treated at 1100°F for one hour in an argon atmosphere and then slow-cooled. Since these bolts were heated above the original tempering temperature, bolt strength was also reduced, and magnetic properties of the steel may have been affected. Two other bolts of the same type were heat treated at 800°F using the same process. This treatment could be expected to affect residual stresses (although not eliminate them) without drastically affecting other bolt properties.

Barkhausen response as a function of shank load was measured before and after the stress-relief step on all four bolts. Data from the two bolts subjected to the 800°F heat treatment is plotted before and after treatment in Figure 59. The data indicates a slight increase in Barkhausen response after heat treatment. The results from the two bolts heat treated at 1100°F are plotted in Figure 60. Since bolt strength was reduced by this heat treatment, these bolts were re-loaded to only 75% of the original proof load value. Here, the effect of heat treatment is substantial. The Barkhausen amplitude is greatly increased for both bolts after heat treatment, indicating a reduction of compressive residual stress.

It should be noted that the observed changes in the Barkhausen response after heat treatment may not be solely due to residual stress effects, since changes in the magnetic properties of the bolt steel introduced by heat treatment could also be involved. However, the trends observed here

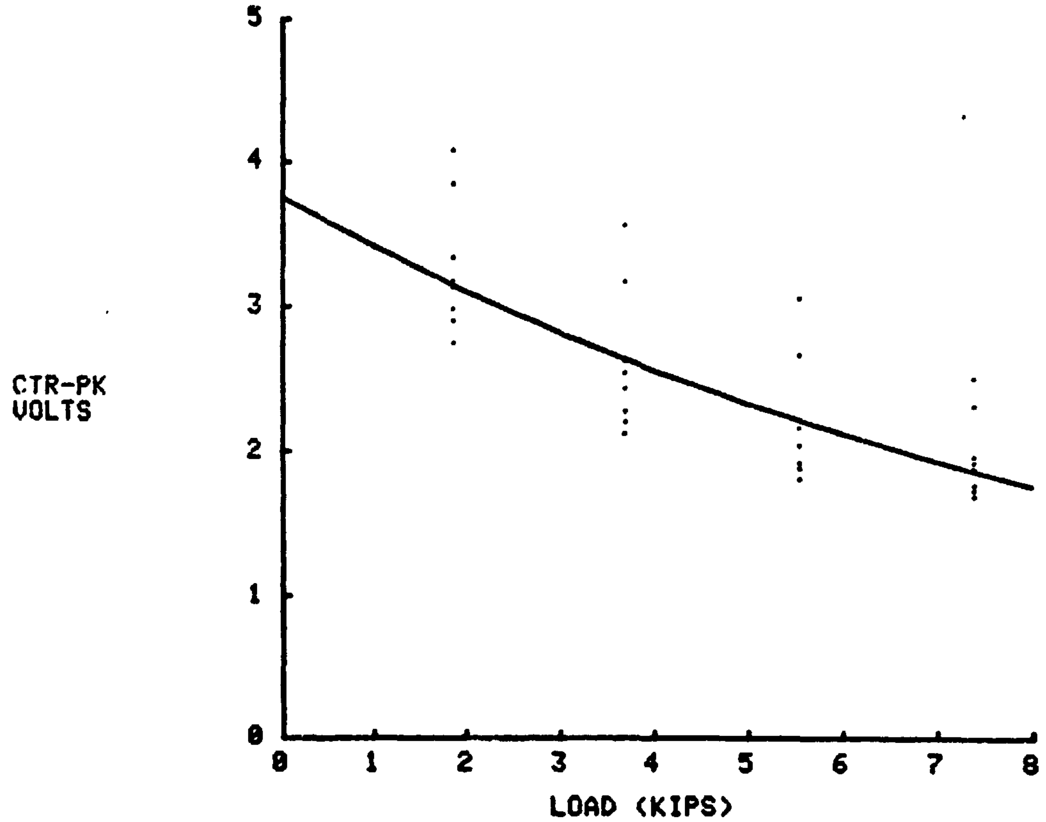

Figure 52a. 3/8-in. Bolts (10) Uncorrected Barkhausen Data

4534

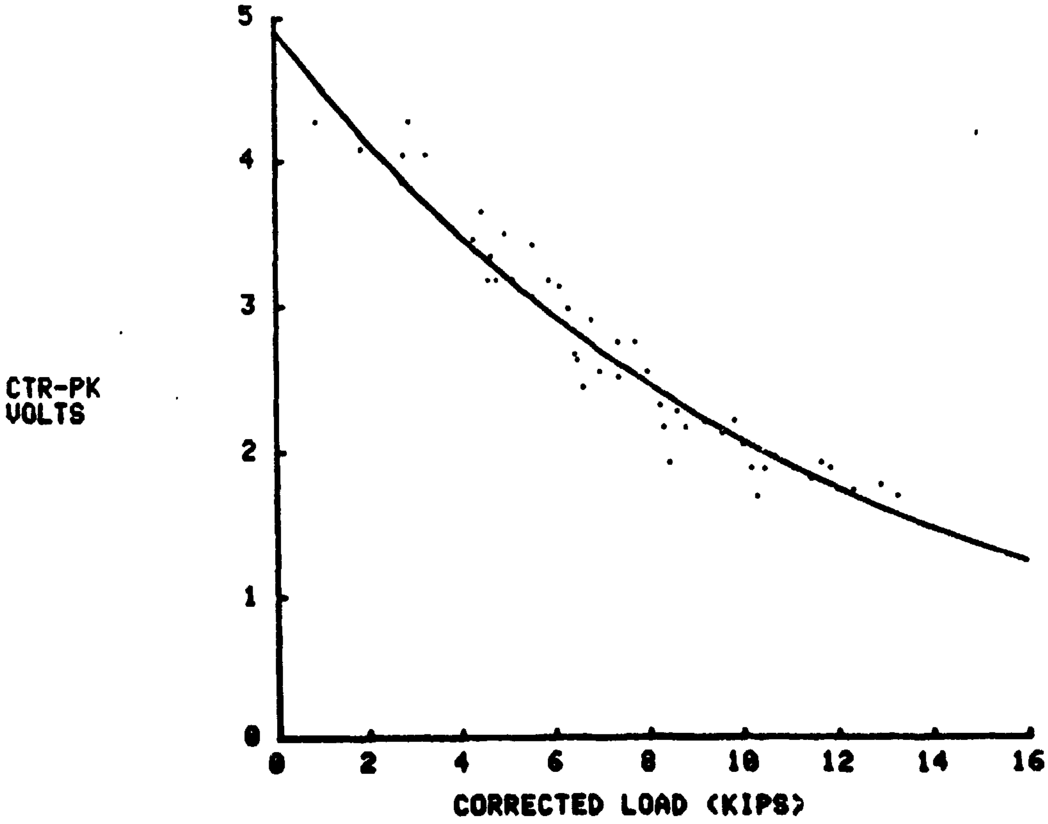

Figure 52b. 3/8-in. Bolts (10) Corrected for Residual Stress

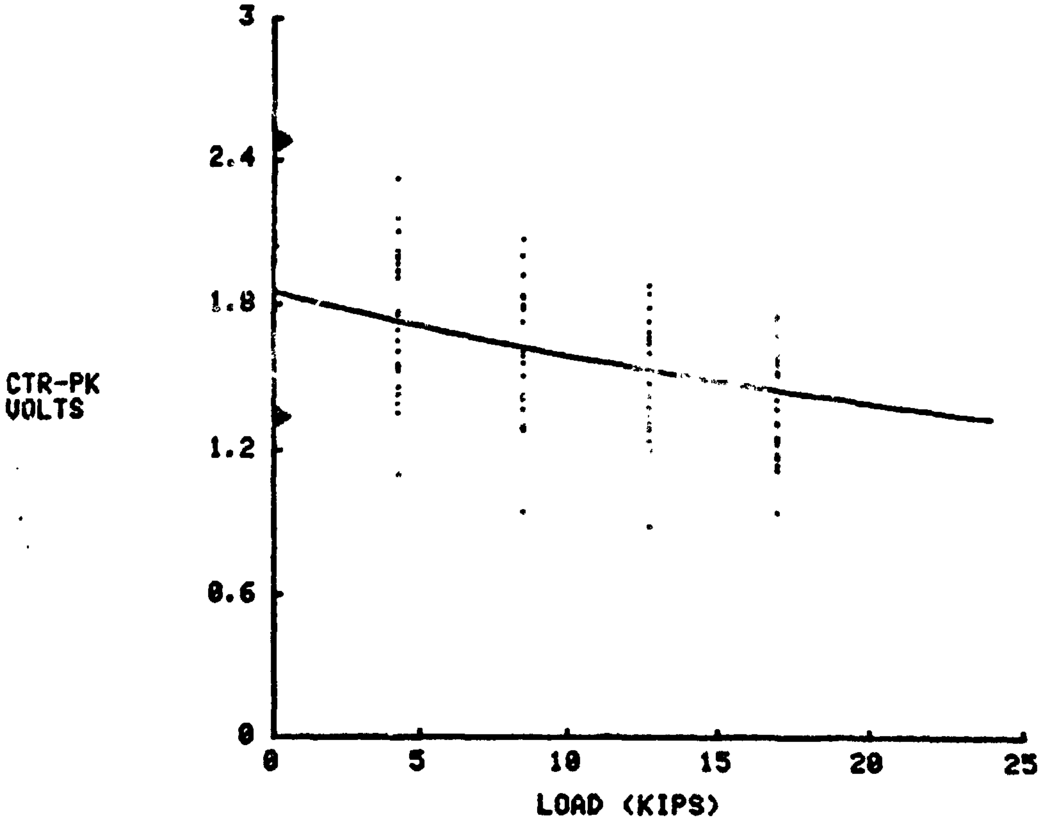

Figure 53a. 1/2-in. Bolts (25) Uncorrected Barkhausen Data

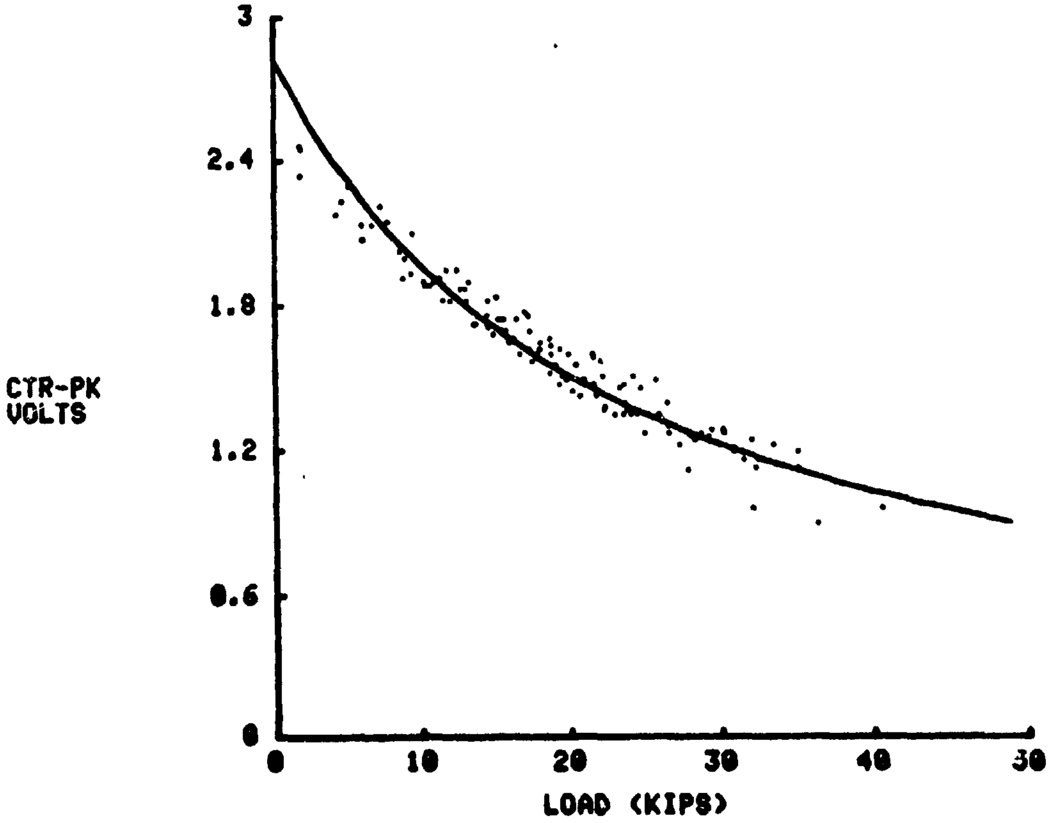

Figure 53b. 1/2-in. Bolts (25) Corrected for Residual Stress

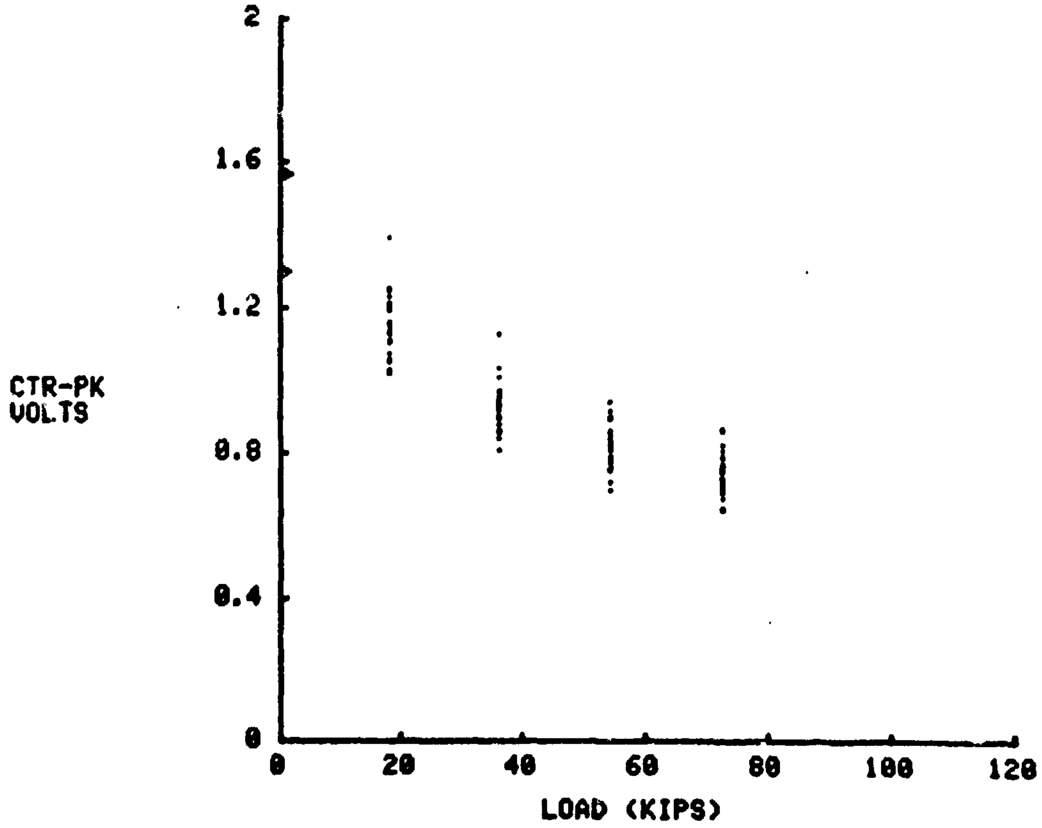

4536

Figure 54a. 1-in. Bolts (25) Uncorrected Barkhausen Data

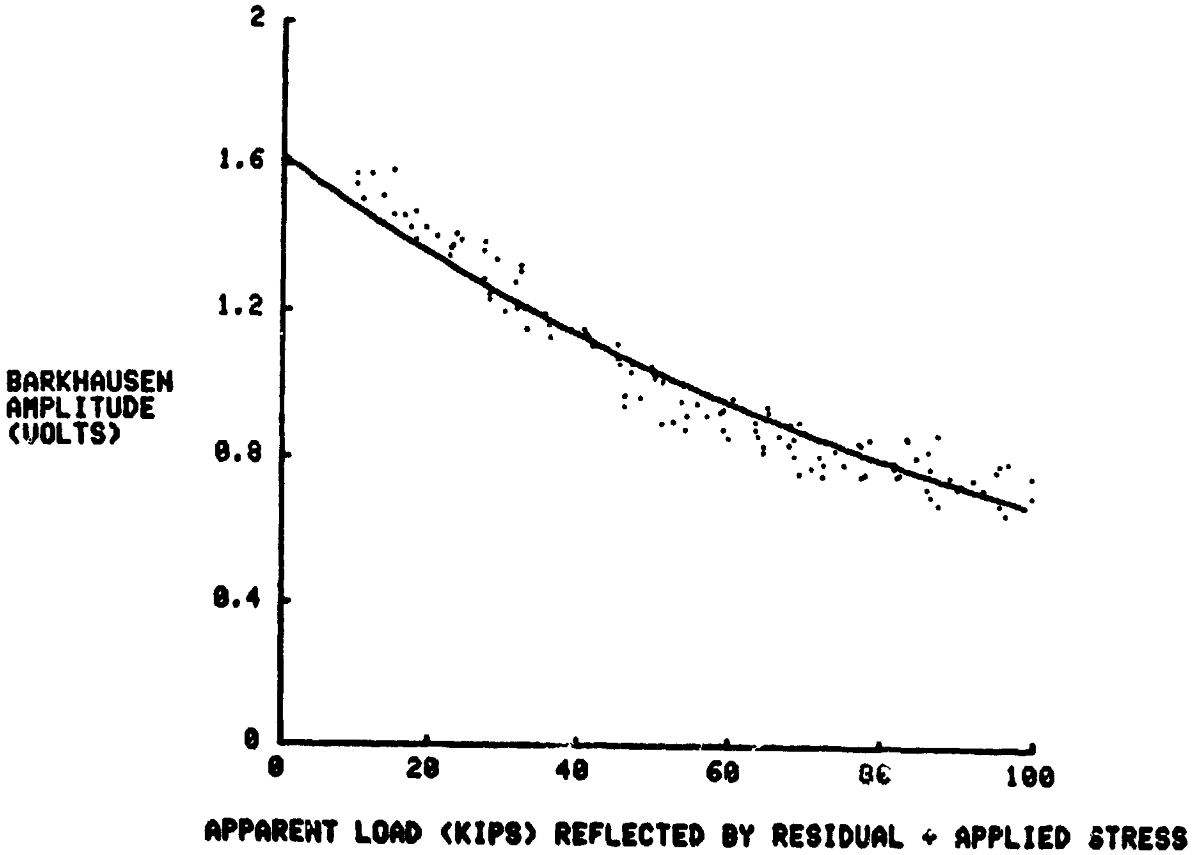

Figure 54b. 1-in. Bolts (25) Corrected for Residual Stress

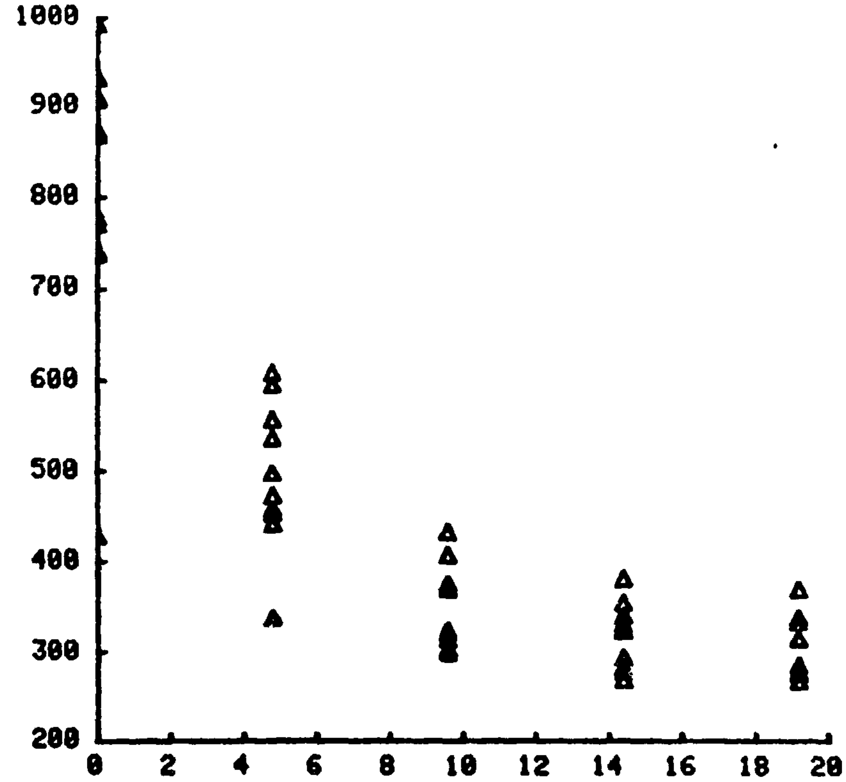

Figure 55a. 1/2-in. MS90727 Bolts (10), First Run Inner Probe, Uncorrected

4537

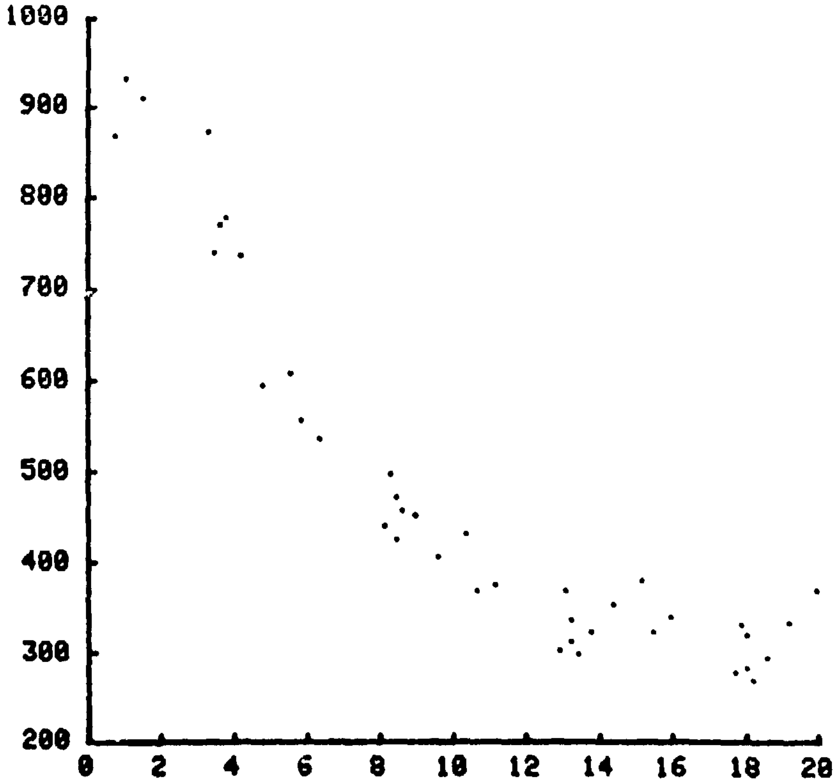

Figure 55b. 1/2-in. MS90727 Bolts (10), Corrected for Residual Stress

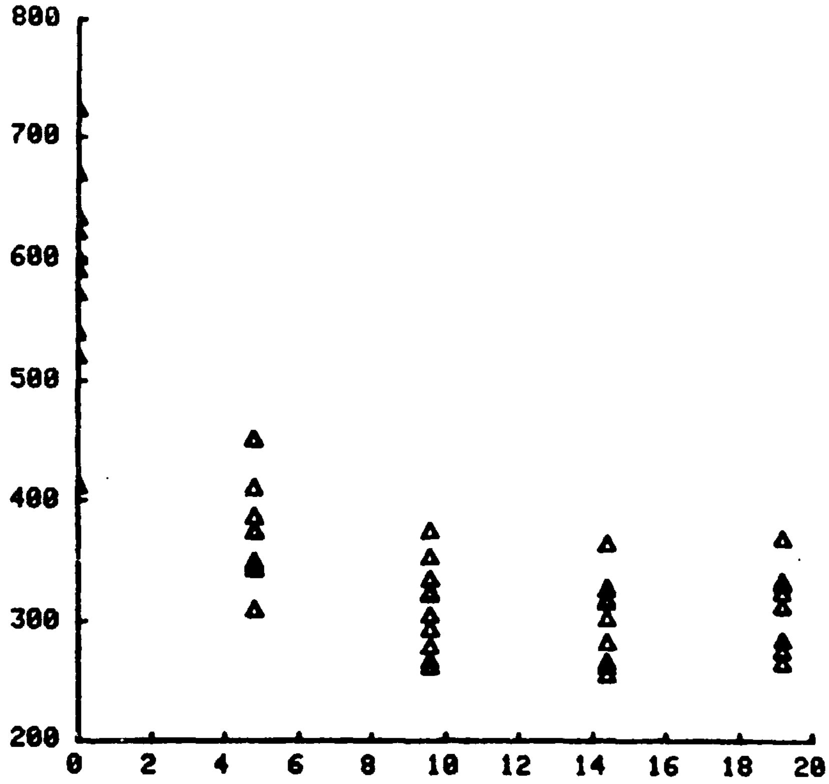

Figure 56a. 1/2-in. MS90727 Bolts (10), Second Run Inner Probe, Uncorrected

4538

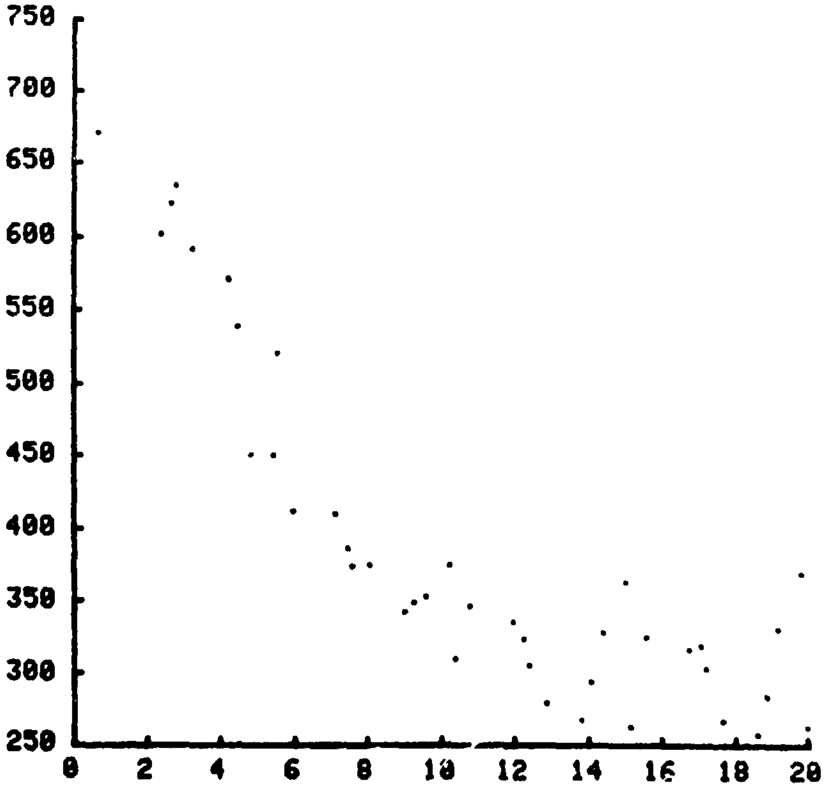

Figure 56b. 1/2-in. MS90727 Bolts (10), Corrected for Residual Stress

4539

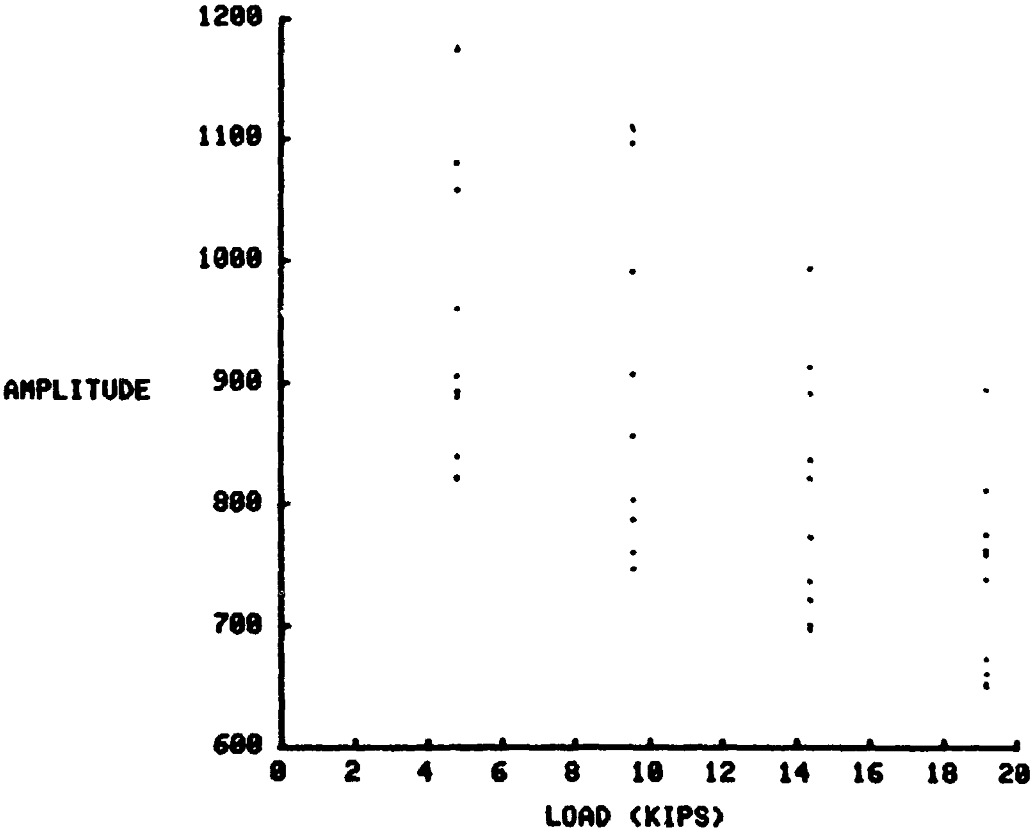

Figure 57a. 1/2-in. MS90727 Bolts (10), First Run, Outer Probe, Uncorrected

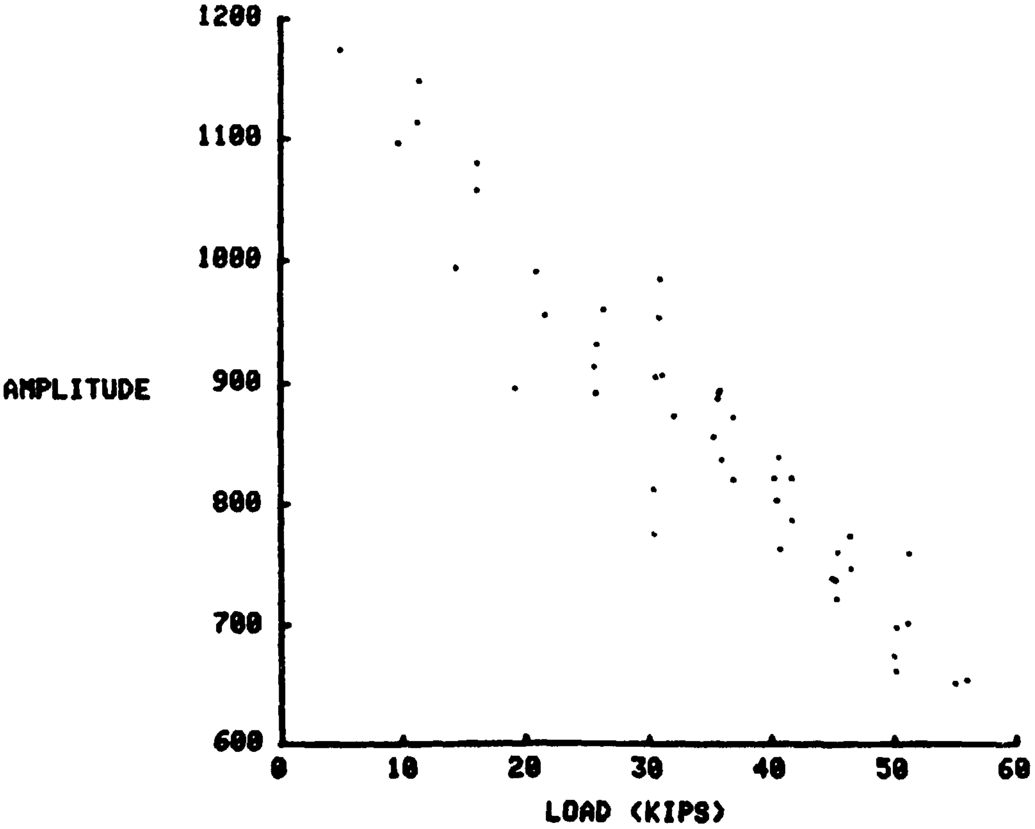

Figure 57b. 1/2-in. MS90727 Bolts (10), Corrected for Residual Stress

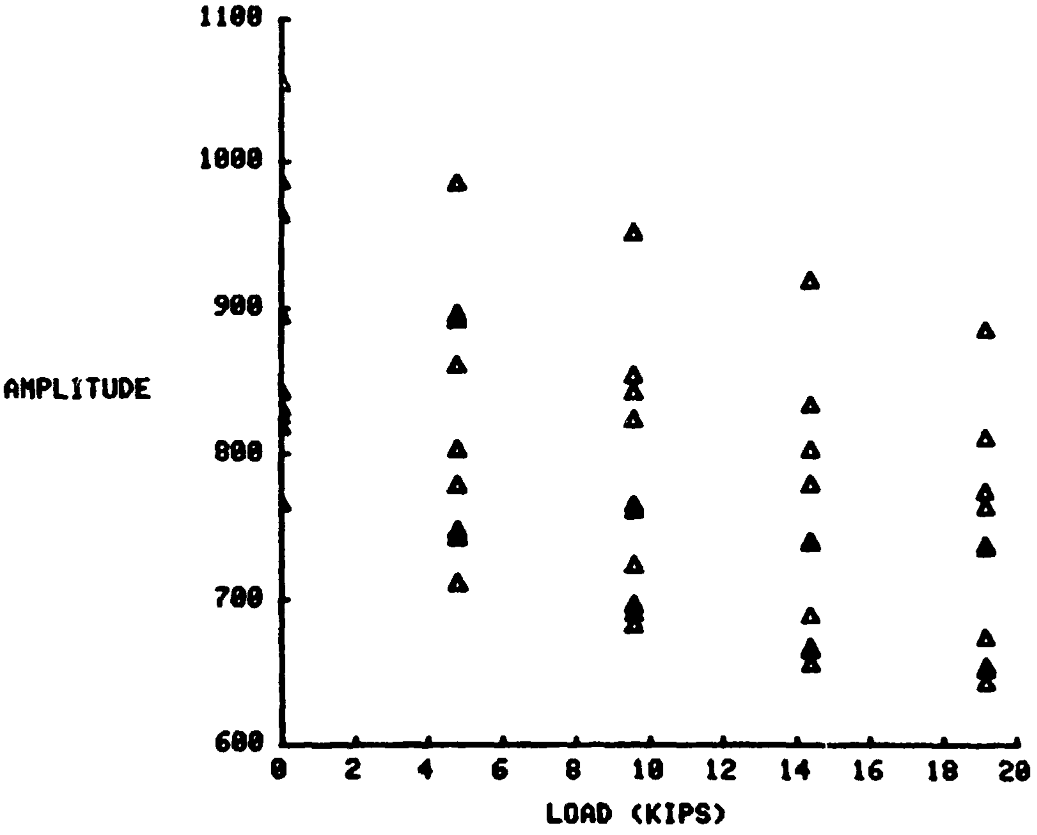

4540

Figure 58a. 1/2-in. MS90727 Bolts (10), Second Run, Outer Probe, Uncorrected

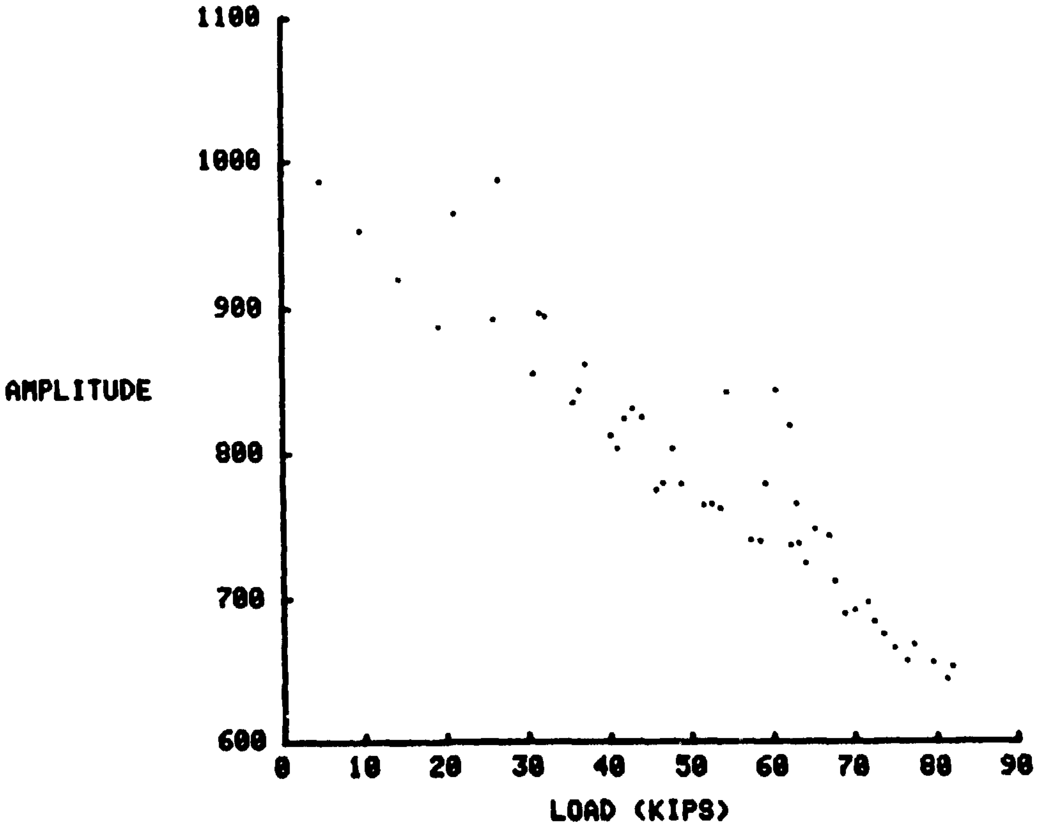

Figure 58b. 1/2-in. MS90727 Bolts (10), Corrected for Residual Stress

FIGURE 59.
40727 BOLTS #4 & 7
ORE AND AFTER 800 F HEAT TREATMENT

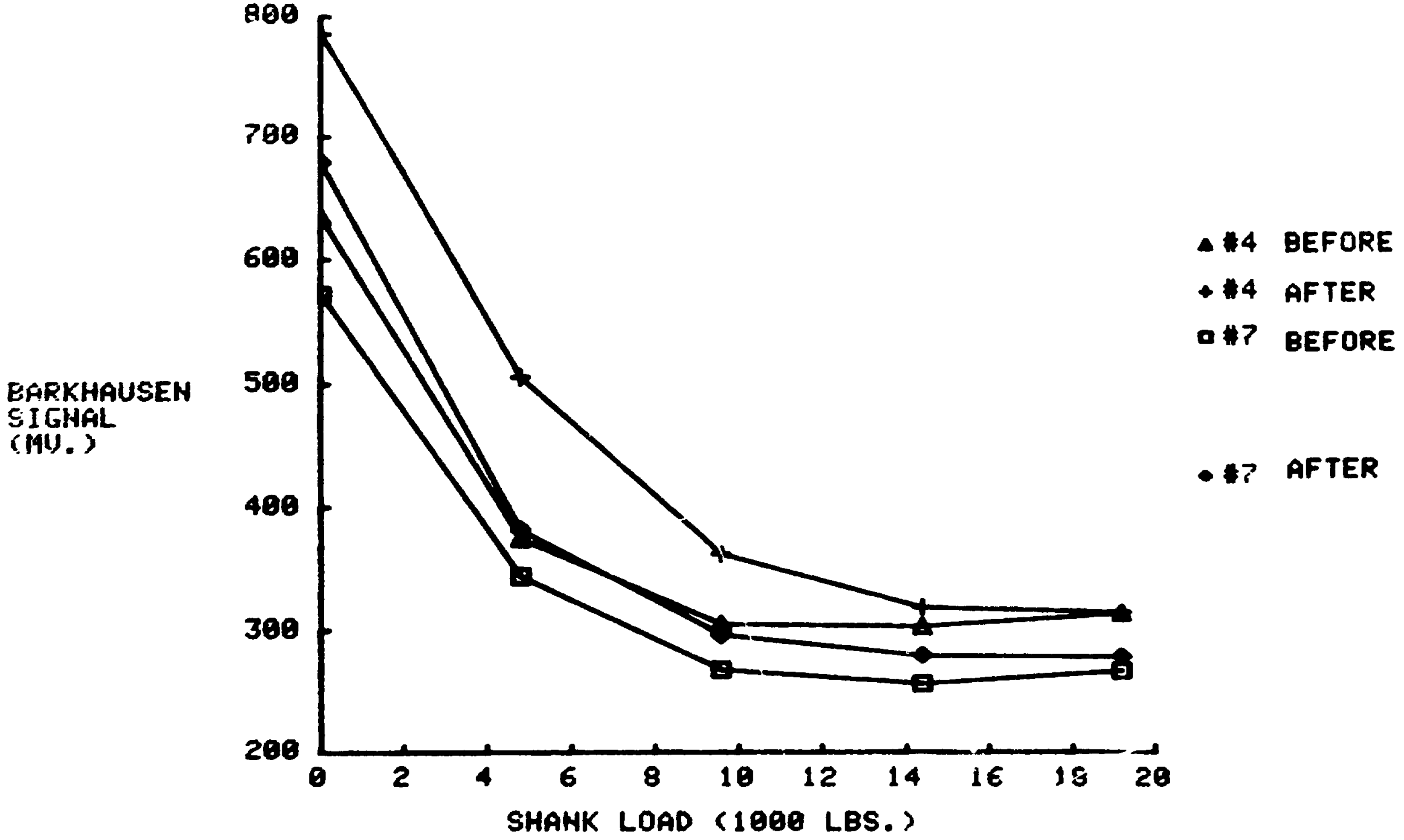

FIGURE 60.
90727 BOLTS #8 & 9
BEFORE AND AFTER 1100 F HEAT TREATMENT

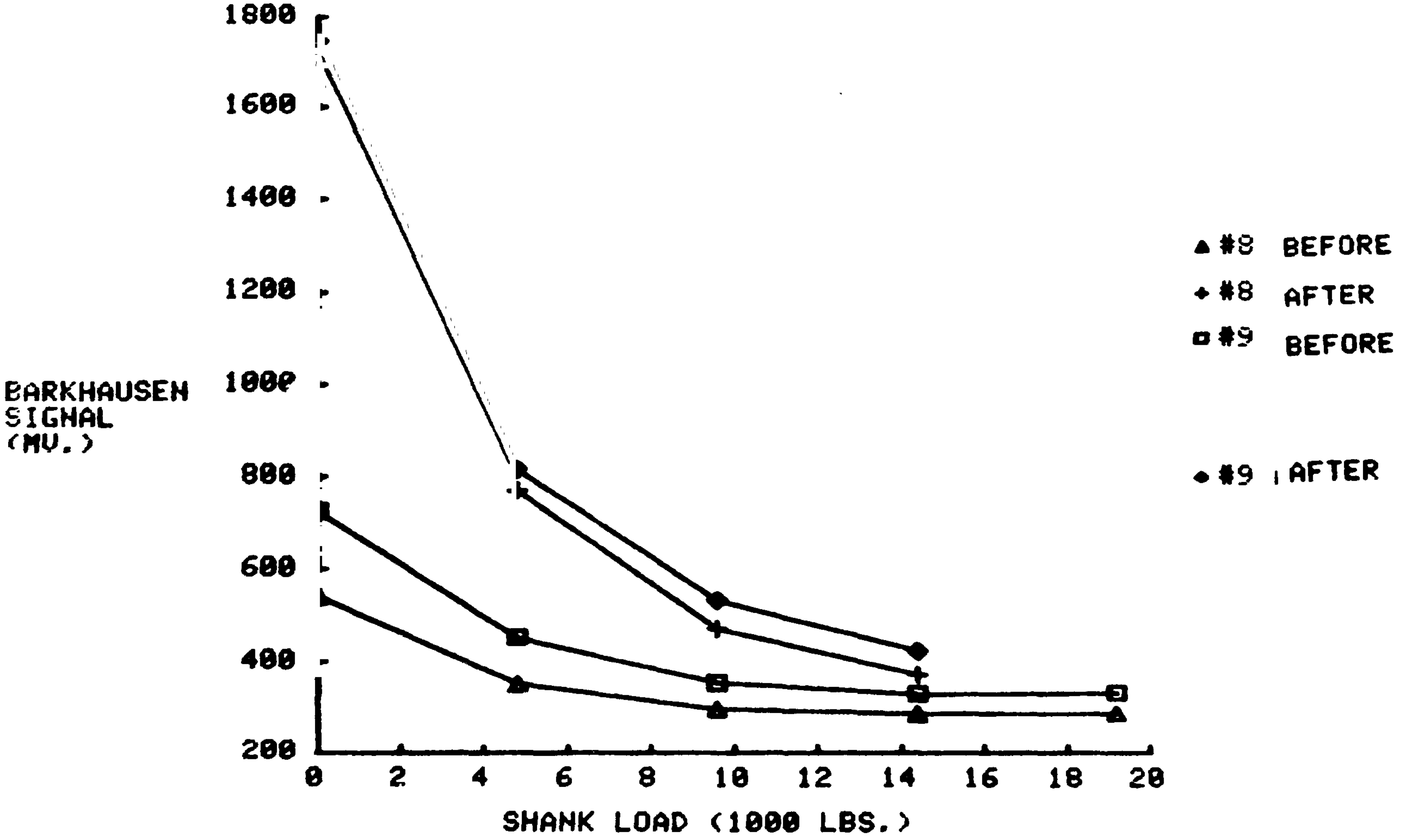

agree with anticipated behavior from residual stresses. Also, the heat treatment experiment and the stress-axis correction discussed in the previous section are both consistent in suggesting that residual stresses in the bolts are a major contributing factor in the observed Barkhausen response and associated scatter in the data.

Experiments with MS21250 Aircraft Bolts

In addition to the hex-head bolts, a group of aircraft-type bolts were also examined. These bolts are of a 12-point, external-wrenching type, with an ultimate tensile strength of 180 ksi. Figure 17, page 60, is a drawing of the bolt taken from MIL STD MS21250. Note that the head configuration geometry is much more complex than the previously examined hex head bolts. The specification allows a flat, round, or conical shape for the bottom of the hole inside the bolt head. Bolts examined had a flat bottomed hole.

Results from the finite element stress analysis in Chapter VI show that the bottom center of the hole experiences a compressive radial surface stress with shank load (Figure 14, page 57) similar to the hex-head bolts. The axial surface stress along the inside diameter of the bolt head wall, however, experiences a high tensile stress (Figure 19, page 62) especially near the bottom corner. A Barkhausen stress measurement in this area would permit this tensile stress component to be monitored, resulting in a larger Barkhausen signal which would increase with applied shank load.

Barkhausen measurements were performed on a total of six of these bolts, utilizing the same equipment setup as with the hex head bolts. Magnet pole pieces were constructed to conform to the special bolt heads and magnetization was accomplished in a direction across the bolt head, in a manner similar to the hex head bolts. A square Barkhausen inductive pickup probe measuring 1.27 x 1.27 mm was constructed for stress indication measurements. This relatively small probe size enabled measurements at the center of the hole bottom with sufficient clearance from the hole sides to insure isolation from the large tensile stress present at the corners. The probe was also suitable for separate measurements around the inside wall at the corner to measure the tensile stress induced by shank loading. Figure 61 is a photograph of the Barkhausen setup as adapted for measurements on the hole bottom of the MS21250 bolts.

Load values applied to each bolt were 0, 5750, 11,500, 17,250, and 23,000 lbs. where 23,000 lbs. represents 90% of yield stress at the effective stress area at the threads. Figure 62 is a plot of the data for all six bolts. The mean of measurements for the six bolts is plotted along with the standard deviation. If a similar analysis to that used with the hex head bolts is applied here, a worst case indicates that a Barkhausen reading of 490 mV could represent shank load variations from 1,500 to 23,000 pounds, or a 93% variation.

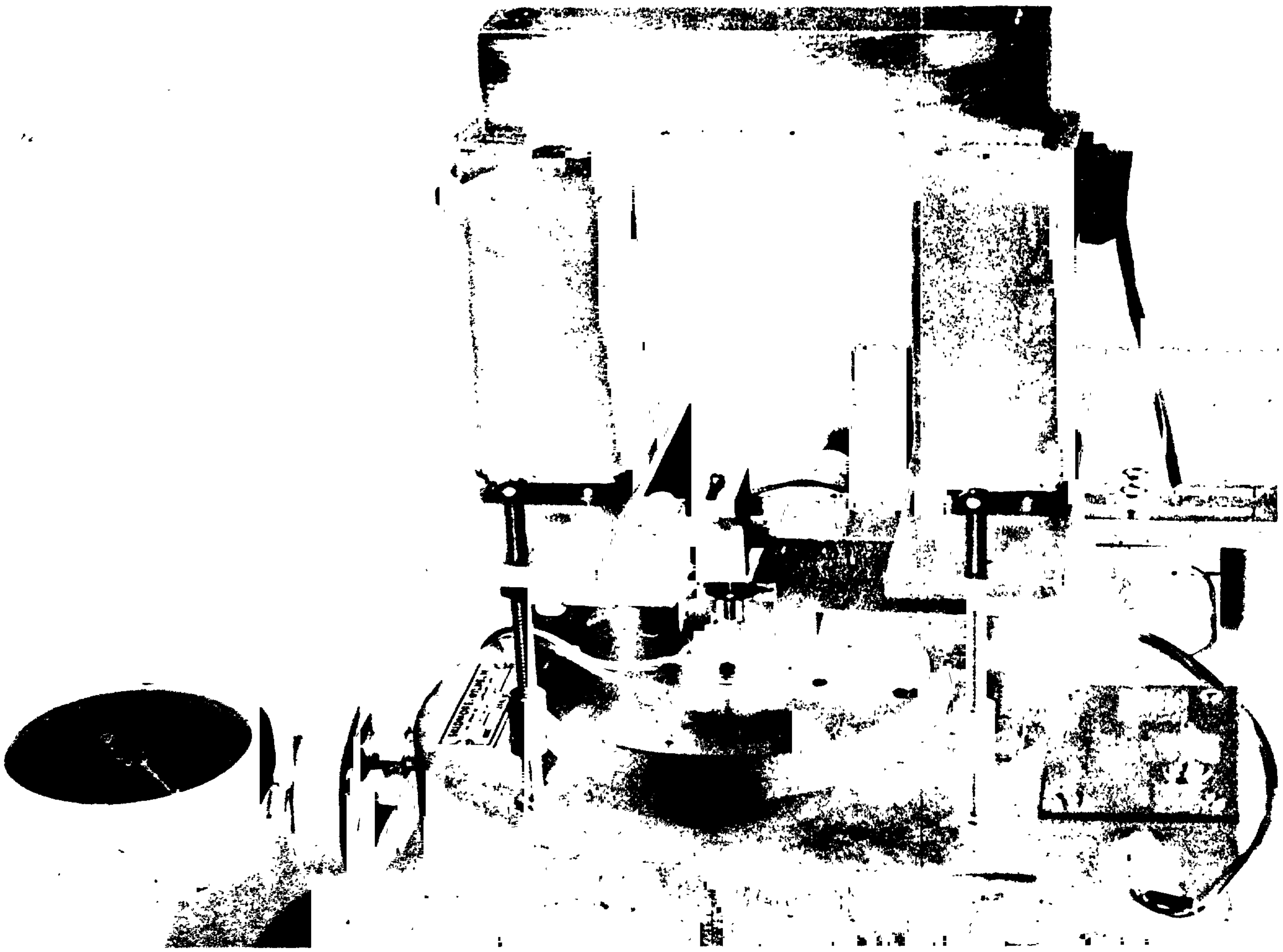

FIGURE 61. LOADING FIXTURE AS MODIFIED FOR BARKHAUSEN EXPERIMENTS WITH MS21250 12-POINT AIRCRAFT BOLTS

ORIGINAL PAGE IS
OF POOR QUALITY

FIGURE 62.
MS21250 BOLTS 1/2IN.
MEASUREMENTS ON HEAD
BOLTS #1-#6

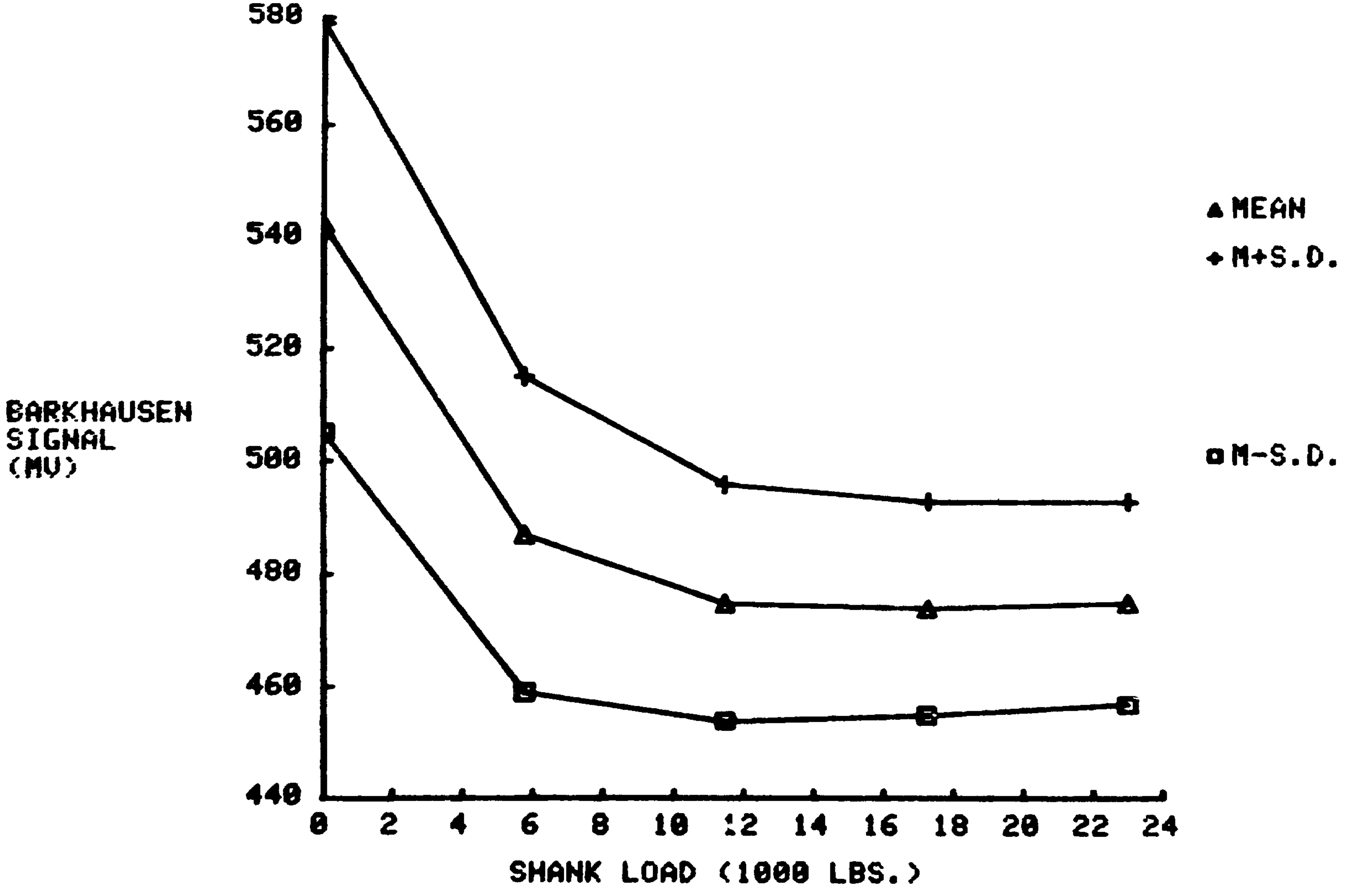

To determine the repeatability of Barkhausen response on a single bolt, measurements were made on one bolt at four different orientations around the head, obtained by rotating the bolt with respect to the magnet and probe. Figure 63 is a plot of the results for the four positions. Data scatter is greatest at 25% of full load where maximum signal variation due to position is 6%. This scatter is significant, since the total signal change is only 13% from zero to full load.

Barkhausen saturation effects also represented a serious problem with these bolts. From the plot in Figure 63, it can be seen that stress saturation occurs at 50% of full load.

In addition to the previous experiments, measurements were taken on the inside wall of the bolt head to determine if the tensile stress present there could be used as a better indicator of shank tension than the compressive stress at the bottom of the hole. Measurements were made on the same bolt as in Figure 63, again at four orientations. The center of the probe was located 1.4mm from the bottom of the hole. Figure 64 is a plot of the results. Appreciable scatter is evident in this data also, with the worst scatter at full load. At this load, a 15% variation in signal level with position is observed, large compared to the 19% average overall signal change from zero to full load.

Scatter in the data from these measurements is not surprising, since the same variables present in the previous (compressive stress) measurements are also influential here. In addition, it is expected that tensile stress on the inside wall would be strongly influenced by the exact configuration of the inside corner, since a sharper corner should produce a greater stress gradient. Since the bolt specification does not specify tolerances at this location, variations are likely. The bolts examined did indeed have rough areas at various positions on this inside corner which could have influenced the results.

Residual Stress Considerations in MS21250 Bolts

It could be anticipated that residual stress effects in these bolts should be at least as prevalent as those experienced with the hex-head bolts. The data analysis method usilizing the stress-axis correction was also applied to the MS21250 bolt measurements made at the center of the head. Figure 65 is a plot of all the original data points and Figure 66 is a plot of the corrected data. The results in this case are not as coherent as observed with the hex-head bolts. The early saturation of the Barkhausen response tends to prevent utilization of a simple correction technique in this case. The large data scatter observed with these bolts is also probably influenced by difficulties with magnetic coupling which, of course, cannot be corrected in a simple way.

FIGURE 63.
MS21250 BOLT #1 BARKHAUSEN SIGNAL
VS LOAD AT 4 ORIENTATIONS, PROBE
AT CENTER

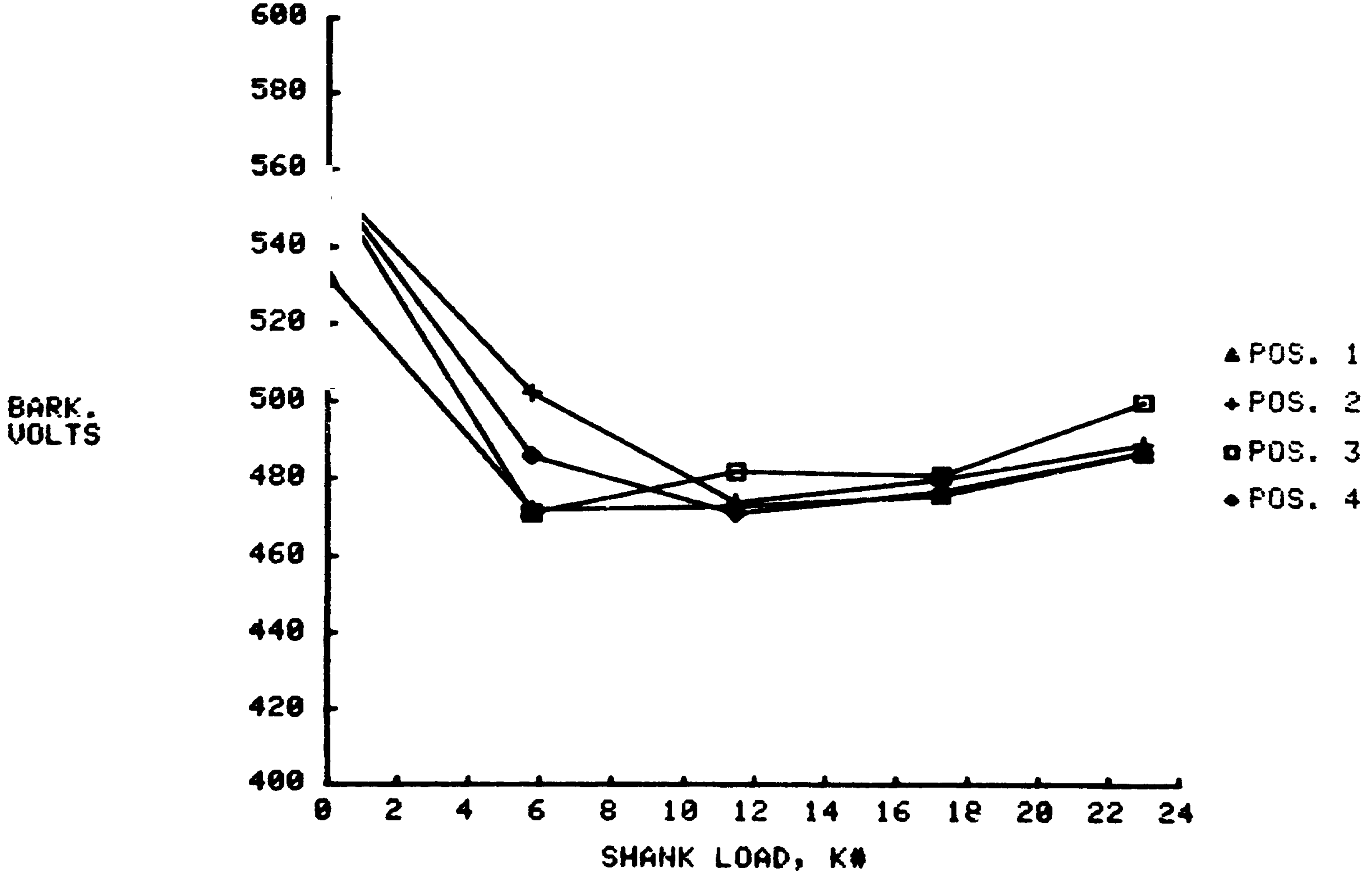

FIGURE 64.
MS21250 BOLT #1 BARKHAUSEN SIGNAL VS. LOAD AT
4 ORIENTATIONS, PROBE ON INSIDE WALL, .055" FROM BOTTOM

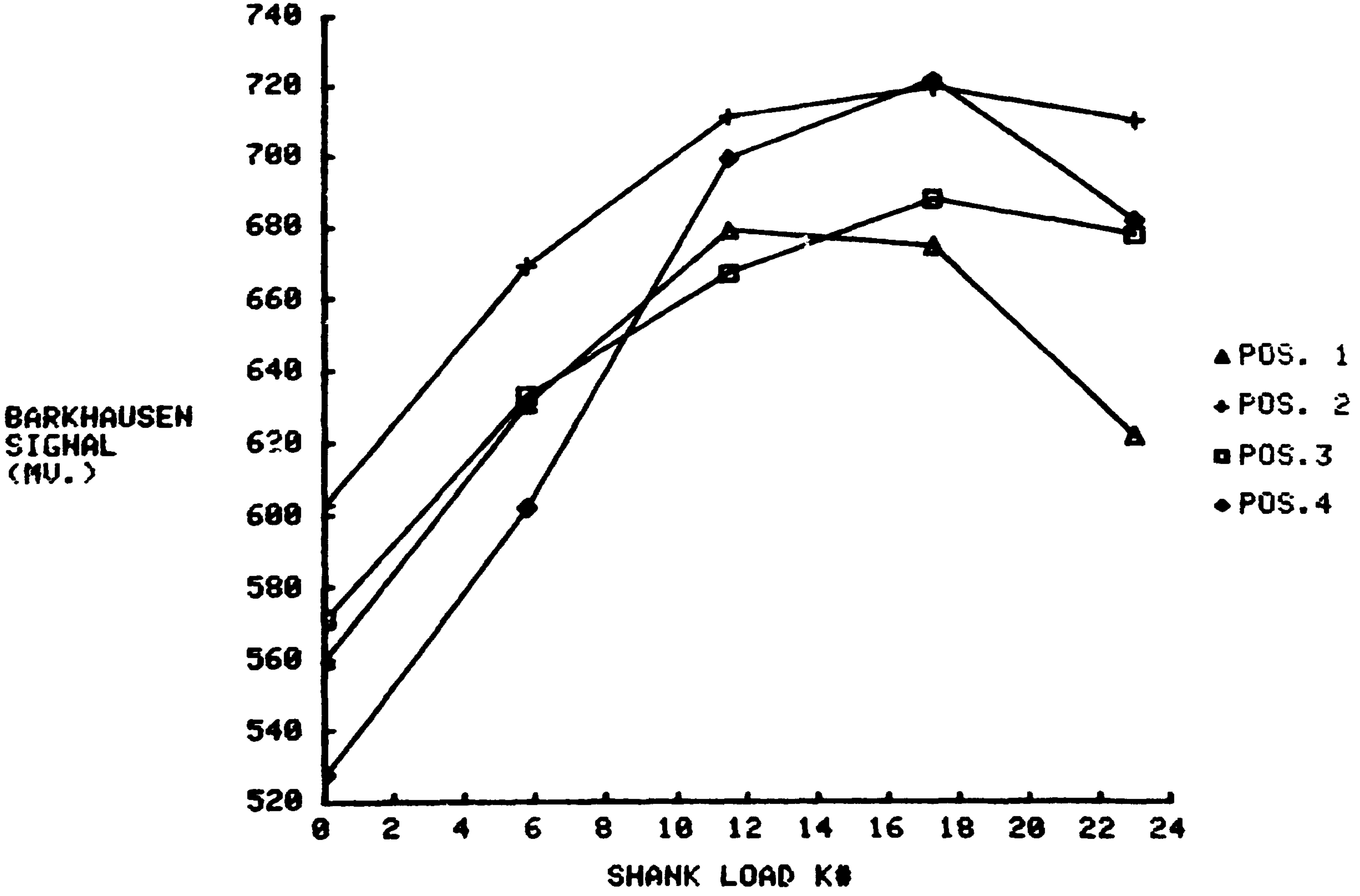

FIGURE 65.
MS21250 BOLTS
UNCORRECTED DATA

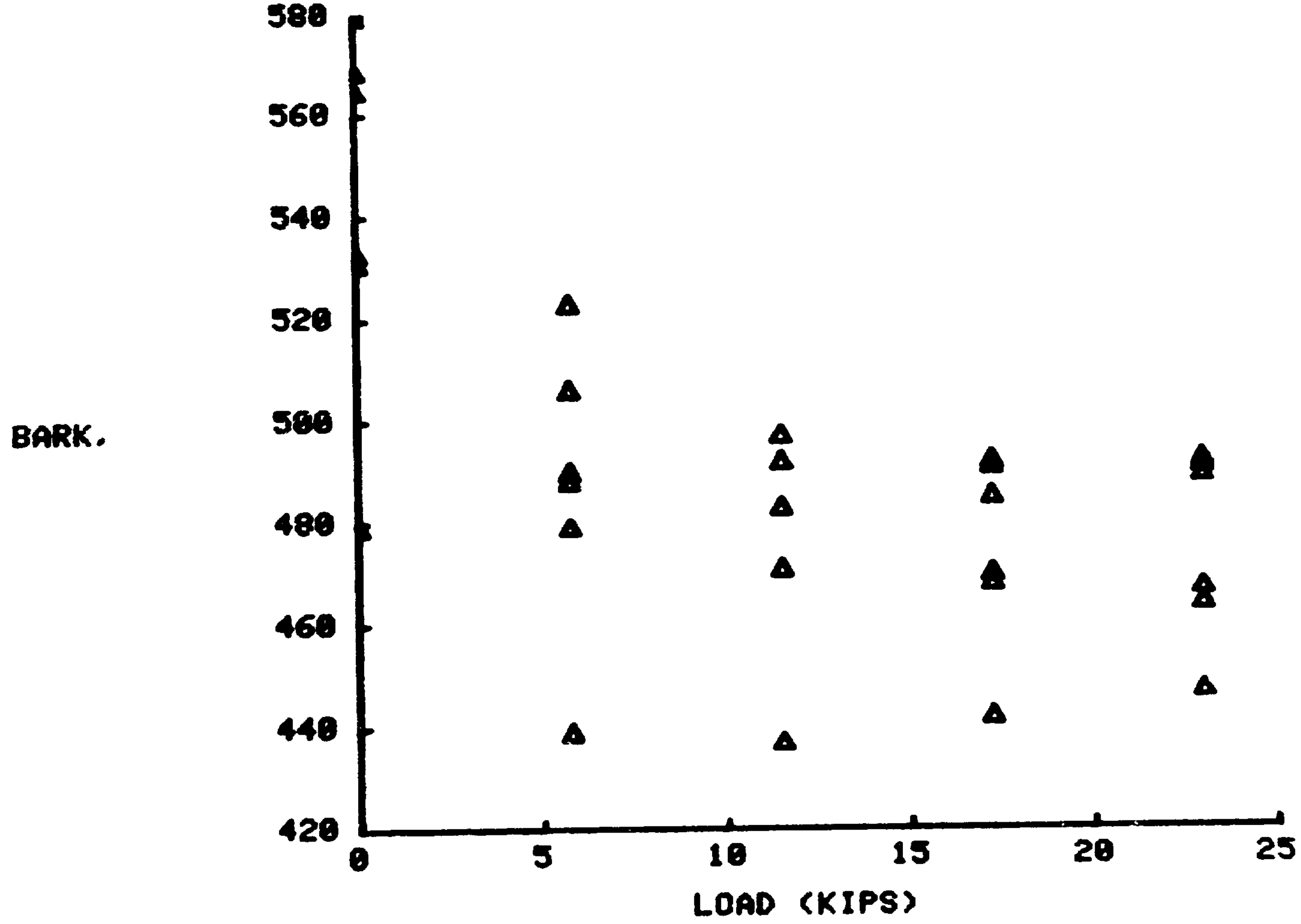

FIGURE 66.
MS21250 BOLTS
CORRECTED FOR RESIDUAL STRESS

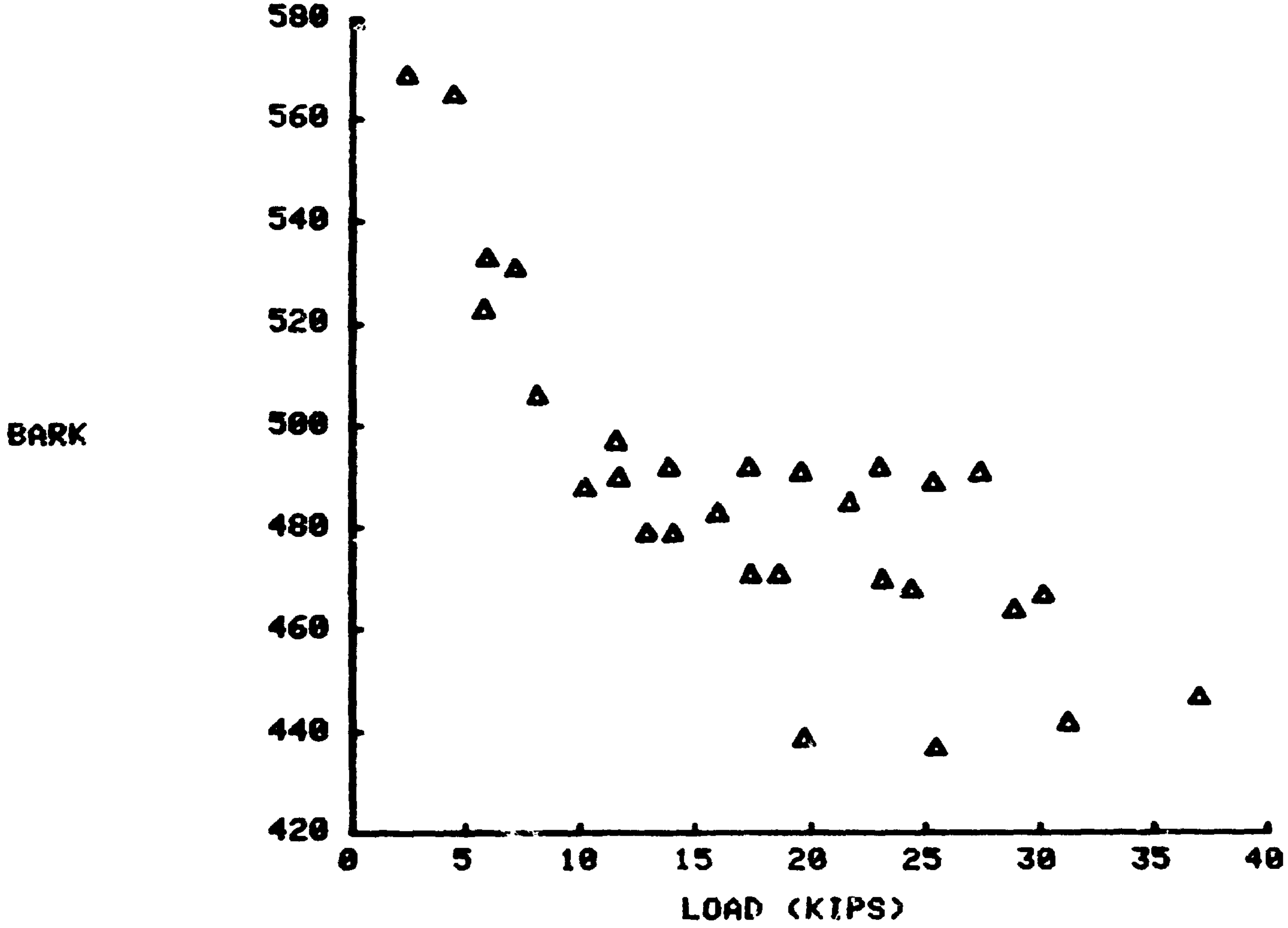

Residual Stress Experiments with MS21250 Bolts

An experiment was performed on the MS21250 bolts to attempt to reduce residual stresses by heat treatment in a manner similar to that applied to the hex head bolts. Two bolts were measured in "as received" condition, and then heat treated at 800°F and the load measurements repeated. The same two bolts were then heat treated again at 1100°F and final Barkhausen measurements vs. load taken. The results are plotted separately for both bolts in Figures 67 and 68. Since bolt strength was lowered after the 1100°F heat treatment, the bolts were reloaded to only 75% of full load. Barkhausen response after the 800°F heat treatment increased slightly in amplitude, which may indicate a partial relief of compressive residual stress. The 1100°F heat treatment resulted in a much larger increase in the Barkhausen no-load signals. This large signal change tends to show a marked relief of compressive residual stress.

As with the hex head bolts, it should be realized that changes in the Barkhausen signal accompanying heat treatment may also be influenced by changes in magnetic properties of the material introduced by the heat treatment process. The trends observed here are, however, consistent with the expected behavior of residual stress conditions and tend to reinforce the belief that residual stress conditions are present in the MS21250 bolts as well as the hex head bolts.

Acoustic and Ultrasonic Methods

Sound is acoustic energy, the mechanical vibration of the atoms in a medium. The motion of acoustic energy through a medium is analogous to wave motion in a fluid. Figure 69 is an illustration which can be interpreted in two ways: the wave-like oscillation can be thought of as the position of one atom varying with time, or it can represent the relative position of many atoms in space as a sound vibration occurs. In the spatial picture one can define the wavelength, i.e., the distance in space from one wave crest or area of compression to the next. In the time domain one can define the period as the time between passage of two wavecrests past a point. The frequency of the wave is the inverse of this period, i.e., the number of cycles per unit time. Finally, one can go to a space and time picture and define the velocity of the wave, i.e., distance the crest moves during one period of vibration divided by the period.

Ultrasonic waves,arbitrarily defined as acoustic waves of high frequency, travel through a medium via the interaction between atoms. This interaction can be pictured as though tiny springs connected neighboring atoms, the simplest theory of ultrasound, in which the spring constants are related to the elastic constants of the material. In an isotropic material all of the spring constants will be the same, but in an anisotropic material they will be different.

FIGURE 67.
[illegible]21250-05
BEFORE AND AFTER HEAT TREATMENT AT 800 AND 1100 F.

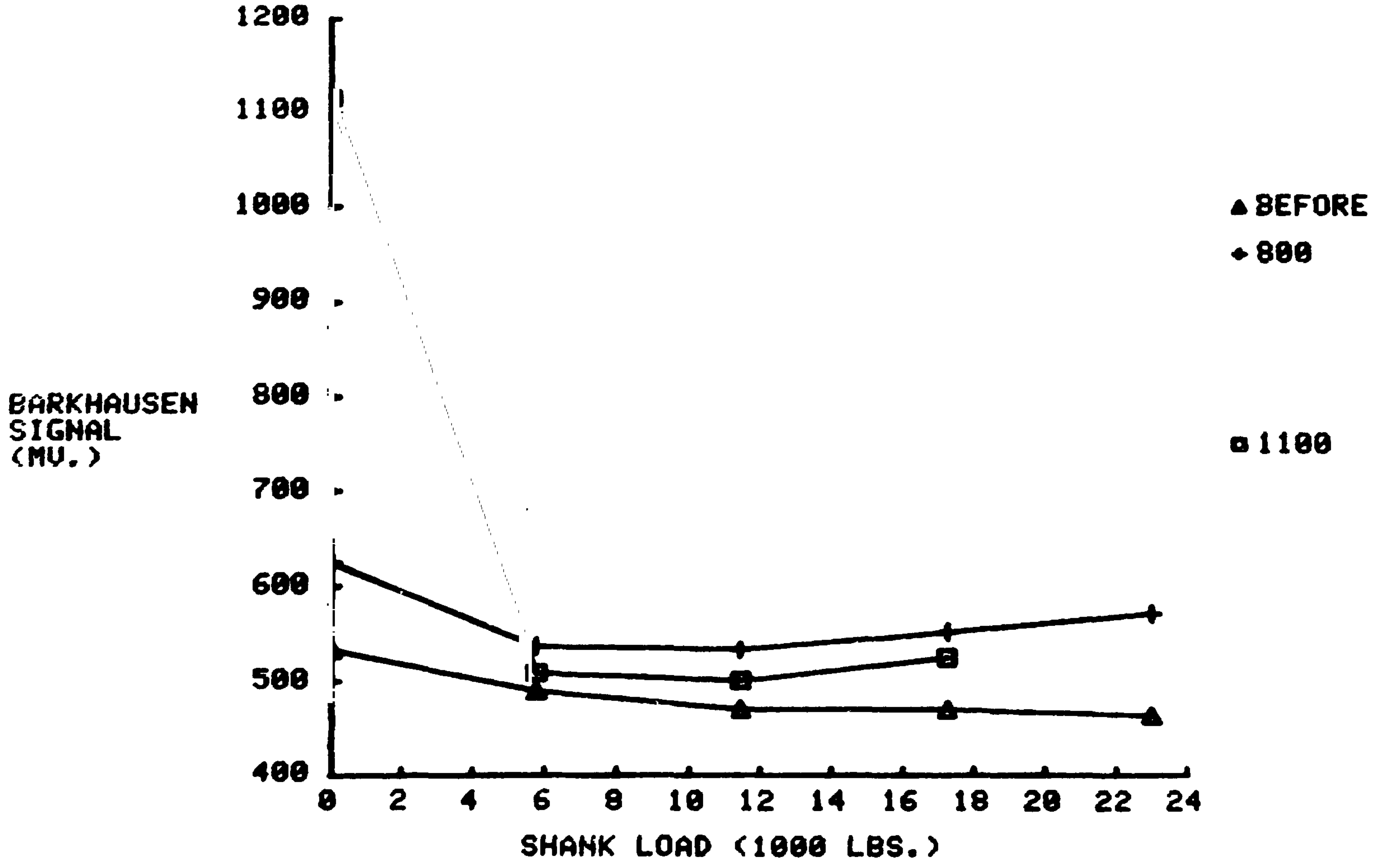

FIGURE 68.
1250-06
FORE AND AFTER HEAT TREATMENT AT 800 AND 1100 F.

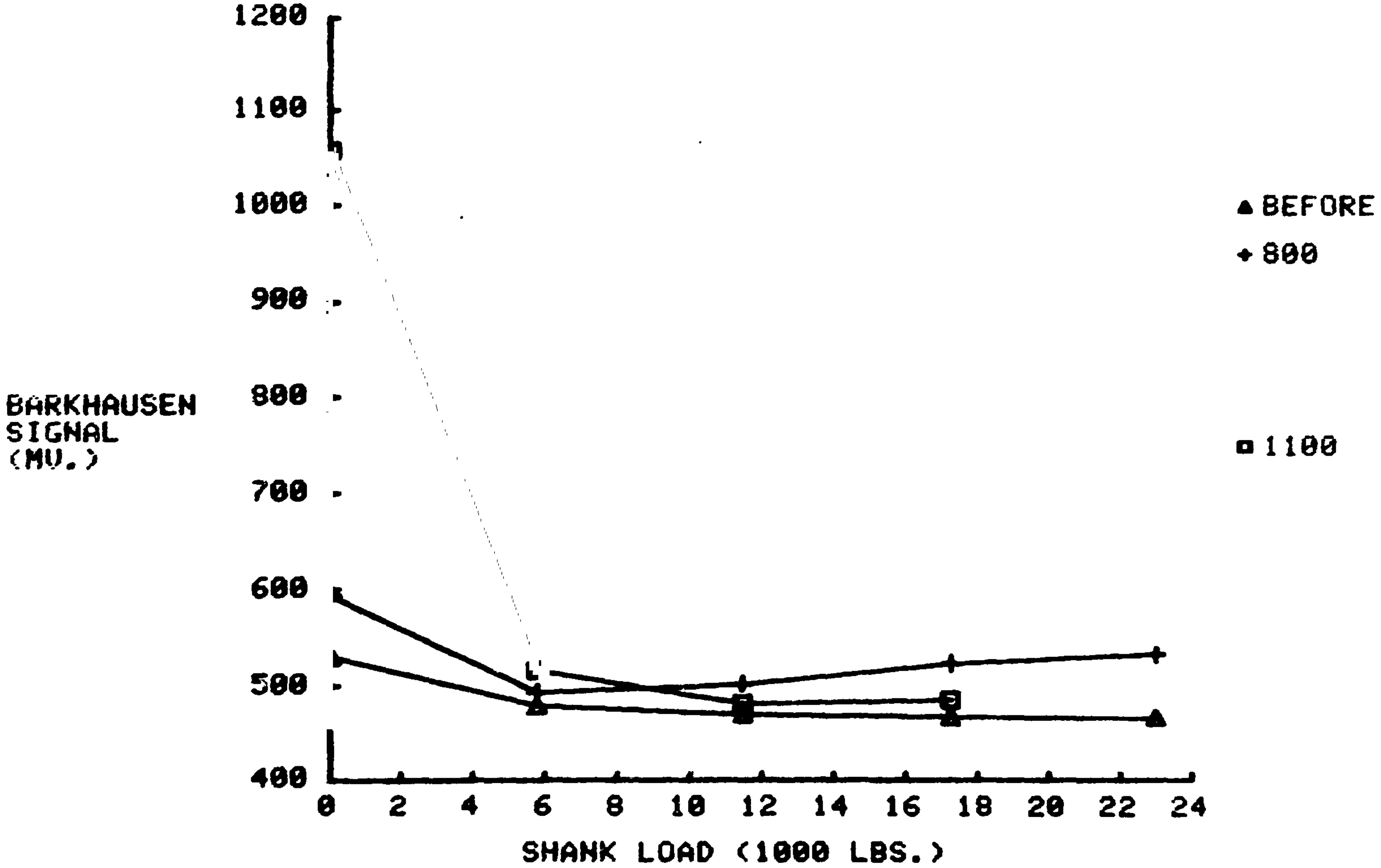

FIGURE 69: PLOT OF ATOMIC POSITION IN AN ULTRASONIC WAVE.

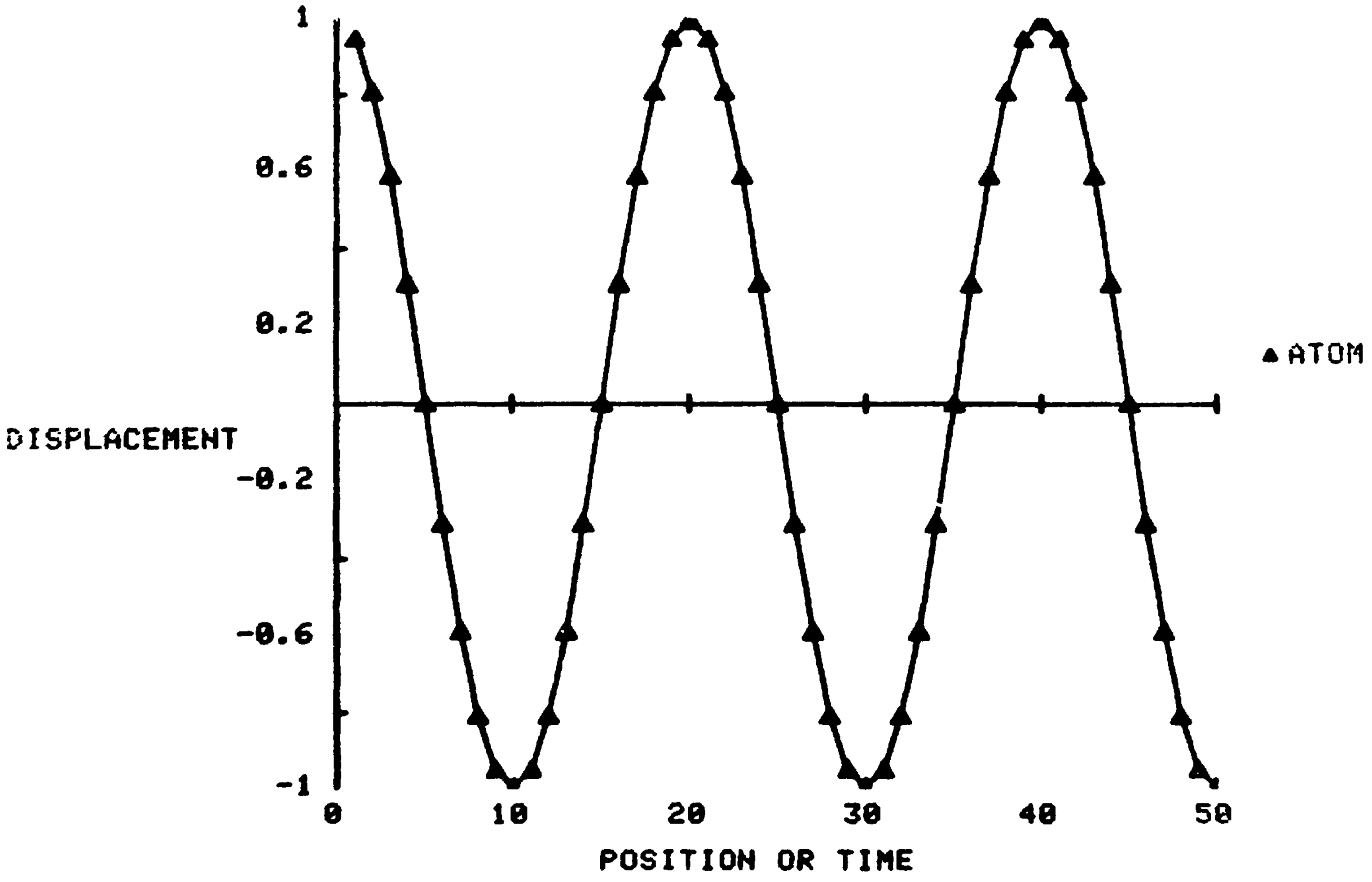

Mathematical analysis of this model leads to the recognition of two modes for ultrasonic waves: longitudinal and shear. Longitudinal waves can be pictured as waves which travel along a line of atoms with the vibration of the atoms parallel to the direction of wave propagation. In a shear wave the atomic vibration is perpendicular to the direction of wave propagation. There is only one possible longitudinal wave mode, but many shear wave modes can be propagated in a medium since the vibration of atoms in the shear wave can be in any direction in a plane perpendicular to the direction of propagation. The concept of polarization is used to distinguish between these different directions of atomic motion in the shear wave. In an isotropic medium, shear waves of any polarization can be propagated without distortion and all travel at the same velocity. In an anisotropic medium, only two polarization modes can be propagated without distortion and they travel at different velocities.

Application of Acoustic Energy to Stress Measurement

The application of stress to a solid medium produces several changes in the material including elongation, changes in elastic constants, changes in damping of atomic vibrations, and spectral response. These changes are reflected in corresponding changes in ultrasonic velocity, attenuation, or frequency spectrum which are subject to measurement. There are nine acoustic or ultrasonic methods capable of measuring these stress induced changes:

Acoustic Impact
Sonic Vibration
Acoustic Emission
Pulse-Echo
Transmission
Resonance
Surface Wave
Critical Angle
Shear Wave Birefringence

Only two of these techniques, pulse echo and resonance, have a quantitative interpretation basis. They are thus the primary candidates for successful application to the measurement of stress in fasteners. Acoustic impact also has some promise, and was felt worthy of investigation. Shear Wave birefringence has received recent attention and has the potential ability of determining bulk stress.

The other techniques are probably inapplicable for a variety of reasons. Critical angle ultrasonics requires that the part be immersed for inspection, which is obviously impractical for bolted joints. To use the sonic vibration technique, the part must be vibrated and the response compared to that of a standard via holography; this would be an impossible task in a practical situation, and interpretation of the results is very nebulous. Acoustic emission has a similar problem, since interpretation of results is unrefined and lacks specificity. Transmission ultrasonics requires access to both ends of the bolt, and detection of stress via surface wave transmission, an experimental technique, only measures surface stress. Since other more developed techniques can measure surface stress, the surface wave technique was not considered of great interest.

Longitudinal Wave Techniques

Both resonance and pulse echo techniques make use of longitudinal waves, and both have been used to measure stress effects in bolts. A pulse echo system is commercially available (the Douglas-Erdman instrument(14) which measures elongation of a bolt due to preload. The ROUS System(15) developed at NASA-Langley Research Center is a resonance system which is affected by both elongation and changes in the elastic constants produced by stress. The instrument is at present being prepared for commercial production. In addition, the Air Force Systems Command is funding an on-going research effort to attempt to develop a pulse echo system with 5% accuracy using commercially available equipment(16). Both the ROUS and the Erdman system propagate longitudinal waves down the length of the shank of the bolt and measure strain resulting from stress. A comparison of these two methods shows that one is basically the inverse of the other. In the pulsed system, the round-trip time is given by(17)

$$T = 2L/V \tag{7}$$

where

L = one-way path length and
V = is the ultrasonic velocity

In the resonance approach, the resonant frequency is approximately(18)

$$F_J = JV/2L \tag{8}$$

where

J = an integer.

This leads to

$$\Delta T/T = -\Delta F_J/F_J \tag{9}$$

From Hooke's Law(19) and acousto-elastic theory(20) it can then be shown that

$$\frac{\Delta T}{T} = -\frac{\Delta F_J}{F_J} = \left[\frac{1}{E} + \frac{2l + \lambda + \frac{\lambda+\mu}{\mu}(4m + 4\lambda + 10\mu)}{6(2\mu + \lambda)(\lambda + 2\mu/3)}\right] S \tag{10}$$

where

E is Young's Modulus,
μ and λ are 2nd order elastic constants,
l, m are 3rd order elastic constants,
s is strain

Shear Wave Techniques

The use of shear wave birefringence to measure stress has been proposed for many years(21,25), but no application in a practical instrument has been reported. For an isotropic medium subjected to a uniaxial stress the two allowed shear wave modes are polarized such that one is perpendicular and one parallel to the stress direction. The velocities of propagation of these waves are, respectively,

$$V_{\parallel} = \sqrt{\mu/\rho_0 - \frac{T}{3k_0\rho_0}\left[2\lambda - m + n/2 + \lambda n/2\mu\right]} \tag{11}$$

$$V_{\perp} = \sqrt{\mu/\rho_0 + \frac{T}{3k_0\rho_0}\left[\lambda + 2\mu + m + \frac{n\lambda}{4\mu}\right]} \tag{12}$$

where μ, λ are second order Lame' constants, m, n are third order Murnagham constants, k_0 is the bulk modulus, ρ_0 is the density, and T is the uniaxial stress.

Assuming the stress effect on the velocity is small, one has approximately:

$$V_{\perp} \cong \sqrt{\frac{\mu}{\rho_0}}\left[1 + C_{\perp} T\right] \tag{13}$$

$$V_{\parallel} \cong \sqrt{\frac{\mu}{\rho_0}}\left[1 - C_{\parallel} T\right] \tag{14}$$

where

$$C_{\perp} = 1/2\left[\frac{\lambda + 2\mu + m + n\lambda/4\mu}{3\mu k_0}\right] \tag{15}$$

$$C_{\parallel} = 1/2\left[\frac{2\lambda - m + n/2 + \frac{\lambda n}{2\mu}}{3\mu k_0}\right] \tag{16}$$

also defining

$$\Delta V \equiv V_{\perp} - V_{\parallel} \tag{17}$$

and

$$V_{AVE} \equiv 1/2(V_{\perp} + V_{\parallel}) \cong \sqrt{\frac{\mu}{\rho_0}} \tag{18}$$

$$\frac{\Delta V}{V_{ave}} \cong kT \qquad (19)$$

where

$$k = \frac{4\mu + n}{8\mu^2} \qquad (20)$$

For an anisotropic medium the allowed shear waves are polarized perpendicular and parallel to the preferred direction. In the absence of stress the two velocities are different and thus any zero stress difference is attributed to anisotropy. Thus in the presence of a uniaxial stress parallel or perpendicular to the preferred direction, one would have

$$V_{\perp} = V_{\perp o} \left[1 + C_{\perp} T \right] \qquad (21)$$

$$V_{\parallel} = V_{\parallel o} \left[1 - C_{\parallel} T \right] \qquad (22)$$

$$\frac{\Delta V}{V_{ave}} = \frac{\Delta V_o}{V_{ave}} + kT \qquad (23)$$

where ΔV_o is the zero stress difference in the velocities.

Further complications will arise if the stress direction is not parallel to the preferred direction. In this case the residual stress and the applied stress add vectorially resulting in a constantly changing preferred direction. Thus as the uniaxial stress changed one would have to rotate the wave source to track the preferred polarization.

Mechanical Impact Techniques

In a manner analogous to experimental measurement of electrical circuit characteristics, properties of a mechanical system can be determined by exciting the system and measuring the system response. One of the most informative characteristics which can be measured by this method is system frequency response. Resonant frequencies and attenuation slopes, which are important parameters of system behavior, can be readily identified from the frequency response curve. In electrical technology it is usual practice to excite the circuit under test with a sinusoid and measure steady-state system response at a number of frequencies; alternatively, a swept-frequency sinusoid may be used to accomplisn automatic plotting of frequency response curves. However, excitation of mechanical systems with sinusoidal waveforms often is not practical, so the equally valid impulse excitation technique is generally used.

The transfer function of a system is defined as the ratio of (1) the LaPlace transformation of the system response time function to (2) the LaPlace transformation of the forcing (i.e., system input) time function. System frequency response is the magnitude of the transfer function with the quantity $j\omega$ (where j is the complex variable operator and ω is angular frequency) substituted for the LaPlace transformation variable s. Because of the close mathematical relationship between the LaPlace transformation and the Fourier transformation, system frequency response is also identically equal to the magnitude of the ratio of (1) the Fourier transformation of the system response time function to (2) the Fourier transformation of the forcing (system input) time function.

The LaPlace transformation and the Fourier transformation of a mathematically perfect impulse (i.e., infinite amplitude, zero duration, and unity amplitude-duration integral) are unity. Thus, if a system could be excited with a mathematically perfect impulse, the transfer function would be simply the LaPlace transformation of the system response time function and the frequency response would be equal to the Fourier transformation of the system time response. This special property of the mathematically perfect impulse is the reason why impulse testing is useful and attractive. However, mathematically perfect impulses cannot be produced in the real world, so transfer functions and frequency responses often must be computed as ratios of the appropriate transformations. In a practical situation, the Fourier transformation of a physically realizable impulse may be sufficiently constant over the desired frequency range that a satisfactorily accurate frequency response can be obtained from the Fourier transformation of the system response.

Limited experiments were conducted employing the impulse excitation method of determining system frequency response on fasteners. In one case, the impulse was delivered by dropping a steel ball on the head of the bolt under test or by striking the bolt head with a mallet, and frequency response was determined assuming that the input impulse was "perfect" (at least in the frequency of interest). In a second set of experiments, the input impulse was delivered by an instrumented hammer, in which case frequency response was determined by computing the ratio of Fourier transformations. Experimental details are presented in a later section of this report.

Acoustics Experiments

The purpose of the acoustics experiments was to evaluate and compare selected sonic and ultrasonic methods of measuring stress. The primary concern was the accuracy with which the preload stress in a bolt could be determined, using generic calibration. This was evaluated by making measurements on several similar bolts and comparing the results.

A second concern was the accomplishment of post-loading measurement of stress which is particularly difficult with ultrasonic methods because of the low magnitude of the measurement parameters. Also, any special fastener preparation, such as machining, polishing, etc. was carefully evaluated. Because of the limited scope of the program, questions of long-term stability, temperature effects, and statistical behavior of a large fastener population could not be investigated.

Four acoustic techniques received experimental evaluation. These consisted of a commercially available pulse-echo extensometer (the Douglas-Erdman System), the NASA-developed ROUS resonance system, a shear-wave birefringence system, and a method known as the acoustic impact technique (AIT).

The ROUS System

NASA Langley Research Center has developed a system called the Reflection Oscillator Ultrasonic Spectrometer (ROUS) which makes use of several ultrasonic parameters that reflect stress. This developmental system was evaluated by the SwRI project team at the invitation of NASA Langley personnel in April, 1977. A block diagram of the system is shown in Figure 70.

When applied to a fastener, stress affects several parameters of the fastener, including its resonant frequency. These frequency changes are monitored by the closed-loop oscillator connected to a transducer which reportedly permits changes in frequency of 1 part in 10^7 to be detected, reflecting very small changes in applied stress.

For the evaluation experiments, three types of threaded fasteners were furnished to Langley several weeks in advance of the test. These consisted of five each titanium (6Al-4V, NAS678), steel (Grade 8, MS90727-119), and aluminum hex-head bolts (2024-T4). NASA personnel were asked to prepare the fasteners in any way deemed necessary. This preparation involved grinding the ends to a smooth finish and drilling small holes in opposite sides of the heads. These holes were used to mount the transducer. Additional identical bolts of two types did not receive special preparation, to assess the effectiveness of the system on bolts in an "as received" condition. Table X presents descriptive data on these bolts.

Table X

Bolt Material	Shank Length	Shank Diameter	Yield
Steel - Grade 8	2.92" ± .004	.492"	150 ksi
Aluminum 2024-T4	2.95" ± .014	.494"	62 ksi
Titanium 6Al-4V	3.43" ± .007	.496"	160 ksi

4122

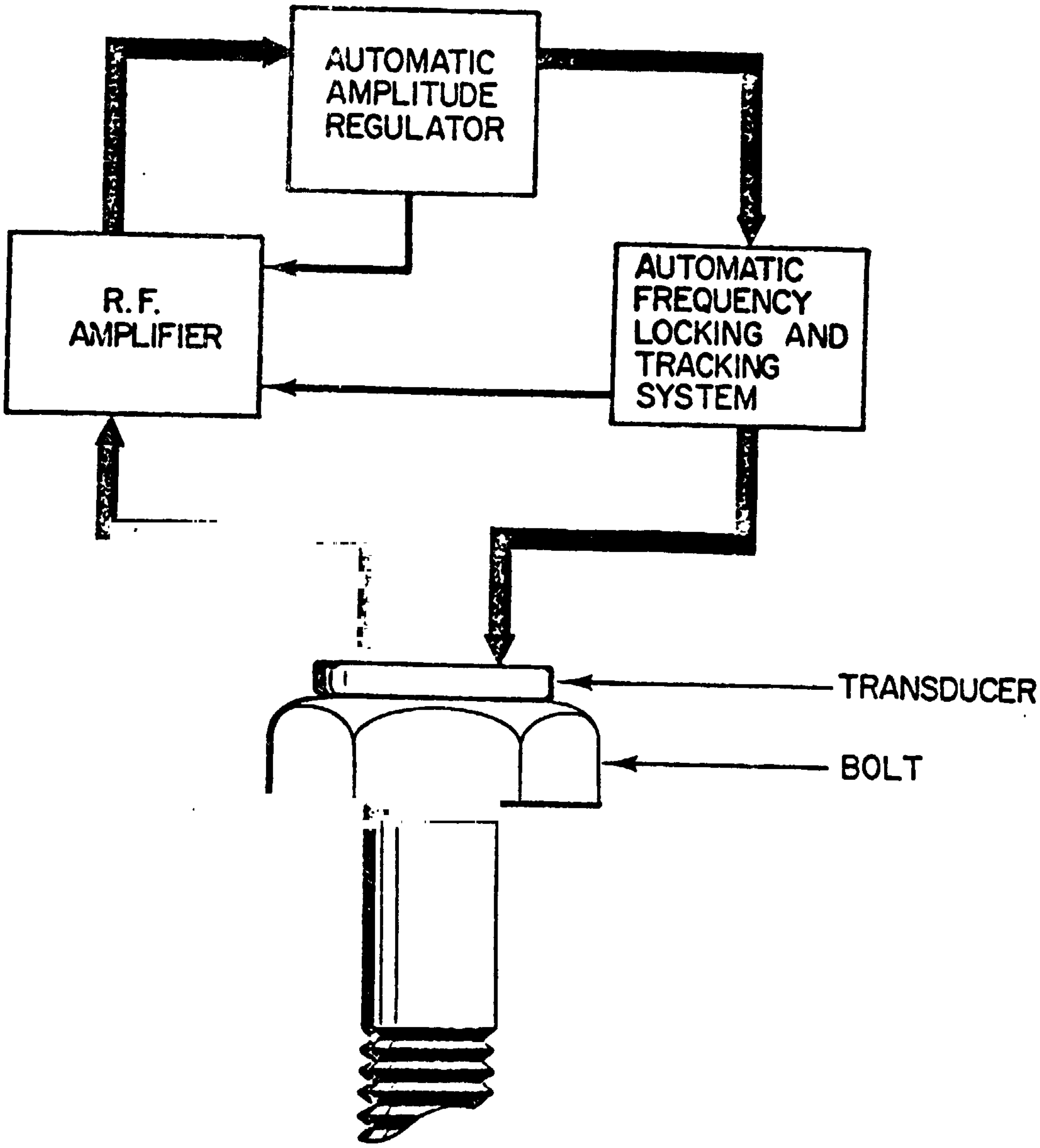
AUTOMATIC AMPLITUDE REGULATOR
R.F. AMPLIFIER
AUTOMATIC FREQUENCY LOCKING AND TRACKING SYSTEM
TRANSDUCER
BOLT

FIGURE 70. BLOCK DIAGRAM OF ROUS SYSTEM FOR MEASURING SHIFT IN RESONANT FREQUENCY OF BOLT vs. LOAD. (Ref. 15)

Resonance measurements were made on each bolt up to a load value near yield. The linearity and reproducibility of the system were excellent. The variation from bolt to bolt was slight ($\leq$ 3%), including those bolts with no preparation at all, in an "as received" condition. Operation of the system to determine preload is quite simple. The bolt is mounted in a load cell with the transducer attached, and tuning for initial resonance is accomplished by means of one control and two meters. One meter indicates the relative strength of the resonance, and the other the slope, from which the "peak" is isolated. Some discrimination and operator judgement is necessary in determining which resonance peak to use, but once a particular resonance is selected, a switch locks the system onto that peak, and no further adjustment is necessary. With different bolts of the same type, only slight readjustment was required to realign the system. Table XI gives a summary of the absolute measured resonant frequency of each bolt at no-load, and the total change in frequency at the maximum stress given. Figures 71 through 75 are plots of frequency shift vs. load for bolts of each type, together with least-squares curve fit to the data.

Table XI

Bolt No.	F_o (MHz)	F(kHz)	Load (KSI)
Steel			
St 1	6.3037	32.7	70.7
St 2	6.3161	33.2	71.3
St 3	6.3335	32.6	71.7
St 4	6.3293	33.0	71.8
St 5	6.3308	33.1	71.1
Aluminum			
Al 1	6.2504	80.6	53.3
Al 2	6.2627	47.1	33.8
Al 3	6.2675	47.	33.8
Al 4	6.2738	46.5	33.9
Al 5	6.2698	45.9	33.6
Al 6	6.2726	47.0	33.9
Titanium			
Ti 1-1	6.063	38.0	79.4
Ti 1-2	6.2884	69.7	144
Ti 2	6.071	37	79.4
Ti 3	6.055	36	79.1
Ti 4	6.077	38	79.1
Ti 5	6.0840	38.6	79.0
Ti 6-1	6.1719	37.5	79.2
Ti 6-3	6.0728	37.3	78.9

Al-6 and Ti-6 were bolts "as received" from the manufacturer.

FIGURE 71: FREQUENCY SHIFT DATA FOR THE STEEL BOLTS WITH LEAST SQUARES FIT TO DATA PLOTTED.

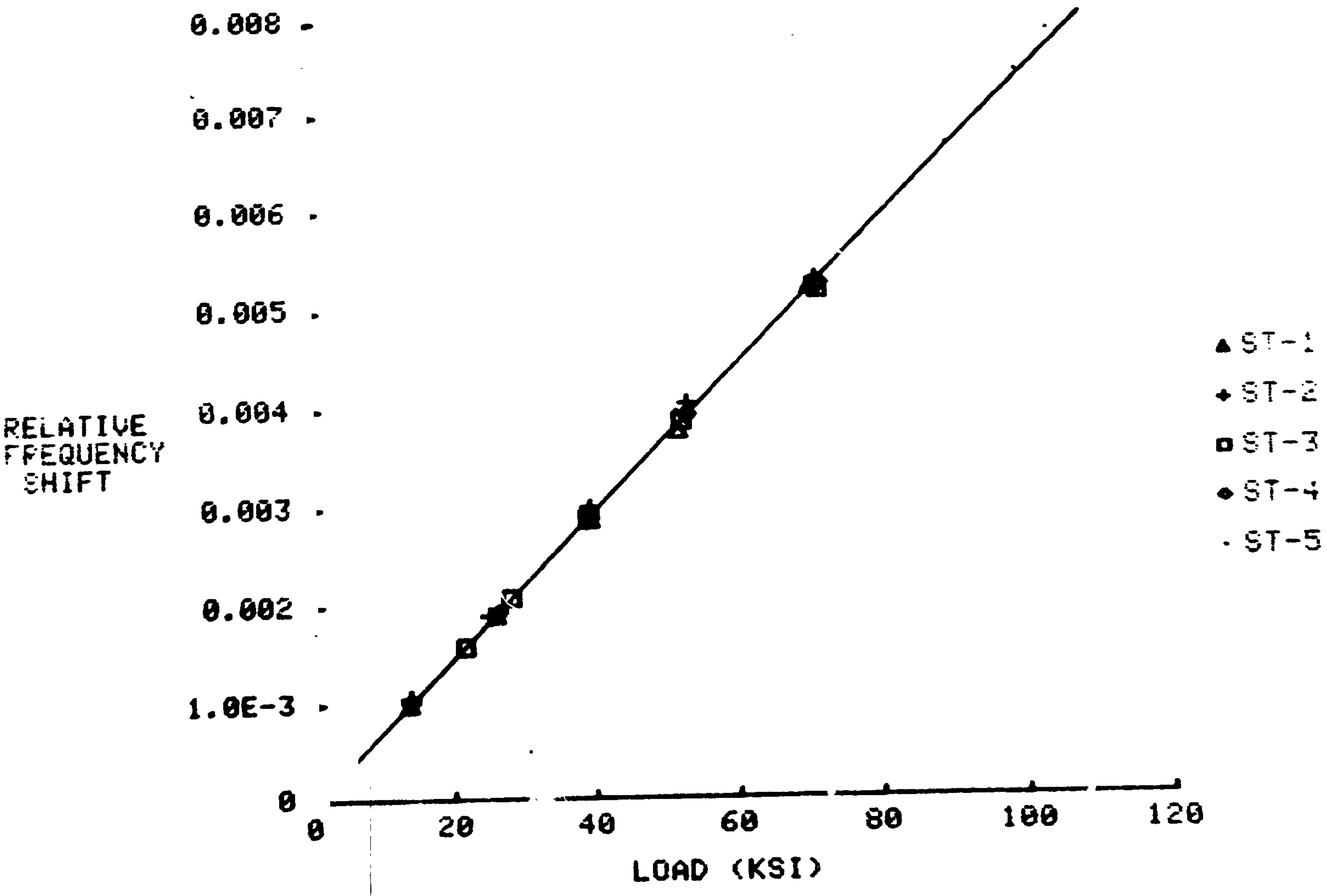

FIGURE 72: FREQUENCY SHIFT DATA FOR THE ALUMINUM BOLTS WITH LEAST SQUARES FIT TO DATA PLOTTED.

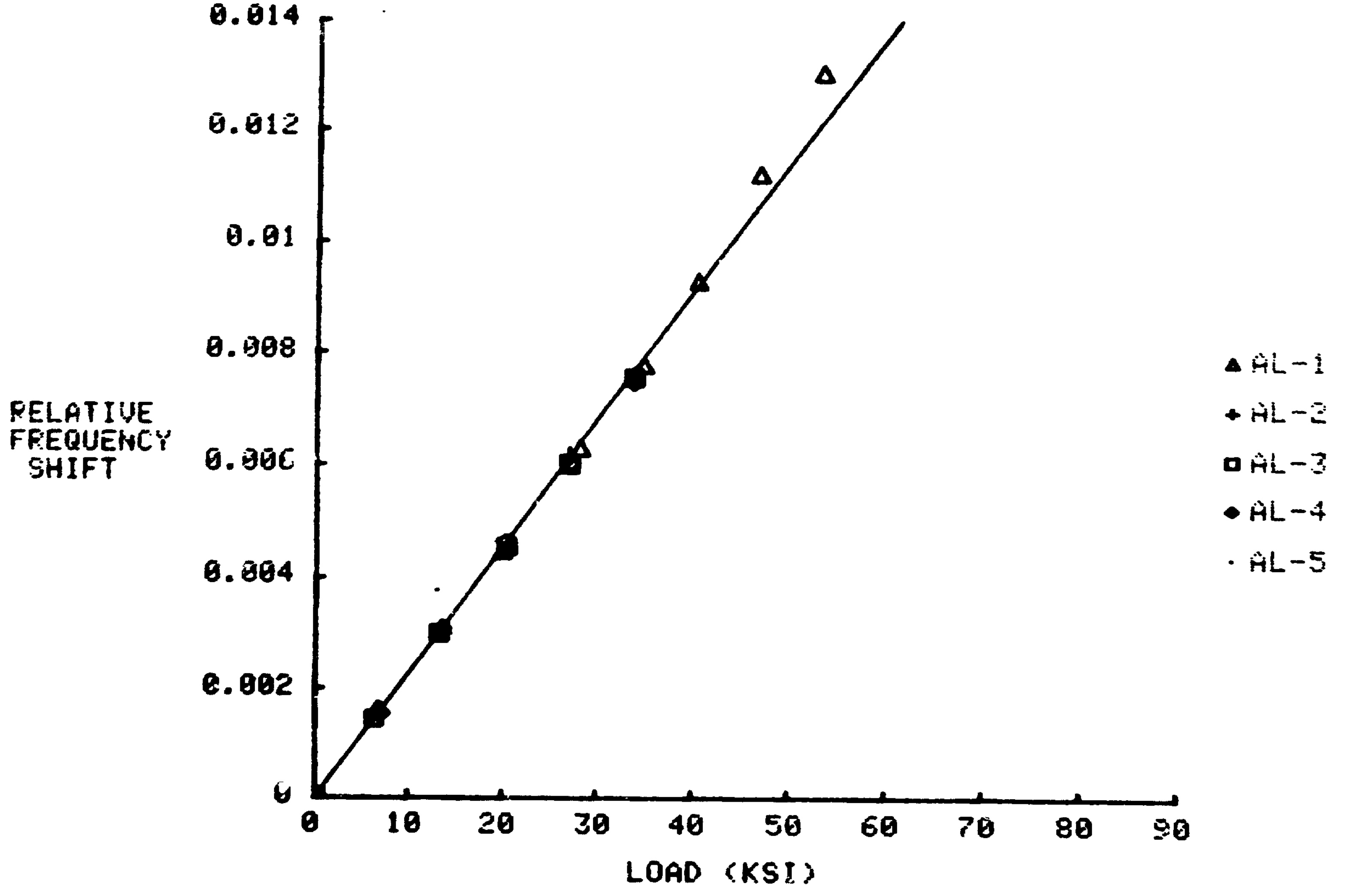

FIGURE 73: FREQUENCY SHIFT DATA FOR THE TITANIUM BOLTS WITH LEAST SQUARES FIT TO DATA PLOTTED.

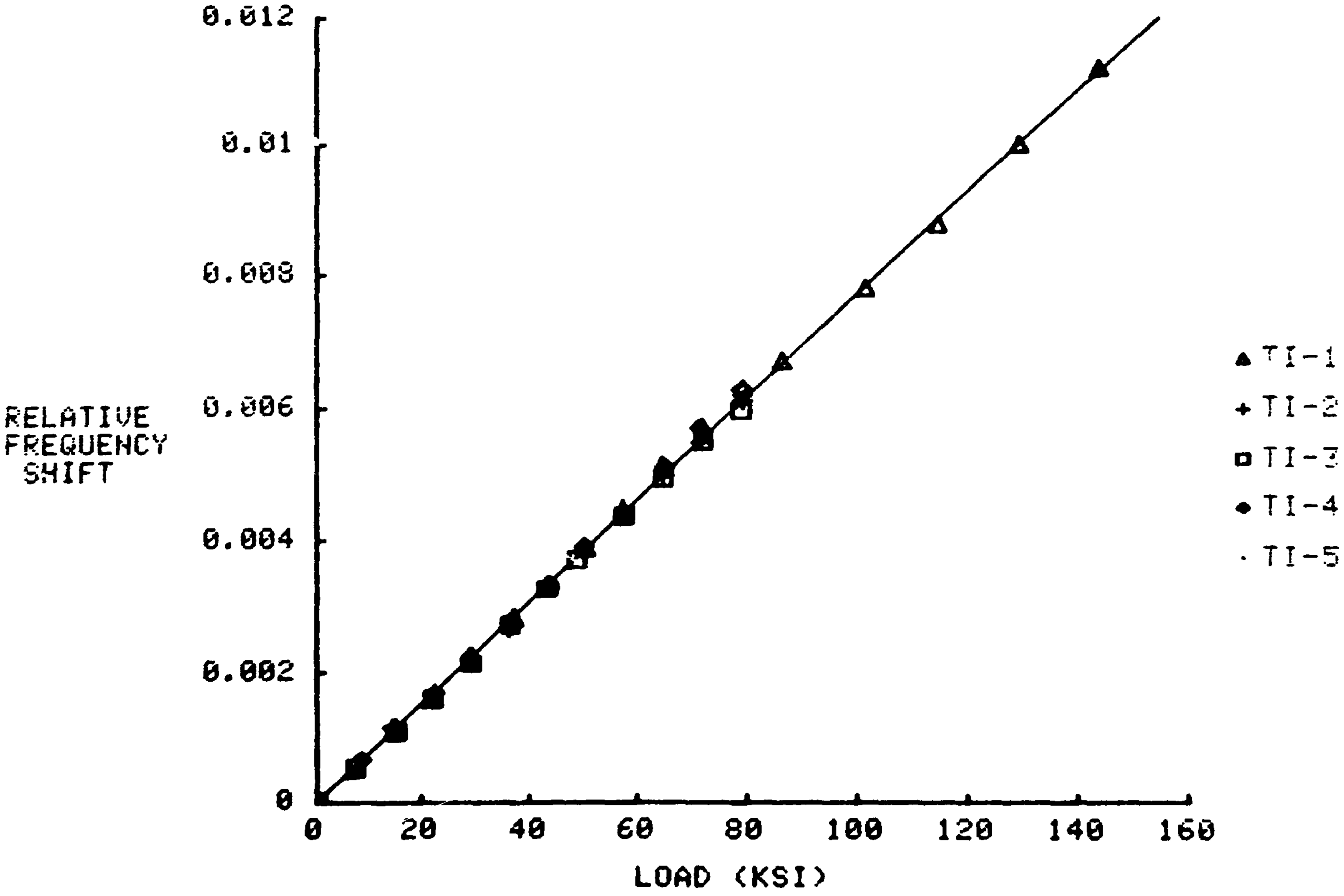

FIGURE 74: FREQUENCY SHIFT DATA FOR THE "AS RECEIVED" ALUMINUM BOLT WITH LEAST SQUARES FIT TO DATA PLOTTED.

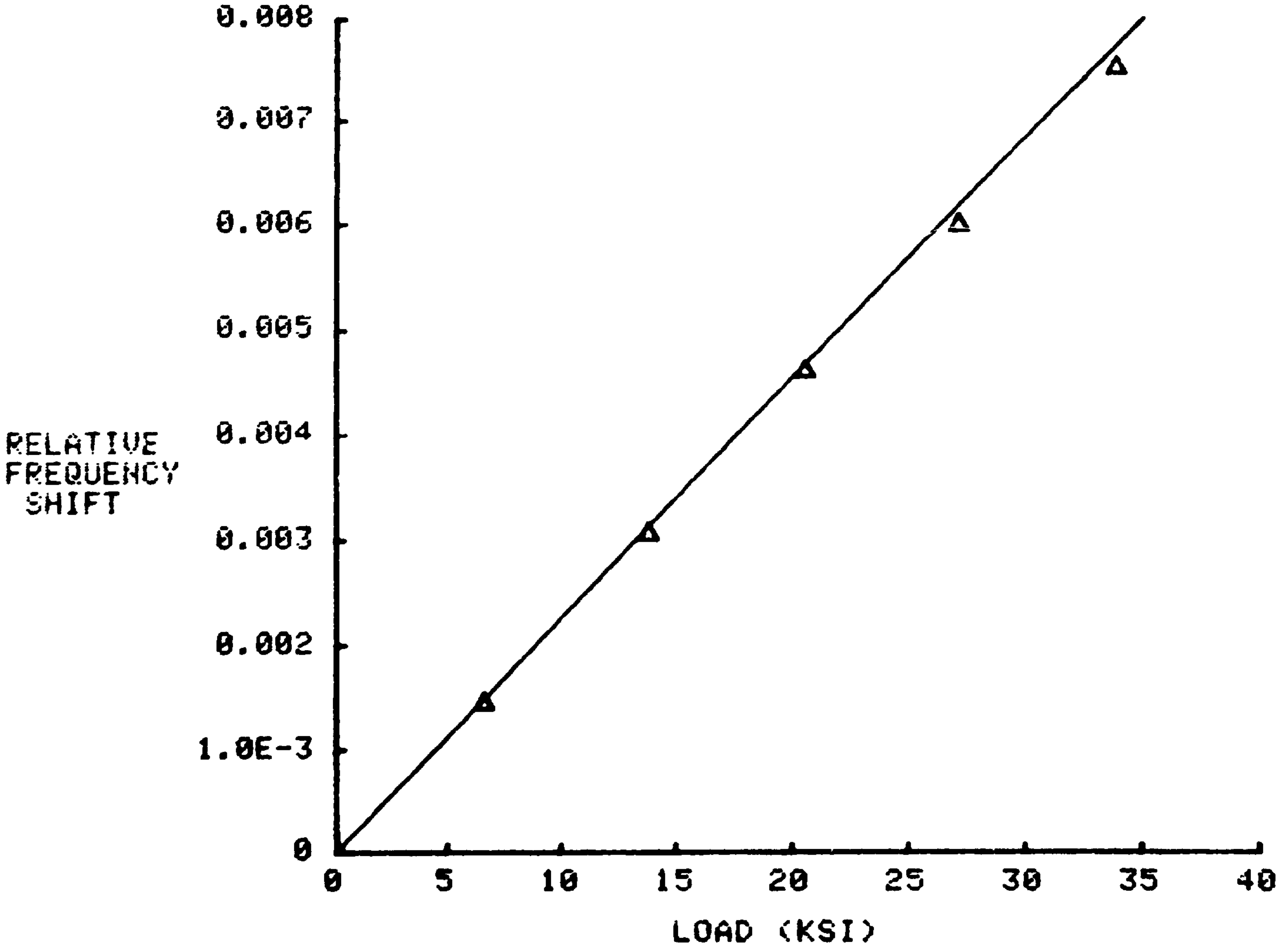

FIGURE 75: FREQUENCY SHIFT DATA FOR THE "AS RECEIVED" TITANIUM BOLT AT TWO RESONANT FREQUENCIES. WITH LEAST SQUARES FIT TO DATA.

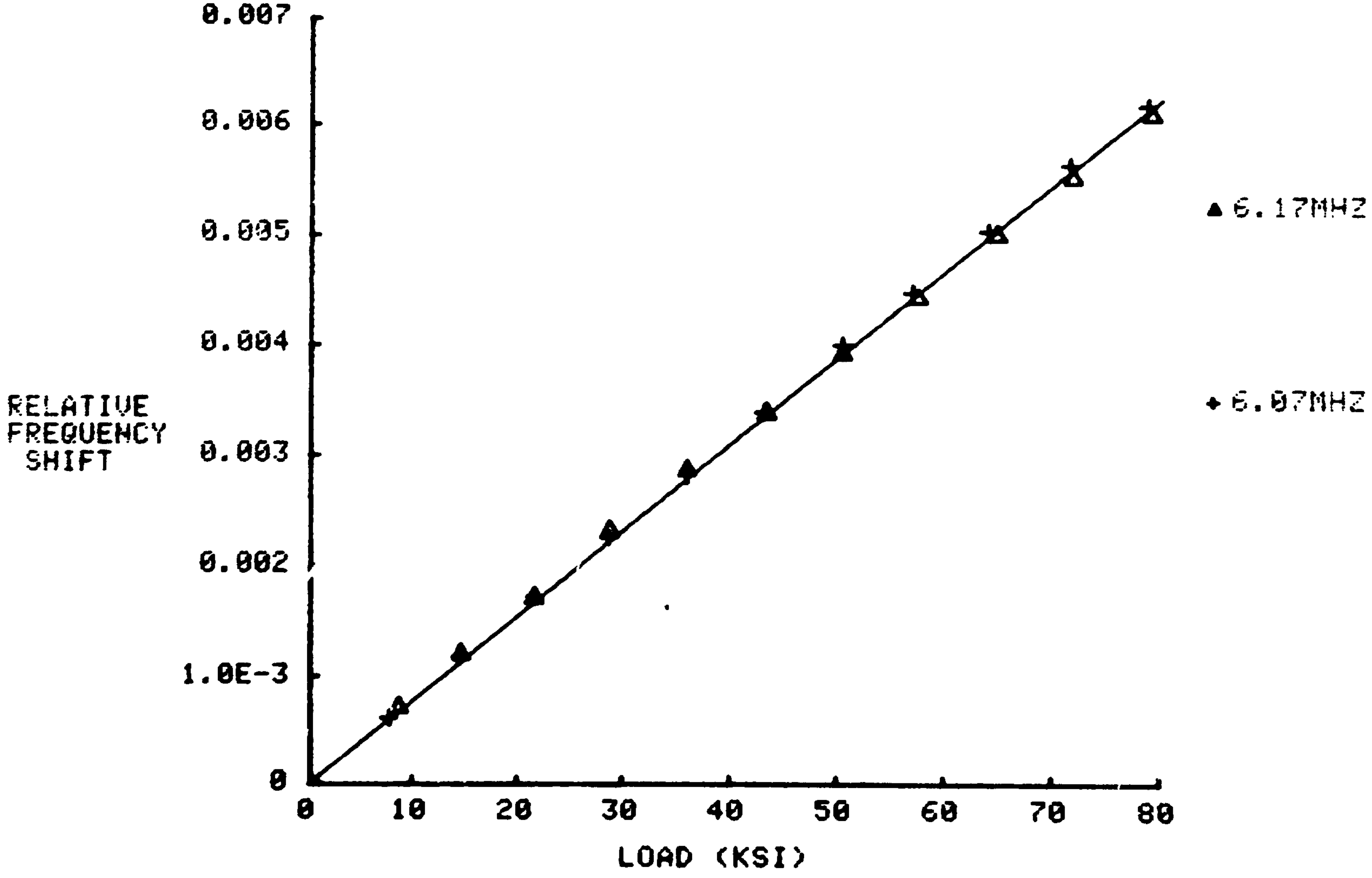

Evaluation of ROUS Data

The equation for frequency shift with stress is,

$$\frac{\Delta F}{F} = KS \tag{24}$$

where K is a constant which depends on the elastic constants of the material. From the experimental data a value for K can be calculated and compared to the theoretical value for each material. Table XII gives the calculated values of K, together with the theoretical values in the case of steel and aluminum.

Table XII

Bolt No.	K (1/ksi)	% Deviation from Average
St 1	7.33×10^{-5}	+ 0.4
St 2	7.37×10^{-5}	+ 1.0
St 3	7.18×10^{-5}	- 1.6
St 4	7.26×10^{-5}	- 0.5
St 5	7.35×10^{-5}	+ 0.7
Average	7.30×10^{-5}	
Theoretical	5.3×10^{-5}	-27.4
Al 1	2.42×10^{-4}	+ 9.5
Al 2	2.23×10^{-4}	+ 0.9
Al 3	2.22×10^{-4}	+ 0.5
Al 4	2.18×10^{-4}	- 1.4
Al 6	2.21×10^{-4}	0
Average	2.21×10^{-4}	
Theoretical	5.4×10^{-4}	+144
Ti 1-1	7.89×10^{-5}	+ 1.4
Ti 1-2	7.89×10^{-5}	+ 1.4
Ti 2	7.68×10^{-5}	- 1.2
Ti 3	7.52×10^{-5}	- 3.2
Ti 4	7.91×10^{-5}	+ 1.8
Ti 5	8.03×10^{-5}	+ 3.3
Ti 6-1	7.67×10^{-5}	- 1.3
Ti 6-3	7.78×10^{-5}	+ .1
Average	7.77×10^{-5}	

With the scarcity of data available on the elastic constants of structural alloys, it is surprising that the theoretical numbers even roughly agree with the measured values. Also, no particular care was taken to ensure reproducibility of coupling. In one case, the transducer was dropped during the experiment and was dislodged from its case. On the remainder of the bolts, an improvised mounting system was used to hold the transducer in place. This appeared to have no adverse effect on the operation of the system.

The results of this limited evaluation indicate that the approach is practical as a means of fastener tension control, assuming it can be incorporated in suitable torquing equipment. The model used in this evaluation was a laboratory device, operated under laboratory conditions on a limited number of bolts. Under such conditions, at least, preparation of the surface of the bolt does not seem to be critical, requiring only a relatively smooth area about 3/8" diameter on the top of the head. The system can accurately measure preload of a given threaded fastener, if a calibration for the type fastener is available. A remaining question is the complexity of a suitable calibration system in a field instrument. It is possible that a calibration curve for each MIL-STD would be adequate, and this should be evaluated. The developer of this system has indicated that length and bolt size should not affect the calibration, although no verification has been made. The effect of alloying on the calibration is not known. Measurement on a large statistical sample of bolts procured from different manufacturers is now essential.

Douglas-Erdman Extensometer

The only commercially available instrument located during the study is an ultrasonic pulse-echo device which measures fastener elongation. The sales representative for this system, the Raymond Engineering Co., arranged an instrument evaluation for the project team at the Raymond manufacturing plant in Middletown, Connecticut, in August, 1977.

The system consists of an instrument housing and cable-connected transducer. The housing is relatively large, weighing 22 pounds. It has four controls on the front panel: power, function, vernier, and alarm-set. The POWER switch allows selection of three modes: thickness (T), elongation (ΔT), or vernier (V). In each mode the measured parameter value is displayed in five digits on an LED readout. The VERNIER control continuously tunes the zero setting for elongation measurements. The ALARM control allows selection of both a visible and an audible alarm to indicate when a desired elongation has been obtained. This alarm signal can be applied to a servo to control automated torquing devices. A voltmeter on the front panel monitors the amplitude of the echo on which the instrument operation is based. Finally, a BNC connector on the front panel attaches the appropriate ultrasonic transducer cable.

The rear panel of the instrument contains a GAIN control to provide limited compensation for the strength of the echo signal, and two BNC connectors. The connectors are provided for an external oscilloscope. Internal adjustments within the instrument for automatic gain control, total gain, and initial delay, calibrate the instrument for specific applications (a factory, or trained technician function).

Operation of the Extensometer

In operation, a short ultrasonic pulse is transmitted through the length of the bolt. The echo from the opposite end activates a ΔT ramp generator which has been calibrated to the particular bolt type under test. The ramp generator is de-activated by a reset pulse, positioned by the VERNIER control on the front panel. This control is adjusted for a specified readout before the bolt is loaded. As the bolt is loaded, the echo arrives at a later time, because of the elongation. The change in arrival time is displayed on the LED readout. The accuracy of the readout is dependent on the factory calibration which, in turn, depends on an independent measurement of the elongation in a sample bolt with load. For the experiments performed for the project team, a micrometer was employed, readable to the nearest .0001". However, the instrument itself is capable of accuracy to the nearest .00001", so that improvement in calibration procedure should be possible.

Preparation of the calibration specimen (not each bolt measured) is critical, since thickness variations must be controlled within .00001" for ultimate precision. Bolts with ground ends were used for calibration in the evaluation demonstration. Measured variations using a flat table and dial indicator were of the order of .0005". Thus, at present at least, the calibration procedure limits the system accuracy. The instrument itself is capable of at least three times the present usable accuracy.

Extensometer Experiments

Bolts of the same three types (steel, aluminum and titanium) used in the ROUS experiments were used with the extensometer. Bolts under test were mounted in a model J, Skidmore-Wilhelm tester, and a drop of glycerine mixed with water (1:3) was applied to the head of the fastener for transducer coupling. For the steel bolts, a magnet was used to hold the transducer in place. For the aluminum and titanium bolts a special holder was fabricated with a set screw.

The extensometer was set to the proper calibration for the type fastener under test and the VERNIER adjusted for specified pre-torque readout. Torque was applied to the nut on the opposite end of the bolt and length readings made at 25%, 50%, 75% and 100% of proof load. All readings were made as soon as possible after reaching a new load value to minimize relaxation effects.

Tests were performed on the steel fasteners in three states of preparation: (a) ground on both ends, (b) filed head only, and (c) as received. Measurements were only made on aluminum and titanium bolts with ground ends.

Table XIII contains the measured values of elongation for nine steel bolts. These results are plotted in Figures 76 and 77. A statistical analysis of these results gives a standard deviation percentile of less than 3%.

Table XIV contains values of elongation for a single bolt (#1) with ground ends, cycled five times. Table XV is the same information for an as-received bolt (#10). This data is plotted in Figures 78 and 79. The percent deviation is about 1%. Table XVI contains the measured elongation at full load, after removing and replacing the transducer five times on two separate bolts.

Table XVII lists the elongation measurements at full load for an as-received bolt (#9) at approximately 0°C, 25°C and 50°C. The total change in length from 0°C to 50°C was measured by the extensometer to be 3.04 mils.

Table XVIII contains the elongation data for an aluminum bolt ground on both ends. The effect of varying the calibration setting by a small amount was also measured on this bolt. The results are plotted in Figures 80 and 81 Table XIX contains the elongation data on a titanium bolt ground on both ends. Figure 82 is a plot of this data.

Post-Installation Load Determination

The only approach to the post-installation inspection of a loaded fastener with this instrument involves (a) recording the length after pre-load determination at installation, (b) resetting the Vernier to the recorded value when a later inspection is required, and (c) measuring the new indicated elongation and relating it to load. To give a preliminary evaluation of this procedure, an experiment was run 24 hrs. following the elongation measurement on one of the bolts. Using the same instrument, the transducer was replaced on the bolt, the Vernier reset to the recorded voltage and the elongation remeasured. The measured elongation after 24 hrs. had changed from 10.22 mils to 9.24 mils, approximately 10%. The bolt was then loosened, and the no-load reading had changed nearly 8% of which temperature may have played a large part. Considering variations in instruments and conditions under practical situations, attempting to determine load at a later time by the elongation method is likely to show only limited accuracy.

Table XIII

Nine 1/2" Grade 8 Steel Bolts, one loading cycle
Elongation (Mils)

Load (kips) \ Bolt #	1	2	4	5	6	7	8	9	10	% Dev.
0	0	0	0	0	0	0	0	0	0	
7.5	2.42	2.44	2.36	2.34	2.41	2.51	2.36	2.33	2.40	2.5
15.0	4.98	4.87	4.86	4.77	4.93	5.00	4.77	4.77	4.94	1.8
22.5	7.49	7.29	7.45	7.28	7.49	7.51	7.34	7.30	7.52	1.3
30.0	10.21	9.79	10.16	10.01	10.11	10.17	10.02	9.93	10.12	1.3
0 Return	0.14	0.21	0.22	0.25	0.20	0.29	0.20	0.29	0.35	

Table XIV

1/2" Steel Bolt (#1) with ground ends, five loading cycles
Elongation (Mils)

Load (kips) \ Cycle #	1	2	3	4	5	% Dev.
0	0	0	0	0	0	0
7.5	2.55	2.48	2.49	2.49	2.51	1.1
15.0	5.12	5.01	5.01	5.02	5.04	.9
22.5	7.70	7.55	7.52	7.56	7.64	1.0
30.0	10.36	10.12	10.11	10.12	10.13	1.1
0 Return	0.41	0.13	0.11	0.12	0.15	

Table XV

1/2" Steel Bolt (#10), as received, five loading cycles

Elongation (Mils)

Load (kips) \ Cycle #	1	2	3	4	5	Dev.
0	0	0	0	0	0	0
7.5	2.46	2.46	2.44	2.44	2.42	0.7
15.0	5.02	4.98	4.97	4.95	4.95	0.6
22.5	7.54	7.46	7.44	7.40	7.42	0.7
30.0	10.00	9.94	9.89	9.84	9.90	0.6
0 Return	0.24	0.20	0.13	0.07	0.12	

Table XVI

Two Grade 8 Steel Bolts at full load
(transducer removed and replaced five times)

Elongation (Mils)

Trial \ Bolt #	4	1
1	10.16	9.81
2	10.33	9.71
3	10.18	9.83
4	9.91	9.70
5	10.17	9.70
Ave	10.15	9.75
% Dev	1.5	0.7

Table XVII

Effect of Temperature on Grade 8 Steel Bolt #9, zero to proof load.
Elongation (Mils)

Temp / Load (kips)	~0°C	RT(~25°C)	~50°C
0	0	0	0
30	10.19	9.93	10.13
0 Return	0.47	0.29	0.25

Table XVIII

Effect of Error in Calibration Setting on Aluminum Bolt
Elongation (Mils)

Cal Setting / Load (kips)	5.9	6.0 (correct)	6.1
0	0	0	0
1	1.20	1.32	1.34
2.5	3.10	3.16	3.22
4	5.27	5.42	5.45
5	6.49	6.68	6.60
0 Return	--	0.29	--

Table XIX

Titanium Bolt

d (kips)	Elongation (Mils)
0	0
5	4.56
10	9.40
15	14.92
19	19.24

FIGURE 76: ELONGATION MEASURED BY DOUGLAS-ERDMAN INSTRUMENT ON GRADE 8 STEEL BOLTS WITH PREPARED ENDS.

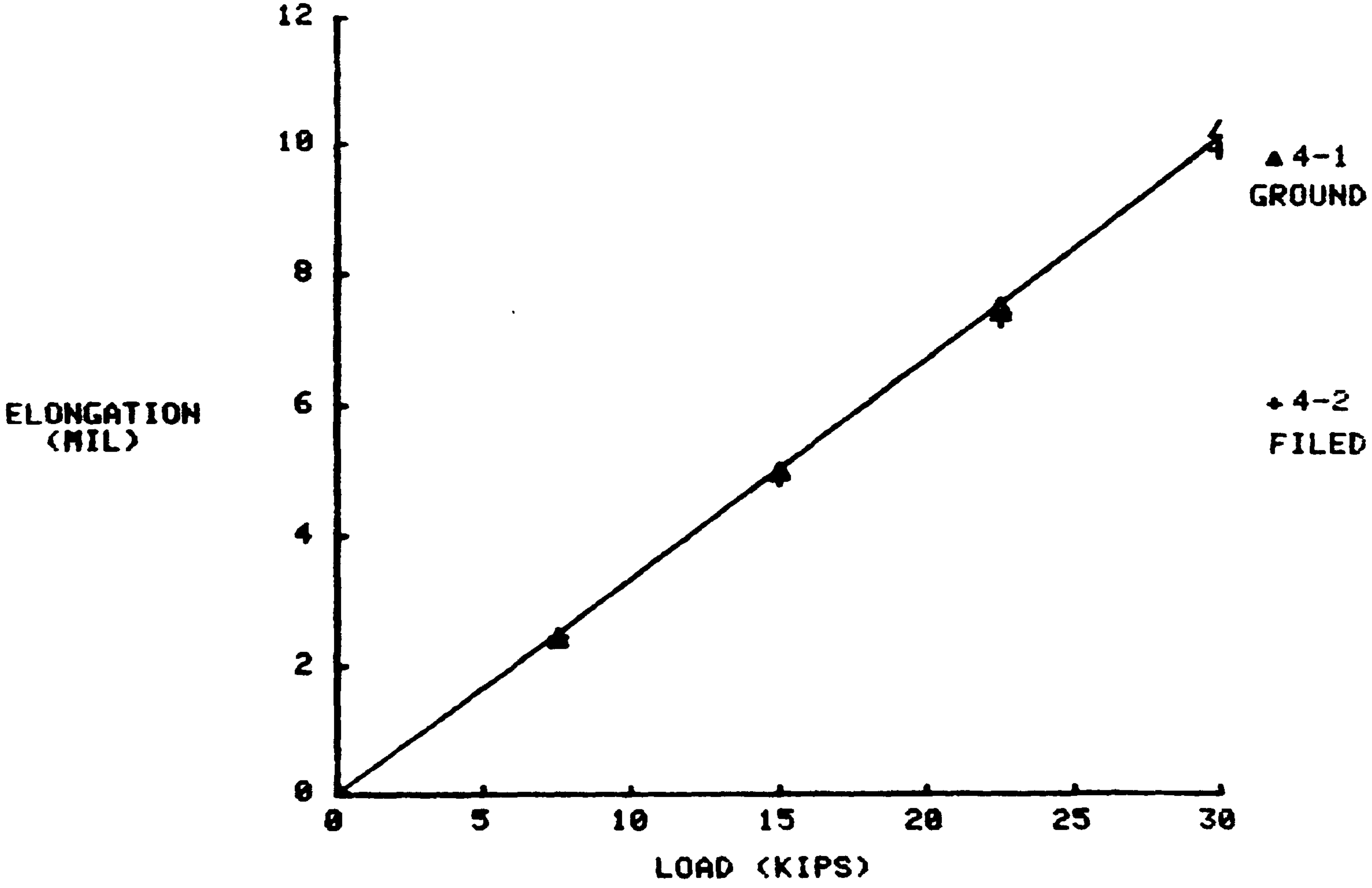

77: ELONGATION MEASURED BY DOUGLAS-ERDMAN INSTRUMENT ON UNTOUCHED GRADE 8 STEEL BOLTS.

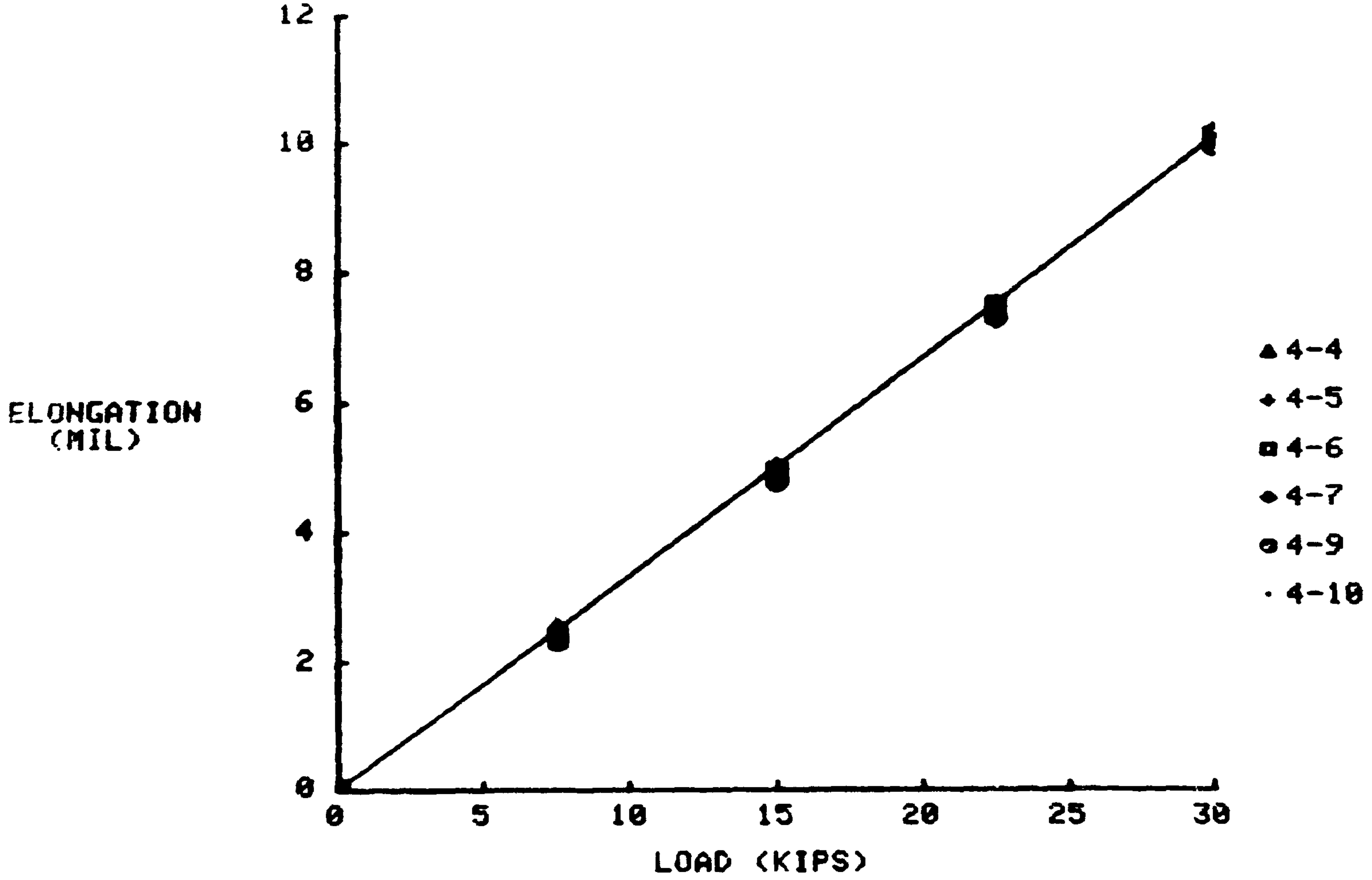

IGURE 78: VARIATION WITH CYCLING OF THE ELONGATION MEASUREMENTS ON A GRADE 8 STEEL BOLT WITH GROUND ENDS (4-1).

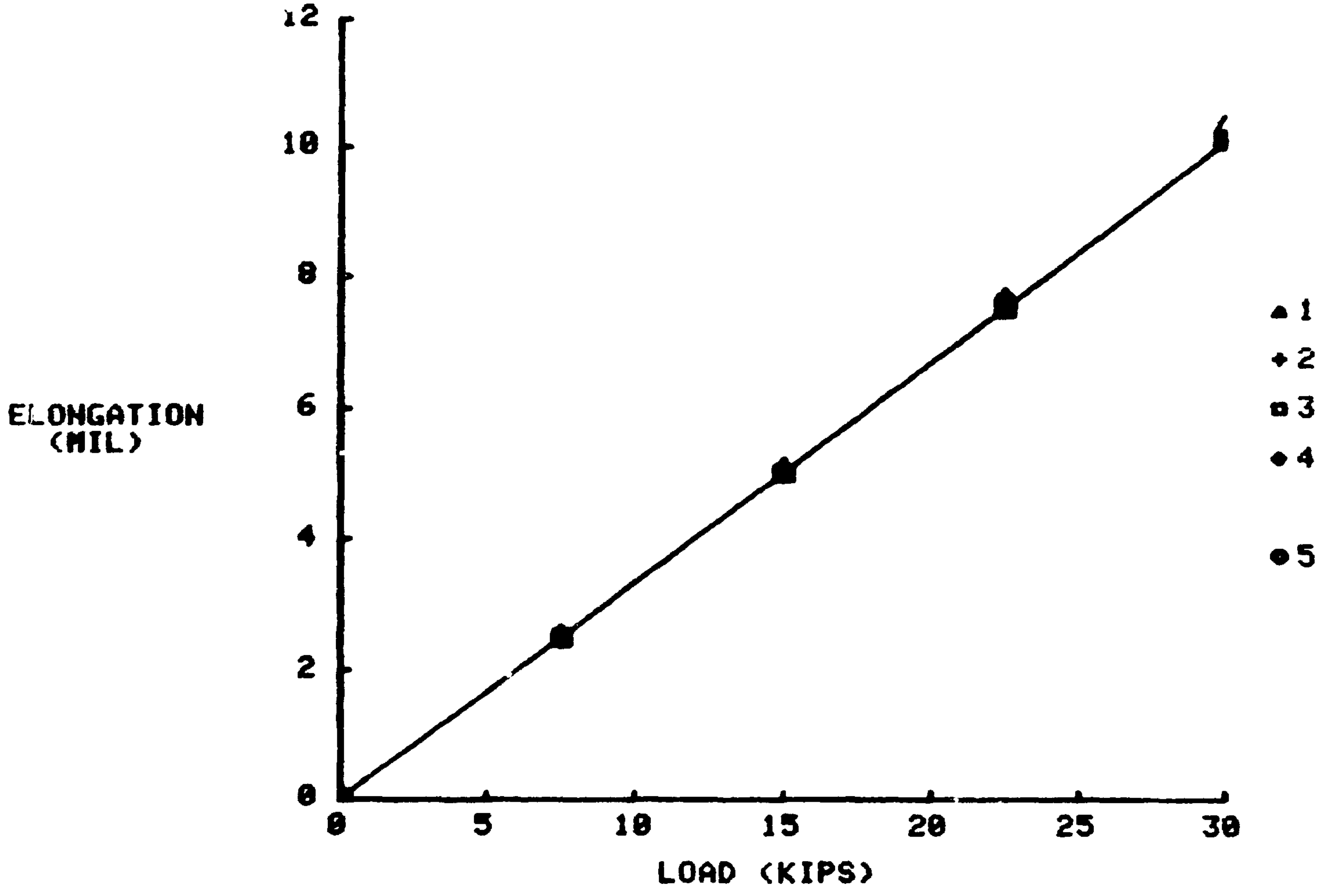

IGURE 79: VARIATION WITH CYCLING OF THE ELONGATION MEASUREMENTS ON A GRADE 8 BOLT WITH UNPREPARED ENDS.

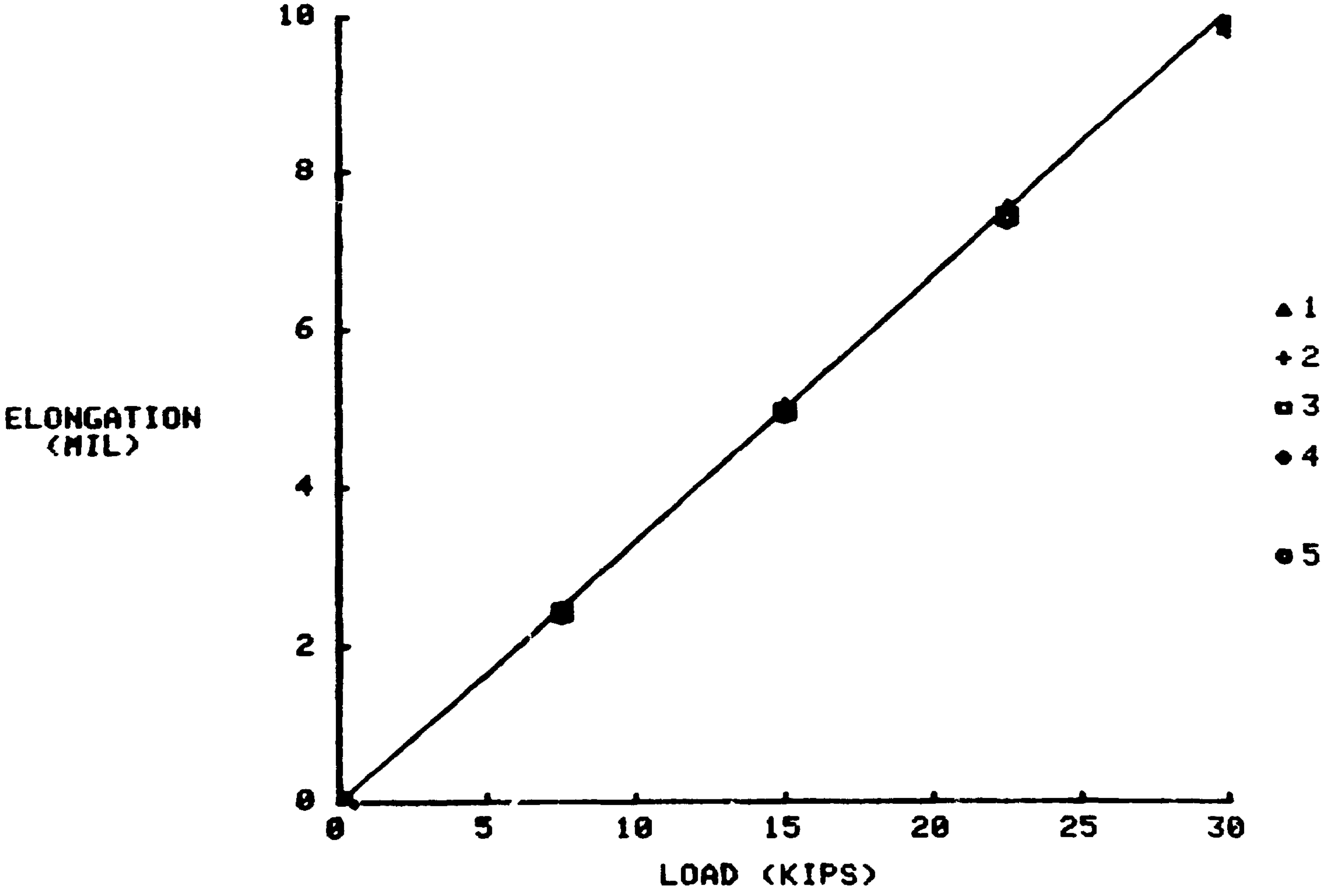

FIGURE 80: ELONGATION OF AN ALUMINUM BOLT MEASURED BY THE DOUGLAS-ERDMAN INSTRUMENT.

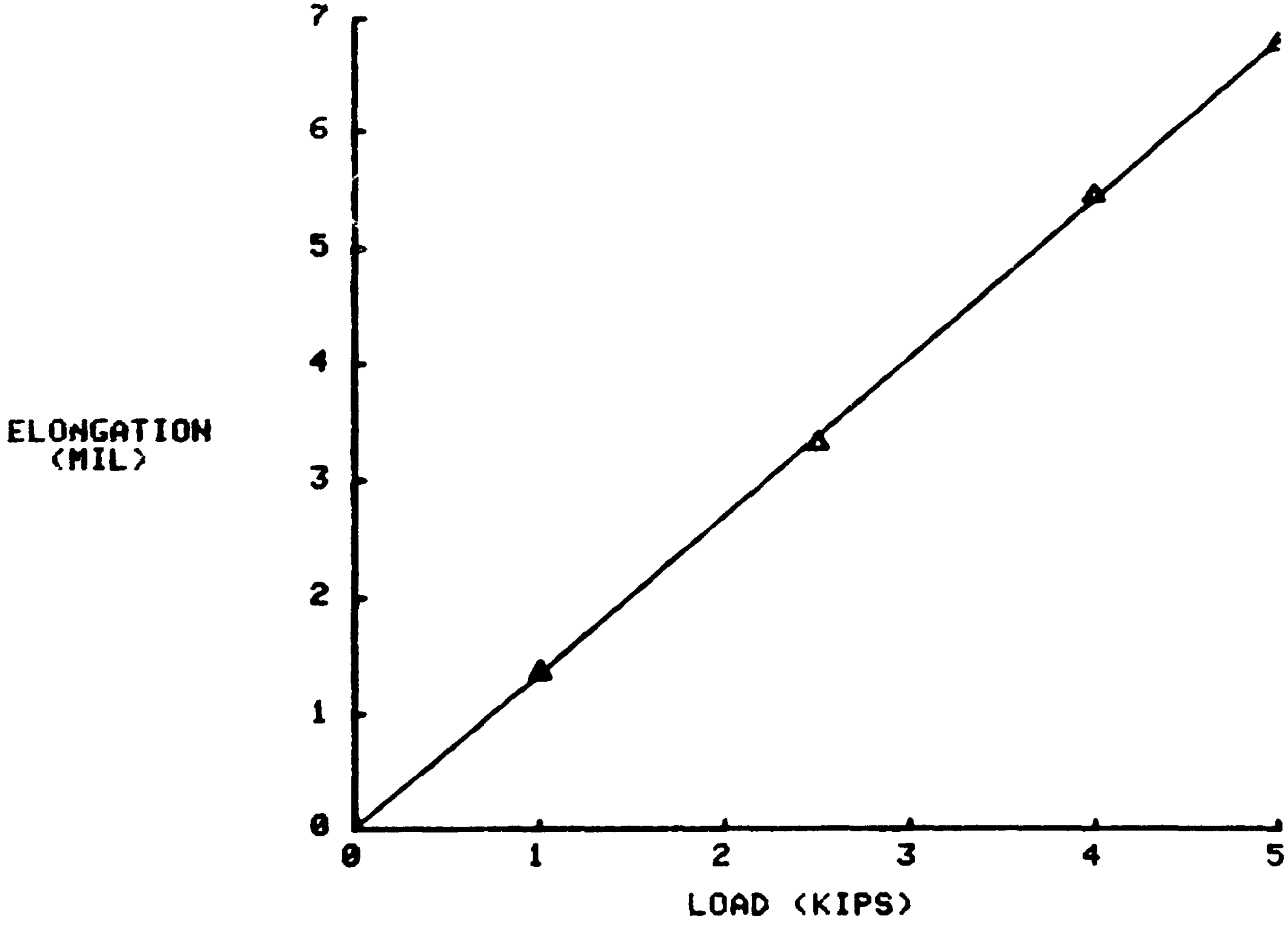

FIGURE 81: VARIATION IN ELONGATION MEASUREMENTS WTIH CHANGES IN CALIBRATION SETTING FOR ALUMINUM BOLT.

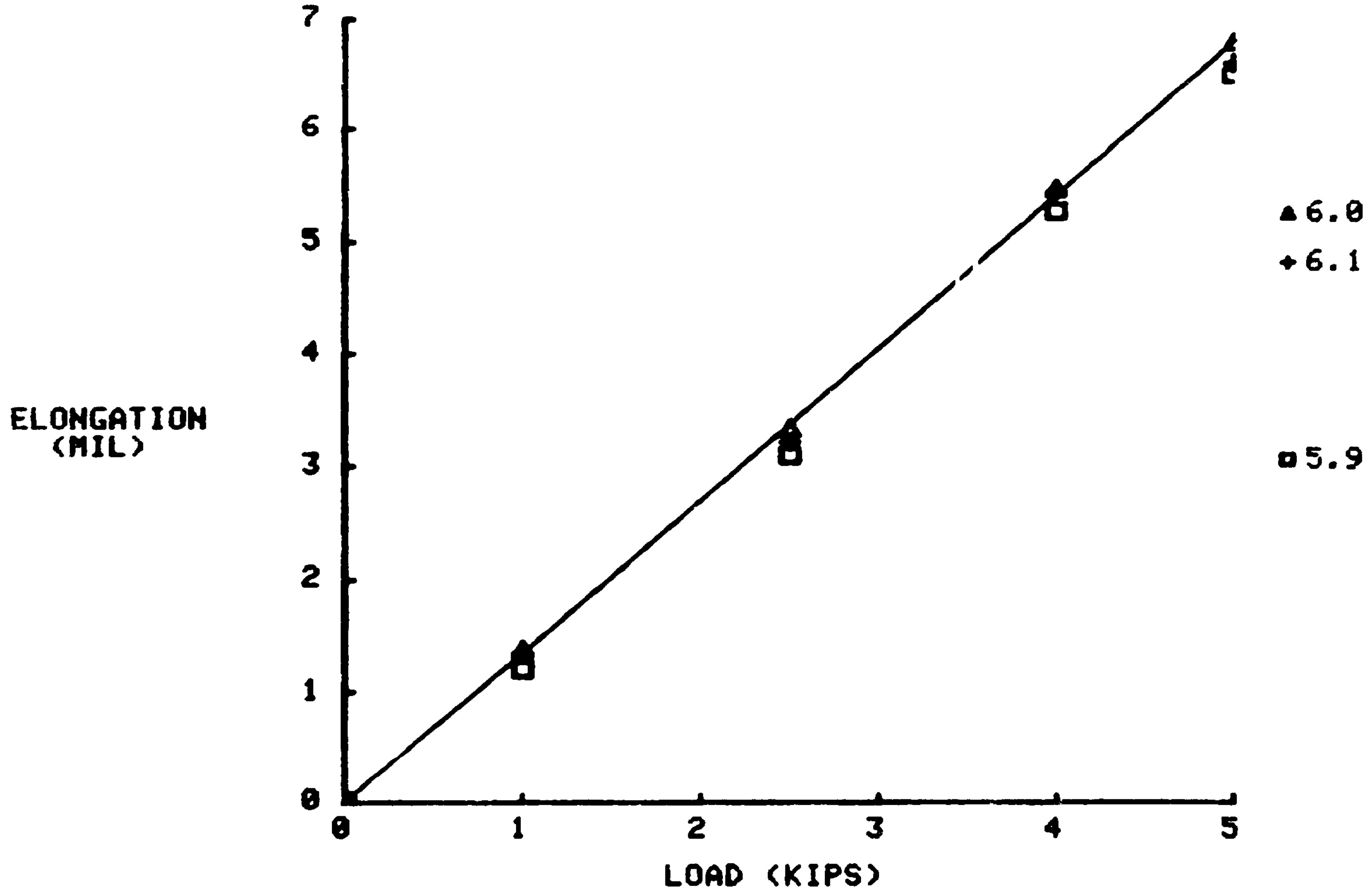

FIGURE 82: ELONGATION MEASUREMENTS ON A TITANIUM BOLT USING THE DOUGLAS-ERDMAN INSTRUMENT.

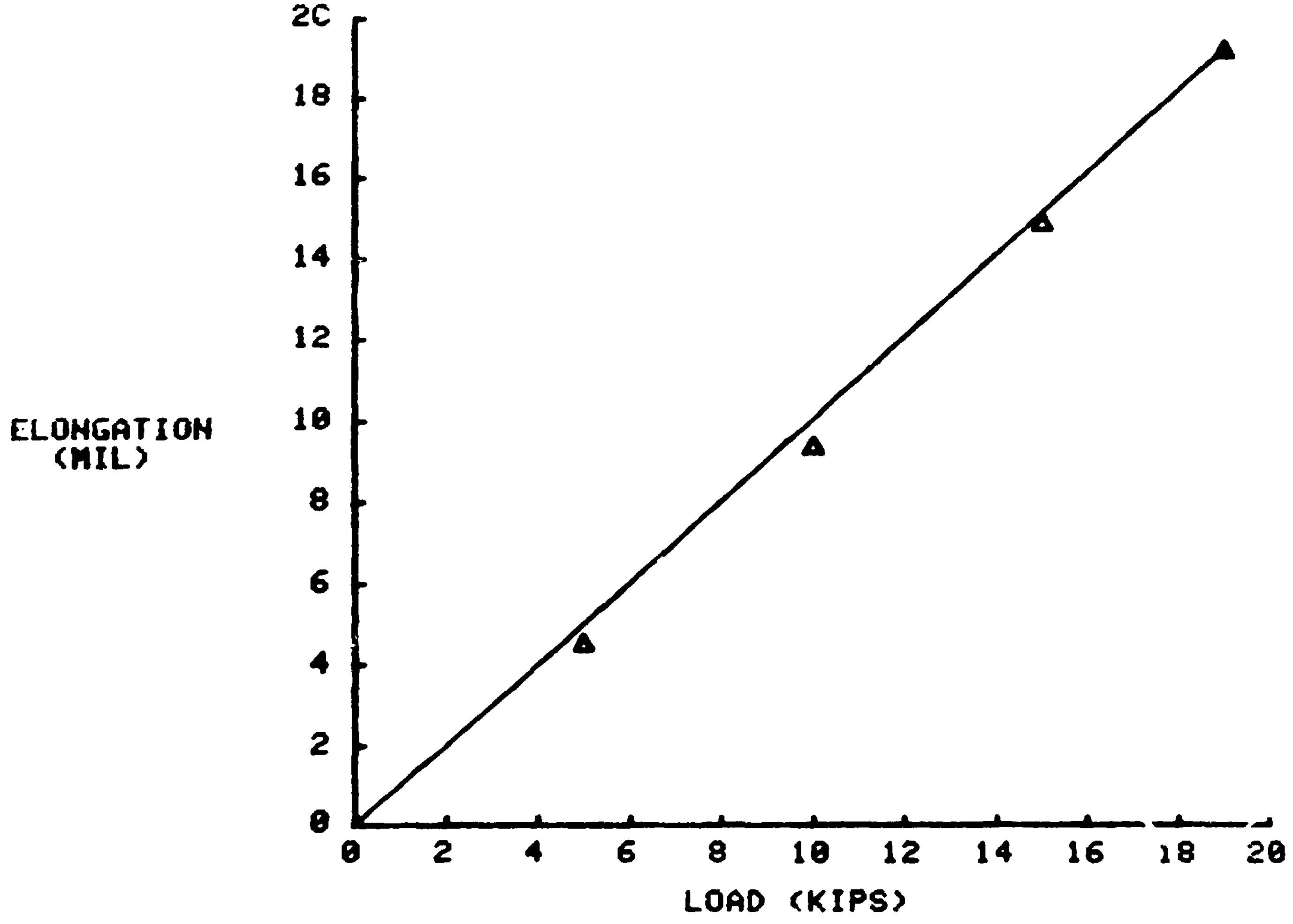

Results of Extensometer Evaluation

This instrument is capable of making elongation measurements with high accuracy. Translating these into preload values depends upon calibration of the instrument against a standard of the bolt type being measured. The manufacturer claims an overall preload measurement accuracy of ±3% which was easily met in the limited evaluation made in this project.

Only minimal bolt preparation for preload measurement appears to be necessary. The as-received grade 8 bolts certainly gave acceptable performance, although the heads of these bolts had raised grade markings and the threaded ends had a slight cup. However, proper control of placement and coupling of transducer would be required to use the device under these conditions, and in the field on production equipment, prepared bolts are likely to be necessary.

Implementing the system with production equipment would be difficult. The application of couplant, placement of the transducer, and instrument set-up represent significant time steps, and each requires some skill. However, in those applications of sufficient criticality to warrant the effort, the instrument is no doubt a useful one. Improvement is certainly possible, and would include automatic zero adjustment and the use of a dry couplant fixed to the transducer.

Data scatter determination for a large population of bolts from different manufacturers and material lots should be made.

Developers of this system are to be congratulated for a significant step in improved tension control accuracy.

Shear-Wave Birefringence Experiments

During the course of the project, the opportunity to acquire the of an accurate ultrasonic velocimeter specially designed for birefringence experiments arose. A program of stress investigation sponsored by the Department of Transportation (Contract DOT-FH-11-9133) was in progress during approximately the same time period at SwRI in which birefringence was a major subject for study. A high-accuracy pulse-overlap velocimeter was designed and constructed for the study,and its application to the measurement of fastener stress already determined to have good potential, could be considered experimentally.

The application of the birefringence technique to bolts is for the purpose of determining the bulk stress in the bolt head. Since the average stress in the head of a hex-head bolt is axial compression (from the finite element analysis), transmission of shear waves across the flats with two separate polarizations, one parallel and one perpendicular to the stress direction, enables the determination of the difference in velocity of the two, and the calculation of the stress. Since the measured stress effect is an average of the stress effect at each point along the path of the acoustic wave, some idea of the expected magnitude of the effect was estimated by averaging the computer-generated stress values from the finite element analysis. This calculation for the head of a hex-head bolt yielded an average axial stress of approximately 10% to 20% of the axial stress in the shank. Although the stress effect in the head is much smaller than that in the shank, the head is accessible to the birefringence measurement while the shank is not.

The proper procedure for measuring shear wave birefringence is to locate the pure mode orientations and make measurements of V and ΔV (the average and differential velocity) along these preferred orientations. One would prefer to be able to select a beam direction exactly perpendicular to the stress, which may not be parallel to the shank (due to residual stress effects). However, hex-head bolts permit only three separate directions of propagation (across each pair of flats, from one side to the other). These directions, 60° apart in orientation, permit alignment resolution of only 30°. The alignment problem is illustrated in Figure 83 which shows the echo patterns for the three directions of propagation in one of the bolts. Alignment with the principle axis is indicated by an echo pattern which defines an exponential envelope. Thus, the orientation shown by Figure 83, C and F, is selected as the best of the three. The experimental procedure was first to locate the "best" orientation of the bolt head, and then make birefringence measurements for that orientation.

Velocity measurements were made on ten 5/8-in. Grade 8 steel bolts (AN8) of the type used in the magnetics experiments. The experimental arrangement is shown in Figure 84, with the special rotatable transducer for defining the parallel and perpendicular polarization directions. Bolts were loaded in the Skidmore-Wilhelm load cell, as in previous experiments.

Additionally, a single aluminum bolt and a titanium bolt were measured, to determine the feasibility of the method, in those materials.

Later, data from four 3/4-in. (A325) steel bridge bolts were obtained from the results of the DOT project. These are also included, and used in an analysis of the data scatter

Results of Birefringence Experiments

Table XX contains the birefringence measurements ($\frac{\Delta V}{V}$) on the ten 5/8-in. steel bolts. From page 135 equation (23) the stress at any shank load, y can

ORIGINAL PAGE IS
OF POOR QUALITY

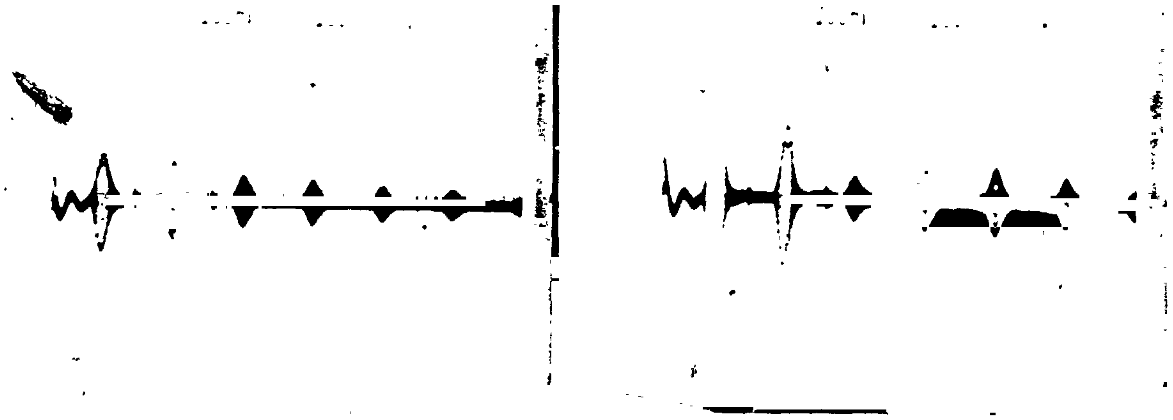

A. ORIENTATION 1, NO LOAD

D. ORIENTATION 1, PROOF LOAD

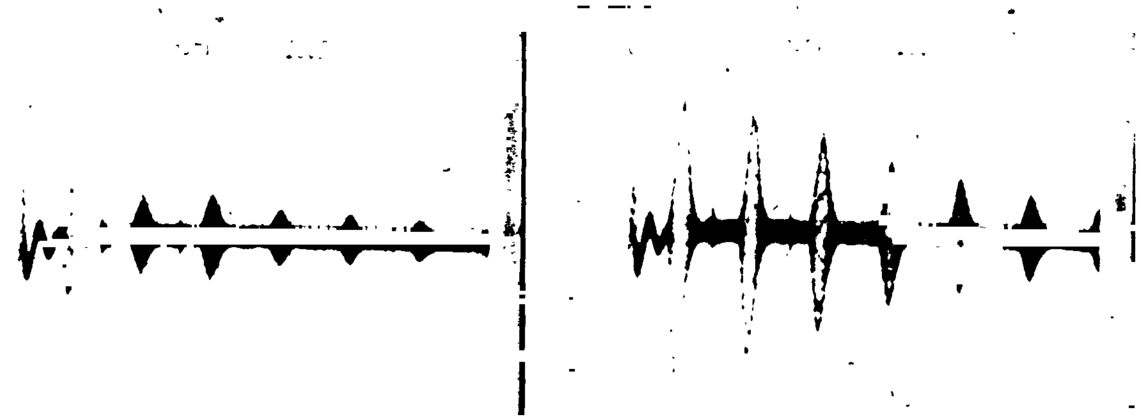

B. ORIENTATION 2, NO LOAD

E. ORIENTATION 2, PROOF LOAD

4341

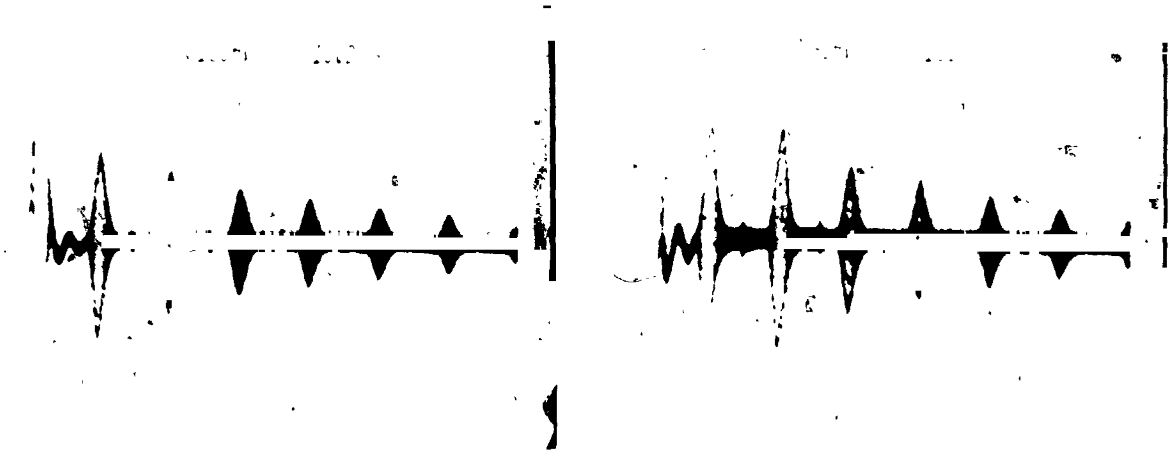

C. ORIENTATION 3, NO LOAD

F. ORIENTATION 3, PROOF LOAD

FIGURE 83. ECHO PATTERNS FOR VARIOUS ORIENTATIONS OF PROPAGATION OF 5 MHz ULTRASONIC WAVE THROUGH 5/8" GRADE 8 STEEL BOLT HEAD

4340

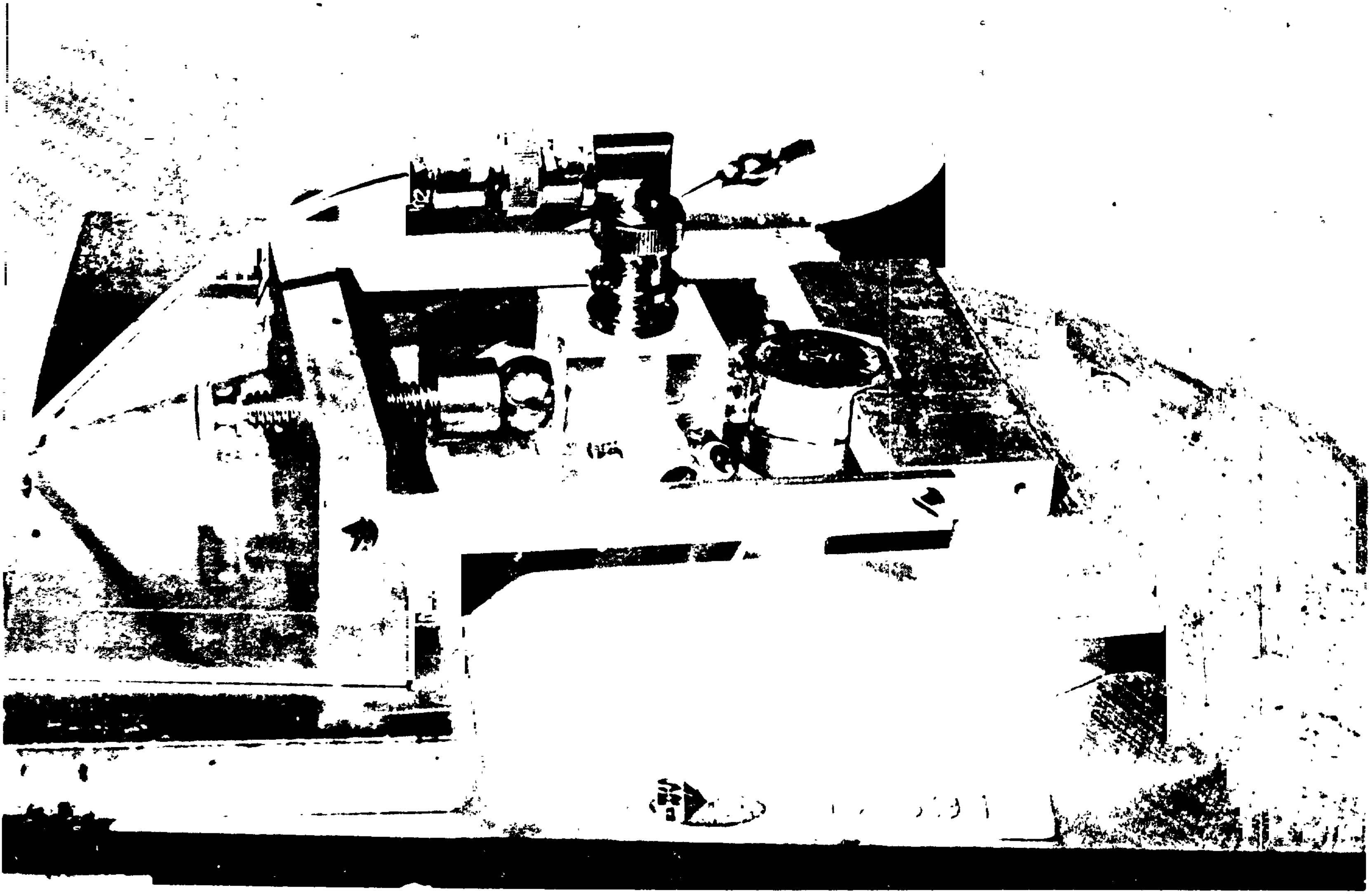

FIGURE 84. EXPERIMENTAL ARRANGEMENT FOR MEASUREMENT OF ULTRASONIC BIREFRINGENCE EFFECT ON HEX-HEAD BOLT DURING LOADING. The 5 MHz transducer can be rotated through 90°.

Table XX

Shear Wave Birefringence of 5/8" Grade 8 Steel Bolts at 0, 10, 20, 30 Kips Shank Load

Shank Load	0	10			20			30		
Bolt #	$\left(\frac{\Delta V}{V}\right)_{10}$	$\left(\frac{\Delta V}{V}\right)_{20}$	Indicated Load (Kips) based on meas. no-load	Indicated Load (Kips) based on avg. no-load	$\left(\frac{\Delta V}{V}\right)_{20}$	Indicated Load (Kips) Meas.	Indicated Load (Kips) Avg.	$\left(\frac{\Delta V}{V}\right)_{30}$	Indicated Load (Kips) Meas.	Indicated Load (Kips) Avg.
1	0.00205	0.00242	9	9	0.00273	17	17	0.00318	27	27
2	0.00174	0.00220	11	4	0.00257	20	13	0.00303	31	24
3	0.00220	0.00265	11	15	0.00295	18	22	0.00348	31	35
4	0.00204	0.00257	13	13	0.00303	24	24	0.00355	36	36
5	0.00212	0.00257	13	13	0.00303	22	24	0.00356	34	36
6*	0.00258	0.00296	9	22	0.00321	15	27	0.00358	24	37
7*	0.00199	0.00237	9	8	0.00262	15	14	0.00310	27	25
8*	0.00164	0.00209	11	1	0.00250	21	11	0.00295	31	22
9	0.00220	0.00258	9	13	0.00295	18	22	0.00341	29	33
10	0.00182	0.00212	7	2	0.00257	18	13	0.00303	29	24
Ave.	0.00204	0.00244	10	10	0.00282	19	19	0.00329	30	30
Std Dev	0.00027	0.00028	2	6	0.00025	3	6	0.00025	4	6
%	13%	11%	20%	60%	9%	15%	30%	8%	12%	20%

---

* Readings on these bolts were taken for the three possible directions of propagation through the head and averaged.

be expressed in terms of the birefringence as

$$T = \frac{\left(\frac{\Delta V}{V}\right)_y - \left(\frac{\Delta V}{V}\right)_o}{k} \qquad (25)$$

In Figure 85, the measured values of $\frac{\Delta V}{V}$ from Table XX are plotted vs. the respective shank loads. The constant k is the slope of the linear fit to the data in Figure 85, or, in this case, k = 4.11 1/kip. The indicated load can then be calculated from the measured birefringence. For a post-load measurement, an average value of no-load birefringence would have to be employed, so the indicated load was also calculated using an average value for the bolts under test. This is the second entry in the indicated load column for each load point in Table XX. A statistical analysis of these results was run giving the indicated standard deviations. Note that full load can be measured within 20% on these bolts, using the average no-load reading. Thus, with the present instrumentation a post-load measurement could also be made with 20% accuracy. The relatively large amount of data scatter shown in Figure 85 can be attributed to two principal causes: (1) resolution of the instrumentation (±0.0002") and (2) variation in alignment with respect to the principal stress axis. The resolution can be improved if results warrant, but the fundamental problem of alignment with respect to the principal stress axis is more serious.

In Table XXI, data from three of the bolts show the variation with direction of propagation through the bolt head. This is assumed to be caused by uneven stress distribution in the head probably the result of residual stresses present before the bolts were loaded. In Figure 86, the data from one bolt is plotted.

Table XXII and Table XXIII present the birefringence data for an aluminum bolt and a titanium bolt, respectively. Figures 87 and 88 are plots of the data from these two bolts. Apparently there are no unforseen difficulties in using the method with these two materials.

The acoustic constant for steel is 0.00005/ksi as measured by Noronha and Wert(25), and confirmed in separate experiments at SwRI. Thus, the average stress in the head at full load for the steel bolts, is about 25 ksi. This is a reasonable figure since finite element analysis modeling of hex-head bolts has shown the average stress in the head due to shank load, to be 1/5 to 1/10 the shank stress. In the test bolts, shank stress was about 100 ksi at 30 kips load.

In order to study the reproducibility of the measurement, a statistical analysis was run on the data at each load point. The average value, standard deviation, and percentile deviation were included in Table XX. These percentages ranged from 8 to 13%.

FIGURE 85: FIT TO DATA ON (10) 5/8" STEEL BOLTS (GRADE 8) WITH STANDARD DEVIATION BOUNDARIES PLOTTED.

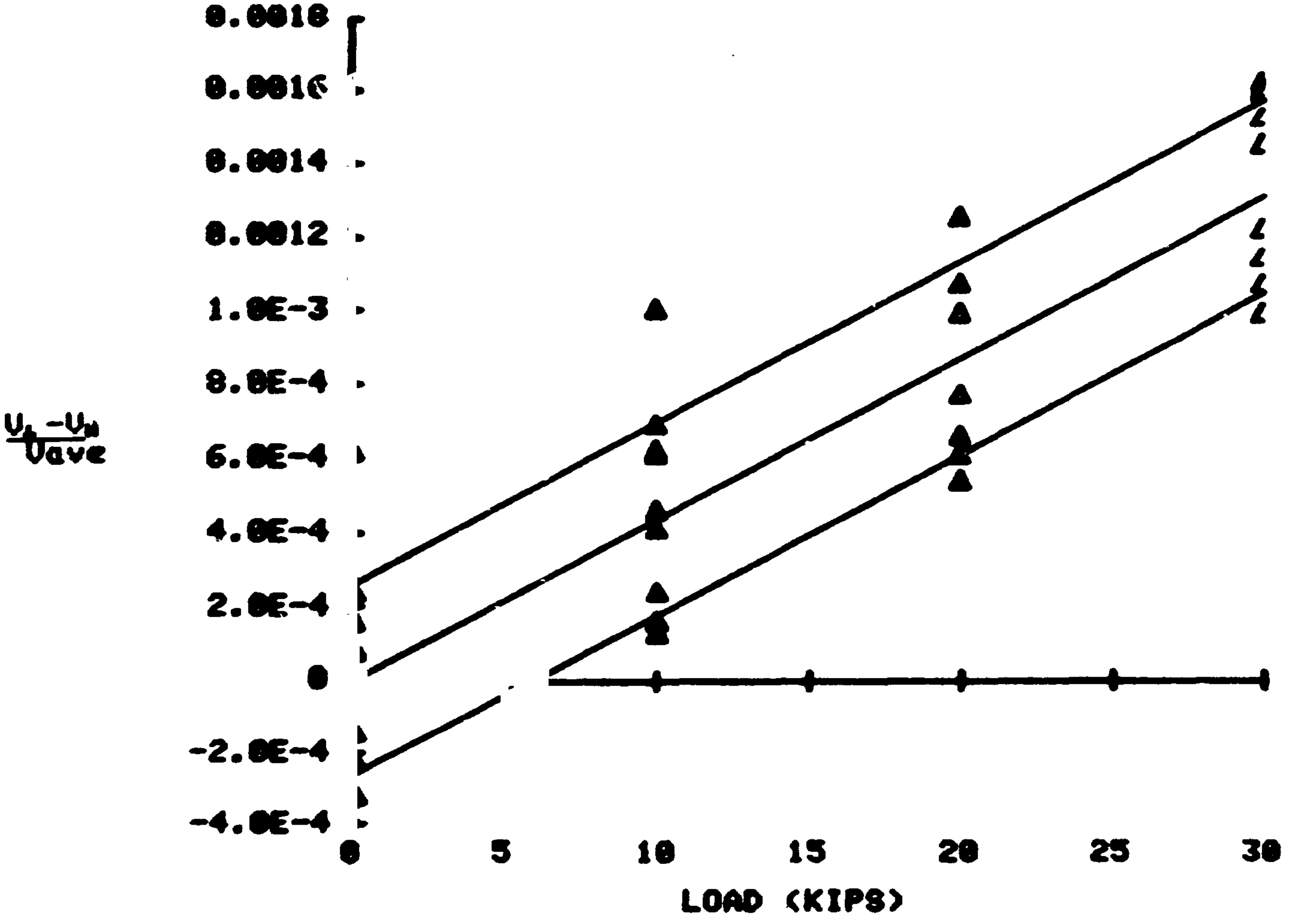

TABLE XXI. VARIATION OF SHEAR WAVE BIREFRINGENCE WITH ORIENTATION OF BOLT HEAD

Bolt #	Orient #	$\left(\frac{\Delta V}{V}\right)_0$	$\left(\frac{\Delta V}{V}\right)_{10}$	$\left(\frac{\Delta V}{V}\right)_{20}$	$\left(\frac{\Delta V}{V}\right)_{30}$	$-\overline{\left(\frac{\Delta V}{V}\right)}_0$	% Deviation
6	1	0.00242	0.00272	0.00303	0.00348	0.00090	-13
6	2	0.00273	0.00311	0.00341	0.00379	0.00121	+18
6	3	0.00258	0.00296	0.00318	0.00356	0.00098	- 5
Ave		0.00258	0.00296	0.00321	0.00361	0.00103	
7	1	0.00227	0.00265	0.00303	0.00325	0.00126	+14
7	2	0.00204	0.00242	0.00272	0.00310	0.00111	0
7	3	0.00166	0.00204	0.00249	0.00295	0.00096	-14
Ave		0.00199	0.00237	0.00275	0.00310	0.00111	
8	1	0.00181	0.00219	0.00265	0.00310	0.00146	+11
8	2	0.00151	0.00197	0.00235	0.00280	0.00116	-11
8	3	0.00159	0.00212	0.00250	0.00295	0.00131	0
Ave		0.00164	0.00209	0.00250	0.00295	0.00131	

ORIGINAL PAGE IS
OF POOR QUALITY

FIGURE 86: PLOT OF BIREFRENGENCE FOR THE THREE ORIENTATIONS OF PROPAGATION THROUGH THE BOLT HEAD FOR BOLT #6.

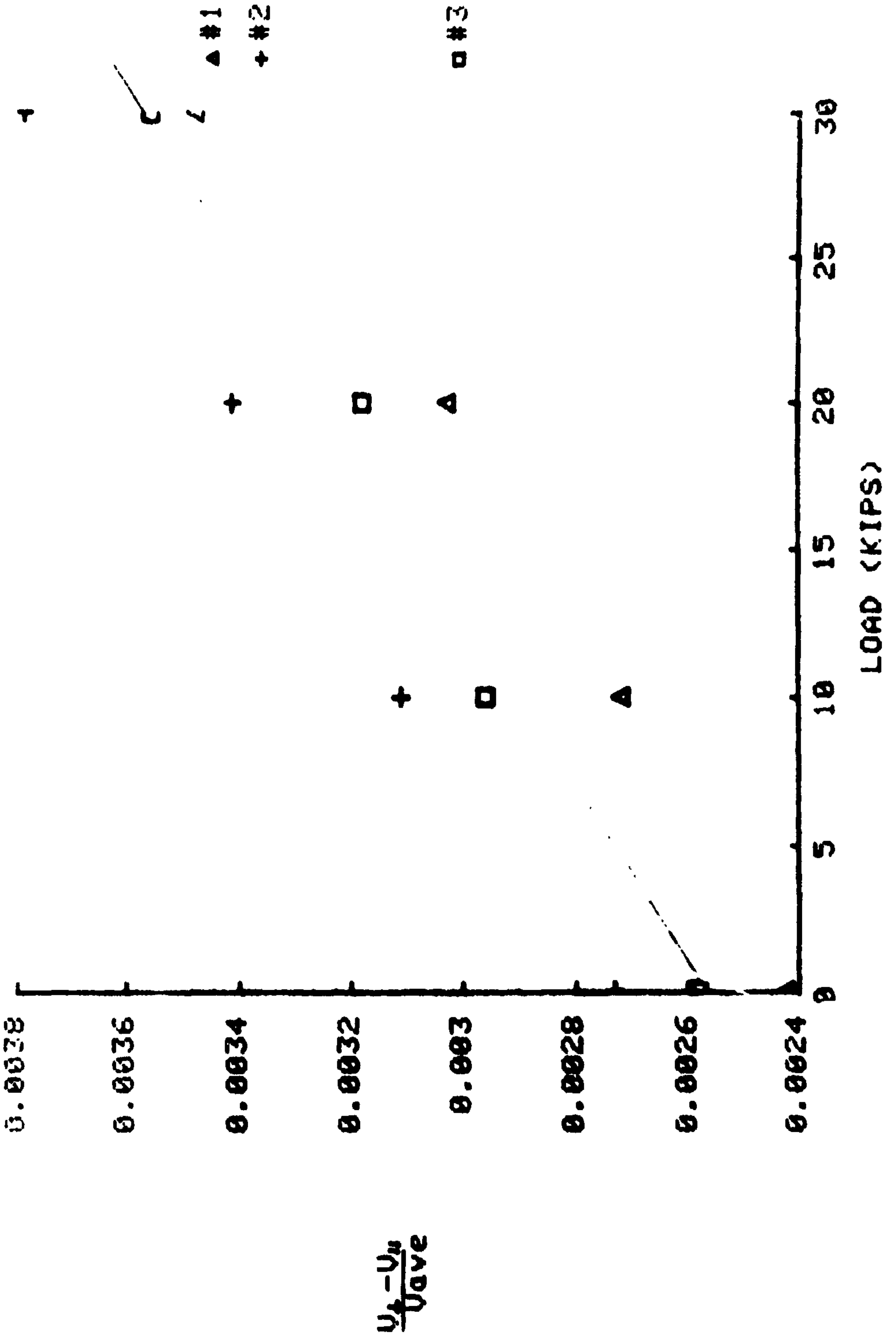

TABLE XXII

SHEAR WAVE BIREFRINGENCE DATA FOR AN 1/2-IN. ALUMINUM BOLT

Load	$\frac{\Delta V}{V}$	$\frac{\Delta V}{V} - \left(\frac{\Delta V}{V}\right)_0$
0	0.00047	0
2-1/2	0.00087	0.00040
5	0.00118	0.00071

TABLE XXIII

SHEAR WAVE BIREFRINGENCE DATA FOR AN 1/2-IN. TITANIUM BOLT

Load	$\frac{\Delta V}{V}$	$\frac{\Delta V}{V} - \left(\frac{\Delta V}{V}\right)_0$
0	-0.00657	0
5	-0.00617	0.00040
10	-0.00593	0.00064
15	-0.00570	0.00087
19	-0.00546	0.00111

FIGURE 87: BIREFFENGENCE IN AN 1/2" ALUMINUM BOLT.

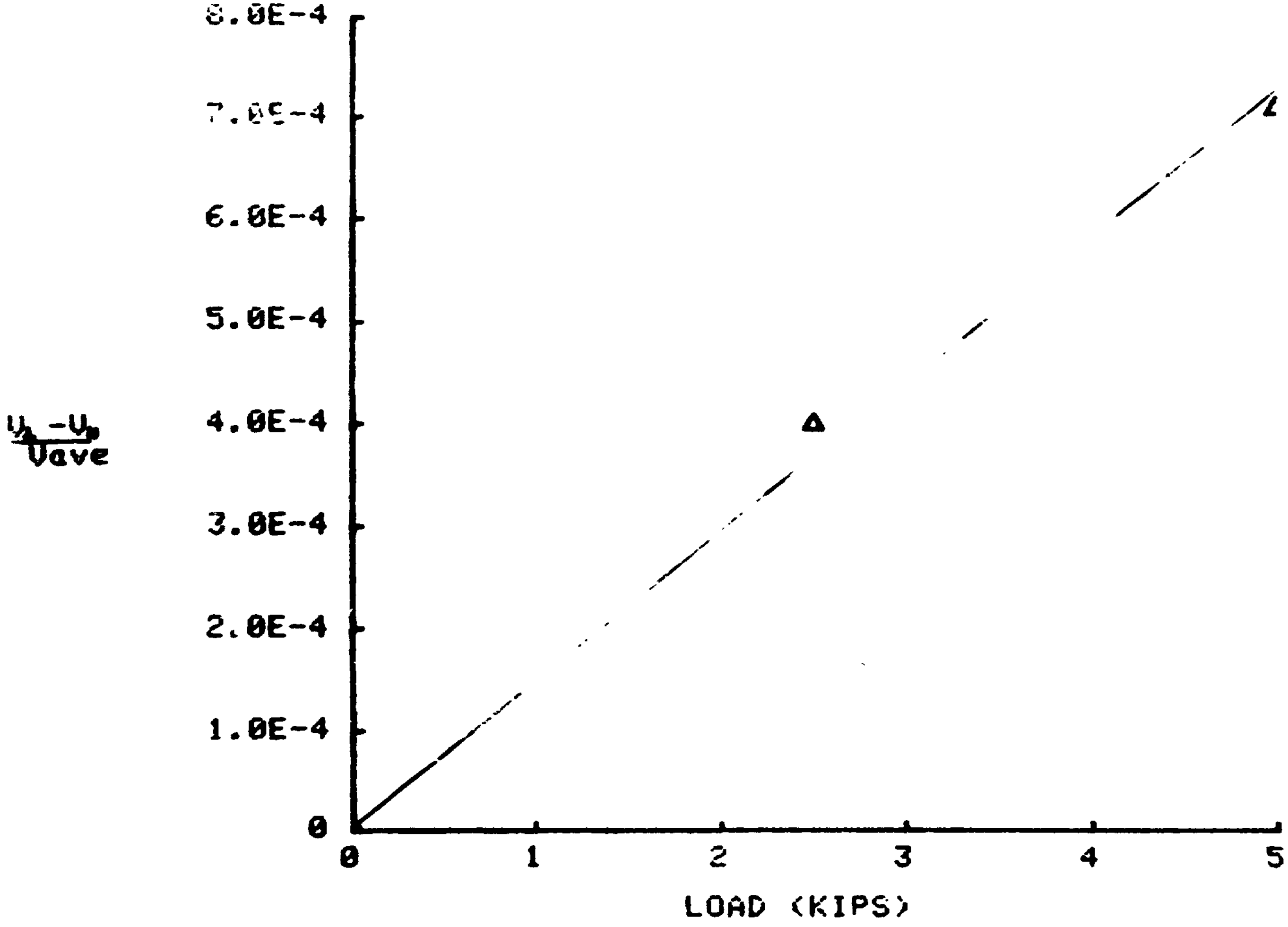

FIGURE 88: BIREFRENGENCE IN A 1/2" TITIANIUM BOLT

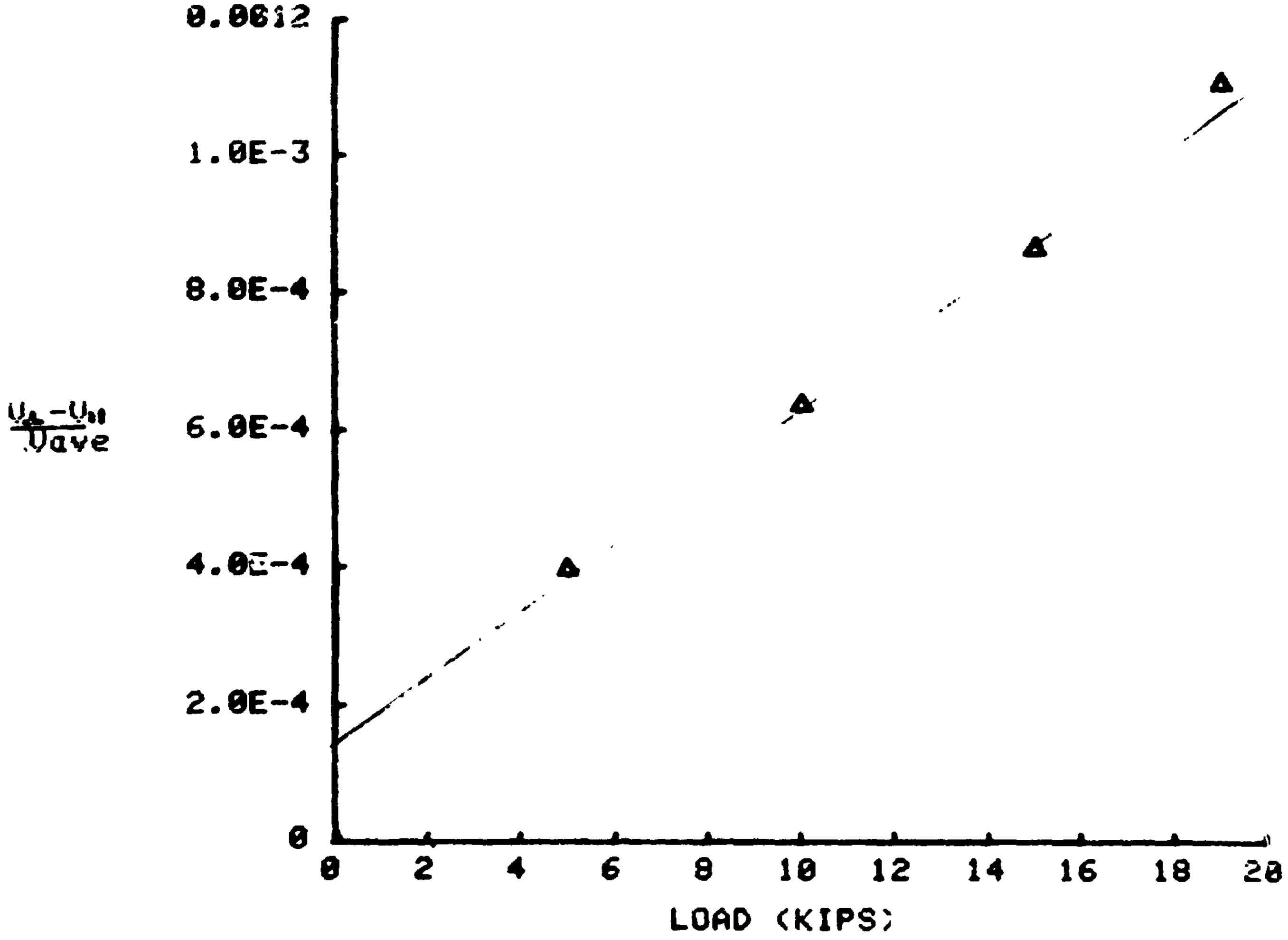

In the DOT project, similar experiments were performed using four 3/4-in. bridge bolts (A325), in a Skidmore-Wilhelm load cell arrangement. Velocity measurements were made in the three possible directions across the flats on each bolt head. Table XXIV contains the data obtained at loads from 0 to 25 kips in 5 kip steps. Figure 89 is a plot of this data with the least squares linear fit to the data. A statistical analysis is also given in Table XXIV. The typical percentile deviation is about 20%.

However, for post-installation measurements, it would be necessary to use an average no-load value, and the corresponding values are shown in the final column of Table XXIV. It is apparent from inspecting these data that the largest variation in indicated load is the result of differences in orientation. By selecting the "best" beam direction for each bolt, the values in Table XXV are calculated. Using these results, the percentile standard deviation is less than 10% in each case. Even when the average no-load value is used, the birefringence at full load produces indicated load value variation corresponding to a 12% standard deviation. This is very encouraging for post-load measurement applications. The exact cause of the variation introduced by orientation direction needs further investigation.

Conclusions from Birefringence Experiments

The results of these experiments demonstrate that hex-head bolts yield birefringence measurements from which average bulk stresses in the head can be calculated. To the extent that these stresses reflect true shank stress, the method shows considerable promise. The effect is linear, so that practical calibration should be possible for bolts of the same type. Aluminum and titanium apparently yield equally good results. The accuracy of the instrumentation used can be improved with little difficulty.

Further evidence was obtained which points to residual stress effects as being a major contributor to data scatter, giving confirmation to the results of the magnetics experiments.

Mechanical Impact Techniques

In conducting all of the mechanical impact tests, a 1/2-20 hex-head bolt was modified by machining the top of the head flat. The modified bolt was mounted in a Skidmore-Wilhelm Tension Tester, in a similar arrangement to that used in the other experiments. In each test a piezoelectric accelerometer was mounted on the bearing plate of the tension tester such that center-to-center distance between the accelerometer and the bolt was 28mm. In some tests a second accelerometer was used. Four separate experiments, discussed in the following subparagraphs, were conducted.

Table XXIV

Shear Wave Birefringence Data on Four 3/4-In. Bolts (A325)

Bolt	Orientation	$\left(\frac{\Delta V}{V}\right)_0$	$\left(\frac{\Delta V}{V}\right)_5$	$\left(\frac{\Delta V}{V}\right)_{10}$	$\left(\frac{\Delta V}{V}\right)_{15}$	$\left(\frac{\Delta V}{V}\right)_{20}$	$\left(\frac{\Delta V}{V}\right)_{25}$	$\left[\left(\frac{\Delta V}{V}\right)_{25}-\left(\frac{\Delta V}{V}\right)\right]$	$\left[\left(\frac{\Delta V}{V}\right)_{25}-\overline{\left(\frac{\Delta V}{V}\right)_0}\right]$
1	1	0.00163	0.00186	0.00209	0.00232	0.00263	0.00302	0.00139	0.00068
1	2	0.00233	0.00256	0.00287	0.00326	0.00349	0.00364	0.00131	0.00128
1	3	0.00155	0.00186	0.00194	0.00225	0.00248	0.00271	0.00116	0.00037
2	1	0.00217	0.00240	0.00286	0.00325	0.00348	0.00364	0.00147	0.00128
2	2	0.00295	0.00303	0.00318	0.00333	0.00349	0.00387	0.00092	0.00153
2	3	0.00140	0.00171	0.00186	0.00209	0.00233	0.00256	0.00116	0.00022
3	1	0.00287	0.00310	0.00333	0.00348	0.00364	0.00387	0.00100	0.00153
3	2	0.00271	0.00295	0.00302	0.00318	0.00341	0.00357	0.00086	0.00123
3	3	0.00256	0.00272	0.00303	0.00334	0.00365	0.00381	0.00125	0.00147
5	1	0.00264	0.00287	0.00310	0.00341	0.00372	0.00396	0.00132	0.00162
5	2	0.00256	0.00280	0.00295	0.00311	0.00326	0.00342	0.00086	0.00108
5	3	0.00273	0.00296	0.00311	0.00335	0.00366	0.00381	0.00108	0.00147
Ave.		0.00234	0.00257	0.00277	0.00303	0.00327	0.00349	0.00115	0.00115
	Std. Dev.	0.00054	0.00050	0.00050	0.00050	0.00050	0.00047	0.00072	0.00047
	%	23%	19%	18%	17%	16%	15%	19%	41%

FIGURE 89: SHEAR WAVE BIREFRENGENCE ON FOUR 3/4" STEEL BOLTS.

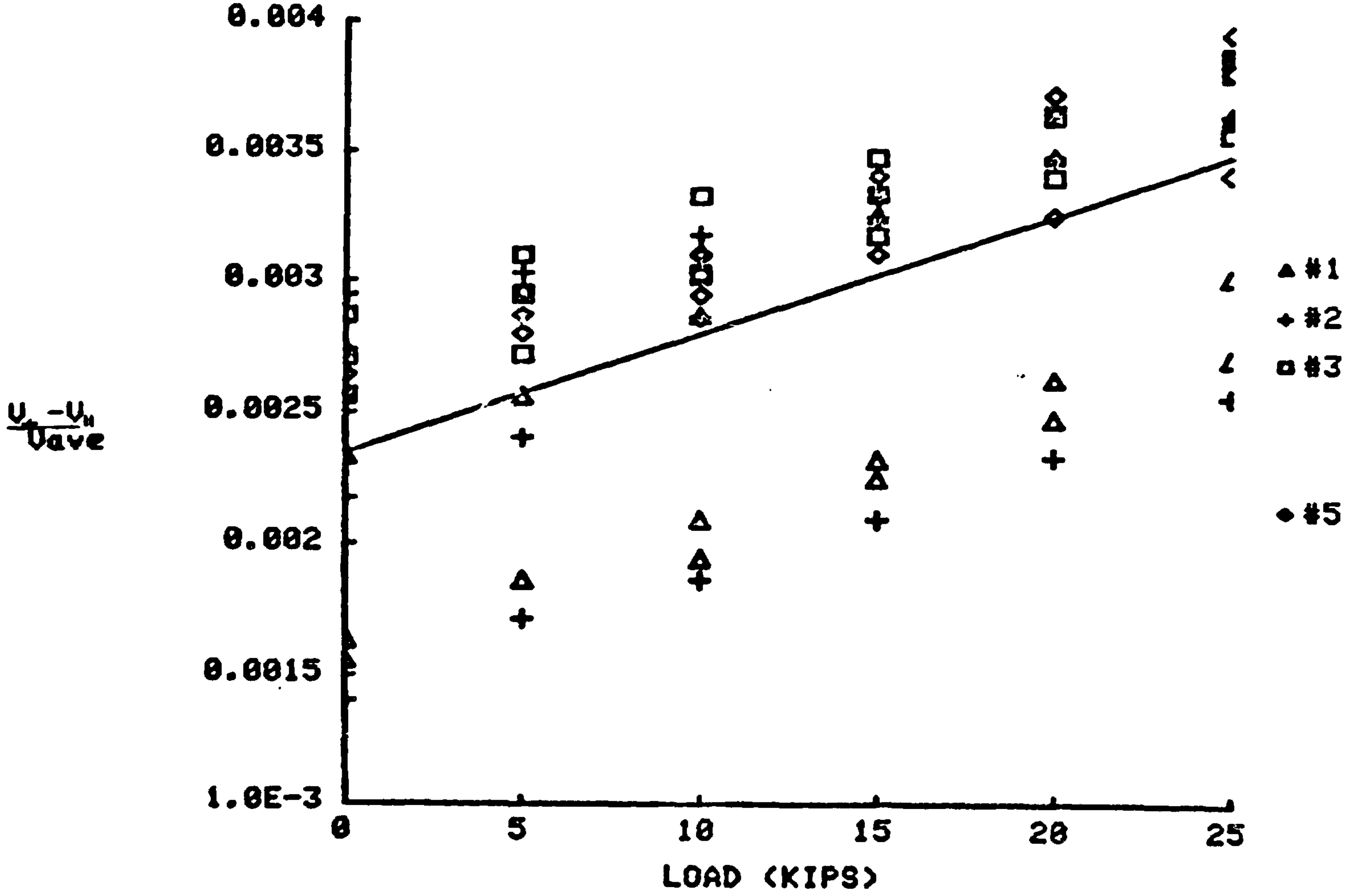

TABLE XXV

Shear Wave Birefringence Data for Selected Orientations

Bolt #	$\left(\frac{\Delta V}{V}\right)_0$	$\left(\frac{\Delta V}{V}\right)_{25}$	$\left(\frac{\Delta V}{V}\right)_{25}-\left(\frac{\Delta V}{V}\right)_0$	Indicated Load(kips)	$\left(\frac{\Delta V}{V}\right)_{25}-\overline{\left(\frac{\Delta V}{V}\right)_0}$	Indicated Load (kips)
1	0.00233	0.00364	0.00131	24.2	0.00122	23
2	0.00217	0.00364	0.00147	27.2	0.00122	23
3	0.00256	0.00381	0.00125	23.1	0.00139	26
4	0.00264	0.00396	0.00132	24.4	0.00154	29
Ave	0.00242	0.00376	0.00135	24.7	0.00134	25
Std Dev	0.00020	0.00016	0.00009	1.7	0.00016	3
%	8%	4%	7%	7%	12%	12%
Max % Dev	10%	5%	9%	9%	15%	15%

Preliminary Ball-Drop Impact Experiment

Two Columbia Research Laboratories Model 306-H Piezoelectric Accelerometers having resonant frequencies of 25 kHz were mounted on the bearing plate of the Skidmore-Wilhelm Tension Tester as shown in Figure 90. Output of each accelerometer passed through a Bruel and Kjaer Model 2619 Unity-Gain Preamplifier and a Bruel and Kjaer Model 2608 Measuring Amplifier to the input of a Bell and Howell Model CPR4010 Instrumentation Tape Recorder. FM record and playback modules having bandwidths from dc to 20 kHz were used. Tape speed was 30 in. /s. A 55-g steel ball was dropped repeatedly from a height of 47cm onto the head of the bolt under test. A tubular guide was used to ensure that the ball struck the bolt on each drop. Additionally, the ball was caught after first impact to prevent bouncing. Responses were recorded for ten drops of the ball with the bolt loose, snug, and tensioned to 25, 50, 75 and 100 percent of its 19, 200-lb proof load.

The data tape was reproduced into a Biomation Model 8100 Transient Recorder, output of which was monitored by an oscilloscope. One accelerometer response for each bolt tension condition was photographed from the oscilloscope screen. These time responses are illustrated in the left-hand column of Figure 91. It was observed during playback of the tape that accelerometer time response was not consistent from drop to drop for the same bolt tension condition. Examination of the oscilloscope trace photographs indicated no waveform feature which could be related directly to bolt tension. The typical response waveform had an initial bipolar swing of approximately 100-μs duration followed by an approximately 19-kHz ringdown. While the characteristics of the ringdown varied from one bolt load condition to another, no consistent and reproducible pattern was observed.

Recorder output was also played into a Rockland Model FFT512/S Real-Time Spectrum Analyzer which computed and displayed the Fourier transformation of accelerometer time response. With the assumption that the mechanical impulse was "mathematically perfect", the Fourier transformation displayed by the Rockland analyzer was equivalent to system frequency response. Frequency response curves corresponding to the six previously mentioned time responses are presented in the right-hand column of Figure 91. It was observed that the frequency response curve for a particular bolt load condition was not repeatable from one ball drop to the next. Although there are some noticeable variations in frequency response among the various bolt load conditions, there appears to be no feature of the frequency curve which can be consistently and reproducibly related to bolt tension.

ORIGINAL PAGE IS
OF POOR QUALITY

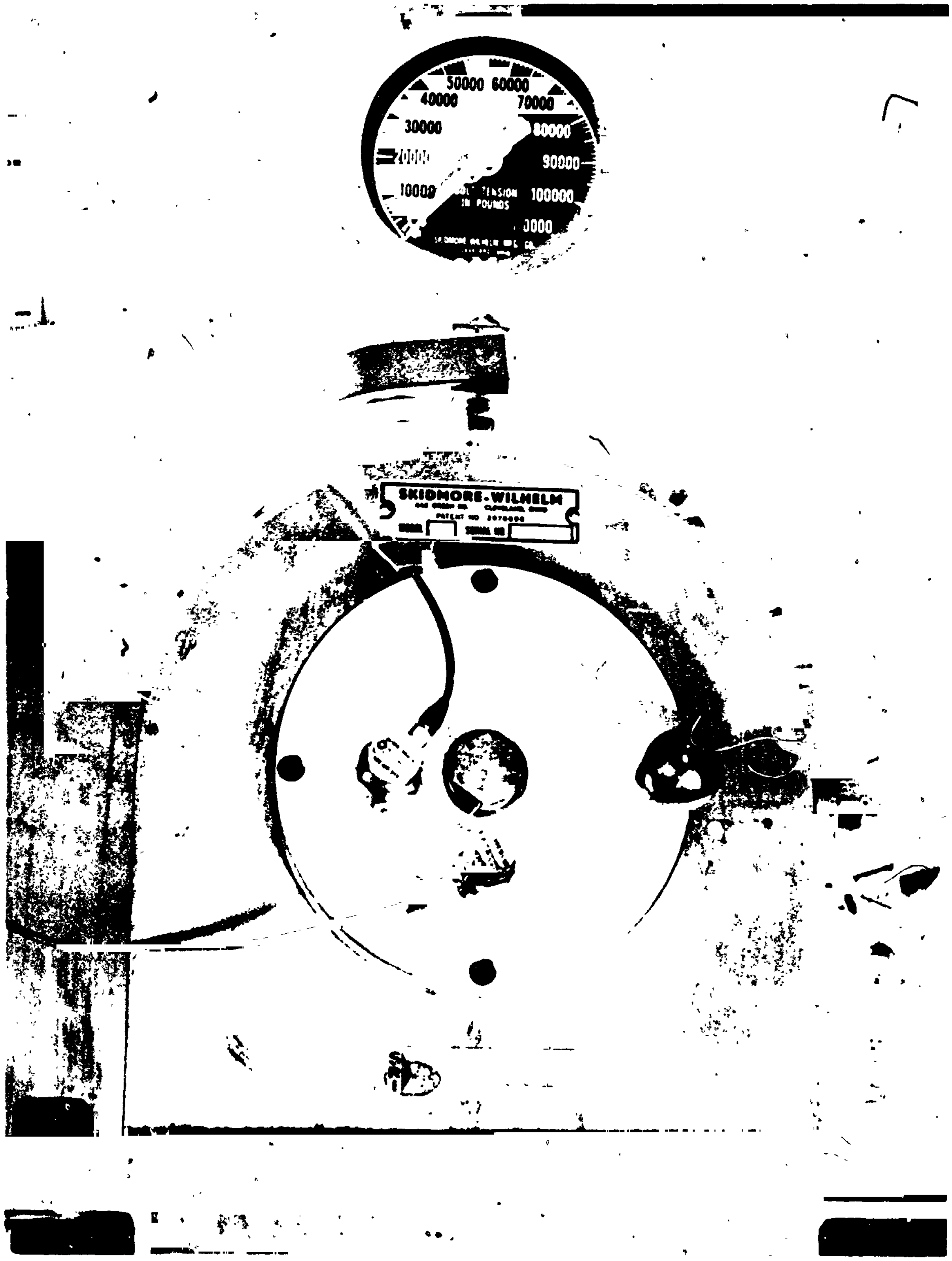
50000 60000
40000
70000
30000
80000
20000
90000
10000
100000
TENSION IN POUNDS
SKIDMORE-WILHELM

4542

FIGURE 90. INSTRUMENTATION FOR BALL-DROP EXPERIMENT.

4543

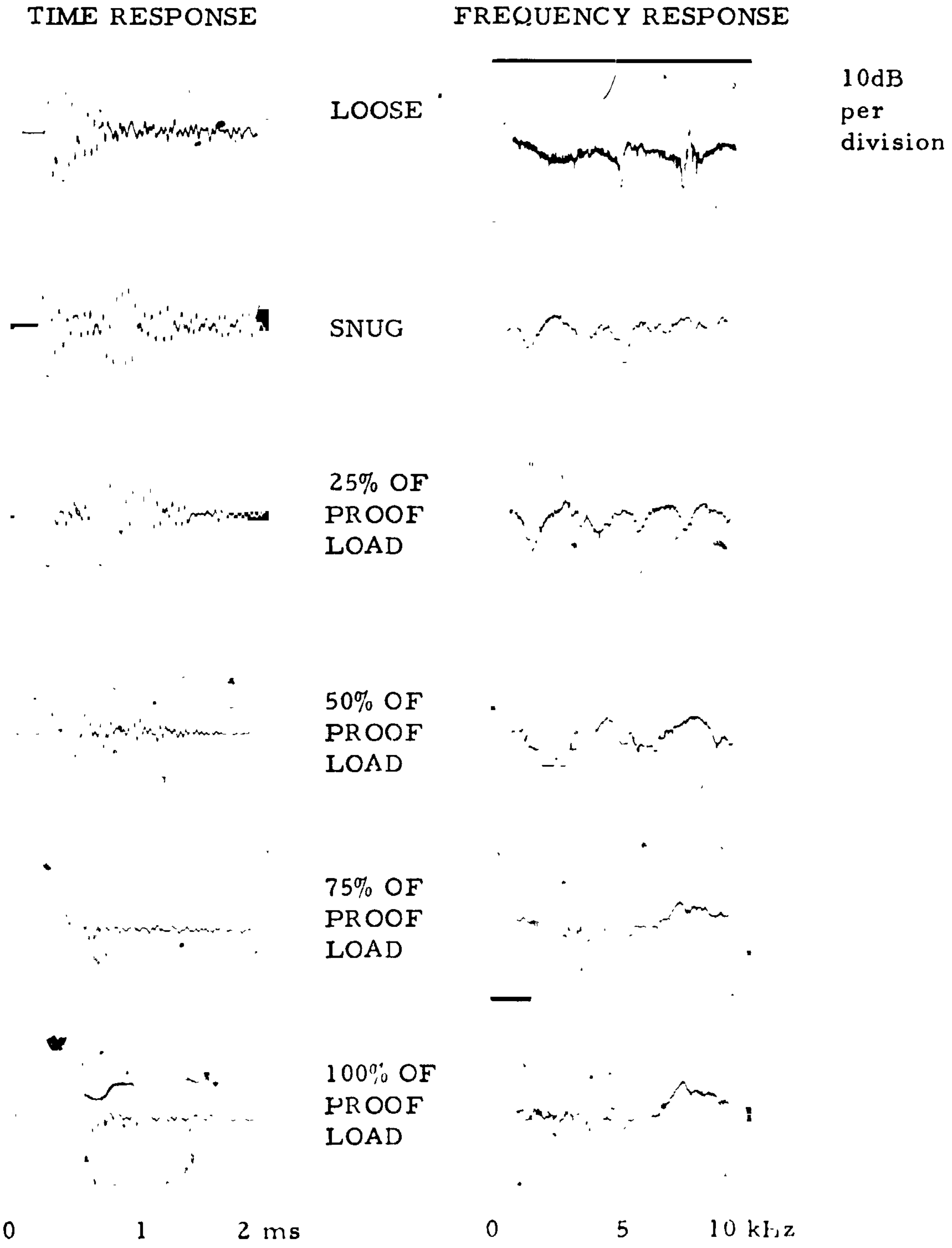

FIGURE 91. ACCELEROMETER TIME RESPONSES AND SYSTEM FREQUENCY RESPONSES OBTAINED FROM BALL-DROP TESTS.

Transverse Impact

For the transverse impact experiment, one Columbia Research Laboratories Model 306-H Piezoelectric Accelerometer was mounted on the bearing plate of the Skidmore-Wilhelm Tension Tester, and a second accelerometer of the same type was mounted on the bolt head. Mechanical impact was delivered to one flat of the bolt head using a pin punch and a small metal mallet. Impact delivered by this technique was transverse to the axis of the bolt under test. Accelerometer responses were recorded for ten impacts with the bolt loose, snug, and tensioned to 25, 50, 75 and 100 percent of its 19, 200-lb proof load.

It was determined that responses obtained by this method were not consistent from one impact to the next, so no further analysis was conducted.

Instrumented Hammer Impact

A PCB Piezotronics, Inc. Model K291A Dynamic Mechanical Impedance Measuring Kit was employed to determine bolt frequency response. The PCB Piezotronics Model K291A Kit includes (1) a small hammer, the striking face of which is instrumented with a piezoelectric force transducer; (2) two piezoelectric accelerometers of differing characteristics; (3) two power units; and (4) necessary cables. A PCB Piezotronics, Inc. Model 302A Accelerometer having a 45-kHz resonant frequency was mounted on the bearing plate of the Skidmore-Wilhelm Tension Tester as shown in Figure 92. Mechanical impulse excitation was delivered by the small hammer from the Dynamic Impedance Measurement Kit, and the face of the hammer was instrumented with a PCB Piezotronics, Inc. Model 208A03 Force Transducer which had a resonant frequency of 70 kHz. Outputs of the accelerometer and the force transducer were passed through PCB Piezotronics, Inc. Model 480 Power Units to the two input channels of a Zonic Technical Laboratories Fast Fourier Transform Analyzer equipped with a Tektronix Graphic Terminal and a Tektronix Hardcopy Unit. This apparatus is illustrated in Figure 93. The trigger circuit of the Zonic analyzer was set to respond to the force transducer waveform. The head of the test bolt was struck lightly with the force-transducer end of the hammer which (1) introduced a mechanical impulse into the bolt and (2) triggered operation of the Zonic analyzer. The analyzer was programmed to (1) plot time responses of both force transducer and accelerometer outputs to ensure that neither signal overloaded the analyzer, (2) compute frequency spectra (i. e., Fourier transformations) of both force transducer and accelerometer outputs, and (3) compute the system frequency response (i. e., accelerometer output Fourier transformation divided by force transducer output Fourier transformation). As expected, the hammer introduced a clean, unipolar mechanical impulse which had essentially flat spectral content to the cutoff frequency of the anti-aliasing filter in the Fast Fourier Transform analyzer. Spectral content of a typical mechanical impulse is illustrated in Figure 94.

ORIGINAL PAGE IS
OF POOR QUALITY

FIGURE 92. FREQUENCY MEASUREMENT APPARATUS EMPLOYING AN INSTRUMENTED HAMMER.

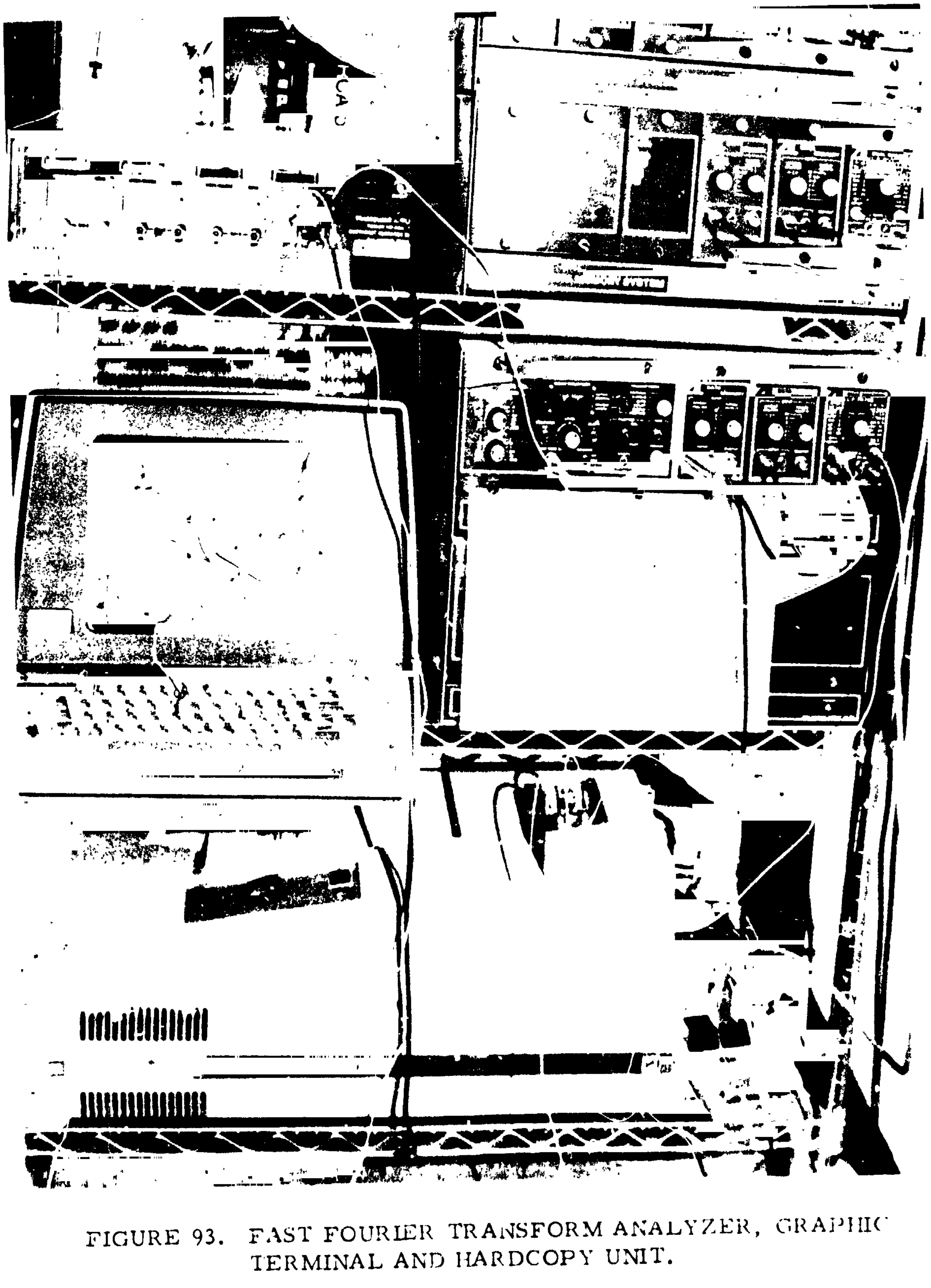

FIGURE 93. FAST FOURIER TRANSFORM ANALYZER, GRAPHIC TERMINAL AND HARDCOPY UNIT.

4545

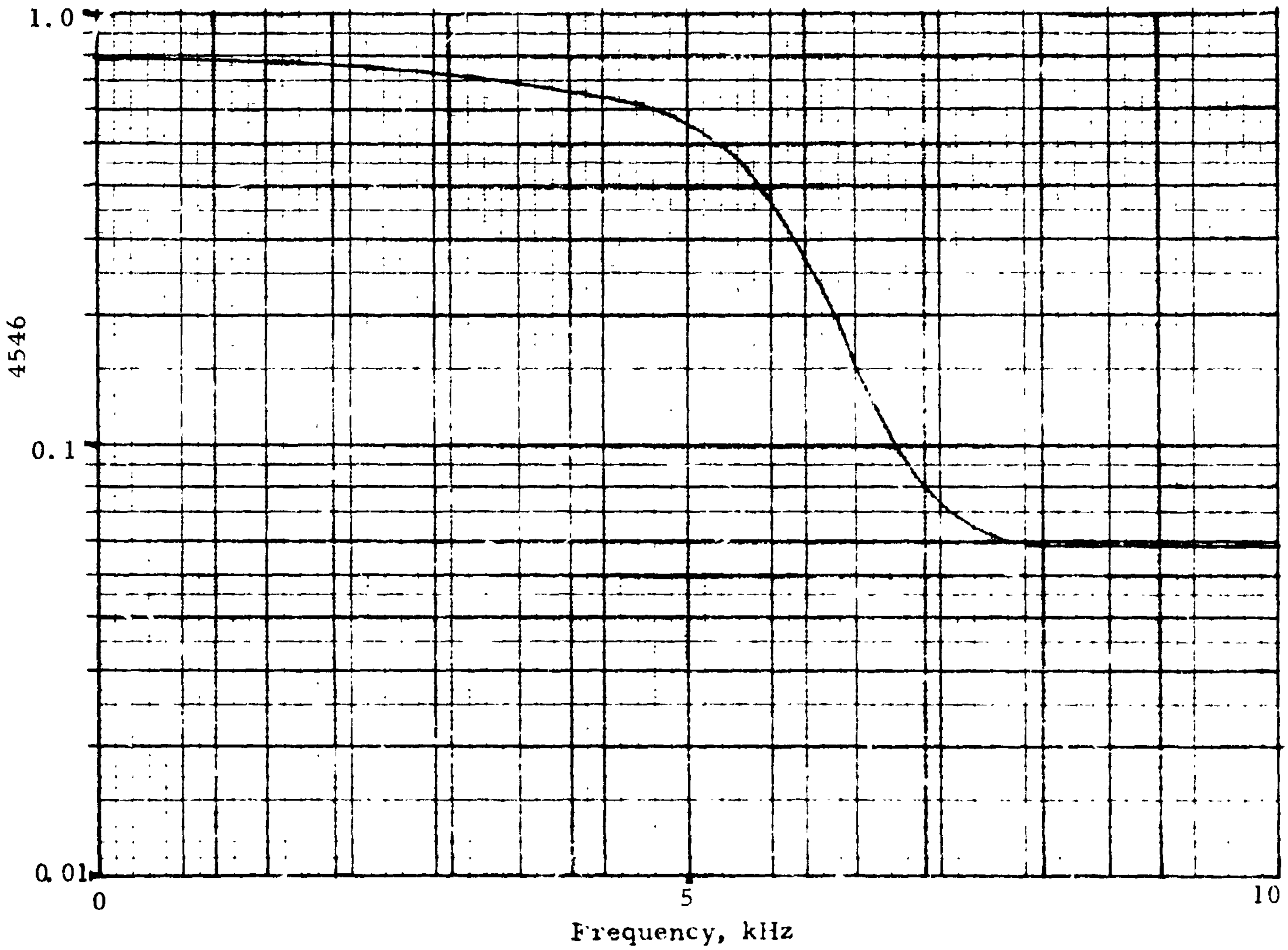

FIGURE 94. FREQUENCY SPECTRUM OF MECHANICAL IMPULSE.

Frequency response curves computed for the bolt snug and in tension at 31, 63 and 94 percent of proof load are presented in Figures 95 through 98, respectively. Comparison of the curves in Figures 95 through 98 reveals that frequency responses for the three loaded conditions were essentially identical. Marked differences between frequency response with the bolt snug but unloaded and any of the tensioned cases were observed. In the range of approximately 1 to 4.5 kHz, frequency response with the bolt snug exceeded that of the tensioned bolt by 10 to 30 dB. Also in the vicinity of 6 kHz, frequency response in the snug case exceeded that in the tensioned cases by approximately 10 dB. As with the frequency responses, phase responses in the three tensioned cases were quite similar in basic structure, but they did differ in fine detail. However, the phase response curve for the snug bolt differed significantly from those of the tensioned bolts.

Instrumented Hammer Impact with Modified Fixture

In an effort to create a more realistic situation for testing the hammer impact method, the test fixture was modified as shown in Figure 99. The bolt under test was passed through (1) central holes in two 12.7-mm thick steel disks, (2) a hexagon nut which had been drilled to clear the body of the test bolt, (3) the bearing plate of the Skidmore-Wilhelm Tension Tester, and (4) the nut of the tension tester. The two steel disks thus represented two plates secured by a bolt and a nut. As in previous hammer impact tests, a PCB Piezotronics, Inc. Model 302A Piezoelectric Accelerometer was mounted on the top disk 28mm from the center of the bolt under test. The small hammer instrumented with a PCB Piezotronics, Inc. Model 208A03 Piezoelectric Force Transducer was used to strike the bolt head to introduce a mechanical impulse. PCB Piezotronics, Inc. Model 480 Power Units interfaced between the transducers and the respective inputs of the previously mentioned Zonic Technical Laboratories Fast Fourier Transform Analyzer.

The head of the bolt was struck and frequency response curves were computed for the bolt snug and tensioned to 34, 63 and 89 percent of proof load. Frequency response curves computed for these test conditions are presented in Figures 100 through 103, respectively. Additionally, the hammer was used to strike the top plate of the test fixture at a position 90° from the accelerometer location and at approximately the same distance from the bolt as the accelerometer. Again, frequency response curves for the bolt snug and tensioned to 34, 63 and 89 percent of proof load were computed. Frequency response curves for these latter conditions are illustrated in Figures 104 through 107, respectively.

ORIGINAL PAGE IS
OF POOR QUALITY

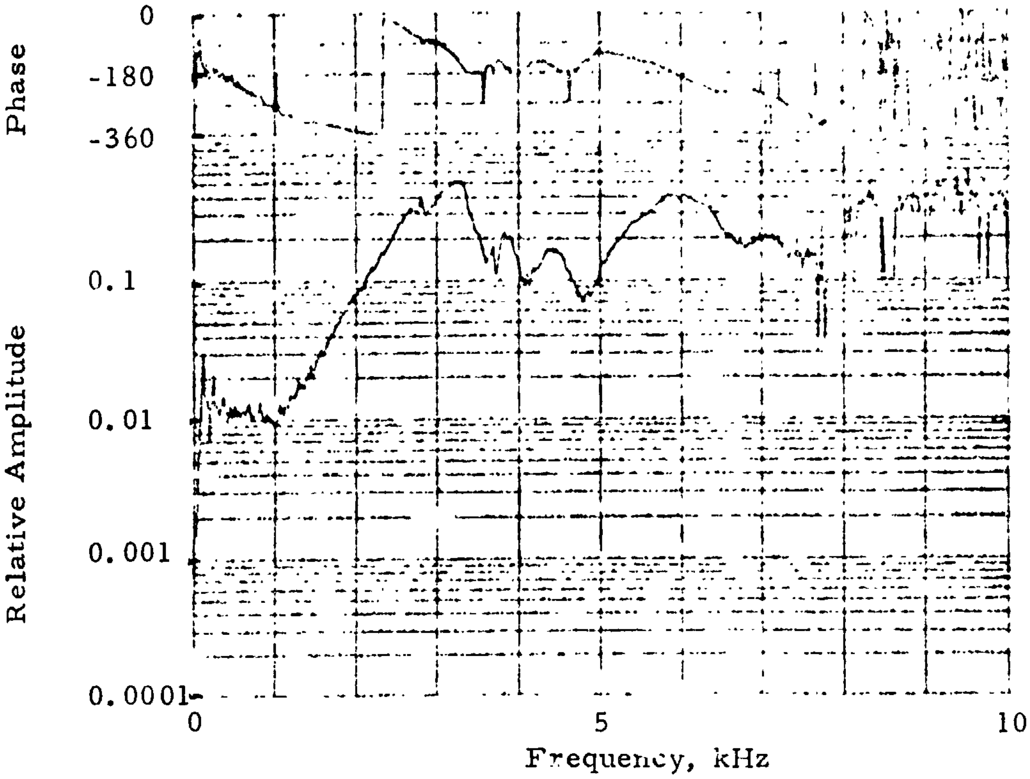

4547

FIGURE 95. FREQUENCY RESPONSE WITH BOLT SNUG.

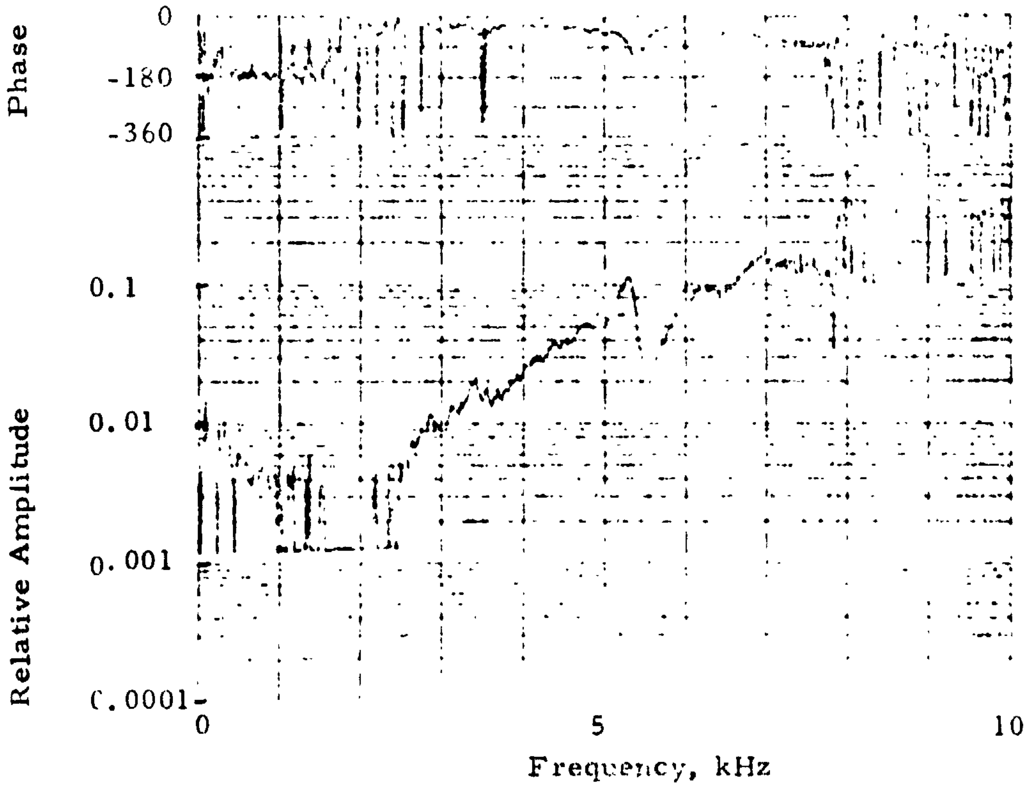

FIGURE 96. FREQUENCY RESPONSE WITH BOLT LOADED TO 31% PROOF LOAD.

ORIGINAL PAGE IS OF POOR QUALITY

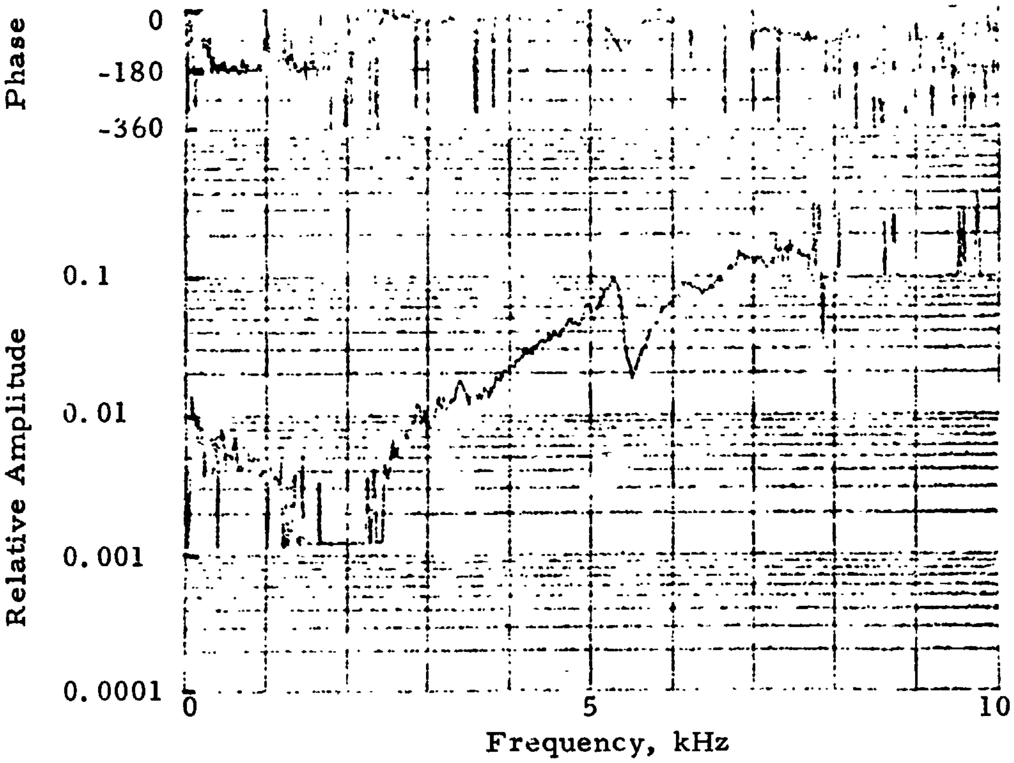

4548

FIGURE 97. FREQUENCY RESPONSE WITH BOLT LOADED TO 63% OF PROOF LOAD.

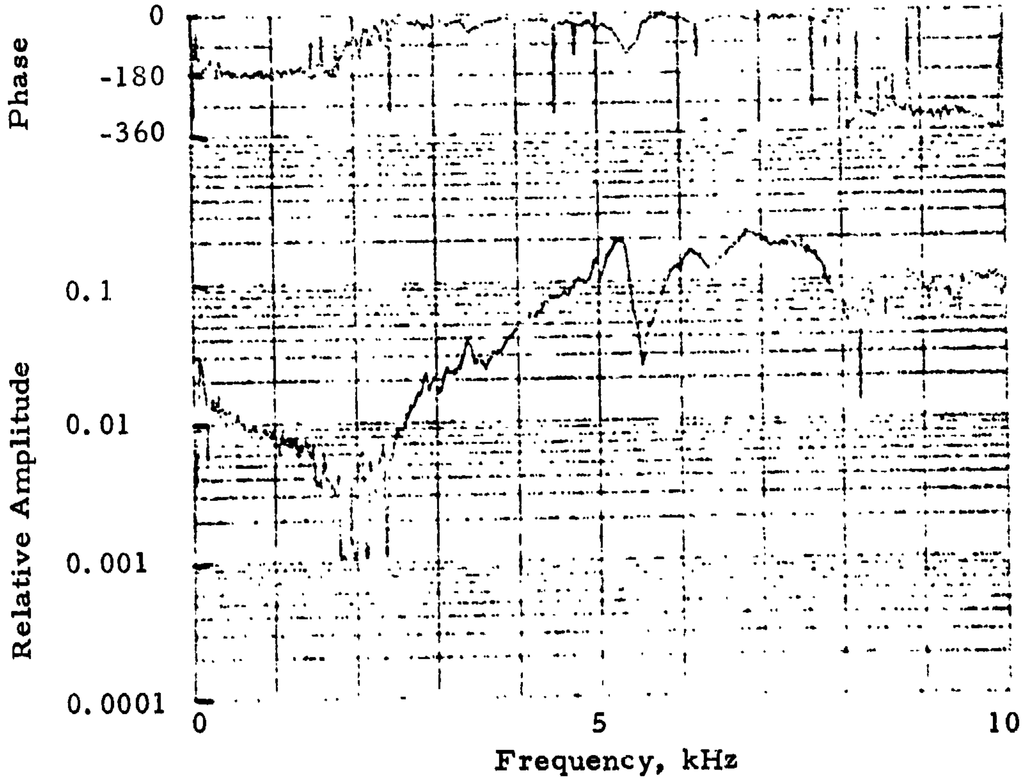

C-3

FIGURE 98. FREQUENCY RESPONSE WITH BOLT LOADED TO 94% OF PROOF LOAD.

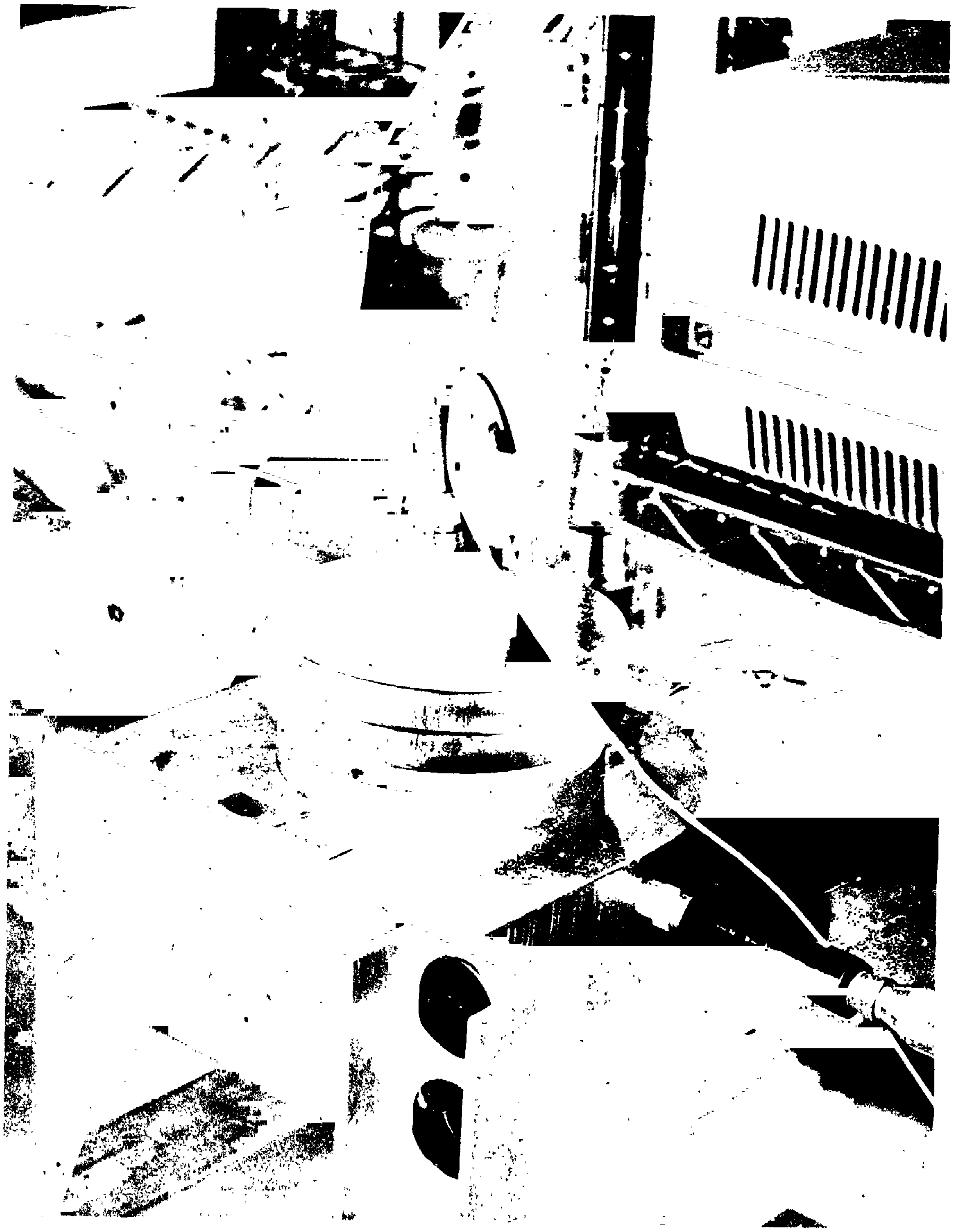

4549

FIGURE 99. MODIFIED HAMMER-IMPACT APPARATUS.

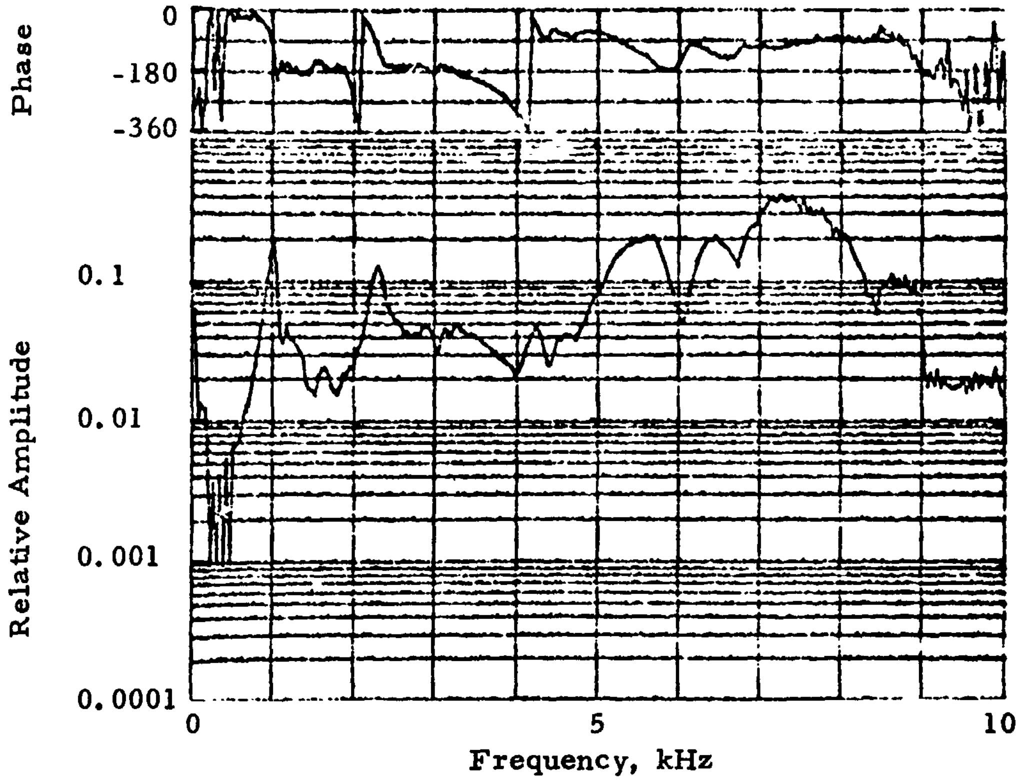

FIGURE 100. FREQUENCY RESPONSE OF MODIFIED FIXTURE WITH BOLT SNUG AND IMPACT ON BOLT HEAD.

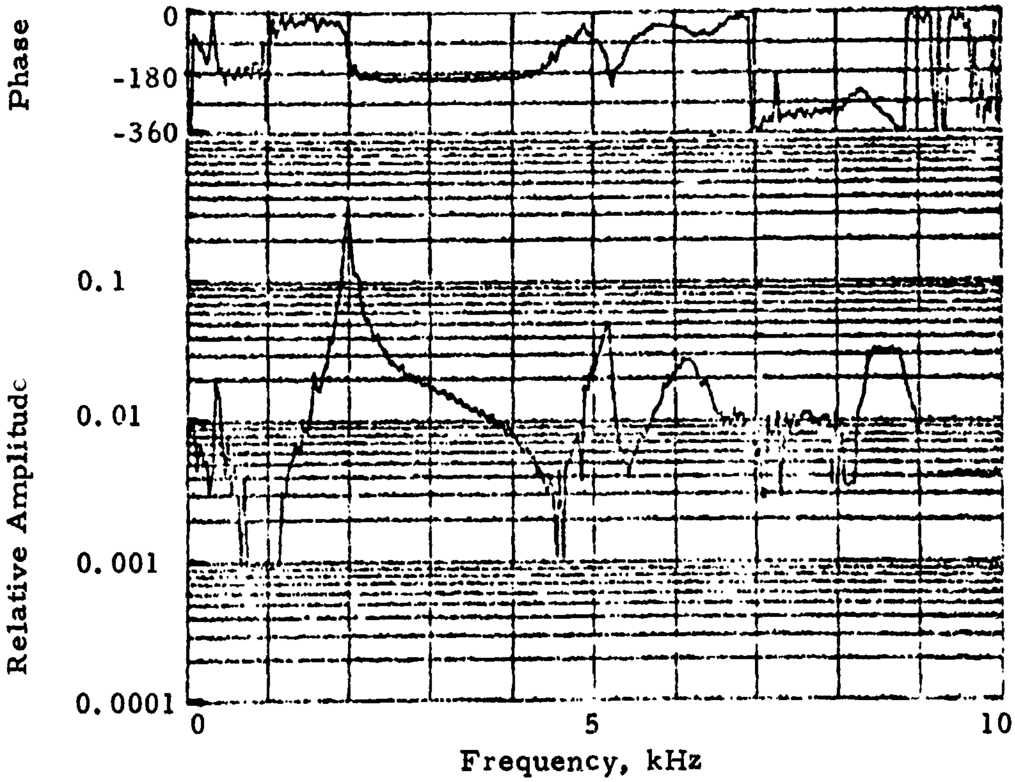

FIGURE 101. FREQUENCY RESPONSE OF MODIFIED FIXTURE WITH BOLT LOADED TO 34% OF PROOF LOAD AND IMPACT ON BOLT HEAD.

4550

ORIGINAL PAGE IS
OF POOR QUALITY

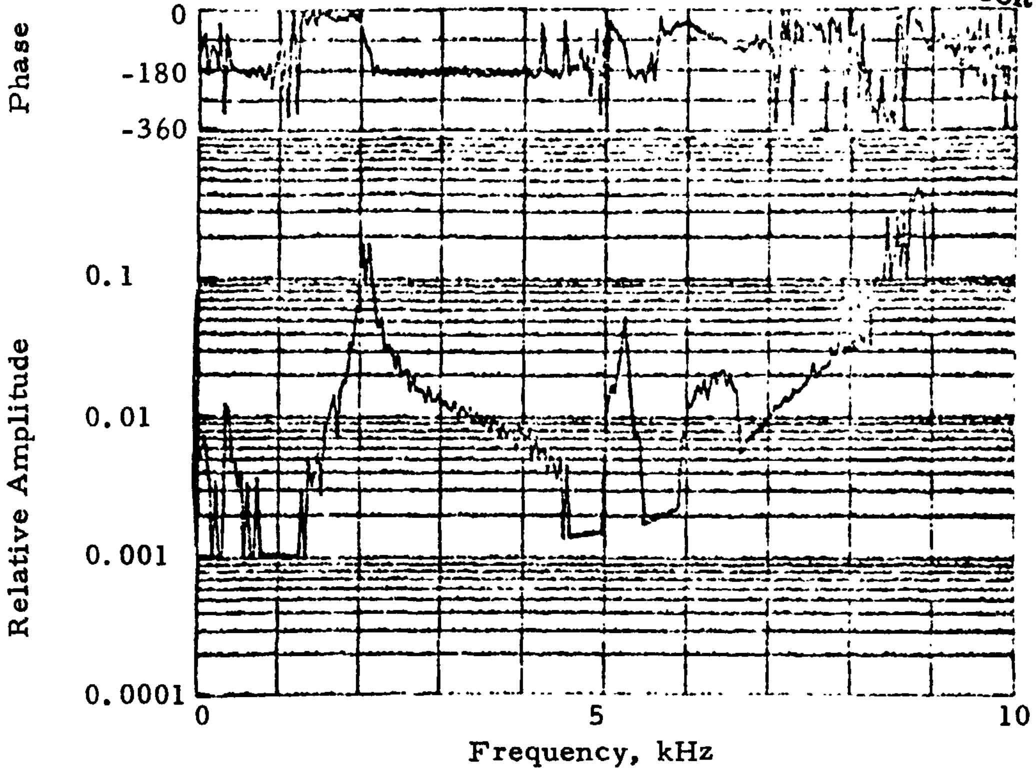

4551

FIGURE 102. FREQUENCY RESPONSE OF MODIFIED FIXTURE WITH BOLT LOADED TO 63% OF PROOF LOAD AND IMPACT ON BOLT HEAD.

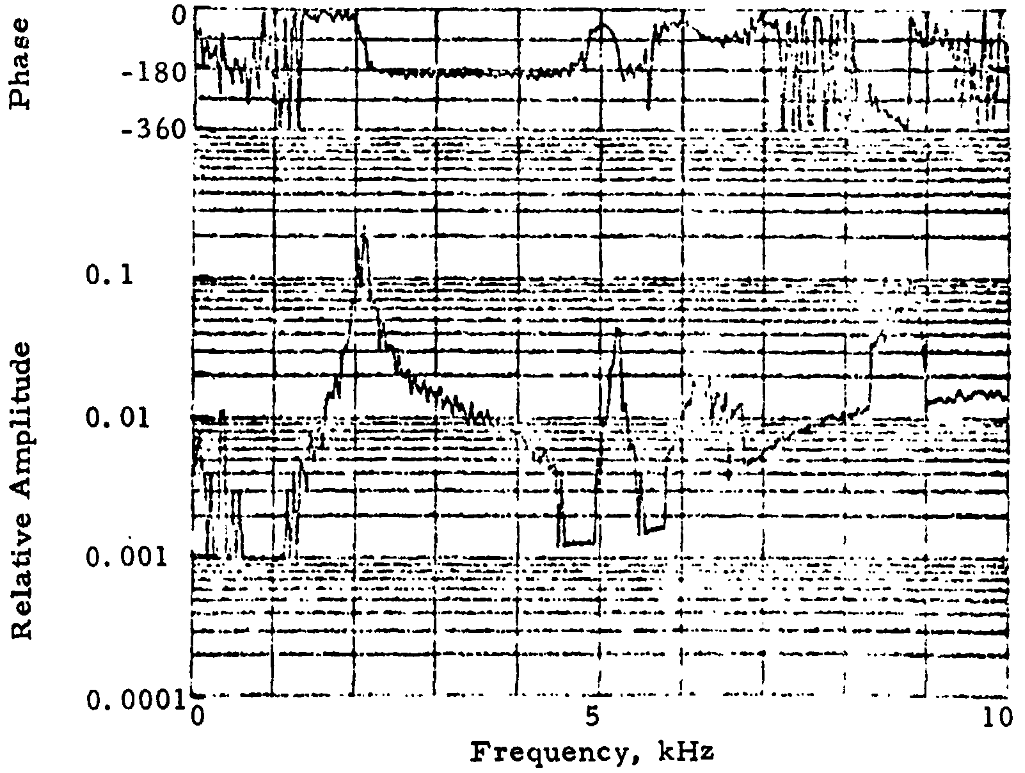

FIGURE 103. FREQUENCY RESPONSE OF MODIFIED FIXTURE WITH BOLT LOADED TO 89% OF PROOF LOAD AND IMPACT ON BOLT HEAD.

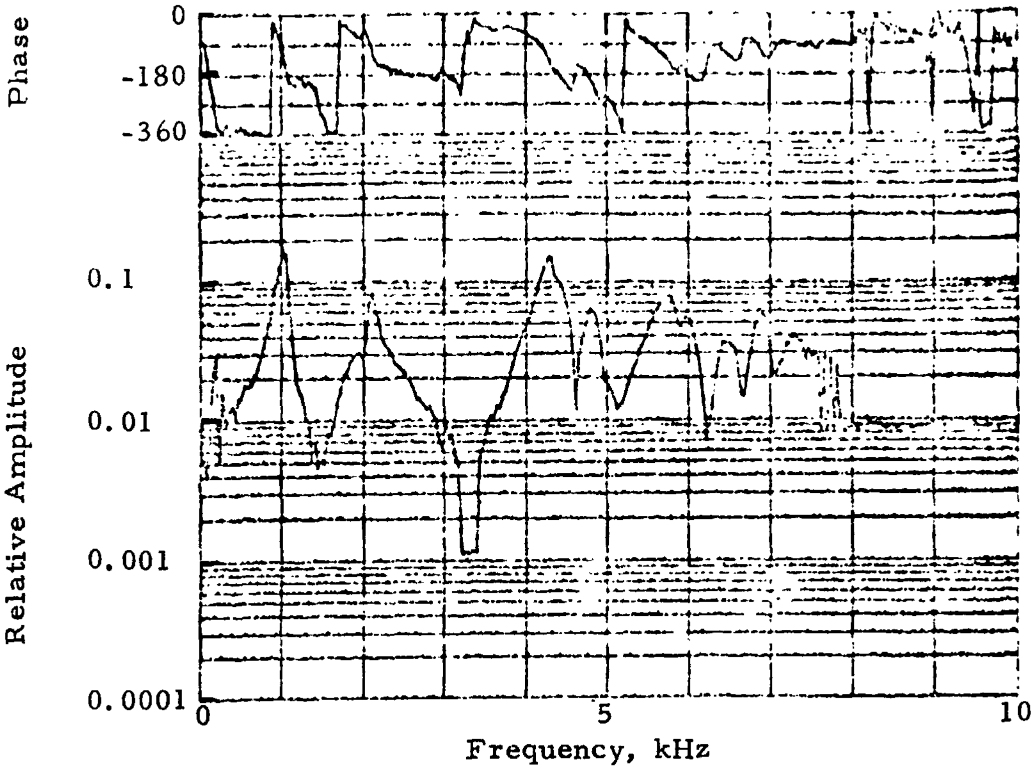

4552

FIGURE 104. FREQUENCY RESPONSE OF MODIFIED FIXTURE WITH BOLT SNUG AND IMPACT ON TOP PLATE.

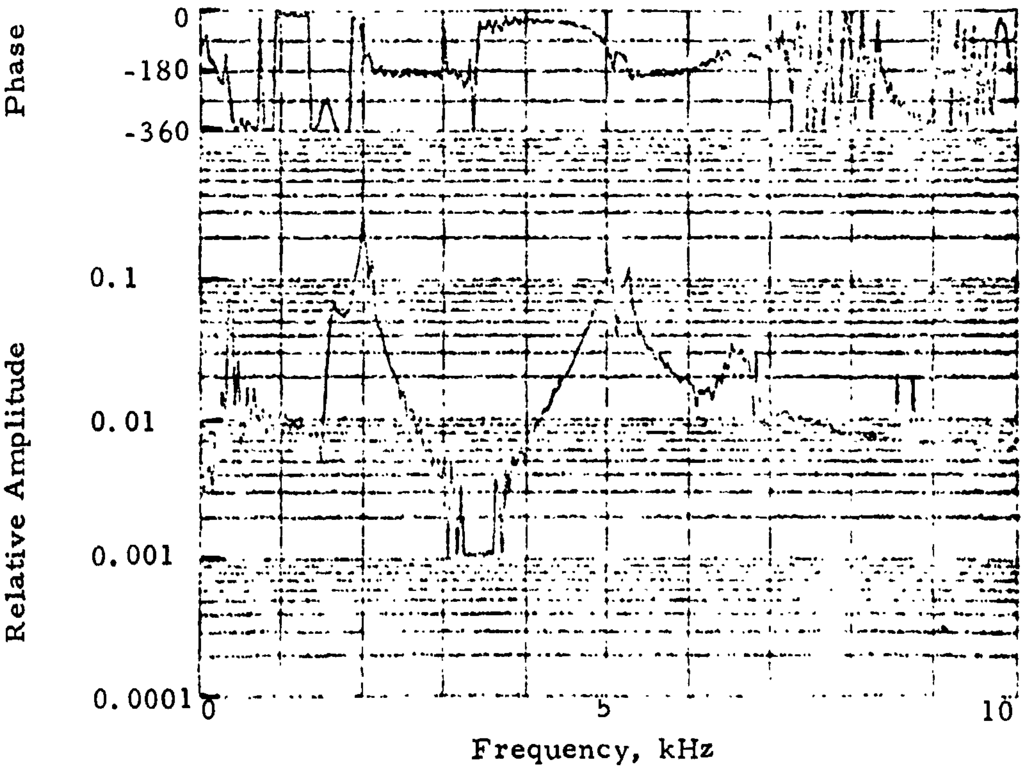

FIGURE 105. FREQUENCY RESPONSE OF MODIFIED FIXTURE WITH BOLT LOADED TO 34% OF PROOF LOAD AND IMPACT ON TOP PLATE.

ORIGINAL PAGE IS OF POOR QUALITY

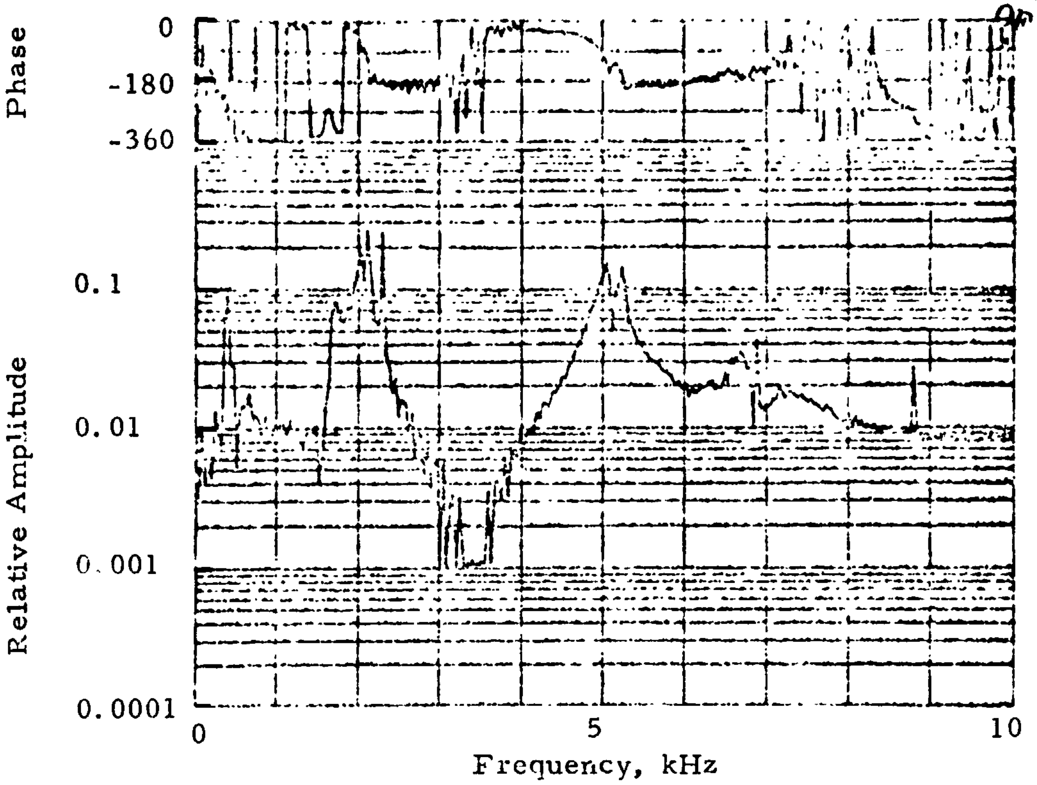

4553

FIGURE 106. FREQUENCY RESPONSE OF MODIFIED FIXTURE WITH BOLT LOADED TO 63% OF PROOF LOAD AND IMPACT ON TOP PLATE.

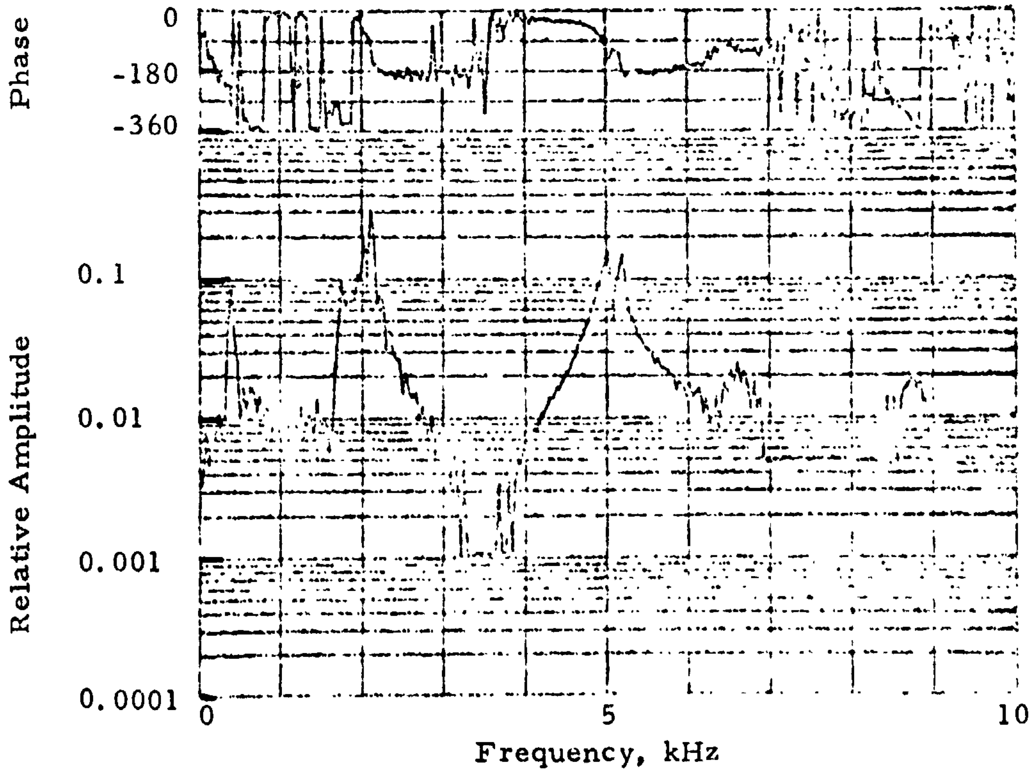

FIGURE 107. FREQUENCY RESPONSE OF MODIFIED FIXTURE WITH BOLT LOADED TO 89% OF PROOF LOAD AND IMPACT ON TOP PLATE.

Examination of these eight curves shows, as previously observed, that frequency response with the bolt snug differs markedly from frequency response with the bolt in tension. However, frequency response is essentially independent of tension in the range tested. Frequency response curves for the two locations of mechanical impulse introduction had a number of similarities, but were not identical.

Conclusions from Acoustic Impact Experiments

Experiments with the acoustic impact technique indicated that this method can readily detect the difference between a bolt which is snug (i. e., too tight to turn with the fingers, but without appreciable tension) and a bolt tensioned to even a relatively small fraction of the proof load. However, no feature of either the time response waveforms or the frequency response curves which could be quantitatively correlated with bolt tension was observed. The rather extensive apparatus required to implement this technique (i. e., a Fast Fourier Transform analyzer) is a distinct disadvantage of the method.

VIII. CONCLUSIONS AND RECOMMENDATIONS

Conclusions

1. Friction at the time of installation accounts for approximately 90% of the torque required to install a fastener. Conditions affecting friction are highly variable and cause considerable uncertainty in the actual preload resulting from a specific torque value. Use of a properly calibrated torque wrench produces preload data scatter of at least 30%. Under practical conditions of operator and torque wrench variability, scatter can be considerably higher than this.

2. Due to uncertainties in the fastener torque-tension relationship, considerable variability is noted in torque recommendations between various sources. Torque recommendations are always conservative to prevent overstressing the fasteners. This results in a condition in which fasteners are generally under-utilized at a considerable penalty in weight or number of properly stressed fasteners.

3. Torque recommendations generally do not reflect a statistical approach to the data, making it impractical to predict reliability of fasteners installed according to a specific torque schedule.

4. Various methods of tension control are effective in reducing preload scatter. Such tension control methods include directly stressing the fastener, applying torque with feedback control, and direct tension measurement. Accurate tension control can produce average weight savings of 30% or more by allowing fewer or smaller properly stressed fasteners for a given load requirement.

5. While a number of special fasteners, washers, and other load indicating devices are available, only one commercial instrument capable of directly measuring preload was located. This is an ultrasonic pulse-echo system for measuring fastener elongation.

6. A total of 14 NDE methods were located which had apparent applicability to the measurement of fastener stress. After a careful engineering assessment, six of these methods were selected for experimental evaluation. These included two ultrasonic methods for measurement of elongation, two magnetic approaches to the measurement of surface stress, and two ultrasonic techniques for the measurement of bulk stress.

7. Ultrasonic pulse-echo, the available commercial system, was demonstrated to be capable of measuring elongation with high accuracy. Preload determination from these elongation measurements appears

possible with an accuracy (preload scatter) of $\pm 3\%$. Its usefulness as a post-installation inspection device for fastener load is doubtful, however.

8. The ultrasonic resonance approach (ROUS) utilizing a developmental laboratory system, was also shown to be capable of measuring elongation with high accuracy. Preload determination with accuracy at least as great as the pulse-echo system is possible, but like the pulse-echo system, its practical application appears to be limited to installation purposes rather than later inspection.

9. A finite-element computer analysis indicated that tensile stress in the shank of a fastener is reflected in surface stresses in the head, mainly compressive, which can be used to determine preload and post-installation load. The analysis further showed, however, that within the dimensional tolerances now allowed in commercial fasteners, variations in stresses in the head of a fastener resulting from a given shank load could be as great as 20%. Thus, measurement of shank stress by sensing stress in the head with high accuracy would require specially selected fasteners with close dimensional tolerances.

10. The Barkhausen noise (magnetic) approach was demonstrated to be sensitive to surface stresses on the heads of fasteners in the range required. However, data scatter was found to be excessive in most cases. Analysis of this problem indicated three principal causes: First, residual stresses, largely the result of manufacturing steps, appear to affect preload determination significantly. Second, Barkhausen noise, in common with other magnetic parameters, exhibits a stress saturation effect at relatively low values of stress which makes preload a non-linear function of the magnetic signal. Third, dimensional variations were shown to affect surface stresses in the head for a given shank load.

11. Shear-wave birefringence, measured by determining the ultrasonic velocity of polarized shear waves traveling across the head, was shown to be an effective means of measuring average bulk stress in the head. The effect is linear, and correlates well with preload. However, it suffers common problems with any method based on fastener head measurements: dimensional variations result in data scatter, and residual stresses affect shank stress determination.

12. The acoustic impact technique (AIT) was not found to be effective in the determination of preload, but can determine whether a bolt is "tight" or "loose". This might be a valuable adjunct to routine inspection of non-critical fasteners, but it cannot be used to determine shank stress.

13. Of the methods evaluated, only the Barkhausen effect and ultrasonic birefringence appear to form the basis for post-installation measurements of load. Of the two, the birefringence approach is the more promising for two principal reasons: First, it does not suffer a stress saturation effect, and second, it may be feasible, by a system of frequency analysis, to separate the effects of residual stress from anisotropy.

14. No method was found capable of making accurate post-installation load measurements on standard fasteners. The principal requirement for an "NDE Grade" bolt, would be more accurate head dimensions, and reduction in residual stresses.

Recommendations

1. For critical applications, experimental torque-preload data should be taken from representative fasteners of the type and under the identical conditions to be used, to establish a torque schedule. These data are preferred over the manufacturers' recommendations where maximum fastener performance is desired.

2. Effort is recommended to implement instrumented tension control for critical fastener applications, using either the pulse-echo or the ultrasonic resonance techniques. The present instruments may be somewhat crude and inconvenient to operate from a practical standpoint, but their improvement and eventual acceptance will depend upon a determined effort to implement the systems. The potential saving in fastener weight alone should more than offset the effort required.

3. A study of residual stress effects in fasteners is recommended. It may be that relatively simple specifications, particularly with regard to heat treatment, could greatly alleviate a serious problem in developing post-installation inspection methods.

4. For post-installation inspection, consideration should be given to a new, special category of bolt which would be designated "NDE Grade". Such fasteners would be dimensioned with somewhat tighter tolerances in the critical head dimensions, and treated in manufacture in such a way that residual stresses would be minimized.

5. Extended study of a shear-wave birefringence system on a statistically significant number of fasteners is recommended. Improved accuracy and stability over the laboratory instrument used in the experiments discussed in this report is well within the capability of ultrasonic technology and such an instrument should be constructed. Such study should include investigation of frequency analysis methods of isolating the effects of residual stresses.

REFERENCES

1. Fisher, J. W., and Struik, J. H. A., Guide to Design Criteria for Bolted and Riveted Joints, John Wiley, New York, 1974.

2. Maney, G., "Predicting Bolt Tension," Fasteners, Vol. 3, No. 5, 1946.

3. Brenner, H. S., "Development of Technology for Installation of Mechanical Fasteners," Contract NAS 8-20799, AD No. N71-26568, 1971.

4. Rice, E. E., "Safer Tightening for Bolted Joints," Machine Design, Vol. 48, No. 15, June 24, 1976.

5. Chesson, E. and Munse, W., Studies of the Behavior of High-Strength Bolts and Bolted Joints, Eng. Exper. Sta. Bul . No. 469, Univ. of Ill., Urbana, 1965.

6. "Air Tools Take a Giant Step in Fastening," Iron Age, March 8, 1976.

7. Finkelston, R. J., "The Joint Control Fastening System," Soc. of Manufacturing Engrs. Paper AD74-422.

8. SAE J429h, Mechanical and Material Requirements for Externally Threaded Fasteners, Sept. 1974.

9. Vary, A., "Nondestructive Evaluation Technique Guidebook," NASA SP-3079, Lewis Research Center, 1973.

10. Reimherr, R. N., Barton, John R., "Evaluation of Barkhausen Noise Analysis as a Method for Measuring In-Place Bolt Tightness," Final Report, Contr. No. DAAE07-76-C-1561, U. S. Army-TARDCOM, December 1976.

11. Rollwitz, W. L., "Magnetoabsorption," Progress in Applied Materials Research, Vol. 6, edited by E. G. Stanford, J. H. Fearon and W. J. McGonnagle, Heywood, 1964.

12. Bozarth, R. M., Ferromagnetism, D. Van Nostrand Company, Inc., 1951.

13. Barkhausen, H., "Zwei mit Hilfe der Neuen Verstarker Entdeckte Erscheinurrgen," Physik, Z. 20, 401-403 (1919).

14. Erdman, D. C., "Ultrasonic Measurement of Fastener Strain on Bolts and Studs Ranging in Length from 2 Inches to 12 Feet". Papre presented at ASNT National Fall Conference, Houston, Texas, September 1976.

15. Heyman, J. S., "A Selfexciting Ultrasonic Reflection CW System", NASA Langley Research Center, Hampton, VA. 1976.

16. Couchman, J.C., Progress Report, Contract No. F33615-76-C-5251, Air Force Materials Laboratory, 1976.

17. McFaul, H. J., "An Ultrasonic Device to Measure High Strength Bolt Preloading," Mat. Eval. 22, 244 (1974).

18. Hegman, J. S., "Ultrasonic Bolt Stress Monitor," Ind. Res., Oct. 1976.

19. Symon, K. R., Mechanics, Addison-Wesley, Reading, Mass. (1964).

20. Hughes, D. S. and Kelly, J.L., "Second Order Elastic Deformation of Solids," Phys. Rev., 92, 1145 (1953).

21. Benson, R. W. and Raelson, U. J., "Acousto-Elasticity," Prod. Eng., 30, 56 (1959).

22. Smith, R. T., "Stress-Induced Anisotropy in Solids - The Acousto-Elastic Effect", Ultrasonics, July-Sept., 135 (1963).

23. Crecraft, D. ., "Ultrasonic Measurement of Stresses," Ultrasonics, April, 117 (1968).

24. R liffe, B. J., "A Review of the Techniques using Ultrasonic Waves for the Measurement of Stress within Materials," British Journal of NDT, II, 48 (1969)

25. Noronha, P. J. Chapman, J. R., and West, J. J., "Residual Stress Measurement and Analysis using Ultrasonic Techniques," J. Test. Eval. 1, 209 (1973).